Ghent University
Faculty of Science
Department of Molecular Genetics

Analysis of inter- and intracellular infection strategies during the legume-rhizobia symbiosis

Ward Capoen

Thesis submitted in partial fulfillment of the requirements for the degree of Doctor (Ph.D.) in Science: Biotechnology

Academic year 2005-2006

Promotor: Prof. Dr. Marcelle Holsters
Co-promotor: Prof. Dr. Sofie Goormachtig

Jury members

Promotor

Prof. Dr. Marcelle Holsters (secretary)
Dept. Plant Systems Biology
Flanders Interuniversity Institute for Biotechnology (VIB)
Ghent University

Co-promotor

Prof. Dr. Sofie Goormachtig
Dept. Plant Systems Biology
Flanders Interuniversity Institute for Biotechnology (VIB)
Ghent University

Promotion commission

Prof. Dr. Erik Remaut (chairman)
Dept. Molecular Biomedical Research
Flanders Interuniversity Institute for Biotechnology (VIB)
Ghent University

Prof. Dr. Lieve Gheysen
Dept. Molecular Biotechnology
Ghent University

Prof. Dr. Monica Höfte
Dept. of Molecular Biotechnology
Ghent University

Prof. Dr. Dirk Inzé
Dept. Plant Systems Biology
Flanders Interuniversity Institute for Biotechnology (VIB)
Ghent University

Dr. Giles Oldroyd
Dept. of disease and stress biology
John Innes Centre
Norwich, UK

Dr. Tom Beeckman
Dept. Plant Systems Biology
Flanders Interuniversity Institute for Biotechnology (VIB)
Ghent University

Table of content

Chapter 1

The legume-rhizobia symbiosis and symbiotic nitrogen fixation

Worldwide importance of legumes

Legume plants are of vital importance, representing a quarter of the world's primary crop biomass and a third of human dietary nitrogen and of the world's vegetable oil production, legumes are second only to the grass family (Graham and Vance, 2003). Adding to this, 88% of all legumes tested so far can engage in a symbiotic interaction with a group of gram-negative bacteria called rhizobia, that, under nitrogen limiting conditions, induce new organs on the plant roots, called nodules, in which the bacteria reduce atmospheric nitrogen and provide the plant with a nitrogen source (Mylona et al., 1995). This symbiotic nitrogen fixation (SNF) has long been exploited by farmers in crop rotation schemes to restore soil fertility. Moreover, legume-based agriculture systems are more efficient at retaining carbon and nitrogen in the soil than systems based on chemical nitrogen fertilizer, allowing for a more environmentally sound approach to agriculture (Drinkwater et al., 1998).

In the past decade, legumes have advanced to the forefront in plant research, partly due to the establishment of two well-supported model legumes, *Medicago truncatula* and *Lotus japonicus* (Oldroyd and Geurts, 2001; Riely et al., 2004). Because of their small diploid genomes, selfing capabilities and amenability for both forward and reverse genetics, the pending genome sequence and dense genetic maps, they have rapidly taken center stage in legume research, pushing away other models like pea (*Pisum* sativum), soybean (*Glycine max*), alfalfa (*Medicago sativa*) and several more.

Evolution of symbiotic nitrogen fixation

Although the use of model plants has undeniable advantages, the sheer magnitude of biodiversity in the legume lineage harbours many aspects that cannot be addressed using just these models. The legume family (Leguminosae), with more than 18 000 species and 650 genera, is the 3rd largest angiosperm family (Soltis et al., 1995). It has 3 subfamilies, the Mimosoideae, Papilionoideae and the Caesalpinoideae, the two first comprising monophyletic clades, whereas the latter is paraphyletic in nature. 90% of all the Mimosoideae and Papilionoideae studied form nodules, opposed to 30% of all Caesalpinoideae studied (Soltis et al., 1995). It is widely acknowledged that Papilionoideae are evolutionary the most derived subfamily, followed by the Mimosoideae and finally the Caesalpinoideae as the most basal legume subfamily. Parsimony analysis suggests that within the legumes, nodulation evolved independently at least on three separate occasions (Doyle, 1998).

Although symbiotic nitrogen fixation (SNF) is best studied within the legume family, a number of other plant groups can also form nitrogen-fixing nodules. Besides legumes, only *Parasponia andersonii* belonging to the Ulmaceae family is also able to form nodules upon infection with rhizobia (Doyle, 1998).

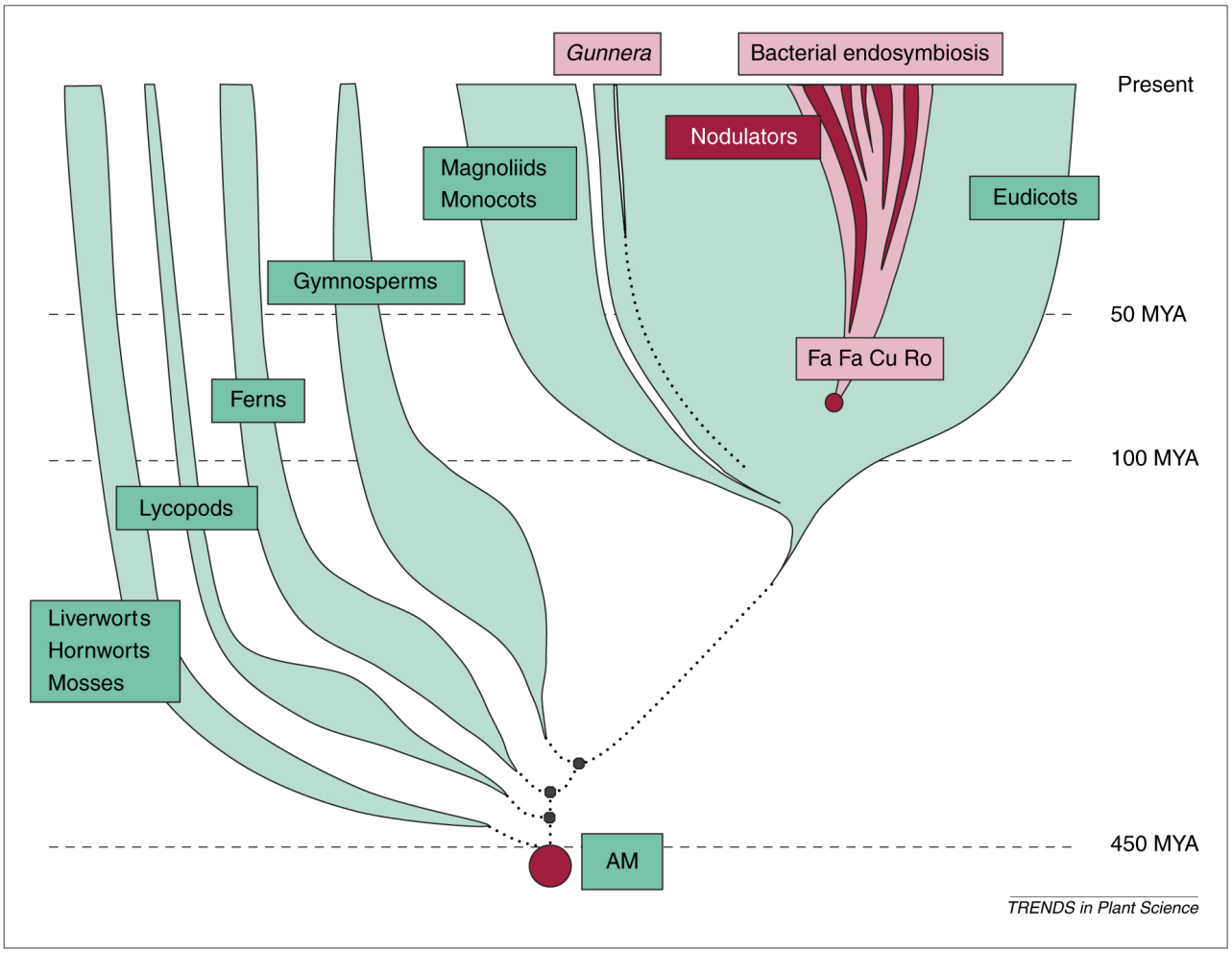

Fig.1 Evolution of endosymbiosis
The arbuscular mycorrhizal symbiosis is thought to have evolved about 460 million years ago. Colonization of land by plants is assumed to be a direct result of this event. Root nodule symbiosis probably arose some 65 million years ago in the Eurosid I clade (in the orders Fabales, Fagales, Cucurbitales and Rosales), and probably developed several times indepently. One other nitrogen fixing symbiosis that probably evolved independtly is the interaction between *Gunnera* and the cyanobacteria *Nostoc*. Reprinted from Kistner, C. and Parniske, M. (2002) Trends Plant Sci 7, 511-8.

The gram-positive actinomycete *Frankia* can form nodules on members of eight angiosperm families (Gualtieri and Bisseling, 2000). Both rhizobia-legume and Frankia-actinorhizal interactions all belong to the Fa Fa Cu Ro clade (for Fabales, Fagales, Cucurbitales and Rosales) of the Eurosids I group of flowering plants (Fig. 1) (Soltis et al., 1995; Kistner and Parniske, 2002). Somewhere in evolution, a predisposition event occurred that enabled these lineages to evolve a nitrogen fixing symbiosis. It is thought that within this clade, bacterial endosymbiosis then evolved several times independently (Kistner and Parniske, 2002). Finally, certain cyanobacteria can form a nitrogen-fixing symbiosis with members of the Gunneraceae. This is usually not considered a true form of bacterial endosymbiosis since the cyanobacteria colonize existing glandular tissue of the plant and no novel organ is formed to accommodate the microsymbionts (Gualtieri and Bisseling, 2000).

Where symbiotic nitrogen fixation is restricted to a small subgroup of flowering plants,

another, more ancient, symbiotic interaction is more universal within the plant kingdom. The majority of land plants can form a intimate relationship with fungi of the Glomales order. In this symbiosis, fungal hyphae penetrate the epidermis and proceed toward the inner cortical cell layers of the root. Here they differentiate into highly branched intracellular structures, called arbuscules (Harrison, 1999; Kistner and Parniske, 2002). Hence, symbiosis is often referred to as Arbuscular Mycorrhization (AM). AM symbiosis essentially results in a huge extension of the root system and allows for a more efficient phosphorous and mineral uptake. AM is a widespread feature of plant life, most land plants will engage in it. Given this fact and given the presumed origin some 400 Million years ago, it is possible that this association was a major advance that enabled plants to first colonize land. Several legume mutants that are impaired in nodule formation are also impaired in AM formation (Fig. 1)(Kistner and Parniske, 2002). For this reason, it is thought that legumes have partially recruited certain endosymbiotic functions from the older AM symbiosis, and will be discussed in further detail in the section on early signaling in symbiosis .

Nodule formation and morphological diversity

In what follows, a general description will be given of the morphological series of events that lead to a nodule, i.e. infection events, nodule development and nodule maturation. Although several variations on this theme occur in nature, the nodulation of *M. truncatula* and *L. japonicus* will be used as a paradigm and pertinent variations on this system will be discussed, either in parallel or in subsequent paragraphs. A comprehensive overview of the molecular aspects of early events will follow.

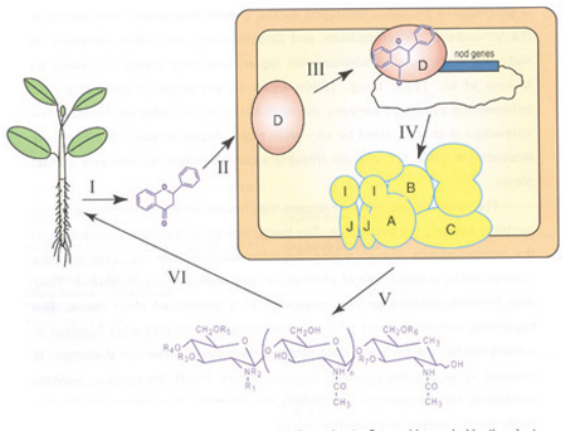

Fig. 2 A molecular cross-talk lies at the basis of symbiosis
Plant roots exude a complex mixture of compounds into the rhizosphere, including several flavonoids (I). These flavonoids are specifically bound by the bacterial nodD protein (II), which then acts as a transcriptional regulator that activates the transcription of the *nod* genes (III). The *nod* gene products are necessary to produce and secrete the bacterial signal molecule, the Nod factor (IV). Nod factor in turn acts as a potent morphogenic signal that is specifically recognized by the plant, presumably via LysM domain containing receptor-like kinases. This recognition is the start signal for a range of processes that will lead to the development of a nitrogen fixing root organ, the nodule, in which the bacteria will reside.

Recognition and molecular cross talk

Plant roots exude a large number of compounds into the rhizosphere, among which a spectrum of flavonoids. Rhizobia can perceive some of these flavonoids via the NodD protein. NodD is a transcriptional activator that, after binding specific flavonoids, initiates transcription of genes that in their promoters contain a highly conserved DNA sequence, the *nod* box (Fig. 2) (Brewin, 1991; Perret et al., 2000). These genes are referred

to as *nod* genes and their gene products are responsible for the production and secretion of a major signaling molecule that will prime the plant for nodule formation. Functional analysis showed that mutations in certain *nod* genes conferred a complete block in nodulation, such as *nodABC*, and since these genes were interchangeable between different rhizobial strains, they were called the common *nod* genes (Brewin, 1991). Others cannot functionally complement each other and are called the host specific *nod* genes (reviewed in Schultze et al., 1994). The extracellular signal responsible for virtually all early plant responses was identified as an N-acetyl-D-glucosamine oligomer with an acylation at the non-reducing sugar and a number of strain specific decorations at both the non-reducing and reducing sugars, e.g. sulphation, methylation, fucosylation, carbamoylation, arabinosylation (reviewed in (D'Haeze and Holsters, 2002)). The signal was named the Nod factor (NF) and it was found that the *nod* genes were responsible for its production (Fig. 2). The common *nod* genes *nodABC* are responsible for the production of the NF backbone as they encode an acyl transferase, a chitooligosaccharide deacetylase and a N-acetylglucosaminyltransferase respectively (Schultze et al., 1994). Their concerted action produces an N-acetylglucosamine backbone that carries an acyl chain at its non-reducing end. Host specific *nod* genes add different moieties to this basic structure, conferring host specificity to the molecule. NF are secreted into the rhizosphere, where they will be are recognized by the plant.

NF are potent morphogens that show biological activity at picomolar concentrations (D'Haeze and Holsters, 2002), making it likely that they are recognized by specific plant receptors. Within hours of NF recognition root hair tips in the zone just behind the apical meristem swell and start to deform (Gage and Margolin, 2000; D'Haeze and Holsters, 2002). Bacterial attachment results in the formation of an infection focus and the root hair deforms further, curling around the infection focus. In order to do this, extensive reorganization of the root hair cytoskeleton is a prerequisite. Already within the first 10 minutes of NF recognition, drastic changes in the distribution of the root hair cytoskeleton are visible and more changes occur over the next few hours (Lhuissier et al., 2001; D'Haeze and Holsters, 2002). Within minutes, a depolymerization of fine actin bundles is seen in the root hair tips of *Phaseolus vulgaris,* reversing again within 1 hour (Cardenas et al., 1998). From this point on, the root hair tip swells and reinitiation and redirection of tip growth ensues. The continuous reorientation of tip growth around a fixed signaling center, i.e. an attached microcolony of rhizobia eventually forms a curl that entraps the microcolony (Esseling et al., 2003). This curling involves massive reorientation of the microtubule cytoskeleton. Some 18 hours after inoculation, the nucleus migrates towards the tip of the root hair and microtubules start to form a connecting structure between the tip and the nucleus (Timmers et al., 1999). During the curling of the root hair, microtubules converge on the center of the curl. It needs pointing out here that although purified NF are sufficient to induce deformations, they do not induce tight

curling of the root hair tip. It has been suggested that positional information from bacterial attachment is necessary to maintain the redirection of root hair tip growth long enough to allow the root hair to form this curl (Gage, 2004). It is now that the bacteria are ready to invade the root hair (Fig. 3).

Infection thread initiation and progression

Local cell wall hydrolysis and invagination of the root hair plasma membrane marks the initiation of a tube like structure that starts to progress within the infected root hair (Patriarca et al., 2004). Infection threads are tubular structures consisting of primary cell wall, surrounding both bacteria and a matrix consisting of extracellular glycoprotein (Brewin, 2004). Actively dividing bacteria are thought to drive IT thread progression in combination with peroxide-driven cross linking and solidification of the matrix behind this tip (Brewin, 2004). Microtubules form a dense network reflecting the path of the progressing IT. This process is maintained throughout the cortical cell layers until the growing IT reaches the incipient primordium (Timmers et al., 1999) (Fig. 3).

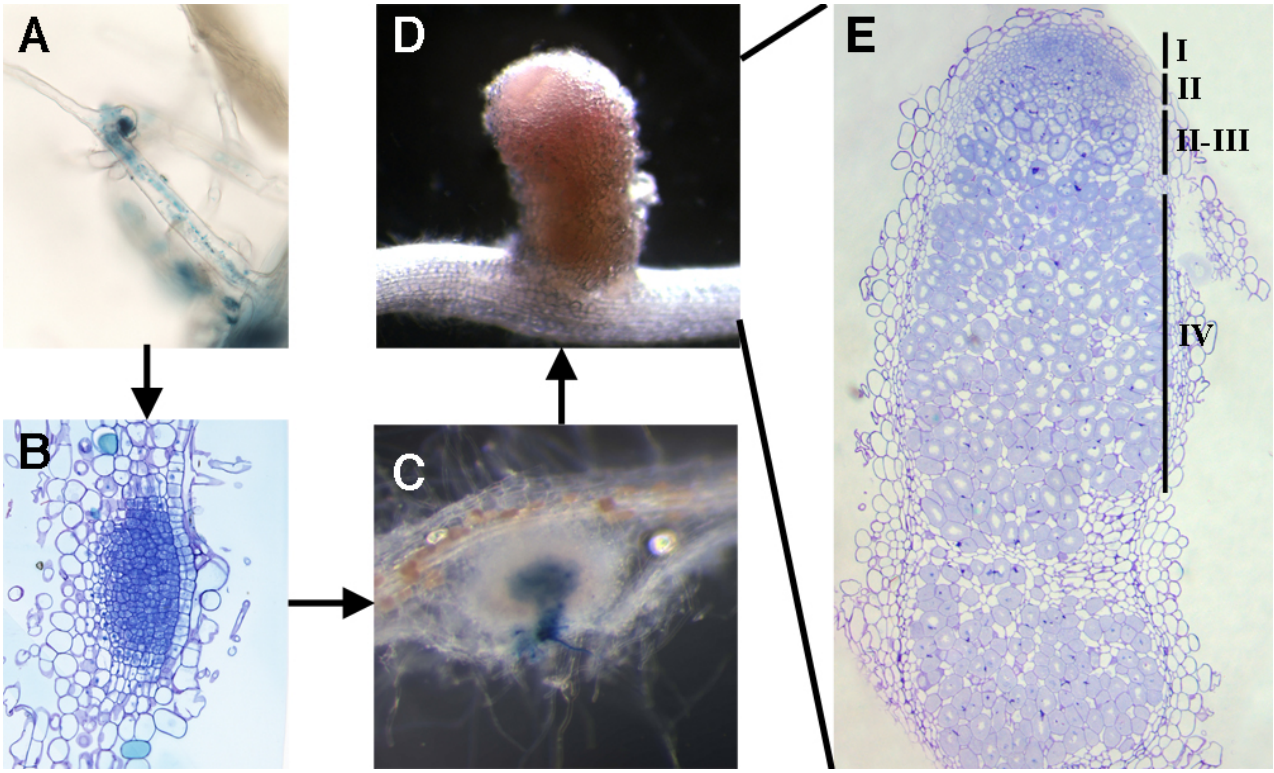

Fig. 3 Morphological stages of indeterminate nodule development
Upon recognition of Nod factors (NF), the root hairs start to deform and will eventually form a tight curl around a bacterial microcolony (A). This microcolony serves as a signaling center for the redifferentiation of inner cortical cells which will start to divide and form a nodule primordium (B). Bacteria will invade the root hair and a tubular structure of plant origin, the infection thread will grow toward the developing nodule primordium, where bacteria will be released into the primordium cells (C). The nodule will develop further and the apical nodule meristem will continue to give of new cells that also become invaded by bacteria, leading to a cylindrical nodule (D). A cross section through a mature indeterminate nodule shows a clear zonation with an apical meristem (I), the progeny of which becomes infected with bacteria (II). Both plant and bacterial cells will then differentiate (II-III) and become mature fixing tissue (IV).

Nodule formation

Roughly at the same time as root hair curling, changes can be observed in the inner cortex and the pericycle of the root. Pericycle cells next to protoxylem poles are activated and an outward going gradient of dedifferentiating cells leads to the formation of a cluster of cells that have regained totipotency, the nodule primordium. This dedifferentiation is preceded by rearrangements of the microtubule cytoskeleton (Timmers et al., 1999). Activation and dedifferentiation of pericycle or cortical cells follows a similar pattern in which the nucleus migrates towards the center of the cell surrounded by a dense microtubular network (Timmers et al., 1999). Cortical cells of the young primordium can be recognized at this stage by the cytoplasmic strands that traverse the vacuole. These strands usually contain the centrally located nucleus (Timmers et al., 1999). Recent findings suggest that this primordium formation is closely linked to the establishment of a symplasmic field that reaches from the protophloem throughout the growing primordium. Modulation of the exclusion limit of plasmodesmata results in the progressive recruitment of new cells into the primordium (Complainville et al., 2003). Since this expansion of the symplasmic field precedes subsequent cell division, it is possible that the transport of certain signaling compounds lies at the basis of primordium formation (Complainville et al., 2003).

Meanwhile, outer cortical cells undergo significant changes in preparation for of IT passage. The nuclei of these cells migrate towards the center of the cells and the cytoplasm rearranges to form radially oriented cytoplasmic bridges, called pre-infection threads (PITs) (van Brussel et al., 1992). The PITs are formed in cells that prepare to receive the progressing IT and seem to guide the IT in the right direction. These cytoplasmic strands initially develop in a similar manner as in cells that will form the nodule primordium. However, unlike primordium cells, these PIT containing cells do not complete the cell cycle and arrest in the G2 phase, as shown by *in situ* hybridization with a mitotic cyclin (Yang et al., 1994). When the IT reaches the bottom of the epidermis. The IT crosses the space between the epidermis and the outer cortical cell layer, subsequent cell wall weakening occurs at the connection between cell wall and PIT, resulting in the invagination of the plasma membrane and the reinitiation of an infection thread (Gage, 2004). The nodule primordia are eventually invaded by the progressing ITs and these ITs ramify throughout the growing primordium. Finally, bacteria are released from infection threads into the cells that will become the nitrogen fixing tissue.

Bacterial release and symbiosome formation

It is still poorly understood how the switch is made between infection thread growth and bacterial release is made. When ITs reach a cell that will be infected, cell wall modifications in the IT cause ruptures or loosening of the cell wall and this allows for bacteria to be released into the cytoplasm, surrounded by a plant derived membrane (Brewin, 2004). These infection droplets will then start to differentiate into fully functional symbiosomes. The outer membrane of this droplet will change in composition from a plant plasma membrane

like structure into a peribacteroid membrane. Association with certain glycoproteins is observed and a vast array of proteins are specifically found in these membranes, no doubt playing roles in cell-organelle communication and transport of nutrients to and from the host (Brewin, 2004; Catalano et al., 2004). The bacteroids continue to divide, filling up the entire cytoplasmic space of the infected cells and the peribacteroid membranes can divide at the same pace or not, resulting in either symbiosomes with few or a larger number of bacteroids per symbiosome, depending on the species.

It needs to be noted that although bacteria are released from ITs, they remain extracytoplasmatic since they remain surrounded by plant-derived membranes (Parniske, 2000). This allows the plant to retain control of its microsymbiont. By keeping it inside a prelytic compartment, it can break of the symbiosis at its own discretion, e.g. in case of defective nitrogen fixation (Parniske, 2000). Symbiotic bacteria are unique in their ability to transgress plant cell walls and it is thought that this trait might have been a pivotal step in the evolution of bacterial endosymbiosis. No known pathogens, nor AM fungi have this ability, thus needing to force their way into the plant in order to penetrate. This is different to bacterial endosymbiosis, where the plant contributes actively to cell wall passage and release into the cytoplasm (Parniske, 2000).

Nodule maturation and nodule type

In most temperate legumes, a number of distally located cells will not be infected by bacteria and become meristematic. While the other primordium cells are invaded by bacteria and develop into cells that fix nitrogen, these meristematic cells continue to produce progeny that will become infected and differentiate into fixing tissue (Patriarca et al., 2004). This continuous addition of new fixing tissue gives these nodules a distinct oval shape and all developmental stages of nodule formation stay visible throughout the life of a nodule. A typical section through a nodule shows an apical meristem, an adjacent zone of continuous infection (the infection zone), a transition zone in which bacteria differentiate into nitrogen fixing bacteroids and a fully differentiated fixation zone (Fig. 3). This fixation zone consists of large plant cells filled with thousands of symbiosomes and uninfected cels interspersed throughout. Older nodules also have a zone of dieing cells where symbiosomes are degraded, nutrients are remobilized and returned to the host, the senescence zone (Patriarca et al., 2004). This nodule type is called the indeterminate type and is typical for legumes such as *M. truncatula* and *P. sativum*.

Another type of nodule, typified in *L. japonicus* and *G. max* do not have a persistent meristem. Initially, meristematic cells can be seen throughout the primordium until all cells become infected with bacteria and nodules grow through cell expansion. These nodules typically have a round shape and are called determinate nodules (Patriarca et al., 2004).

Chapter 2

Nod factor perception and signal transduction

Nodules are complicated organs that need a diverse array of pathways to be integrated flawlessly to allow the formation of a mature nodule. The molecular basis underpinning this is still poorly understood. Recently however, the identity of a number of key integrators has been unravelled. In what follows, a state of the art will be presented of the molecular nature of host-microbe recognition and signal transduction in legumes.

Cell biological events following NF recognition

Legume root hairs respond to Nod factor within seconds after application. These responses are varied and are usually NF structure specific, suggesting intervention of highly specific NF receptors in the process. In what follows, an overview of most known cell biological changes upon bacterial or NF recognition will be presented. In a next paragraph, an attempt will be made to integrate this information into a genetic background, reviewing genes and proteins known to be involved in these early responses and their putative roles during NF perception.

Ion Fluxes and membrane depolarization are the earliest known responses to NF

Within 10 minutes of NF addition, a number of extremely rapid responses can be detected in responsive alfalfa root hair tips. One early change is the rapid alkalinization of alfalfa root hair cytosol, reaching a maximum as little as three minutes after NF application (Erhardt et al., 1992; Felle et al., 1995). Both sulphated as non-sulphated NF induced the response and worked additively, suggesting different perception systems for the two NF structures (Felle et al., 1996). The O-acetyl group of the *Sinorhizobium meliloti* NFs was of no consequence for this response. Interestingly, high concentrations of N-acetylchitooligosaccharides also induced the alkalinization, suggesting that a similar mechanism might recognize these distinct molecules (Felle et al., 1996). This is particularly interesting in respect to the possible evolutionary origins of NF perception. Given the structural resemblances between chitin elicitors and NF, it seems plausible that NF perception evolved from the more ancient chitin perception system.

Following this alkalinization, within 10 minutes of NF addition, a significant membrane depolarization event occurs (Felle et al., 1995). Following an initial, short hyperpolarization (1-3 mV), the membrane depolarizes in a NF concentration dependent manner, with a maximum at 25 mV (10^{-7} M Nod factor). The membrane then returns to its ground state membrane potential within 20 minutes. Tetrameric NF were more efficient than pentameric NF, no strong difference was visible with O-acetylated NF although the response was slightly more rapid and finally non-sulphated NF, nor chitotetraose triggered the respons. These findings correlate remarkably well with the root hair deformation and cortical cell activation abilities of the respective NF, suggesting a molecular link between both. Interestingly, non-sulphated NF and chitotetraose could induce cytosolic alkalinization without inducing membrane depolarization, suggesting independent

perception systems for different NF structures (Felle et al., 1995). These differences in NF structure requirements for different host responses will be further discussed in a next chapter.

The most rapid physiological response identified to date however, is the rapid influx of calcium ions into alfalfa root hair cells upon NF application (Felle et al., 1998). This is part of a number of ion fluxes in root hairs that are thought to form the basis of the previously discussed membrane depolarization. The influx of Ca^{2+} ions preceeds membrane depolarization and alkalinization. Subsequently, an efflux of Cl^- ions could be measured concomitantly with the depolarization event, suggesting that both are caused by the calcium flux (Felle et al., 1998). This ion imbalance is then neutralized by a K^+ efflux that occurs at the moment of membrane repolarization (Felle et al., 1998). It has proven difficult to link all these observations into a firm model since no evidence so far exists for a specific role for these events in nodule initiation. Moreover, causal links are often difficult to discern since responses can sometimes be uncoupled using NF with different structures, suggesting a more complex network of responses rather than a simple linear model of ion flux action in the root hair cell. Substantial research has gone into the identification of the ancestral pathway from which this NF induced ion signaling network would be derived. It has been shown that chitooligosaccharide elicitors can induce similar processes as NF in alfalfa, albeit with different kinetics and effects (Felle et al., 2000). Although chitotetraose had no discernable effects on any ion flux tested, higher order chitooligosaccharides such as chitopentaose or chitooctaose did. It has been shown that both $(GlucNAc)_8$ and NF induce rapid extracellular and subsequent intracellular alkalinization and membrane depolarization, but that recovery after NF treatment is not complete, whereas for $(GlucNAc)_8$ hyperpolarization and extracellular and intracellular acidification were observed (Felle et al., 2000). It seems that $(GlucNAc)_8$ and NF are perceived by another recognition mechanism with partly overlapping signal transduction mechanisms. It is proposed by Felle *et al.* (2000) that the different responses that start to occur downstream can account for differences in gene expression, i.e. that $(GlucNAc)_8$ induced acidification of the cytosol would be one of the signals for defense gene expression, whereas NF induced alkalinization is a mechanism by which defense gene expression can partly be suppressed, a prerequisite for the establishment of a successful symbiosis (Felle et al., 2000).

Nod factor induced Ca^{2+}-spiking

Shortly after the influx of calcium ions at the root hair tip, another, different type of change in calcium concentrations becomes apparent. About 10 minutes after NF application, rhythmic calcium oscillations can be detected mostly in and also around the nucleus of growing root hair cells (Fig. 4) (Ehrhardt et al., 1996; Oldroyd and Downie, 2006). By means of microinjection, Ehrhardt and coworkers introduced calcium sensitive dyes into root hair

cells and then visualized changes in cytosolic calcium concentrations upon challenge with NF. Chitotetraose was unable to induce spiking and furthermore, NF structural restraints for spiking induction were found that were of a similar nature as restraints for nodulation, i.e. NF of bacterial strains that do not nodulate alfalfa did not induce spiking

(Ehrhardt et al., 1996). Spiking can be described as a function of several variables, in *M. truncatula* the average time between two spike maxima is around 106 seconds (Oldroyd et al., 2001a). The shape of the spike in all legumes investigated so far is also very typical, an initial sharp and rapid burst leads to a maximum calcium concentration within 10 seconds, whereas the return to basal levels is slower, resulting in an asymmetric spike shape (Ehrhardt et al., 1996; Walker et al., 2000; Harris et al., 2003).

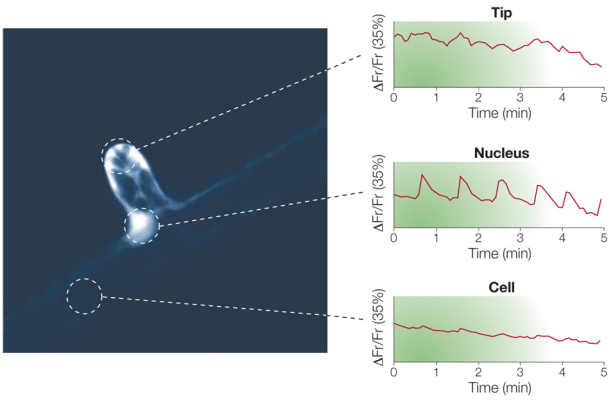

Fig. 4 NF induced, nuclear Ca^{2+} spiking in legume root hairs
Within minutes of NF perception, rhythmic Ca^{2+} oscillations (or Ca^{2+} spiking) can be seen in and around the nucleus. These oscillations can readily be visualized by microinjecting Ca^{2+} sensitive dyes into susceptible root hair cells. Measuring dye intensities in different parts of the cell shows the strictly nuclear and perinuclear localization of these oscillations. Reprinted from: Oldroyd, G.E. and Downie, J.A. (2004) Nat Rev Mol Cell Biol 5, 566-76.

It is thought that Ca^{2+}-spiking is a major component of the NF signal transduction and for this reason considerable research has gone into this phenomenon. Pharmacological analysis implicated phospholipase C in the pathway leading up to spiking, as inhibitors of PLC activity could block NF induced Ca^{2+}-spiking (Engstrom et al., 2002). Also, the involvement of Type IIA calcium pumps was inferred from the fact that CPA can block spiking (Engstrom et al., 2002). The use of Ruthenium Red as a specific inhibitor of the ryanodine receptor and of EGTA and La^{3+} as calcium influx inhibitors further implicated both internal and external calcium stores (Pingret et al., 1998). Calcium pumps are the prime candidates for generation of Ca^{2+}-spiking from internal Ca^{2+} stores. Whereas release from the store would occur along its concentration gradient towards the cytoplasm and nucleus, resequestration into the internal store would require ATP hydrolysis, making it an energetically demanding process (Oldroyd and Downie, 2004, 2006).

Future research will no doubt be instrumental in the further dissection of Ca^{2+}-spiking and it will be interesting to see which proteins are involved in the basic spiking machinery in plants. The involvement of calcium specific channels and pumps seems likely, but the secondary signals that trigger spiking are still elusive, although phospolipases might be involved. However, spiking also can be modulated more subtly than merely by an on/off switch. Spiking frequency can be modulated by endogenous molecules and this would be important for downstream signaling. Significant progress has been made in the

understanding of how spiking is regulated, and it appears that this pathway integrates several signals, resulting in what might be process-specific Ca^{2+}-signatures. Among these upstream signals are NF, ethylene, jasmonate and possibly more, still unknown factors.

Firstly, Ca^{2+}-spiking is a NF structure specific process and subtle changes to NF structures radically alter spiking responses. Wild type *S. meliloti* NF are able to induce spiking at concentrations as low as 10^{-12} M, and cumulative defects in NF structure progressively lower the activity of Ca^{2+}-spiking induction (Oldroyd et al., 2001b). Non-sulphated NF induced spiking but activity was 30 000 fold lower than wild type NF (Oldroyd et al., 2001b). O-acetylation seemed less critical, resulting in a 100 fold reduction in activity, whereas modification of the acyl chain did not significantly alter activity (Oldroyd et al., 2001b). Surprisingly, when added at high concentrations chitotetraose induced spiking (10^{-4} M) and sulphated chitotetraose was 1000 fold more active than non-sulphated chitotetraose (Oldroyd et al., 2001b). Mutants that no longer support spiking also did not respond to any of these alternative elicitors which suggests that spiking induction by chitin and sulphated chitin occurs via the same pathways as for wild type NF (Oldroyd et al., 2001b).

The first regulator of NF dependent spiking discovered was the gaseous plant hormone ethylene. It had previously been demonstrated that ethylene has an inhibitory effect on nodulation on various levels. Transcripts of ACC oxidase, an ethylene biosynthetic gene accumulate opposite of protophloem poles, which led to the hypothesis that ethylene can inhibit cortical cell division. This would explain why nodules are preferentially formed at protoxylem poles and why this positioning mechanism is lost in *skl,* an ethylene insensitive, hypernodulation mutant of *M. truncatula* (Heidstra et al., 1997; Penmetsa and Cook, 1997). Ethylene also regulates the number of infection threads, so ethylene should impact on a process upstream of IT initiation (Penmetsa and Cook, 1997). Ethylene can indeed affects Ca^{2+}-spiking profoundly. Ethylene is involved in desensitizing the plant to NF, as higher NF concentrations can overcome the inhibition of Ca^{2+}-spiking by ethylene. Additionally, ethylene can block spiking after it's commencement, suggesting that ethylene is also involved in spiking maintenance (Oldroyd et al., 2001a). Finally, *skl* plants showed a lower frequency of Ca^{2+}-spiking, so ethylene is probably involved in determining spiking frequency (Oldroyd et al., 2001a).

Whereas ethylene seems to speed up spiking, it was recently found that jasmonic acid (JA) slows spiking down (Sun et al., 2006). As for ethylene, JA is involved in the determination of sensitivity to NF, the maintenance of spiking and the frequency of spiking (Sun et al., 2006). JA has an opposite effect to ethylene, it slows spiking significantly. Ethylene enhances JA's effect on spiking frequency, since lower concentrations of JA are necessary to inhibit spiking in *skl* compared to wild type plants (Sun et al., 2006). Interplay between these two pathways may very well be the major determining factor for spiking frequency. It is

also likely that slowing down spiking inhibits gene expression in *M. truncatula*. Using the NF induced ENOD11 promoter fused to GUS as a marker for NF signaling, Sun and coworkers were able to show that the number of cells responding to NF gradually decreased with increasing JA concentration. A shift in the population of cells with suitable spiking frequencies might account for such changes, it would also explain why plants have gradually less nodules with rising concentrations of JA (Sun et al., 2006).

Although the downstream effects of Ca^{2+}-fluxes during NF signaling remain elusive for now, it is reasonable to assume that both Ca^{2+} flux and spiking have a function during nodulation. It is quite clear that the sources of Ca^{2+} ions are different, since influx of ions from outside the cells are responsible for the initial flux and intracellular stores, presumably the ER and nuclear envelope are involved in Ca^{2+}-spiking (Felle et al., 1998; Oldroyd and Downie, 2006). In animal systems, it is widely recognized that calcium oscillations and transients can induce changes in gene expression, with differences in amplitude, frequency, duration and localization as the major information sources for specificity (Dolmetsch et al., 1997; Fields et al., 2005). By analogy, it is likely that Ca^{2+} signaling in legume root hairs serves a similar purpose and the recent identification of several transcription factors known to act directly downstream of spiking reinforces this hypothesis (Oldroyd and Downie, 2004, 2006), as will be discussed in more detail in a following paragraph.

Evidence for other signal transduction pathways involved in NF signalling

So far, great strides have been made in identifying putative NF receptor proteins and effector proteins presumed to play a role in gene expression during the early stages of nodulation. However, the mechanistic links between these two remain elusive and mutants for this part of the pathway are lacking, possibly due to redundancy or lethality. Nevertheless, pharmacological approaches using known inhibitors and antagonists of signal transduction pathways have shed some light on the mechanisms that relay the initial NF signal to downstream processes such as Ca^{2+} signaling and gene expression.

The first report on a possible role for heterotrimeric G proteins in NF signaling dates back nearly a decade (Pingret et al., 1998), when it was shown that the heterotrimeric G protein activator mastoparan and its more active analog mas7, but not the inactive mas17 induced ENOD12 expression in alfalfa and ENOD11 expression in *M. truncatula* (Charron et al., 2004). Similarly the heterotrimeric G protein antagonist pertussis toxin abolished NF induced ENOD12 expression (Pingret et al., 1998). Subsequently it was shown that mas7 but not mas17 is able to induce root hair deformation in *Vicia sativa* (den Hartog et al., 2001).

Heterotrimeric G proteins are signal transduction elements in animal systems were they sense light, odorants, sweet and bitter molecules, and numerous hormones and

neurotransmitters (Assmann, 2002). Mammalian effector proteins include adenylate cyclase, cyclic GMP phosphodiesterase, phosphoinositide 3-kinase, the phosphoinositide (PI)-phospholipase C, phospholipase D, the TUBBY transcription factor, K^+ and Ca^{2+} channels (Assmann, 2002). Heterotrimeric G proteins have been implicated in processes such as sphingolipid elicitor signal transduction, hyperpolarization sensitive calcium channel activation and fungal pathogen disease resistance in plants and the list grows rapidly (Aharon et al., 1998; Suharsono et al., 2002; Trusov et al., 2006). Moreover, agonists and inhibitors of animal heterotrimeric G proteins also seem to be able to modulate pathways in plants, pointing towards a high degree of structural similarity between plant and animal proteins, although mastoparan was also able to activate a MAP kinase phosphorylation cascade independently of heterotrimeric G proteins, suggesting additional targets in plants (Miles et al., 2004). In any case, a target for mastoparan must exist in plants and it will be interesting to see whether or not this is indeed a heterotrimer G protein complex.

Given the possible role for G proteins in NF signal transduction, several studies focused on possible effector molecules that would transduce this signal from the plasma membrane to other cellular compartments. Pingret and coworkers (Pingret et al., 1998) showed the possible role of the phosphoinositide pathway using inhibitors of phospholipase C, which converts phosphatidylinositol 4,5-bisphosphate (PIP_2) into inositol 1,4,5-trisphosphate (IP_3) and diacylglycerol (DAG). DAG is rapidly phosphorylated by DAG kinase into phosphatidic acid (PA) and can be removed by PA kinase, which converts it to diacylglycerol pyrophosphate (DGPP) as a regulatory mechanism. Another, more direct source of PA is phospholipase D mediated degradation of structural lipids (Munnik et al., 1998; Munnik, 2001; Meijer and Munnik, 2003). Based on ENOD11 expression, it was shown that inhibiting PLC activity abrogated NF signaling in alfalfa and also NF induced calcium spiking in *M. truncatula* (Pingret et al., 1998; Engstrom et al., 2002). Both mastoparan and NF induce PLC and PLD activity in *V. sativa* as measured through PA accumulation (den Hartog et al., 2001). In order to discriminate between a general elicitor like activation of PA production and NF specific PA production, alfalfa cell cultures were treated with either NF or chitotetraose and xylanase (den Hartog et al., 2003). Whereas elicitors triggered only PLC derived PA production, NF stimulated both PLC and PLD derived PA accumulation, suggesting specific responses to different stimuli (den Hartog et al., 2003). Possible roles for phosphoinositide signaling upon NF recognition are still unclear, but in animals it is known that these molecules can induce calcium release from internal stores, so a role in the induction and regulation of Ca^{2+}-spiking seems plausible.

Epidermal NF perception and signalling

Hunting down the NF receptors

It had long been assumed that NF were perceived by the plant by at least one and maybe more receptor complexes. A landmark paper in this respect proposed the presence of two distinct types of NF receptors, each with specific roles in the process. This two receptor model has been the paradigm for NF perception ever since (Ardourel et al., 1994). Using mutant *S. meliloti* strains with altered NF structures, Ardourel and coworkers elegantly showed that several core processes of nodulation can be uncoupled using different mutant strains, suggesting distinct signaling cascades leading up to these processes. They used three mutant strains, a *nodFE*, a *nodL* and a *nodF/nodL* double mutant which have a different acyl chain, lack an O-acetyl moiety at the non-reducing end or both, respectively (Ardourel et al., 1994). Both the *nodFE* and *nodL* strains displayed a delay in nodulation, they induced less IT initiation events, but once initiated, infection proceeded as wild type and nodules were formed. The double mutant however, had a more severe phenotype. Double mutants induced more deformation of root hair cells and even other epidermal cells and cortical cells were activated, as assayed by amyloplast accumulation, but no ITs were initiated (Ardourel et al., 1994). This shows that tip growth and deformation can be uncoupled from curling, IT initiation from IT progression and infection from cortical cell activation (Ardourel et al., 1994). To explain this, a model was proposed in which two receptors perceive NF at different stringencies and for different purposes. A non-stringent 'signaling receptor' is still able to recognize NF with slight modifications and acts to prime the plant for nodulation. The signaling receptor would be involved in root hair deformation, cortical cell activation and the like. The second type of receptor, the 'entry receptor' would be more stringent and would be involved in infection site establishment, subsequent curling and IT initation (Ardourel et al., 1994). Ecologically, this makes sense since the rhizosphere is teeming with microorganisms and the plant needs to allow only the proper rhizobia in. A non-stringent receptor would prime the plant at the first sign of compatible rhizobia and the stringent receptor would be more selective as to let only the right bacterial strain enter the root hair. This two step cell sorting programme would allow for a diligent but robust screening for compatible microsymbionts (Ardourel et al., 1994).

Nod factor binding sites

Identification of candidate NF receptors can be done via several approaches, one of which is the search for specific binding sites in protein extracts from roots or cell cultures. In this way, several binding sites were identified and characterized. The first to be discovered was a binding site in *M. truncatula* roots, called NFBS1 (Nod factor binding site 1, (Bono et al., 1995)). NFBS1 was found to have a K_d of 86 nM (Bono et al., 1995). No NF substitutions were found to be indispensable for binding (deacetylation, desulphation or saturation of the fatty acid), but chitotetraose was inefficient as a binding competitor. This means that

although NFBS1 is a NF binding protein, it is not likely to be a very specific receptor and might serve another purpose. A similar NF binding site was also found in tomato, albeit at lower concentrations (Bono et al., 1995). A subsequent study using *Medicago varia* cell suspension cultures and ^{35}S labeled NF found a binding site similar to NFBS1 (K_d = 70 nM) and an additional high affinity binding site designated NFBS2 (K_d = 1.9 nM, (Niebel et al., 1997)). Tests for ligand specificity revealed that sulphation was not recognized by NFBS2, but that modifications at the non reducing sugar (i.e, acetylation, fatty acid length and hydroxylation) influenced binding capacity (Gressent et al., 1999). Recently a third NF binding site was identified in *Medicago roots,* NFBS3 is a high affinity binding site with a K_d = 0.45 nM and no selectivity towards the sulphate group, the o-acetyl group nor the number of double bonds in the acyl chain at the non-reducing end was found(Hogg et al., 2006). The identity of all these binding sites remains unclear for now and although they show a certain level of specificity towards NF structure, they are usually not selective for major NF substitutions, for instance, none was selective for the sulphate group that is a prerequisite for nearly all biological activity. It will be interesting to see whether or not these binding sites represent *bona fide* NF receptors.

Lectins and apyrases

On the other hand, certain lectins were found to selectively bind NF. Lectins are carbohydrate binding proteins that are very abundant in seeds, but are also present in root tissue. Heterologous expression in transgenic roots of a pea lectin PSL gene into *Trifolium repens* enabled nodulation by *R. leguminosarum* bv. *viciae*, which doesn't normally nodulate *Trifolium* (Diaz et al., 1995). Another lectin, DbLNP was found in the legume *Dolichos biflorus* to specifically bind NF (Etzler et al., 1999). The protein is an apyrase, showing phosphohydrolase activity that was significantly enhanced upon NF binding (Etzler et al., 1999). Antibodies raised against the DbLNP protein abolished NF induced root hair curling (Etzler et al., 1999). Since the entire protein is predicted to be extracellular, γ phosphate released from ATP or β phosphate from ADP must end up in the extracellular space. Extracellular ATP has been implicated in processes such as membrane depolarization, gravitropism and calcium transients in plants (discussed in (McAlvin and Stacey, 2005)). Similarly, heterologous expression of the soybean apyrase GS52 in *L. japonicus* was able to enhance nodulation (McAlvin and Stacey, 2005). Conversely, introduction of the soybean lectin *Le1* into *Lotus japonicus* led to the induction of nodule like structures induced by *Bradyrhizobium japonicum,* which is not a suitable symbiotic partner for *Lotus* spp. (van Rhijn et al., 1998). Infection threads were formed but aborted in the root hairs. Experiments using bacterial mutants however, showed that attachment of *Bradyrhizobium* was dependent on the *exoB* gene, suggesting exopolysaccharides as ligands rather than NF, moreover NF could not be shown to bind to the lectin *in vitro* (van Rhijn et al., 1998). It was also shown that bacterial attachment was enhanced in plants expression the lectin protein and attachment was lost in control lines

expressing a mutated version of the protein. Although at present much more promising and straightforward NF receptor candidates have been identified (see below), it is still worthwhile to investigate possible roles for these proteins since they might be involved in finetuning of nodulation. Enhanced attachment of bacteria through polysaccharide-lectin interactions might also suffice to allow local NF concentrations to increase above a certain threshold, thus facilitating nodulation. Legumes might have adapted several different lectins to do this, some of which bind EPS rather than NF, some of which have additional apyrase activity whereas others don't. Whichever is the case, these might all just be variations on a common theme of enhancing and tightening the physical association of the symbiotic partners, thus allowing infection.

LysM domain containing receptor-like kinases

To date, several types of LysM domain containing RLKs have been found to be involved in nodulation. In what follows, a comprehensive overview will be laid out of what is known so far of the role of LysM-RLKs in Nod factor perception.

Since NF perception is thought to mediate the earliest plant responses, mutants affected in the very early stages of nodulation have been studied extensively. Investigation of early nodulation mutants in pea resulted in the identification of the *sym2*^{A} allele in the pea variety Afghanistan (Geurts et al., 1997). Plants harbouring the *sym2*^{A} allele can only be nodulated by *R. leguminosarum* bv. *viciae* strains that have a *nodX* mediated acetylation at the reducing end of their NF. Non compatible interactions led to ENOD12 expression, primordium initiation and and root hair curling but hardly ever to IT initiation. When ITs were formed, they always arrested within the root hair cell. A temperature sensitive allele showed that the sym2^{A} gene product was only necessary during the first 2 or 3 days of the interaction (Geurts et al., 1997). Interestingly, the defects in invasion could be overcome by strains containing the *nodO* gene. The NodO protein is secreted and can integrate into membranes, where it is thought to function as a K^+ and Na^+ selective ion channel that is negatively regulated by calcium (Sutton et al., 1994). This is interesting since K^+ and Na^+ are thought to be involved in the membrane repolarization of root hairs cells after NF perception (Felle et al., 1998), implicating this process in signaling for entry of rhizobia. Given the facts that *sym2*^{A} still can form primordia, root hair curls and can still induce gene expression, but is impaired in the bacterial entry step, this made the gene a perfect candidate for the stringent entry receptor. Mapping this allele in pea, which has a very complex genome structure proved so cumbersome, that synteny based mapping in *M. truncatula* was preferred. This led to the identification of a genomic region containing 7 different LysM domain containing receptor-like kinases (called LYK1 through 7) (Limpens et al., 2003). LysM domains are known in prokaryotes and some eukaryotes to be involved in binding peptidoglycan and chitin (Bateman and Bycroft, 2000), making them likely candidates for NF binding proteins. Of the 7 LYK genes, only *LYK3* was found to be exclusively expressed in roots and nodules,

but because of high levels of similarity also *LYK4* was analysed. Both genes have a similar structure, an extracellular domain containing 2 LysM domains is separated from the intracellular serine/threonine kinase domains by a single-pass transmembrane domain. Surprisingly, for both knock down lines, inoculation with wild type *S. meliloti* showed no phenotype and normal nodules were visible. However, when inoculated with a *nodFE* mutant strain with a different acyl chain, *LYK3* knock down resulted in an almost complete block in IT initiation and the few ITs that were initiated aborted in the root hairs (Limpens et al., 2003). Similarly, *LYK4* knock down resulted in abortive ITs when inoculated with the *nodFE* mutant but not with wild type rhizobia (Limpens et al., 2003). Since the pea orthologue sym2 showed specificity to a moiety at the reducing end of the NF, these results are somewhat confounding, but nevertheless they show that LYK3/4 and their putative pea orthologue have specific NF structural requirements for entry and IT initiation. This suggests that the LYK group of LysM-RLKs might be involved in NF perception as entry receptors. Extra credibility to hypothesis comes from the fact that the *hcl* mutant in *M. truncatula* turns out to be mutated in the *LYK3* gene (Ton Bisseling, personal communication). The *hcl* mutant still displays cortical cell activation, root hair deformation and *ENOD11* and *rip1* gene expression, but no microcolonies are being produced and no root hair curling is obvious (Catoira et al., 2001). The main problem in these mutants seems to be root hair curling leading to infection thread formation (Catoira et al., 2001). Analysis of the microtubular cytoskeleton showed that *hcl* was impaired in its ability to induce the asymmetric array of microtubules in root hair curls and also failed to form preinfection threads (Catoira et al., 2001). Interestingly, *hcl* mutants still show NF induced Ca^{2+} spiking (Wais et al., 2000), suggesting that Ca^{2+} spiking might not be a prerequisite for the stringent response. From these data, it seems reasonable to assume that LYK3/HCL is involved in the pathway around the time of the stringent response, i.e. the organization of the infection center and initiation of infection threads, combined with the fact that these genes are LysM RLKs, a strong case can be made for the fact that in *M. truncatula* and pea, these genes are good candidates for the role of ‘entry receptor’.

The picture becomes more complicated given the fact that an *L, japonicus* mutant called *nfr1* impaired in virtually all responses to NF was mapped to a gene with high homology to LYK3/HCL (Radutoiu et al., 2003). Only an attenuated alkalinization was detected in the *nfr1-1* mutant, whereas acidification was seen in the *nfr1-2* line (Radutoiu et al., 2003), indicating that only the chitin sensing pathways is still active in these plants. This is in stark contrast with data for the candidate orthologues of this gene in other plants tested so far, perhaps indicating lineage specific differences in NF perception mechanisms.

Another type of mutants is the NFR5 type. In *L. japonicus,* a mutant similar to *nfr1* was found, called *nfr5,* that showed absolutely no responses to NF and was mapped to be another LysM-RLK (Madsen et al., 2003; Radutoiu et al., 2003). Sequencing analysis

showed orthology with *sym10* from pea, which has a comparable phenotype (Madsen et al., 2003). NFR5 belongs to a different subfamily however, typified by a 1 exon gene, 3 LysM domains and an atypical kinase domain lacking the so called activation loop an an ATP binding site, suggesting that this kinase might not be functional (Madsen et al., 2003; Riely et al., 2006). Similarly, in *M. truncatula,* a mutant with no detectable responses to NF was also found, called *nfp* for Nod factor perception (Amor et al., 2003).

Recently, computer modeling of the LysM domains of the (still unpublished) NFP protein suggested that indeed LysM domains are probably capable of binding NF in a specific manner (Mulder et al., 2006). Several observations were made that may have important implications for the understanding of NF perception. NFP appears to be highly glycosilated, and all 3 LysM domains appear to be able to bind a NF molecule. In two of the three LysM domains, the sulphate group seems to be able to interact with a lysine residue in the domain, the O-acetyl group on the non reducing sugar sits in a hydrophobic pocket in all 3 domains. Finally the acyl chain can wrap around the LysM domains while interacting with several amino acids at the side of the domain. In this model, at least for *M. truncatula* NFP and the main NF of *S. meliloti,* all NF substitutions have specific binding sites (Mulder et al., 2006). This model can be tested through site directed mutagenesis of the predicted interacting residues and this will no doubt shed new light on several questions concerning NF specificity. Interestingly, only one of the predicted glycosilations would interfere with NF binding in the 3rd LysM domain, although probably not enough to completely block binding (Mulder et al., 2006). An important question that will need looking into is the fact that probably 3 NF molecules can bind the same protein. Perhaps a signal amplification can be obtained in this way, or not all 3 domains recognize the same NF with the same specificity, future experiments are likely to address this. A ‘common sym pathway’: convergence of NF signaling and mycorrhizal signaling

Downstream from NF receptors, a wide variety of responses are induced and need to be integrated in order to lead to proper nodulation and rhizobial infection. Great strides have been made in the past decade in identifying genes involved in these early steps of NF signaling and our understanding of what happens in these crucial steps grows rapidly. Interestingly, several plant mutants that are impaired in the initial responses to NF also turned out to be unable to engage in AM symbiosis, as discussed above (Kistner and Parniske, 2002). To date, 5 or 7 genes, depending on the species analysed, are thought to be in this common pathway, several of which have now been cloned and analysed in more detail (Oldroyd and Downie, 2004; Kanamori et al., 2006). This common sym pathway seems to converge upstream of calcium influx, at least 3 of the common genes are upstream of Ca^{2+}-spiking since *LjNup133*, *Mtdmi1* and *Mtdmi2* are impaired in Ca^{2+}-spiking (Wais et al., 2000).

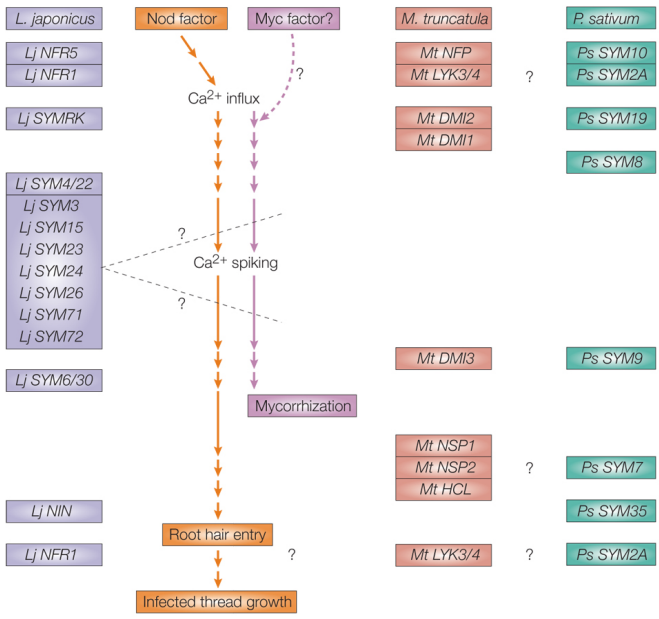

Fig. 5 Overview of known mutants in early nodulation genes in legumes
Mutants involved in early signaling events are represented by species (*Lotus japonicus* (*Lj*; purple), *Medicago truncatula* (*Mt*; red) and *Pisum sativum* (*Ps*; green)) and ordered chronologically. Orthology between genes, either known or inferred based on phenotype (marked '?') is indicated via horizontal alignment. *LjNFR5*, *MtNFP* and *Ps SYM10* encode LysM domain RLKs involved in NF perception. Similarly, *LjNFR1*, *MtLYK3*, *MtLYK4* and *PsSYM2A* also encode LysM-RLKs proposed to be the 'entry receptors' although phenotypes differ significantly between species (see text). Not al common sym genes can be ordered yet due to lack of markers or lack of investigation. Reprinted from: Oldroyd, G.E. and Downie, J.A. (2004) Nat Rev Mol Cell Biol 5, 566-76.

Downstream of Ca^{2+}-spiking lies *Mtdmi3*, with a phenotype similar to the other *dmi* mutants (doesn't make infection), but still capable of Ca^{2+}-spiking (Wais et al., 2000). Similar mutants have been identified in other legumes such as *L. japonicus* and *P. sativum* (Fig. 5), however orthology has not been established for all these mutants and nomenclature is somewhat confusing since *Lotus* and pea mutants both get SYM number (albeit different ones), often making comparison between species confusing. For clarity, the *Medicago* nomenclature will be used as much as possible.

Generally, mutations in common sym genes have an extreme phenotype since they hardly respond to NF (Catoira et al., 2000). Initial screens identified these mutants based on the fact that plant responses were blocked at the stage of root hair deformation. Except for some weak alleles, these mutants only show some ion fluxes and some root hair swelling and branching, but are blocked for subsequent responses. It was not until most genes were assayed for Ca^{2+} spiking that an attempt could be made at chronological ordering of these mutants (Wais et al., 2000; Walker et al., 2000).

The first common sym gene to be cloned was dmi2/SymRK in *M.truncatula* and *L. japonicus* respectively, a leucine rich repeat (LRR) containing receptor-like kinase with 3 LRR domains and a new domain of unknown function called NSL (NORK symbiosis like) domain (Endre et al., 2002; Stracke et al., 2002). Mutants showed a wider zone of root hair deformation, indicating that DMI2/SYMRK is some kind of negative regulator of the initial stages of NF signaling (Stracke et al., 2002). Although first believed to be necessary for root hair deformation, Ca^{2+}-spiking and ENOD expression, recent finding have refined this model. The *dmi2* mutant has an additional, non-symbiotic root hair phenotype, rendering it hypersensitive to mechanical stimuli (Esseling et al., 2004). The mutants is unable to reinitiate cytoplasmic streaming arrest after touch responses, which is physiologically

analogous to turning the responsive root hair into a non-growing, non-responsive root hair (Esseling et al., 2004). Indeed, when care is taken not to provoke the response, root hair deformation can be detected and the deformation will stop when the root hair tip touches its own shank, which invokes the touch response (Esseling et al., 2004). This is accompanied by ENOD11 expression, showing that DMI2 is not essential for these responses, and suggests a new bifurcation in the NF signaling pathway, with calcium influx and root hair curling in a different branch of the pathway than Ca^{2+}-spiking and ENOD11 expression (Esseling et al., 2004). The overlap between touch sensation of root hairs and endosymbiosis signaling is both remarkable and enigmatic (Geurts et al., 2005). No conclusive explanation has been found yet, but several speculative answers can be proposed. DMI2 activity initially stems from the AM symbiosis and was recruited much later by nodulation, mechanical pressure is assumed to be present in both symbiotic interactions however, appresioral pressure of AM fungi and dividing bacteria in the enclosed microcolony are both thought to be sources of mechanical stress (Capoen et al., 2005).

A novel type of plant protein was also found to be an element of the common pathway. Mutants affected in DMI1 no longer show spiking and only swelling of the root hair tips (Catoira et al., 2000). DMI1 is a protein with low overall homology to a ligand gated cation channel from archaea (Ané et al., 2004). Two similar proteins were identified in *L. japonicus*, CASTOR and POLLUX, the latter being the probable orthologue of DMI1 (Imaizumi-Anraku et al., 2005). The homology of the proteins to cation channels invites to speculate about a possible role in NF induced ion fluxes, but subsequent localization of the *Lotus* proteins complicates matters since both proteins localize to the plastids (Imaizumi-Anraku et al., 2005). This type of localization cannot be reconciled with a role in ion fluxes of the plasma membrane and conjecture about a possible function of plastid proteins in early NF signaling is ongoing.

A newly mapped common sym gene encodes a putative nucleoporin (Kanamori et al., 2006). *Lotus* mutant *sym3* (renamed Nup133) is the fourth common sym gene mapped so far and is thought to operate upstream of calcium spiking. Mutants defective in SYM3 show alkalinization of the root hair cytosol, root hair swelling and some branching, similar to the *dmi* phenotypes (Kanamori et al., 2006). In a certain number of cases, however, nodules could be observed at extremely low frequencies, and this at a lower temperature, showing a temperature sensitive phenotype (Kanamori et al., 2006). Ca^{2+}-spiking was never seen, although the presence of an occasional nodule suggests that a minority of root hairs might still be able to spike, although no evidence for this could be found. Interestingly, similar nucleoporins have been identified in *Drosophila* and *Arabidopsis* as part of a pathogen defense pathway, in *Drosophila*, it is required to shuttle two transcription factors to the nucleus (Kanamori et al., 2006). Since the nucleoporin is required for Ca^{2+} spiking, it might shuttle a protein or secondary messenger into the nucleus that triggers spiking. The observation that most

spiking actually occurs in the nucleus and not in the cytosol seems to draw more and more attention to the nucleus as the major compartment involved in NF induced calcium signaling (Oldroyd and Downie, 2006). The speed at which NF can induce Ca^{2+}-spiking (less than 10 minutes) however, does not allow for much transcription and protein synthesis to occur before spiking commences, suggesting that the pathway might be different from what has been observed in *Drosophila*, making shuttling of a secondary messenger more plausible. Whatever the explanation, elucidation of the role of this nucleoporin holds great promise to accelerate our understanding of this enigmatic pathway.

The most downstream common gene to be cloned thus far is dmi3 (Catoira et al., 2000). This mutant differed from the other *dmi* mutants in the fact that *dmi3* plants still show Ca^{2+}-spiking when NF are perceived (Wais et al., 2000). This puts the DMI3 protein directly downstream of Ca^{2+} spiking and indeed, map based cloning showed that dmi3 encodes a calcium and calmodulin dependent protein kinase (CCaMK), making it an appealing candidate to be the Ca^{2+} spiking decoding protein (Lévy et al., 2004; Mitra et al., 2004b). The protein contains a visinin-like domain with 3 EF hands, a calmodulin binding domain within an autoinhibitory loop and a kinase domain, making it structurally similar to animal CAMKII (Lévy et al., 2004; Mitra et al., 2004b). CAMKII is involved in decoding calcium oscillations in both neuronal firing and cardiac contractions, where it autophosphorylates upon Ca^{2+} and calmodulin binding (Eshete and Fields, 2001). Once activated, Ca^{2+}/CaM binding is no longer required and the kinase activity becomes Ca^{2+}/CaM independent, which allows for activity long after the initial Ca^{2+} signal has vanished (Eshete and Fields, 2001).

In dorsal root ganglia neurons, CAMKII activity is correlated with Ca^{2+}-spike duration and frequency, extracellular calcium concentrations and duration of stimulation (Eshete and Fields, 2001). Calcium oscillations in these conditions however, were much faster than what has been detected in legume root hairs, suggesting different kinetics for the spiking decoder in legume root hairs. CAMKII has a basal level of autophosphorylation that is correlated with ambient calcium concentrations and which influences sensitivity to lower calcium transient frequencies (Eshete and Fields, 2001). This suggests that decoding sensitivity of this type of protein can partially be modulated by several factors such as basal phosphorylation status, CaM binding affinity of different isoforms, cytosolic and extracellular calcium concentrations, spiking frequency, spiking amplitude, spiking duration and spiking localization and possibly more factors (De Koninck and Schulman, 1998). Hence, a wide range of signals can be integrated via this protein and would allow for a fairly high discriminatory capability of the protein towards different calcium transients. This would indeed be a prerequisite since DMI3 is involved in at least 2 different biotic interactions, which are known to involve differences in gene expression, this will be discussed in the next paragraph.

Early transcription factors as integrators of NF signaling

NF signal transduction inevitably leads to altered gene expression, and several transcriptional waves are most likely involved (Mitra and Long, 2004). So far, 3 transcription factors have been identified that, based on their early nodulation phenotype, are likely to be involved in the primary transcriptional regulation of nodule initiation.

A transcription factor called NIN (for nodule inception) was identified via transposon tagging, yielding a mutant that showed exaggerated root hair deformation and lack of IT initiation and cortical cell division (Schauser et al., 1999). Via the phenotypic analogy, pea mutant *sym35* was found to be mutated in the pea orthologue of nin (Borisov et al., 2003). NIN contains a previously uncharachterized, putative DNA binding domain and belongs to a small family with representatives in *Arabidopsis,* rice, *Chlamidomonas* and *Dictyostelium* (Schauser et al., 2005). Expression analysis showed that nin transcripts are upregulated in primordium cells and that in determinate nodules, expression is evenly distributed throughout the differentiating nodule, whereas in indeterminate nodule, expression is confined to the nodule meristem and its progeny in the infection zone, showing no expression in differentiated central tissue (Schauser et al., 1999; Borisov et al., 2003). As of yet, no targets of NIN are known, although it is likely that some very early nodule specific transcripts might be under direct transcriptional control of NIN.

Two other early transcription factors recently cloned are NSP1 and 2 (Kalo et al., 2005; Smit et al., 2005). They belong to the plant specific GRAS family of transcription factors (named after the founding members GAI, RGA and Scarecrow). Mutants in these proteins *nsp* and *nsp2* (for nodulation signaling pathway) still respond to NF by root hair branching, but no longer show ENOD11 and ENOD40 gene expression, suggesting a key role in early NF signaling (Catoira et al., 2000; Oldroyd and Long, 2003). It needs pointing out that these NSP proteins are presumed to function directly downstream of Ca^{2+} spiking and of the common pathway, since neither *nsp* mutant is impaired in AM formation. Functional analysis of the two proteins revealed a strict nuclear localization for NSP1, whereas NSP2 localizes to the nuclear envelope from where it relocalizes to the nucleus upon NF application (Kalo et al., 2005; Smit et al., 2005). It is not yet clear in what way NSP1 and 2 are activated upon NF recognition, but the fact that they are downstream of DMI3 and colocalize with the DMI3 protein makes them possible NF signaling specific targets of DMI3 (Kalo et al., 2005; Smit et al., 2005). Downstream targets of NSP protein activity are not yet known. If NSP1 and 2 are indeed regulated by DMI3, it will have to be determined how they are activated specifically upon rhizobial recognition and not upon AM recognition. As NSP1 and 2 are downstream of the divergence of the common sym pathway, they are interesting for studies concerning pathway specification, since these genes are involved in nodulation but not mycorrhization.

Modeling the integration of signaling and entry receptor mediated pathways

As more and more data become available concerning molecular events following NF perception, the model becomes more detailed. The strict linear pathway originating from NF perception over the common sym genes towards root hair curling and nodulin gene expression has over the years made room for a more complex, branching network. Both mycorrhization and nodulation have their own specific signaling pathways that depend on their respective signaling molecules, the so called myc factor and the Nod factor, but signaling also occurs through a shared pathway involving the common sym genes and Ca^{2+} spiking (Fig. 6) (Geurts et al., 2005). Downstream of the common pathway, possibly depending on Ca^{2+} spiking characteristics are the effector molecules, for nodulation presumably being the GRAS type transcription factors NSP1 and 2 (Geurts et al., 2005). Although the absence of mycorrhization in common sym mutants implies a role for Ca^{2+} spiking in this process, so far no reports have been made about this. No doubt this model will become even more elaborate in the near future. Of extreme importance here will be to unravel how signaling receptor and entry receptor pathways interplay. By transcript profiling experiments in mutant backgrounds, it was shown that of a number of very early nodulation induced transcripts that were no longer induced in a *dmi* mutant background, a subset were still being induced in *hcl* background (Mitra et al., 2004a). This subset might well be part of the first wave of transcripts resulting from the activation of the signaling receptor.

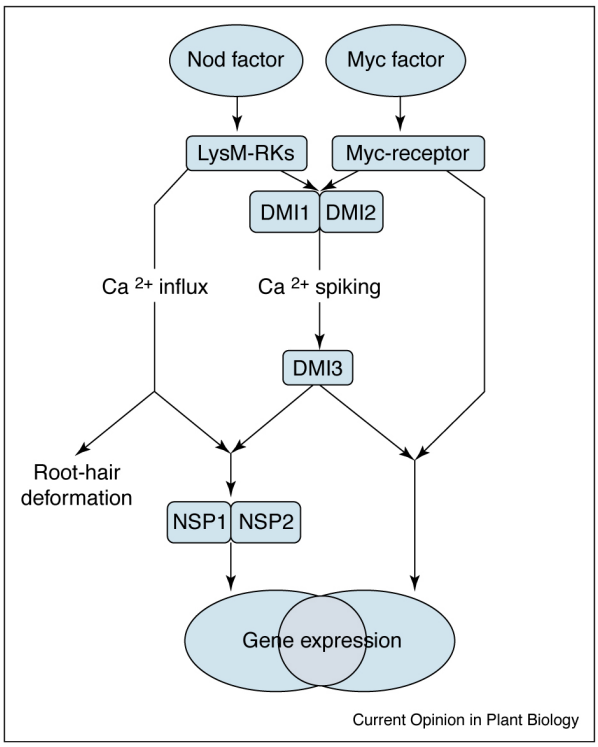

Fig. 6 Nod factor and mycorrhizal signaling via common and specific pathways
Nod factors and the elusive myc factors are probably perceived by specific receptor complexes and downstream signals are transduced via several pathways. NF signaling occurs via a DMI dependent and DMI independent pathway. The DMI dependent, common sym pathway is typified by nuclear and perinuclear Ca^{2+}spiking, probably leading to specific gene expression events. The DMI independent pathway displays a NF dependent Ca^{2+} influx into the root hair. So far, no mutants have been identified in the DMI independent pathway. These different pathways may be responsible for different subsets of gene expression profiles, the combination of which results in nodule formation. Reprinted from Geurts, R., Fedorova, E. and Bisseling, T. (2005) Curr Opin Plant Biol 8, 346-52.

Geurts and Bisseling (2005) propose a model were indeed this first subset of transcripts from the signaling receptor affect the entry receptor pathway, directly or indirectly (Geurts et al., 2005). Functional analysis of signaling

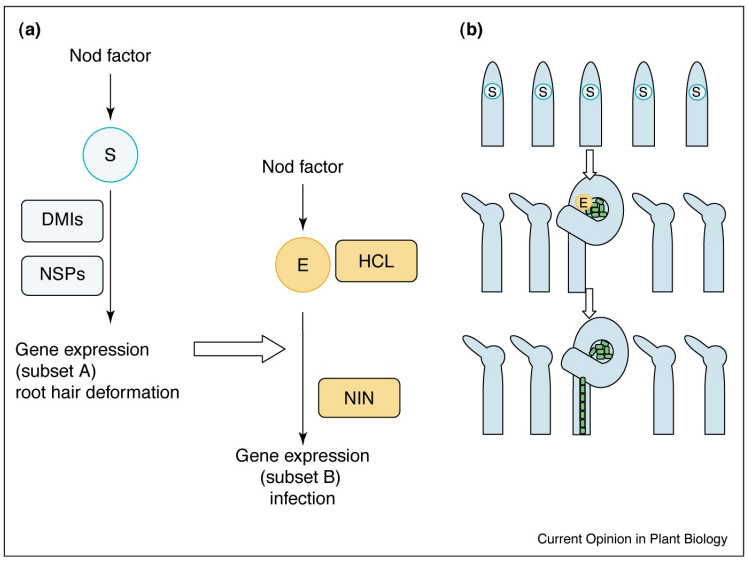

Fig. 7 Model of interaction between signaling and entry receptor complexes

NF are first perceived by the non-stringent signaling receptor complex which presumably signals via a DMI and NSP- mediated pathway. This pathway is responsible for root hair deformation and an first wave of gene expression (subset A). This influences a second pathway, mediated by the stringent entry receptor complex (thought to be HCL/LYK3) and signaling via NIN. This second pathway is responsible for root hair curling, infection thread initiation and gene expression of more nodulins (subset B). Reprinted and modified from Geurts, R., Fedorova, E. and Bisseling, T. (2005) Curr Opin Plant Biol 8, 346-52.

cascades and identification of secondary signaling molecules will be required in order to achieve this fully (Fig. 7).

NF perception and signalling in the cortex

Most of the work discussed thus far is based on biochemical assays at the level of root hair cells and mutants blocked in the early, epidermal responses to NF. Although enlightening and vital to our understanding of NF perception, one should not forget the multitude of processes and cell types that are not of epidermal origin involved in nodulation. Recent reports have started to unveil functions for these genes in deeper cell layers, and this via several approaches. A role for NF perception has long ago been extrapolated from observations that bacterial *nod* genes were highly expressed in the late stages of nodule development, in the infection zone (Sharma and Signer, 1990). This might indicate that perception of NF is still necessary for proper nodule development. Indeed several reports show expression of the LysM RLKs in cells adjacent to the meristem and the whole infection zone. NFR5/SYM10 is expressed in mature pea nodules but not in mature *Lotus* nodules, a discrepancy most easily explained by the fact that the former produces indeterminate nodules and the later determinate nodules (Madsen et al., 2003). Also in *M. truncatula in situ* hybridizations showed the expression of LYK3 and DMI1, 2 and 3 in the infection zone of indeterminate nodules (Limpens et al., 2005).

DMI2/SYMRK is necessary for bacterial release from ITs

Recent work shows that DMI2/SYMRK is not only functional in root hairs, but also at the very late steps of nodule formation, bacterial release into central tissue cells (Capoen et al., 2005; Limpens et al., 2005). Partial knock down of dmi2 transcripts and near total knock down of *SymRK* transcripts in *S. rostrata* showed a novel phenotype in which nodules were still formed, but IT had sack like protrusions and bacteria were not released from ITs, resulting in differentiating but empty nodules (Capoen et al., 2005; Limpens et al., 2005). A further discussion can be found in one of the following chapters of this thesis.

This possible cortical role for DMI2/SYMRK is corroborated by *in situ* hybridizations, transcript analysis and promoter analysis for DMI2/SYMRK, all showing expression of this gene in the infection zone of the nodule, where bacteria are being released from ITs (Bersoult et al., 2005; Capoen et al., 2005; Limpens et al., 2005).

DMI3 gain of function mutation leads to spontaneous nodule formation

No partial knock down experiments are published for dmi3 or dmi1, although their expression is also visible in the infection zone of indeterminate nodules, possibly indicating a at these late stages. However, a previously known phenotype was recently found to correlate with CCAMK gain of function mutations in *L. japonicus* and truncated DMI3 proteins that lack the autoinhibitory domain in *M. truncatula* (Tirichine et al., 2006b; Gleason et al., 2006).

Recently, 3 loci in *L. japonicus* were defined that are responsible for spontaneous nodule formation (Tirichine et al., 2006). Spontaneous nodules were found to be devoid of bacteria, bot otherwise showed most characteristics usually associated with nodules. ENOD2 and nin expression was measured, inhibition by nitrogen and ethylene, central tissue and parenchyma with vascular bundles could be observed, all indicating that spontaneous nodules are genuine nodule structures (Tirichine et al., 2006a). Two loci were found to be recessive while 1 is dominant. One recessive allele (*snf2*) was mapped and identified as a recessive gain of function allele of the DMI3 orthologue in *Lotus* (Tirichine et al., 2006b). Similarly, when the visinin domain and CaM binding/autoinhibitory domain were removed from DMI3, Gleason and coworkers found emerging nodules on *Medicago* transgenic roots (Gleason et al., 2006). These nodules remained empty and the gain of function could not fully complement nodulation. This suggests a dual role for CCAMK in NF signaling and the uncoupling of nodule formation and bacterial infection.

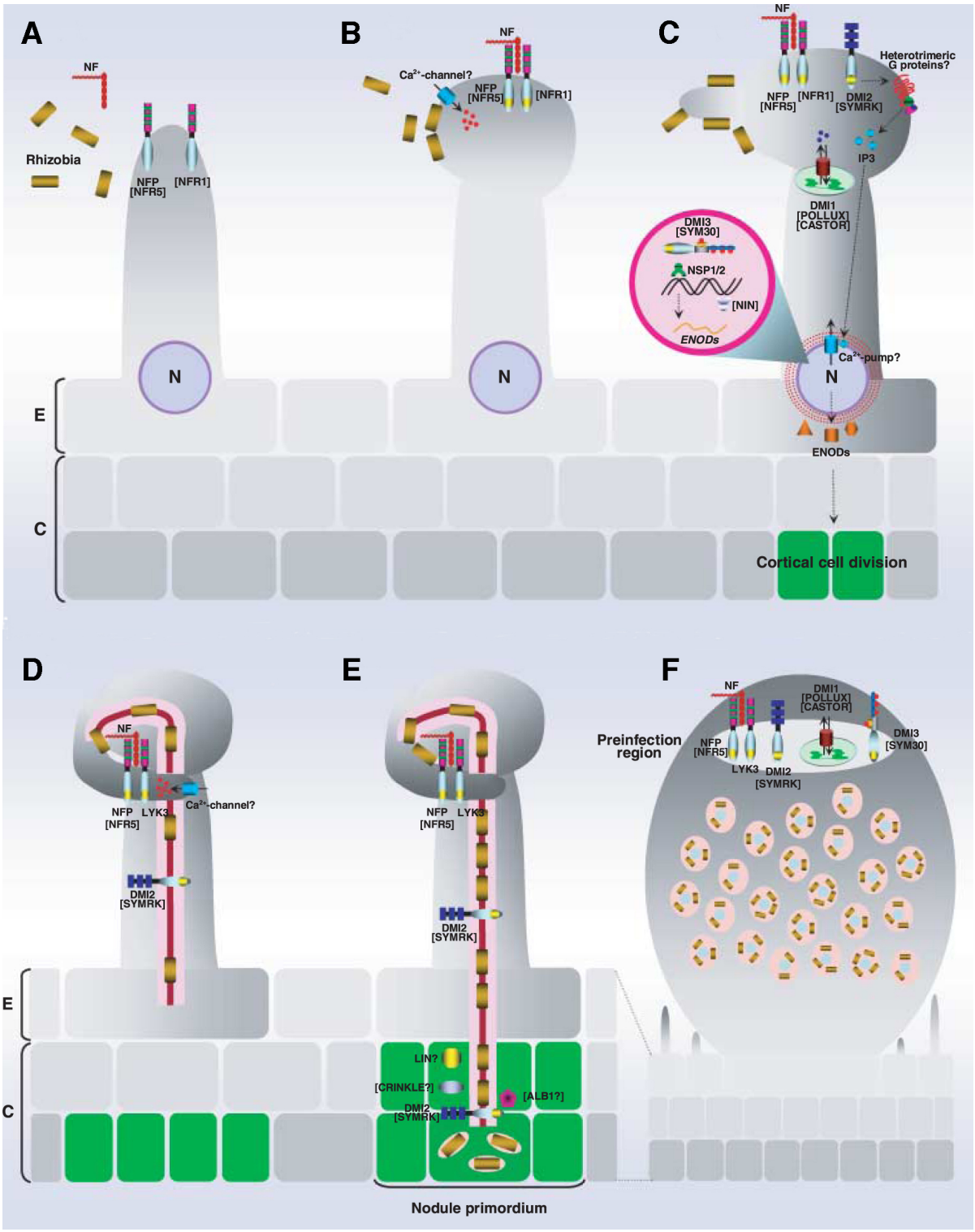

Fig. 8 Overview of Nod factor signaling at various stages of nodulation
A signaling receptor complex consisting of one or more LysM domain RLKs is present in susceptible root hair cells (panel A). Upon NF recognition, an influx of Ca^{2+} ions redirects tip growth and deformation of the root hairs is initiated. Ca^{2+} spiking mediates gene expression in a DMI and NSP dependent manner, possibly also involving heterotrimeric G-proteins (panel C). Root hair deformation leads to a three dimensional curl in which a microcolony is present (panel D). Infection thread initiation is mediated by another NF receptor complex, possibly involving LYK3/HCL. Infection thread integrity and directional growth are controlled partly by DMI2/SYMRK and the infection thread grows towards the incipient nodule primordium (panel E). Bacterial release from the IT is mediated by DMI2/SYMRK and the released bacteria will differentiate into nitrogen fixing bacteroids (panel E). Reprinted from Riely, B.K., Mun, J.H. and Ane, J.M. (2006) Molecular Plant Pathology 7, 197-207.

Unregulated, constitutive kinase activity is sufficient to produce a seemingly mature nodule, whereas the calcium regulation of CCAMK activity somehow seems to alter certain pathways, allowing infection to proceed. This once again shows the pivotal and diverse role of CCAMK in nodule development. It is not clear whether signaling of CCAMK in epidermal cell layers would be sufficient for all these processes to occur, but the previously mentioned expression of DMI3 in the infection zone of the nodule suggests that CCAMK might play a cell autonomous role.

Additional support for these findings come from the complementation of *dmi3* mutant lines with the rice orthologuous CCAMK gene (Godfroy et al., 2006). Strong expression using a 35S promoter resulted in nodule-like structures that contained infection threads but no bacterial release was visible, an even more severe phenotype was observed when complementation was attempted with the endogenous dmi3 promoter sequence, here no ITs could be seen (Godfroy et al., 2006). This suggests that although the rice CCAMK is able to restore nodule formation, it is not able to complement signaling for bacterial invasion. This might be due to the inability of the rice visinin and CaM binding domains to correctly decode calcium signals, 35S driven expression seems to partly compensate for this problem, but bacterial release is still impaired. DMI3 thus is likely to affect 3 different steps of the nodulation process, with different stringencies. The process with lowest stringency requirements is nodule formation, which only requires unregulated, constitutive CCAMK activity. Second, in infection thread initiation and thirdly, the most stringent respons would be bacterial release from infection threads. This is somewhat similar to findings *S. rostrata* and *M. truncatula* were bacterial release required higher expression of dmi2/SymRK than for infection, whereas nodule formation was not affected (Capoen et al., 2005; Limpens et al., 2005).

Concluding remarks

A marked change in our view on NF signaling has occurred over the past few years, mainly thanks to the increasing number of early mutants that has been mapped so far. Although this particular generation of mutants was initially considered specific to the early epidermal stages of nodulation, more and more functional data point towards roles for these genes in the later stages of the nodulation process (Fig. 8). These data firmly place these gene products in the infection zone of indeterminate nodules, no such data are available yet for determinate nodules and it will be interesting to see whether this nodule type has analogous processes during its development.

The groundwork for a better molecular understanding of NF perception and signaling is in place, several key players have been identified and tools for efficient identification of new genes and mechanisms are available. The coming years will no doubt continue to bring new insights into these processes. One of the main challenges for the near future will be to determine to what extent and how existing pathways were recruited and adapted

by nodulation to serve a purpose during root nodule development. A paradigm shift has occurred over the last decade from a view that large numbers of genes were nodulation specific and novel to a line of thought that shows that actually very few genes are indeed exclusively involved in nodulation. Pathways are now known to have been usurped from other tip growth processes, root hair and trichome development, defense responses, meristem formation, touch response, cell division and mycorrhization, and the list keeps expanding. The first generation of mutant screens is coming to an end and new screens (e.g. suppressor screens) are on the way. No doubt functional analysis of the genes identified in this way will allow for significant advances to be made.

Chapter 3

Sesbania rostrata as a model for studying rhizobial invasion

Evolution of alternative infection and nodule types

Root hair curling occurs in all legume subfamilies and phylogenetic and morphological studies corroborate the ancient origins of this invasion (Sprent, 2002). IT formation seems to be an ancient trait, and legumes like *Gleditsia* only contains IT like structures filled with bacteria that are responsive to nitrogenase antibodies (Parniske, 2000), suggesting that infection threads might have arisen early on in evolution of symbiotic nitrogen fixation and possibly even independently from nodule formation (Parniske, 2000). The vastness of the legume family comes with an equally rich range of variations on the themes discussed in part I. Root hair curling invasion is considered as the default pathway in legume nodulation (Sprent, 2002). It would be unwise, however, to neglect other invasion pathways and nodule types since they offer alternative vantage points that will no doubt be useful in interpreting data concerning nodule development as a whole. A large number of legumes do not show the root hair curling invasion. Other, less complex invasion pathways are dispersed throughout the legume family and are now thought to have arisen as specific adaptations to certain environmental conditions that hampered root hair invasion (Sprent, 2002; Goormachtig et al., 2004).

Several different entry modes have been characterized in the past (Fig. 1, reviewed in Guinel and Geil, 2002), and the importance of root hair invasion and epidermal signaling is different for these different invasion strategies. In *Chamaecytisus* for instance root hair infection occurs, but ITs abort in the root hairs and the actual infection that leads to nodule formation originates from intercellular entry (also known as crack entry) through the epidermal and cortical cell layers (Vega-Hernandez et al., 2001). It is possible that IT initiation in root hairs still plays a signaling role but that infection somehow is unable to proceed. Legumes such as Arachis hypogea (groundnut) nodulate at lateral root bases via a form of crack entry that seems to involve adjacent axillary root hairs at the lateral root base, although these root hairs are not infected (Boogerd and vanRossum, 1997). No intracellular ITs could be observed and intercellular invasion results in a primordium that develops in the outer cortical cell layers (Boogerd and van Rossum, 1997). Topologically similar is the crack entry invasion in S. rostrata that proceeds via cracks at the lateral root base and inter- and intracellular infection threads (see next chapter). Mimosa scabrella is invaded intercellularly between two epidermal cells, the bacteria thus gain access to the cortex and inter- and later intracellular ITs grow towards the nodule primordium (de Faria et al., 1988).

Although plants have a tight genetic control over the infection process, a certain amount of leeway seems to be available in the developmental program. A mutant of L. japonicus, root hairless 1, that is impaired in root hair development shows that this obvious obstacle can be overcome. Two different strategies were employed by root hairless 1 (Ljrhl1) to allow invasion in the absence of epidermal root hair cells. Superficially located

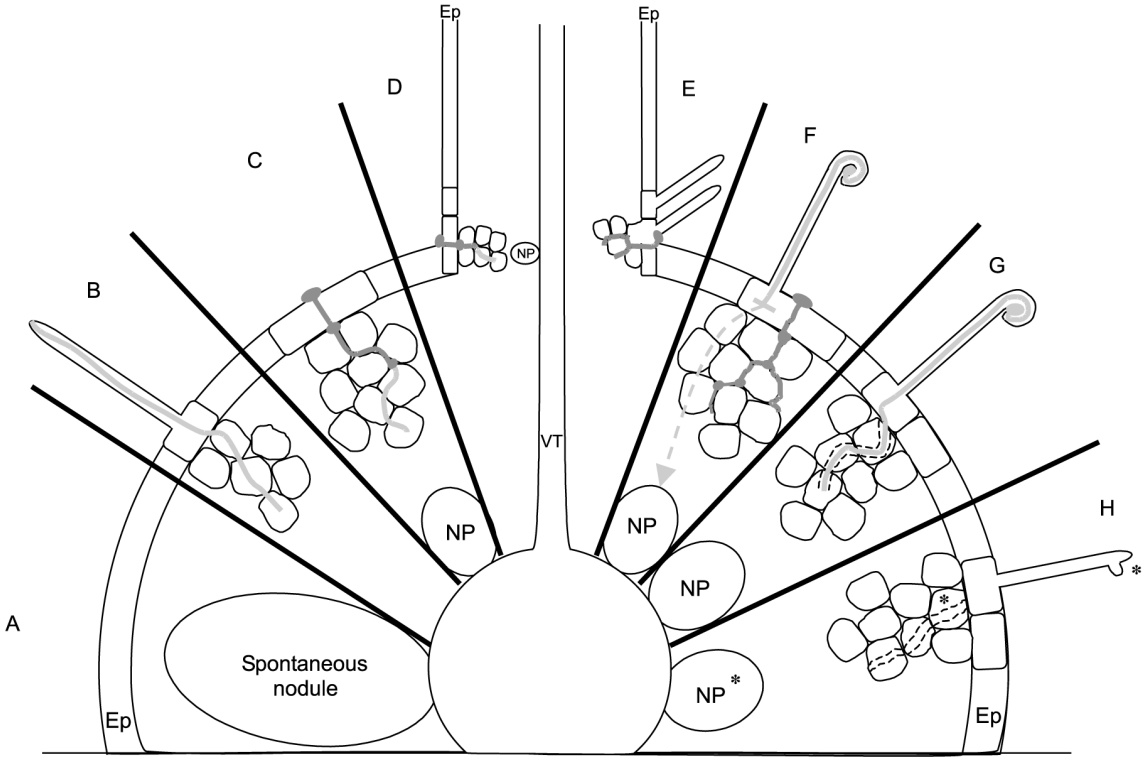

Fig. 1 Infection strategy diversity in legumes.
A. Certain mutants are able to form empty nodules in the absence of rhizobia, showing the strict plant origin of the developmental programme. B. *Gleditsia triancanthos* (Caesalpinioideae) is invaded via root hair cells, but infection does not involve primordium formation and bacteria fix nitrogen within the infection thread. C. *Mimosa scabrella* (Mimosoideae) is infected intercellularly between epidermal cells. Infection switches to intracellular invasion before reaching the incipient nodule primordium. D. *Neptunia natans* (Mimosoideae) and *S. rostrata* (Papilionioideae) are infected via the fissures at sites of protruding lateral root bases. Inter- and intracellular ITs lead the bacteria towards the nodule primordium. E. *Arachis hypogea* (Papilionoideae) is infected through intercellular spaces at the bases of enlarged root hairs. Infection proceeds at lateral root junctions and nodule primordia develop concomitantly. *Chamaecytisus proliferus* (Papilionoideae) is initially infected via curling root hairs, but infection aborts in the root hair and nearby intercellular infection is the actual source of infection of the nodule primordium. (G) In *Pisum sativum*, a Papilionoideae, rhizobia infect via curling root hairs, PIT formation and nodule primordium formation occurs as described in chapter one. H. NF can trigger a multitude of processes in the absence of bacteria, these are PIT formation, root hair deformation, primordium formation, nodulin gene expression. Abbreviations: Ep, epidermis; NP, nodule primordium; VT,

bacteria were found to infect the cortical tissue intercellularly, eventually leading to a fixing nodule (Karas et al., 2005). Also, nodules were visible with infected and curling root hair cells. Upon closer inspection, it turns out that NF induced root hair cell growth is not impaired, and root hairs originating from the outer cortical cell layer emerged and became infected (Karas et al., 2005). These observations are of particular interest in respect to *S. rostrata* since *Sesbania* is very closely related to *L. japonicus*. It seems plausible that intercellular entry can be forced, at least in this lineage, although not efficiently and that *S. rostrata* evolved to expand on this propensity for intercellular invasion.

Sesbania rostrata as model for water-tolerant nodulation

Sesbania rostrata Brem has in the past attracted attention because of a number of peculiarities. *S. rostrata* is a semi-aquatic legume indigenous to the Sahel region of West-Africa, a dry habitat characterized by annual flooding. As an adaptation, *S. rostrata*

has rows of dormant adventitious root primordia along the length of its stem that will emerge and grow upon waterlogging (Goormachtig et al., 1998). These dormant root primordia are also the site of nodule formation upon inoculation with *Azorhizobium caulinodans* (Tsien et al., 1983). No root hairs are present on the stem and bacterial invasion occurs through the fissures caused by the protrusion of the adventitious root primordia (called crack entry or lateral root base nodulation, LRB) (Tsien et al., 1983). This makes the site of early signaling for nodulation much more predictable than in other legumes. Besides this 'stem nodulation', roots also can form nodules via a similar mechanism (Ndoye et al., 1994; Goormachtig et al., 1998; Den Herder et al., 2006). However, crack entry nodulation is not the default pathway and in aerated conditions *S. rostrata* nodulates via root hair invasion (Goormachtig et al., 2004), making *S. rostrata* an ideal model to compare two different infection strategies within one plant species.

The symbiotic interaction between *S. rostrata* and *A. caulinodans*

Lateral root base nodulation on *S. rostrata* occurs upon submergence of the root or inoculation of the stem and the initial cross talk between both symbiotic partners is similar to what has been described for other legumes. Exuded flavonoids, the most predominant being liquiritigenin, induce nod gene expression in *A. caulinodans* via the transcription factor nodD, upon which NF are produced and secreted (Messens et al., 1991). *A. caulinodans* NF are tetra- or pentameric, the acyl chain can be either a mono- or non-saturated C18 or a non-saturated C16 fatty acid, other substitutions at the non-reducing end are a methyl and a carbamoyl group and the reducing end sugar can be decorated with a fucosyl and/or arabinosyl group (Mergaert et al., 1993; Mergaert et al., 1996). The arabinosyl modification at the reducing end has so far only been observed in strains able to nodulate *S. rostrata* (D'Haeze and Holsters, 2002). Bacterial mutants lacking one or more of these decorations show a varying decrease in nodulation efficiency (D'Haeze et al., 2000). Loss of either the fucosyl or arabinosyl group lowers LRB nodulation efficiency slightly, loss of both strongly reduces stem nodulation and, to a lesser extent, root nodulation efficiency (D'Haeze et al., 2000). Additional loss of the carbamoyl group almost completely abolishes nodulation, although sometimes slightly pink nodules were still formed (D'Haeze et al., 2000). The effect of these modifications on root hair curling invasion in *S. rostrata* (see next chapter) is more drastic. When aerated roots are inoculated with ORS571 (1.31U-ΩK), a mutant producing NF that lack the carbamoyl-, fucosyl- and arabinosyl-moieties, a large number of arrested nodule primordia were apparent and root hairs deformed but did not become infected (Goormachtig et al., 2004). This points towards differences in NF stringency between LRB nodulation and RHC invasion, the latter posing more stringent demands on NF structure (Goormachtig et al., 2004). Data in *M. truncatula* suggest stringent and less stringent NF perception complexes involved in entry and signaling, respectively (Ardourel et al., 1994), and it is possible that the stringent entry receptor complex is no

longer needed during crack entry nodulation in *S. rostrata* (Goormachtig et al., 2004).

Upon inoculation, *A. caulinodans* colonizes the fissures that are formed at sites of lateral or adventitious root protrusion and induce the formation of intercellular IPs in the outer cortical cell layers (Fig. 2) (Goormachtig et al., 1998). IP formation shows distinct features of induced cell death. Transmission electron microscopy revealed cell death was preceded by loss of the plasma membrane integrity, fragmentation of the vacuole and the formation of electron-dense precipitates in the cytoplasm (D'Haeze et al., 2003). $CeCl_3$ staining to visualize H_2O_2 accumulation as cerium perhydroxide precipitates revealed massive H_2O_2 production in the apoplasts of some outer cortical cells and these cells showed distinct features of cell death (D'Haeze et al., 2003). H_2O_2 was also present in ITs but not inside bacteria, which were surrounded by a thick layer of low electron-dense material, presumably EPS (D'Haeze et al., 2003). Eventually this space becomes filled with proliferating bacteria. Prior to IP formation, a number of transcripts of genes thought to regulate this process accumulate. Transcripts of a peroxidase gene, *SrPrx1*, accumulate around IPs and *SrPrx1* expression accompanies the growing ITs until they reach the nodule primordium (Den Herder et al., 2006). Peroxidase driven cross-linking of glycoproteins might be involved in the solidification of the matrix present in the IP and

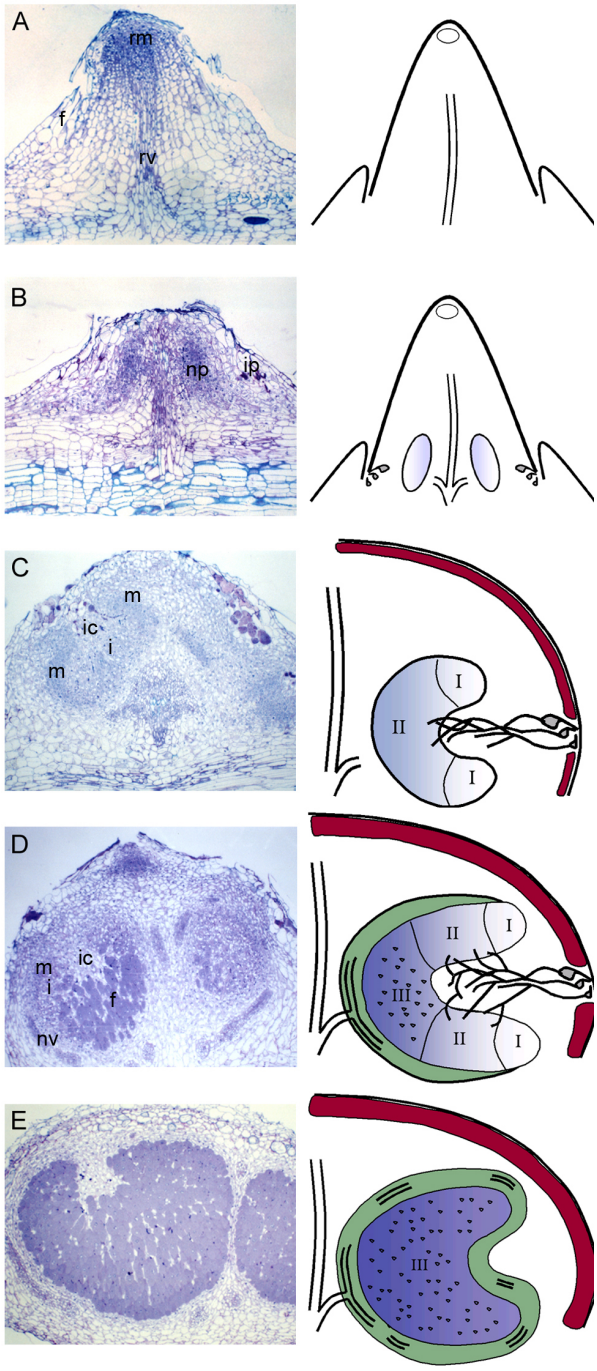

Fig. 2 Lateral root base nodulation in *S. rostrata.* Crack entry nodulation in *S. rostrata* initiates in fissures at sites of lateral or adventitious root protrusion on either stem or root (A). These fissures are colonized by bacteria, from where they induce the formation of infection pockets, a process that involves localized cell death (B). Concomitantly, inner cortical cells will dedifferentiate and will form the nodule primordium (B). Infection threads grow, first intercellularly and later intracellularly, towards the developing primordium (C) and enter the primordium at the basal part of the 'open basket'. Here the primordium cells become infected and the tissue differentiates into nitrogen fixing central cells. At this stage, the developing nodule is zonated, with a meristem, an infection zone and a fixation zone, analogous to an indeterminate nodule (D). Finally, meristem activity ceases and the nodule becomes determinate in size. Abbreviations: rm, root meristem; f, fissure; rv, root vasculature; np, nodule primordium; ip, infection pocket; ic, infection center; I, infection zone; m, meristem; f, fixation zone; nv, nodule vasculature.

ITs (Lievens, 2002). A putative leghemoglobin *Srlb6* is also induced very early and Srlb6 transcripts accumulate around the incipient IP in a NF dependent manner (Goormachtig et al., 1995). Leghemoglobins are usually considered late nodulins because of their role in regulation oxygen delivery to the nitrogen fixing bacteroids. However, in both *S. rostrata* and *V. sativa,* leghemoglobin genes have been found that are expressed well before the onset of fixation, suggesting they might a role in ROS perception or scavenging during early stage of nodulation (Goormachtig et al., 1995, Heidstra et al., 1997). Also, a gibberellin 20 oxidase gene SrGA20ox1 is strongly expressed around IPs and ITs, suggesting a role for gibberellins during early NF signaling in *S. rostrata* LRB nodulation (Lievens et al., 2005). From these IPs subsequent deeper invasion of the cortical tissue occurs (Goormachtig et al., 1998). The bacteria invade the cortical tissue intercellularly at first, then switching to intracellular ITs that finally reach the developing nodule primordium (Goormachtig et al., 1998). Concomitantly with IP formation, inner cortical cells start to redifferentiate to form the nodule primordium (Fig. 2).

Lateral root nodule development in *S. rostrata* is of a chimeric nature in a sense that although starting off as an indeterminate nodule, it switches to determinate nodule formation several days after inoculation (Fig. 2) (Goormachtig et al., 1998). Some three to four days after inoculation, the nodule primordium has taken on the so called 'open basket formation'. Radially symmetric around the IP-zone, a three-dimensional basket shaped primordium is apparent, with meristematic tissue at the distal end of the basket. Proximally, ITs penetrate the primordium in the basal part of the basket, called the infection center (Goormachtig et al., 1998). The ITs now progress through the primordium toward the more distally located cells that are supplied by the active meristem (Goormachtig et al., 1998). At this point, all stages of nodule development can be seen in a single cross section of the nodule, a distal meristem, the adjacent infection zone and the proximal fixation zone, reminiscent of the nodule morphology of an indeterminate nodule. Around 5 days after inoculation however, meristem activity ceases and all cells become infected with bacteria (Goormachtig et al., 1998). From this moment on, the nodule increasingly looks like the globose determinate nodules described previously. About 7 days after initiation, the nodule has matured completely (Fig. 2).

This switch from indeterminate to determinate nodule development can be circumvented when plants are grown in aerated soil. Aerated roots of *S. rostrata* form cylindrical, indeterminate nodules (Fernandez-Lopez et al., 1998). A major factor in the regulation of this phenotypical plasticity is the gaseous plant hormone ethylene since adding ethylene inhibitors to plants grown in hydroponic medium (which favours determinate nodule formation) resulted in the formation of indeterminate nodules (Fernandez-Lopez et al., 1998). Conversely, adding ACC, an ethylene biosynthesis precursor, blocked the formation of indeterminate nodules whereas it favoured determinate nodule formation

(Fernandez-Lopez et al., 1998). Ethylene accumulation might inhibit meristem maintenance in a similar manner as it inhibits nodule formation opposite protophloem poles (see part I). The absence of indeterminate nodules on stems could be explained by the presence of a strong gaseous diffusion barrier present in these nodules, thought to shield the central nodule tissue of stem nodules from excessive oxygen levels, thus blocking ethylene diffusion (Fernandez-Lopez et al., 1998).

Early signaling events during lateral root base nodulation

Based on

D'Haeze, W., De Rycke, R., Mathis, R., Goormachtig, S., Pagnotta, S., Verplancke, C., Capoen, W., and Holsters, M. (2003). Reactive oxygen species and ethylene play a positive role in lateral root base nodulation of a semiaquatic legume. Proc Natl Acad Sci U S A 100, 11789-11794.

Lievens, S., Goormachtig, S., Den Herder, J., Capoen, W., Mathis, R., Hedden, P., and Holsters, M. (2005). Gibberellins are involved in nodulation of Sesbania rostrata. Plant Physiol 139, 1366-1379.

Infection pockets are an intriguing analogue of the micro colony in a curling root hair. Both presumably serve as a signaling center that provides a positional cue and a strong accumulation of Nod factors, in a small space, thus leading to signal amplification. It has been pointed out that hydroponic nodulation comes with its typical high ethylene levels, conditions which inhibit RHC nodulation (Fernandez-Lopez et al., 1998). To investigate this, an extensive study of potential signals and regulators has been performed in an attempt to unravel these signaling networks. The three most studied signals thus far are reactive oxygen species (ROS), ethylene and gibberellins (GA) (D'Haeze et al., 2003; Lievens et al., 2005).

Infection pocket formation, as mentioned previously, shows features reminiscent of cell death. Indeed, using Evans blue staining, bacterial colonization of the outer cortex colocalizes with localized cell death. IP formation is a strictly regulated process that depends on NF. Bacteria that are deficient in NF production such as *A. caulinodans* ORS571-V44, a nodA mutant, are completely blocked in their ability to form IPs (D'Haeze et al., 1998). In coinoculation experiments with ORS571-V44 and ORS571-X15, with altered LPS, it was shown that the X15 mutant can compensate for V44's lack of NF production. Nodules are then formed that are occupied solely by ORS571-V44 while X15 cannot progress beyond the IP stage (D'Haeze et al., 1998).

Several secondary signals play a role in the induction of the IPs. An initial screen for compounds that are likely to be involved in early NF signaling during hydroponic nodulation was based on the responsiveness of dormant axillary root hairs at lateral root bases (Mergaert et al., 1993). These axillary root hairs respond to NF by deforming and forming bushy outgrowths, but they do not become infected with bacteria (Mergaert et al.,

1993). Deformation is NF structure specific and hormonal requirements differ from the requirement for NF induced root hair deformation in legumes such as *M. truncatula.* These requirements correlate well with requirements for NF induced IP formation and nodule formation (D'Haeze et al., 2003). Application of H_2O_2, ethylene or the ethylene biosynthesis precursor ACC can induce root hair outgrowth at these sites, although root hairs are straight as opposed to the deformed root hairs outgrowth induced by NF (D'Haeze et al., 2003). NF induced axillary root hair outgrowth and deformation can be inhibited by adding inhibitors of H_2O_2 production (such as AIB, DPI, Ascorbic acid) and ethylene biosynthesis or perception inhibitors (silver ions, AVG), showing a putative role for H_2O_2 and ethylene in NF signaling (D'Haeze et al., 2003). When pretreatments are performed with these compounds, also hydroponic nodulation is blocked, providing evidence for their role during nodulation (D'Haeze et al., 2003). These data suggest opposite roles for ethylene for nodulation under hydroponic conditions, since exogenous ethylene completely blocks nodulation in *M. truncatula* (Peters and Cristestes, 1989).

Similarly, gibberellins are involved in NF signaling toward IP formation (Lievens et al., 2005). A first clue to a role for GA came with the identification of a differentially expressed gibberellin 20-oxidase that is strongly upregulated during the early stages of hydroponic nodule formation, designated *SrGA20ox1* (Lievens et al., 2001). *SrGA20ox1* is upregulated within hours of inoculation in a NF dependent manner (Lievens et al., 2005). Initial expression can be seen 8 hours after inoculation in the outermost cortical cell layers, surrounding the fissure at lateral root bases where bacteria are present (Lievens et al., 2005). Expression subsequently surrounds the developing IP and follows IT progression, where it is visible in cells surrounding the ITs (Lievens et al., 2005). *SrGA20ox1* finally becomes restricted to the infection zone where bacteria are released from ITs. A possible function of GA during intercellular invasion might be regulation of programmed cell death, analogous to the role of GAs in barley aleurone cell death (Bethke and Jones, 2001).

GA also mediated NF induced axillary outgrowth since GA can induce root hair outgrowth and chlormequat chloride (CCC, a gibberellin biosynthesis inhibitor) can block NF induced axillary root hair deformation (Lievens et al., 2005). Furthermore, application of CCC and several other GA antagonists also inhibits lateral root base nodulation, although bacterial colonization still occurred. CCC application 1 day after inoculation still strongly inhibited nodulation, adding CCC later resulted in a weaker inhibition, suggesting that GA action is required early on in the interaction (Lievens et al., 2005). Conversely, adding GA to plants grown in aerated conditions, favouring root hair curling (see next chapter), blocked nodulation, suggesting opposite effect of GA for initiation of hydroponic and aeroponic nodulation (Lievens et al., 2005).

Later on during development GAs might be necessary for the induction of cortical cell division and nodule differentiation. This is linked to a second *SrGA20ox1* expression

pattern that is not directly dependent on NF. In the developing nodule, *SrGA20ox1* expression is also apparent in the cells adjacent to the nodule meristem, similar to GA20ox expression in cells derived from floral meristems (Komeda, 2004; Lievens et al., 2005). GAs are thought to be involved in meristem differentiation and it seems that a similar mechanism is required for differentiation of nodule meristem cells.

Chapter 4

Infection plasticity in water-tolerant legumes

Published as: Goormachtig, S., Capoen, W., James, E.K., and Holsters, M. (2004). Switch from intracellular to intercellular invasion during water stress-tolerant legume nodulation. Proc Natl Acad Sci U S A 101, 6303-6308.

Rhizobia colonize their legume hosts by different modes of entry while initating symbiotic nitrogen fixation. Most legumes are invaded via growing root hairs by the root hair-curl mechanism, which involves epidermal cell responses. However, invasion of a number of tropical legumes happens through fissures at lateral root bases by cortical, intercellular crack entry. In the semiaquatic legume *Sesbania rostrata*, the bacteria entered via root hair curls under nonflooding conditions. Upon flooding, root hair growth was prevented, invasion on accessible root hairs was inhibited, and intercellular invasion was recruited. The plant hormone ethylene was involved in these processes. The occurrence of both invasion pathways on the same host plant enabled a comparison to be made of the structural requirements for the perception of nodulation factors, which were more stringent for the epidermal root hair invasion than for the cortical intercellular invasion at lateral root bases.

Introduction

Leguminous plants can engage in a symbiotic interaction with rhizobia (nitrogen-fixing bacterial symbionts), resulting in the formation of specialized root organs, the nodules. In the central nodule tissue, internalized bacteria fix dinitrogen to be used by the host. Many legumes are of agronomic importance as major food and feed crops, whereas others have a great potential as green manure. The legume–rhizobia interaction is initiated by a complex signal exchange during which recognition of bacterial nodulation (Nod) factors switches on the nodulation program in the plant. Nod factors are lipochitooligosaccharides that carry different substitutions. Recently, plant genes have been characterized that encode components of the Nod factor receptor-perception complexes (Endre et al., 2002; Stracke et al., 2002; Limpens et al., 2003; Madsen et al., 2003; Radutoiu et al., 2003). In legume symbiosis, bacterial invasion can follow different routes, the best known of which is via root hairs. Rhizobia induce the curling of growing root hairs, are entrapped in the curl, and enter the root hair by local hydrolysis of cell walls and invagination of the plasma membrane. Tip growth toward the base of the root hair results in an intracellular infection thread that proceeds through the cortical cells to reach the nodule primordia, where bacteria are released inside plant cells. The process takes place in the zone of developing root hairs (zone I, (Mathesius et al., 2000)), located just above the root meristem. Root hair invasion is used in pea, bean, soybean, vetch, and alfalfa, and in the model legumes *Medicago truncatula* and *Lotus japonicus* (Vance et al., 1982; Wood and Newcomb, 1989). Another mode of entry, via intercellular invasion at lateral root bases, has been observed in many tropical legumes. The bacteria enter via cracks formed by the protrusion of lateral roots and colonize large intercellular spaces called infection pockets. The mechanism for deeper invasion varies. In *Sesbania rostrata* and in *Neptunia sp*., infection pockets narrow down to form intercellular infection threads, and subsequently intracellular infection threads intrude into the nodule primordium (James et al., 1992; Ndoye et al., 1994; Subbarao et al., 1995; Goormachtig et al., 1998b). In *Aeschynomene, Stylosanthes*, and *Arachis*, invasion progresses by means of cell collapse, and bacteria enter the cells of the nodule primordia by direct uptake from the infection pockets (Chandler et al., 1982; Alazard and Duhoux, 1990; Loureiro et al., 1995; Boogerd and vanRossum, 1997). The process of intercellular invasion has been examined in most detail in the *S. rostrata–Azorhizobium caulinodans* interaction, which has become a model for the study of this type of entry (Goormachtig et al., 1998b; Lievens et al., 2001). On *S. rostrata*, nodules arise not only on the root but also on the stem, at positions of adventitious root primordia (Goormachtig et al., 1998b). These so-called stem nodules are actually adventitious root nodules, and their development is morphologically equivalent to the development of lateral root base nodules. The hormone ethylene, which controls the physiology of aquatic plants (Jackson, 1985), is required for lateral root base nodulation, where it plays a role in the Nod factor-induced cell death that is needed for infection pocket formation (Dazzo et al., 1991; D'Haeze et al., 2003). This ethylene

dependency for nodule initiation is special. Indeed, root hair curl invasion has been found to be either inhibited by or insensitive to ethylene (Guinel and Geil, 2002). In *M. truncatula*, ethylene modulates the calcium spiking that precedes root hair deformation (Oldroyd et al., 2001).

In vetch, ethylene affects preinfection thread formation, thus blocking invasion (van Spronsen et al., 1995). Both root hair and intercellular invasion are Nod factor dependent processes (D'Haeze et al., 2000; Cullimore et al., 2001; Oldroyd, 2001). In *Medicago* sp., pea, and vetch, the Nod factor structure requirements for entry in root hairs are more stringent than those for induction of cortical cell division (Ardourel et al., 1994; Walker and Downie, 2000; Geurts and Bisseling, 2002), suggesting the occurrence of very specific entry receptors. Genes coding for putative entry receptors of *M. truncatula*, pea, and *L. japonicus* have recently been identified (Limpens et al., 2003; Madsen et al., 2003; Radutoiu et al., 2003). Interestingly, during intercellular invasion in *S. rostrata*, bacteria that produce Nod factors without decoration were still active, and functional nodules were still formed, be it at very low frequency (D'Haeze et al., 2000). Although these observations suggest that intercellular invasion may need less stringent structural Nod factor requirements, no conclusions can be reached because root hair invasion and intercellular invasion took place on different host plants. The fact that different entry routes exist to invade the host and to form functional nodules has attracted the attention of many legume biologists. Because of its occurrence in the less evolved groups of legumes, intercellular invasion was proposed to be the more ancient mechanism. On the other hand, legumes that allow intercellular invasion bear only few root hairs, suggesting that intercellular invasion might be an adaptive behavior (Sprent, 2002). We show that under nonaquatic conditions, *S. rostrata* roots, in contrast to hydroponic roots, have plenty of root hairs through which infection proceeds. Root hair infection was inhibited by ethylene and required more stringent Nod factor features than intercellular invasion. Ethylene also affected root architecture and the formation of new root hairs. Other aquatic legumes, such as *Neptunia* sp., also prefer the root hair curling process under nonaquatic conditions. Thus, intercellular invasion is seemingly an adaptation to waterlogging, and the root hair curling process is the default pathway taken by rhizobia to enter legume plants.

Materials and Methods

Plant and Bacterial Growth Conditions.

Seedlings of *S. rostrata* Brem were germinated (Goormachtig et al., 1995) and grown in tubes and Leonard jars (Fernandez-Lopez et al., 1998). L-α-(2-aminoethoxyvinyl)-glycine (AVG), 1-aminocyclopropane- 1-carboxylate (ACC), and Ag_2SO_4 were added to the lower container of Leonard jars or in tubes at final concentrations of 7 μM, 20 μM, and 10 μM, respectively. The tubes and Leonard jars were protected from light. The components were added 2 days before inoculation, except when otherwise indicated. The strains ORS571, ORS571(pRG960SD-32) (Van den Eede et al.,

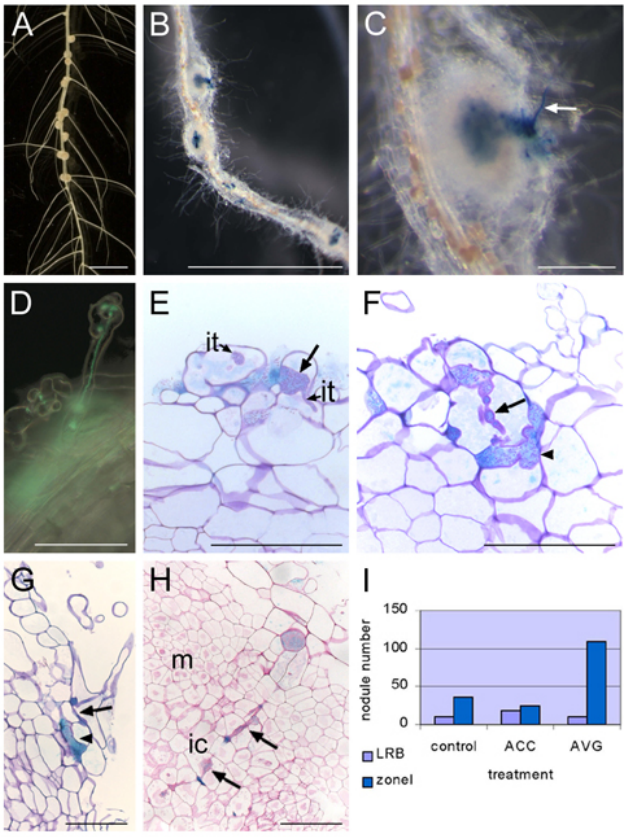

Fig. 1. Features of *S. rostrata* nodulation.
A Nodulated hydroponic *S. rostrata* root, 7 days postinoculation (DPI). Nodules are present at the lateral root bases. *B* GUS staining of a vermiculite-grown root nodulated by ORS571(pRG960SD-32). Nodules are distributed over the root (zone I nodules) 4 DPI. *C* Enlargement of *B*. Arrow indicates GUS-stained root hair. *D* Root hair with an infection thread containing *A. caulinodans* carrying a GFP marker. *E–G* Toluidine blue-stained sections through vermiculite-grown roots, 2 DPI with ORS571(pRG960SD-32), and stained for GUS. Arrows indicate initiating broad infection thread *E*, an intracellular cortical infection thread (*F*), and an intercellular infection thread *G*; arrowheads mark small infection pocket-like structures (*F* and *G*). *H* Ruthenium red-stained section through a developing zone I nodule, 4 DPI with ORS571(pRG960SD-32), and stained for GUS. Arrows indicate intracellular invasion track. *I* Influence of ethylene on lateral root base and on zone I nodulation on vermiculite-grown roots. The histogram presents the number of nodules derived from zone I or from lateral root base infection, 7 DPI, on roots grown in vermiculite (control), on vermiculitegrown roots to which ACC has been added 2 days before inoculation (ACC), and to which AVG has been added 2 days before inoculation (AVG). ic, infection center; it, infection thread; LRB, lateral root base nodule; m, meristem; zonel, zone I nodules. (Bars - 1 cm in *A* and *B*, 1 mm in *C*, and 100 µm in *D–H*.)

1992), ORS571(pBBR5-hem-gfp5-S65T) (W.D'Haeze and M.H., unpublished data), ORS571(4.2K), ORS571(1.2), ORS571(1.11Z-ΩK), and ORS571 (1.31U-ΩK) (D'Haeze et al., 2000) were grown and inoculated as described (Fernandez-Lopez et al., 1998). *Neptunia plena* seeds were germinated according to James et al. (James et al., 1992). The plants were grown in tubes and Leonard jars according to the same protocols as those for *S. rostrata*. *Rhizobium* sp. DUS239 was cultivated as described (James et al., 1992). To construct a strain that is detectable by GFP analysis, the hem-gfp5 cassette was cut from the plasmid pBBR5-hem-gfp5-S65T by XhoI–PstI digestion and introduced into the tetracycline-resistant plasmid pBBR1MCS-3 by standard procedures (Sambrook et al., 1989), creating the plasmid pBBR3-hem-gfp5-S65T. The plasmid was introduced into DUS239 by triparental mating (Sambrook et al., 1989).

Microscopic Analysis.

Staining for β-glucuronidase (GUS) was as described (D'Haeze et al., 1998). For semithin sectioning, the tissues were embedded in Technovit 7100 (Heraeus Kulzer, Wehrheim, Germany), sectioned, and stained with ruthenium red or toluidine blue (Goormachtig et al., 1998a; Van de Velde et al., 2003). GFP analysis was performed according to Van de Velde et al. (Van de Velde et al., 2003). Roots and root hairs were stained with methylene blue (D'Haeze et al., 2000).

Results

S. rostrata Roots, Grown in Vermiculite, Are Invaded via Root Hairs.

Upon inoculation with the *A. caulinodans* strains ORS571(pRG960SD-32) and ORS571

(pBBR5-hem-gfp5- S65T), which can be visualized by GUS staining or fluorescence microscopy, respectively, curled root hairs with infection threads were detected (Fig. 1 C and D). Because this response took place in zone I of emerging root hairs (data not shown), the resulting nodules will be referred to as zone I nodules. Analysis of semithin sections revealed that the bacteria entered the root hairs by sometimes very broad infection threads that narrowed down toward the base of the root hairs (Fig. 1E). Upon leaving the root hair, the infection proceeded through the cortex intracellularly (Fig. 1F) or intercellularly (Fig. 1G), occasionally accompanied by small infection pocket-like structures (Fig. 1 F and G). Progression into the nodule primordium happened by intracellular infection threads (Fig. 1H). On hydroponic roots, the bacteria entered the plant solely by intercellular invasion at lateral root bases (data not shown). On vermiculite-grown roots, both types of invasion occurred, but with a clear preference for zone I nodulation and intracellular root hair invasion (Fig. 1I, control).

Opposite Requirement for Ethylene During Intercellular and Intracellular Invasion.

Previously, we have found that ethylene is required for the intercellular invasion at lateral root bases of *S. rostrata* (D'Haeze et al., 2003). On the other hand, ethylene has been shown to have no or a negative effect on the root hair invasion process (Guinel and Geil, 2002). Is ethylene dependency of lateral root base nodulation in *S. rostrata* linked to the plant or the process? To address this question, we investigated the role of ethylene in root hair invasion (Fig. 1I). Two days before inoculation of vermiculite-grown *S. rostrata* roots, 7 μM AVG, an inhibitor of ethylene synthesis, was added, and nodules were counted 1 week after inoculation. The number of zone I nodules had clearly increased. Similar results were obtained with Ag_2SO_4, an inhibitor of ethylene action (data not shown). In contrast, the amount of zone I nodules decreased when ACC, an ethylene precursor, was added to the medium (Fig. 1I). These results show an opposite ethylene dependence for the intercellular invasion and the root hair invasion, the latter being inhibited by ethylene.

Submergence Blocks Root Hair Invasion.

In *S. rostrata*, root hair distribution and susceptibility to the symbiotic bacteria depend on root growth conditions and are controlled by ethylene. Hydroponic roots hardly had root hairs, the tips were naked (Fig. 2A), and root hairs present at the upper, oldest part of the root did not curl upon inoculation (D'Haeze et al., 2003). On the contrary, when grown in vermiculite, roots were completely covered with root hairs, starting from zone I just above the tip (Fig. 2B). When vermiculite- grown roots were submerged for 24 h or 1 h before inoculation, the root hair invasion was completely blocked, and no zone I nodules were detected 7 DPI (Fig. 2C). Because submergence is known to cause entrapment of ethylene, we examined the putative role of ethylene in prevention of root hair growth and root hair response to nodulating bacteria. When seedlings were transferred to tubes containing 7 μM AVG, the main root and lateral roots were much smaller than those grown without AVG (Fig. 2 D and E),

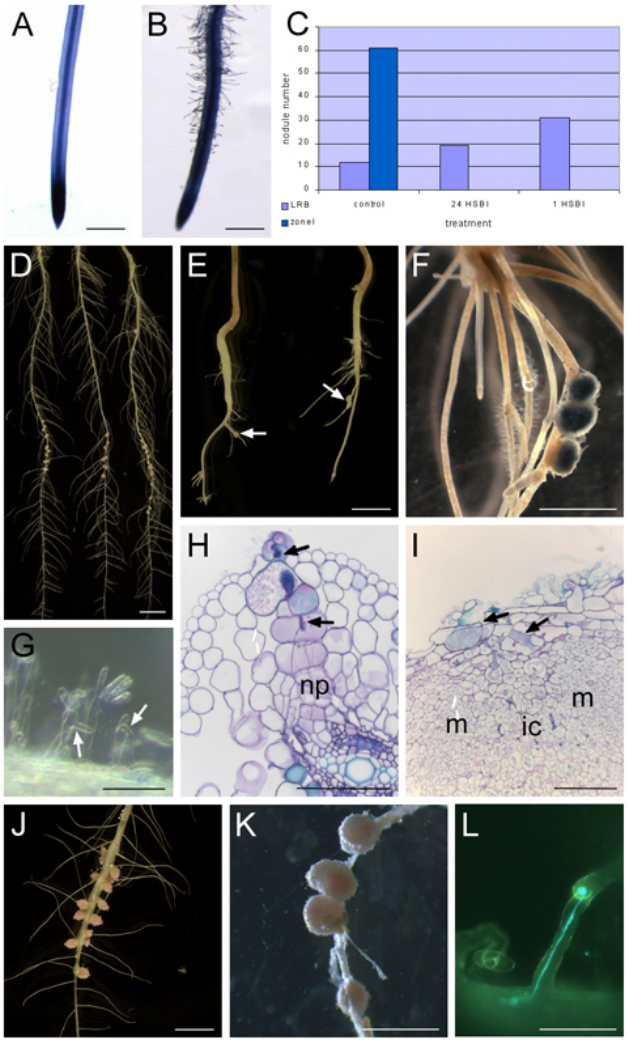

Fig. 2. Comparison of root morphology and nodulation traits between hydroponically and vermiculite-grown S. rostrata and N. plena plants.
A and B. Methylene blue-stained root tip of hydroponically and vermiculite-grown *S. rostrata* root, respectively. No root hairs are detected on the hydroponically grown root tip, whereas the vermiculite-grown root contains plenty. C Influence of submersion on lateral root base and zone I nodule numbers of vermiculite-grown S. rostrata roots. The nodule number is derived from lateral root base or zone I nodulation, 7 DPI on vermiculite-grown roots (control), on vermiculite-grown roots that were submerged 24 h before inoculation (24HSBI), and 1 h before inoculation (1HSBI). D. Nodulated hydroponic roots, 7 DPI. Nodules are located at lateral root bases. E. Nodulated hydroponic root, grown in the presence of AVG, 7 DPI. Nodules are distributed over the root (arrows). F. Hydroponic root grown in the presence of AVG, infected with ORS571(pRG960SD-32), and stained for GUS. G. Root hair deformation and curling on hydroponically grown roots in the presence of AVG, 2 DPI. Arrows mark curled and deformed root hairs. H and I. Toluidine blue-stained sections of developing nodules on hydroponic roots grown in the presence of AVG. Arrows indicate intracellular infection thread (H) and small infection pockets (I). (J) Hydroponically grown nodulated N. plena roots, 7 DPI. Nodules are present at lateral root bases. (K) Vermiculite-grown nodulated N. plena root. Nodules are distributed over the root. (L) Curled N. plena root hair containing an infection thread visualized by GFP-containing Rhizobium sp. DUS239. Abbreviations, see Fig. 1 legend; np, nodule primordium. (Bars - 1 cm in A, B, D–F, J, and K and 100 μm in G–I and L.)

and lateral roots were partially covered with root hairs (Fig. 2F). Inoculation resulted in deformation and curling of the root hairs (Fig. 2G); the nodules were preferentially distributed over the lateral roots (Fig. 2 E and F). Semithin sections through young developing nodules revealed infection threads inside root hairs and a subsequent intracellular track toward the nodule primordia (Fig. 2H). At later stages, also small intercellular infection pockets were observed (Fig. 2I), similarly as for nodule formation in vermiculite-grown roots.

The Versatile Invasion Is Typical for Water-Adapted Legumes.

Are these versatile invasion properties typical for *S. rostrata* or do other semiaquatic legumes have the same behavior? *N. plena* is an aquatic legume that is invaded under hydroponic conditions in a manner very similar to that of *S. rostrata* (data not shown, (James et al., 1992)). *N. plena* seedlings were grown either in tubes or in Leonard jars. As for *S. rostrata*, the root hair distribution differed between the two physiological conditions

(James et al., 1992). Upon inoculation with the microsymbiont *Rhizobium* sp. DUS239, nodules arose at lateral root bases of the

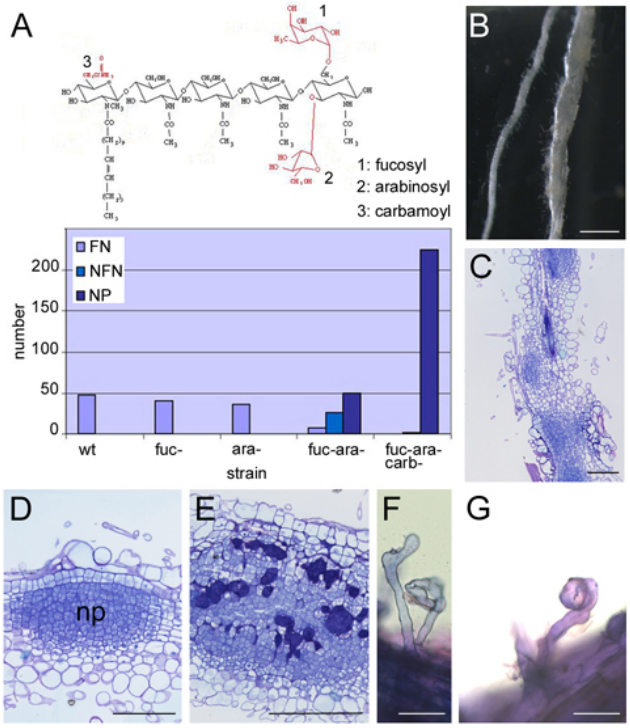

Fig. 3. Nod factor structure requirements for root hair infection on S. rostrata.
(A) Structure of the main Nod factor produced by A. caulinodans ORS571. Substitutions in red are the chemical groups that are removed in the different mutant strains used in the experiment. 1, fucosyl moiety; 2, arabinosyl moiety; and 3, carbamoyl moiety. The histogram shows the number of functional nodules (FN), nonfunctional nodules (NFN), and nodule primordia (NP) caused by zone I infection on vermiculite-grown roots, 7 DPI, infected with wild-type ORS571 or several mutants. Fuc-, ara-, and carb- indicate that the mutant strain produced Nod factors lacking the fucosyl, arabinosyl, or carbamoyl moiety, respectively. Because of the variable nodulation efficiency of different plants, the results presented are the sum of lateral root base or zone I nodules formed on 12 plants. (B) Vermiculite-grown roots infected with ORS571(1.31U-ΩK), 7 DPI. Arrow indicates swollen root. (C) Toluidine bluestained section through a swollen root reveals that the swollen root appearance is due to the presence of a sequence of nodule primordia. (D) Toluidine blue-stained sections through a nodule primordium grown after infection with ORS571(1.31U-ΩK). (E) Toluidine blue-stained section of a colonized nodule primordium grown after infection with ORS571 (1.31U-ΩK). Bacteria are seen in large intercellular spaces between the primordial cells. (F and G) Methylene blue-stained deformed and curled root hairs, respectively, of vermiculite-grown S. rostrata roots after infection with ORS571(1.31U-ΩK). Abbreviations, see Fig. 2 legend. (Bars - 1 cm in B and 100 μm in C–G.)

hydroponic roots and were distributed all over the vermiculite-grown roots (Fig. 2 J and K). To follow bacterial invasion, the plasmid pBBR3-hem-gfp5-S65T was introduced into *Rhizobium* sp. DUS239 (see Materials and Methods), and vermiculite-grown, inoculated roots were analyzed by fluorescent microscopy. As shown in Fig. 2L, root hairs with infection threads were observed.

Nod Factor Structure Requirement Is More Stringent for Root Hair Invasion Than for Intercellular Invasion.

A. caulinodans produces mainly pentameric Nod factors with a common fatty acid, an N-methyl, and a 6-O-carbamoyl group at the nonreducing terminal GlcNAc residue and with a D-arabinosyl, an L-fucosyl, or both at the reducing-end GlcNAc (Fig. 3A, (Mergaert et al., 1993)). By using bacterial mutants that produce well characterized sets of altered Nod factors, none of the Nod factor substituents was shown to be strictly required for lateral root base nodulation, although their synergistic presence determined the nodulation frequency (D'Haeze et al., 2000). Hence, we investigated the Nod factor structure requirements for the root hair invasion of *S. rostrata*. Roots grown in vermiculite were inoculated with ORS571 (4.2K), ORS571(1.2), ORS571(1.11Z-ΩK), or ORS571(1.31U-ΩK), which are strains that produce Nod factors without a fucosyl group, without an arabinosyl group, without reducing-end glycosylations, or devoid of reducing-end glycosylations and carbamoylation, respectively. For each strain, the total number of nodules (primordia) derived from zone I invasion in 12 plants was counted at 7 DPI (Fig. 3A). Inoculation with bacteria producing nonarabinosylated, nonfucosylated, or nonarabinosylated and nonfucosylated Nod

factors yielded 40, 36, and 32 nodules, respectively, barely fewer than during wild-type infection (47 nodules). Only one nonfunctional nodule (with white to slightly pink central tissue; data not shown) was counted on plants inoculated with strain ORS571(1.31U- ΩK), which produces nonglycosylated and noncarbamoylated Nod factors. These plants were yellow, indicating a lack of nitrogen fixation. In the infection with ORS571(1.11Z-ΩK), 25 of 32 nodules were small with a white-to-pinkish central tissue. In the experiments with ORS571(1.11Z-ΩK) and ORS571(1.31U-ΩK), many small nodule-like structures were observed; in the latter case, these were so abundant that the root had a swollen appearance (Fig. 3B). Sectioning through such a swollen root showed multiple nodule primordia (Fig. 3C), consisting of densely packed dividing cells and located in the outer cortex (Fig. 3D). Sometimes these primordia were invaded intercellularly (Fig. 3E). To see at which level the interaction was blocked, vermiculite-grown roots were infected with ORS571(pBBR5-hem-gfp5-S65T), and 45 roots were screened for infection thread formation. Although the root hairs were deformed (Fig. 3F) and curled (Fig. 3G), neither infection threads nor colonization of the curls was observed.

Discussion

To study legume–rhizobium symbiosis, two model plants have been selected, *L. japonicus* and *M. truncatula* (Oldroyd, 2001; Stougaard, 2001; Limpens and Bisseling, 2003). However, not all nodulation-related questions can be addressed with these two systems. For instance, the specific adaptations related to nodulation under aquatic conditions, a trait that is of agronomic importance, requires appropriate study organisms. During the symbiosis between the semiaquatic legume *S. rostrata* and its microsymbiont *A. caulinodans*, bacteria enter the plant intercellularly via cracks at lateral or adventitious root bases (Duhoux, 1984; Ndoye et al., 1994). However, an old and nearly forgotten paper mentioned the presence on *S. rostrata* of curled root hairs that contained infection threads (Olsson and Rolfe, 1985). We show that indeed both ways of invasion occur in *S. rostrata*, but under different conditions. On well aerated roots growing in Leonard jars in vermiculite, nodules do not arise at the lateral root bases, but are distributed mostly over the lateral roots. In contrast to hydroponically grown roots, which are bare, the well aerated roots are covered with root hairs. After inoculation with *A. caulinodans*, zone I root hairs, located near the root tip, are curled and contain infection threads to guide the bacteria to nodule primordium cells. These infection threads are often very broad and interrupted by an intercellular track at the borders between cells. At later stages of nodule development, also small intercellular infection pockets can be observed in the outer cortical regions. Probably, *A. caulinodans* can colonize cracks that appear once the nodule primordium expands from the inner cortex. It is improbable that these bacteria progress within the plant to cause the nodule organogenesis and infection. Indeed, mutant bacteria that produce unsubstituted Nod factors fail to induce functional nodules via root hairs in zone I, although they are able to proliferate in small intercellular pockets. Because *S. rostrata* is capable of switching entry modes when grown

on flooded and unflooded soils, we were curious to investigate the role of ethylene in the control of this versatility. In addition to being involved in various developmental processes, the plant hormone ethylene is also tightly related to flooding-adapted growth. Ethylene, being gaseous, diffuses at a more reduced rate in water than in air, leading to a quick accumulation upon flooding, and is a primary signal that activates water-adapted growth responses in *Rumex palustris* and deepwater rice (Lorbiecke and Sauter, 1999; Voesenek et al., 2003). In *S. rostrata*, ethylene affects nodule meristem maintenance (Fernandez-Lopez et al., 1998) and is necessary for the intercellular invasion at lateral root bases of hydroponic roots (D'Haeze et al., 2003). Ethylene also affects root growth and root hair distribution (this work) . Hydroponically grown roots have no root hairs in zone I, whereas aeroponically grown roots have plenty. Ethylene might be partially responsible for this difference because adding AVG results in a partial restoration of root hair growth on the lateral roots of hydroponic seedlings. In *Arabidopsis thaliana*, ethylene is involved in both root hair initiation and elongation (Schiefelbein, 2000). In hydroponic *S. rostrata* roots, ethylene is necessary for root hair elongation in the axils of lateral roots (D'Haeze et al., 2003) but inhibits root hair initiation (this work), illustrating again the specific physiology of flooding-adapted plants that cannot always be compared with terrestrial plants (D'Haeze et al., 2003; Voesenek et al., 2003). Ethylene also affects the root hair invasion process in *S. rostrata*. When inhibitors of ethylene synthesis or perception are added to vermiculite-grown roots before inoculation with azorhizobia, the numbers of zone I nodules increase, whereas addition of ACC, the precursor of ethylene, reduces root hair invasion. Flooding of roots grown in Leonard jars and thus bearing susceptible zone I root hairs results in a 100% inhibition of root hair infections 1 h before inoculation with *A. caulinodans*. On the contrary, root hairs present on roots grown hydroponically in the presence of AVG were sensitive to curling and to root hair invasion. The difference between the two root hair situations is the presence of ethylene, the accumulation of which is responsible for the root hair curl inhibition upon flooding. Thus, root hair curl invasion in *S. rostrata* is sensitive to ethylene, similar to the situation described for *M. truncatula* and several other legumes (Oldroyd et al., 2001). Intercellular invasion often takes place on plants without root hairs (Sprent, 2002), but in *S. rostrata* the situation is more complex and variable (Sprent, 2002). In this water stress-adapted plant, ethylene is the main switch that determines how the invasion will happen because ethylene prevents root hair growth, inhibits the invasion of accessible root hairs upon submersion, and is necessary for infection pocket formation, which is an essential trait of intercellular invasion ((D'Haeze et al., 2003), this work). How about other flooding-adapted legumes? On hydroponically grown *N. plena* roots, nodules arose at lateral root bases, and infection took place intercellularly as in *S. rostrata*. On the other hand, in Leonard jars nodules were distributed all over the lateral roots, and infection threads were detected within curled root hairs. In the literature on aquatic legumes, we found no further direct support for our observations, mainly because most articles do not focus on

infection. However, between the lines, several authors hint at a versatile infection behavior on aquatic legumes, suggesting that the intercellular invasion was recruited to allow infection in situations where root hair invasion is inhibited (Chandler et al., 1982; Loureiro et al., 1995; James and Sprent, 1999). The observation that *S. rostrata* and *N. plena*, two semiaquatic legumes belonging to different subfamilies, display a similar versatility in entry mode is interesting in view of the interpretation of the evolutionary aspect of infection. *S. rostrata* belongs to the Hologalegina tribe of the Papilionoideae family and *N. plena* to the family of the Mimosoideae (Doyle and Luckow, 2003). It has often been postulated that intercellular invasion would be more ancestral than root hair invasion simply because it looks more primitive and has more characteristics in common with pathogen invasion, from which it could have been derived. On the other hand, Sprent (Sprent, 2002) suggested, on the basis of evolutionary tree interpretations, that root hair invasion would be ancestral. The observation that root hair invasion indeed happens on *N. plena* (under nonflooding conditions) demonstrates that it is more spread among the legume members than previously thought. Moreover, we have shown that the intercellular infection bypasses the root hair invasion inhibition by flooding, suggesting that root hair invasion is the default program. Because in *S. rostrata* the two types of invasion occur, the respective Nod factor structure requirements can be compared. The bacterial Nod factors activate the nodulation program of the legume host. They trigger various responses, such as root hair deformation, root hair swelling, gene expression, and cortical cell division. For nodulation of vetch, pea, and *M. truncatula*, the structural Nod factor requirements for infection thread formation are very stringent, whereas they are less stringent for root hair swelling, root hair deformation, and cell division (Ardourel et al., 1994; Geurts et al., 1997; Walker and Downie, 2000). Concerning the intercellular invasion, *A. caulinodans* mutants that produce Nod factors stripped of carbamoyl and glycosyl substitutions can still induce functional nodules, but the nodulation efficiency drops considerably. Thus, intercellular invasion at lateral root bases, although Nod factor dependent, does not require the recognition of a very strict structure (D'Haeze et al., 2000). By using the same set of mutant strains, root hair invasion was found to present higher structural demands than did intercellular invasion. Whereas removal of one of the reducing-end glycosylations does not diminish the nodulation efficiency, removal of both glycosylations decreases the number of functional nodules and causes the formation of numerous small white nodules and nodule primordia. The effect is most prominent after infection with a mutant that produces Nod factors that lack the reducingend glycosylations as well as the carbamoyl group at the nonreducing end. Functional nodules are no longer observed; only a few nonfunctional white nodules and a huge number of small nodule primordia are present, giving the roots a swollen appearance. Microscopic analysis showed that root hair deformation, swelling, and, to a lesser extent, curling were still detectable, but no infection threads were found. In a very few cases, bacteria are found in intercellular infection pocket-like structures and in intercellular infection threads. These

bacteria do not enter via root hairs but most probably via cracks that inevitably appear when the primordia grow out from the root cortex. They are incapable of invading the plant cells and transforming into bacteroids. Interestingly, aerated roots of *S. rostrata* react to an infectiondeficient strain by allowing many more nodule initiation events. The number of nodule primordia increases according to the level of infection deficiency. A similar event has been observed by Ardourel et al. (Ardourel et al., 1994). (Auto)regulation of nodulation is complex and takes place at several levels, such as control of primordium formation and control of infection site formation (Krusell et al., 2002; Nishimura et al., 2002; Penmetsa et al., 2003; Searle et al., 2003). The latter probably involves ethylene, which negatively regulates the persistence of infection, interfering with the Nod factor signal transduction (Penmetsa and Cook, 1997; D'Haeze et al., 2003). Thus, infection in susceptible zone I would trigger ethylene production, which negatively modulates infection initiation. Because of inability of the mutant strains to efficiently invade the plant, the infection-related autoregulation system is not switched on, leading to an excess of nodulation events. Whereas the *S. meliloti* strains, which cannot invade the root hairs of *M. truncatula*, induce only some cell divisions in the cortex (Ardourel et al., 1994), the corresponding *A. caulinodans* strains induce dense nodule primordia in *S. rostrata*. Probably, the Nod factors produced by the bacteria within the intercellular spaces maintain the cortical cell divisions. The lack of locally high ethylene levels may be the reason why the intercellular bacteria are not able to further progress in the plant. Root hair infection and, especially, infection thread formation are often inhibited by ethylene, and this ethylene inhibition is probably active in the epidermis (Guinel and Geil, 2002). Under aquatic conditions, where ethylene accumulates, this step has to be circumvented; instead, an infection route was recruited in which ethylene is necessary. Although intercellular invasion may look more simple, physiological demands, such as ethylene concentrations, make it as complex as root hair invasion. The differences in Nod factor structure requirements for root hair invasion at the level of the epidermis and intercellular invasion at the level of the cortex provide an interesting challenge to compare epidermal and cortical responses at the gene expression level. Plants have adapted to live in situations of flooding or partial flooding by versatile mechanisms. Whereas *S. rostrata* root nodules develop and function on submerged roots, there is a switch from indeterminate to determinate nodule type (Fernandez-Lopez et al., 1998) and from root hair infection to intercellular invasion. A hope remains to understand the legume symbiosis in such detail that the process can be introduced into important nonlegume crops, such as rice (James et al., 2002). Because rice is also a flooding-adapted plant, intercellular invasion at lateral root bases could well be the preferred mode to be used to let nitrogen-fixing bacteria enter.

Chapter 5

Phenotypic plasticity of rhizobial invasion in semi-aquatic legumes: past, present and questions for the future

Published as: Goormachtig, S., Capoen, W., and Holsters, M. (2004). Rhizobium infection: lessons from the versatile nodulation behaviour of water-tolerant legumes. Trends Plant Sci 9, 518-522.

Water-tolerant legumes provide bacteria with special ways of invading roots to establish N_2-fixing symbiosis upon flooding. On well-aerated roots, root hair curling (RHC) invasion is used, whereas, under hydroponic conditions, rhizobia enter the cortex through cracks at lateral root bases (LRBs). Here, we compare the physiological and anatomical traits of these invasions. During waterlogging, accumulating ethylene inhibits the epidermal stages of RHC invasion. LRB invasion circumvents this step by direct colonization of the cortical tissue. By avoiding the epidermis for bacterial entry under hydroponic conditions, the stringent nodulation (Nod) factor perception systems that are active within the epidermis are not needed. Consequently, LRB invasion might be useful for analysing the requirement for Nod factor perception and other signal transduction systems downstream of the epidermis.

Introduction

Legumes that grow in nitrogen-poor soils have the peculiar ability to obtain ammonia from N2-fixing rhizobial symbionts. To this end, the plant provides specific entry methods for the rhizobia to reach the root nodule primordia and settle as N_2-fixing organelles. Bacterial invasion only occurs after a reciprocal signal exchange that determines the specificity of the interaction. Flavonoids exuded by the plant root turn on the production of nodulation (Nod) factors in rhizobia. Nod factors are lipochito-oligosaccharides that differ in the nature of the fatty acid chain, the number of GlcNAc residues and in substitutions at the reducing and non reducing end sugars. Nod factor recognition turns on the plant nodulation programme that tightly links bacterial invasion to cortical cell division (Oldroyd and Downie, 2004). Different rhizobial invasion processes have been described of which two have been studied in detail. The best-known entry mechanism is the root hair curling (RHC) process (Gage, 2004) (Figure 1, Figure 2a–c). Upon recognition of proper rhizobia, growing root hairs just above the root tip (zone I) start to curl, thereby entrapping a bacterial colony. Within this three-dimensional curl, a local hydrolysis of the cell wall takes place and an intracellular infection thread is made by invagination of the cell membrane (Kijne, 1992). The infection thread proceeds to the base of the root hair and, through cortical cells, reaches the nodule primordium. Hence, via this tubular path, the rhizobia are guided to the target cells for nitrogen fixation. For RHC, the proper Nod factors have to be recognized.

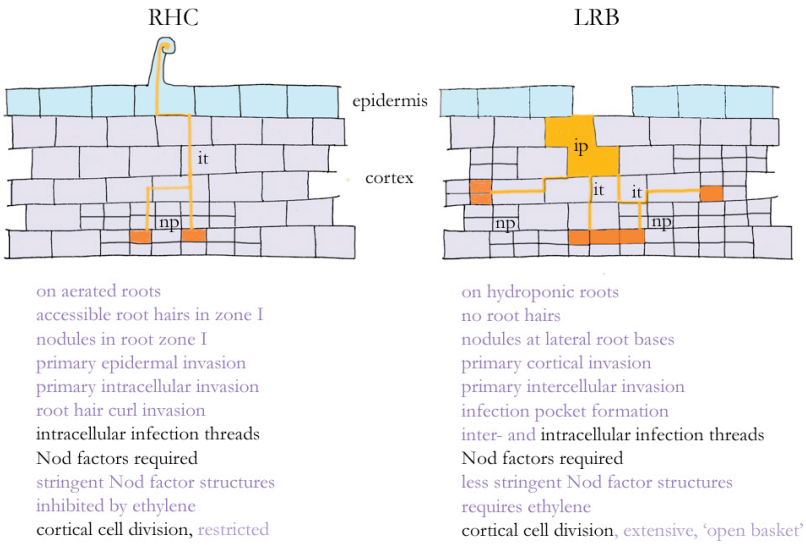

Fig. 1. Comparison of invasion pathways. (Left) Root hair curl (RHC) invasion. The bacteria (orange) are entrapped within the curl and induce the formation of an intracellular infection thread (it) within the root hair. The infection thread proceeds intracellularly towards the cells of the nodule primordium (np) where the plant cells take up the bacteria. (Right) Lateral root base (LRB) invasion. The bacteria (orange) colonize the intercellular spaces between cortical cells and induce the formation of infection pockets (ip), from which intercellular and intracellular infection threads (it) guide the bacteria to the target cells for nitrogen fixation within the nodule primordium (np). Important traits of both invasion pathways that differ or are common are indicated by purple or black text, respectively.

Purified Nod factors provoke root hair deformations and several cellular processes, such as membrane depolarization, ion fluxes across the membrane, H_2O_2 efflux inhibition, Ca^{2+}-influx and Ca^{2+}-spiking (Cullimore et al., 2001; Shaw and Long, 2003). RHC invasion is an epidermal response that occurs in members of the three subfamilies of the Leguminosae (Caesalpinioideae, Mimosideae and Papilionidae) (Sprent, 2002). The last subfamily includes important crops such as soybean, bean and pea and the model legumes *Medicago truncatula* and *Lotus japonicus*, which are all infected in this manner. An intercellular mode of entry takes place at bases of lateral or adventitious roots. Lateral roots are the side roots of the root system, whereas adventitious roots arise from a stem rather than from the primary root. Instead of using the epidermal root hair track, rhizobia directly colonize the subepidermal root tissue, the root cortex. They enter between cells via cracks in the epidermis that originate from lateral or adventitious root protrusion (Figure 1, Figure 2d–f). By inducing local cell death, intercellular infection pockets are formed that are filled with bacteria (D'Haeze et al., 2003). Further invasion varies depending on the species. Lateral root base (LRB) nodulation has been observed in tropical legumes, many (but not all) of which are (semi)aquatic. In *Sesbania rostrata* (Papilionoideae) and in *Neptunia* spp. (Mimosoideae), infection pockets narrow down to form intercellular infection threads and, subsequently, intracellular infection threads intrude into the nodule primordium (James et al., 1992; Goormachtig et al., 1998). Often, intracellular infection threads are also observed to start immediately from the infection pockets. In *Aeschynomene*, *Stylosanthes* and *Arachis* (Papilionoideae), invasion progresses via cell collapse; bacteria from infection pockets are taken up directly by the nodule cells (Chandler et al., 1982; Alazard and Duhoux, 1990; Loureiro et al., 1995; Boogerd and vanRossum, 1997).It is interesting that although *S. rostrata* and *Neptunia* spp. are infected by bacteria via the LRB pathway under hydroponic conditions, RHC invasion was observed in well-aerated roots growing in vermiculite (Figure 2a–c) (Goormachtig et al., 2004). Thus, the two invasion programmes occur in the same plant and the root growth conditions determine how and where the bacteria will colonize the host. Because the versatile invasion routes occur in representatives of the two largest of the three subfamilies, the underlying processes might be fundamental in legumes. Both invasion processes result in a similar product, the nodule, and both depend on the recognition of Nod factors. It is unlikely that two completely independent genetic pathways have evolved to allow nodule formation. Therefore, *S. rostrata* is a useful tool to compare these invasion routes. We illustrate here the differences and similarities between the two routes, and suggest how the study of LRB nodulation will help to solve some infection- related questions that are difficult to address with RHC infection.

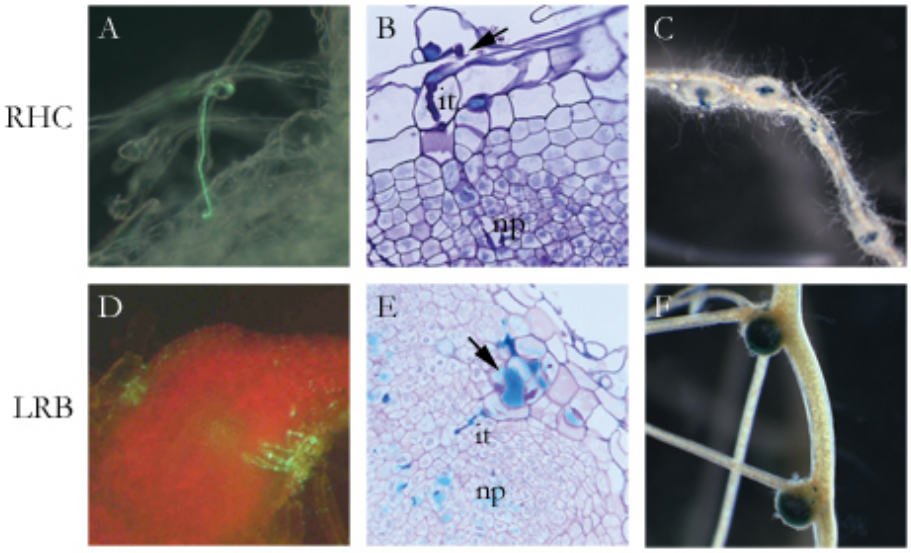

Fig. 2. Two invasion routes provided by the tropical legume *Sesbania rostrata* for its microsymbiont *Azorhizobium caulinodans:*
root hair curl (RHC) infection during aerated growth (A-C) and lateral root base (LRB) intercellular infection during hydroponic growth (D–F). A. *A. caulinodans* labelled with green fluorescent protein enters the root hairs via an intracellular infection thread.B. Toluidine-blue-stained section through a developing nodule after RHC invasion. The arrow indicates the intracellular infection thread (it) within the root hair. C. The end product: nodules are distributed over the root. D. Developing nodule at a lateral root base. The entry track is visualized by bacteria labelled with green fluorescent protein. The infection threads that initiate from the infection pockets are seen as green fluorescent tracks. E. Toluidine-blue stained semi-thin section through a developing nodule. The bacteria are labelled with β-glucuronidase (GUS). The arrow indicates the infection pockets. F. The end product: nodules at lateral root bases. Bacteria are labeled with GUS. Abbreviation: np, nodule primordium. Scale bars A-C, E.F 100 μm; D 500 μm.

Infection pockets are the functional equivalent of the rhizobial colony within the three-dimensional curl.

Bacteria in infection pockets and in the microcolony in the RHC are the last external populations before the microsymbionts enter the host tissues. To form infection threads in root hairs, rhizobia have to be entrapped in an occluded space, usually provided in a three-dimensional curl (the 'shepherd's crook'), although infection threads can also initiate at sites where rhizobia are caught between two adjacent root hairs (Kijne, 1992). By being entrapped in a curl, the rhizobia might produce the crucial amounts of primary signals (such as Nod factors, lipopolysaccharides and extracellular polysaccharides) needed to initiate the plant responses. Thus, the microcolony serves as a signalling centre that allows bacteria to enter the root hair and will also induce division of cortical cells to create the nodule primordium. The same is probably true for the bacterial population in the infection pockets that produces the signals needed to initiate the symbiosis programme. The signal coming from the infection pockets is expected to be stronger than that from the microcolony in the curl because of the larger bacterial populations (infection pockets are the size of one to three cortical plant cells; Figure 1, Figure 2e) (D'Haeze et al., 2003). During LRB nodulation, the nodule primordium develops as a concentric open-basket structure around an infection centre, a trait that might be linked to the high signal levels emitted from the infection

pockets (Figure 1). Inward growth of the plasma membrane against the turgor pressure of the cell is required for intracellular infection thread growth. Cytoskeletal rearrangements (Timmers et al., 1999) and osmotic phenomena could facilitate this process. Entrapment of bacteria to exert a mechanical force on the plant plasma membrane could be achieved by occlusion and insolubilization of extensins via H_2O_2-driven cross linking within the extracellular matrix in the older parts of the infection threads but not in their growing tips (Wisniewski et al., 2000; Rathbun et al., 2002). A family of extensin-like glycoproteins has been identified in the lumen of the infection threads during pea nodulation (Rathbun et al., 2002). An orthologous extensin-encoding gene is expressed in cells around the infection pockets in *S. rostrata* (Goormachtig et al., 1998) (S. Goormachtig et al., unpublished) and H_2O_2 has been localized within the lumen of the infection threads during RHC invasion of *Medicago* and within infection pockets and infection threads during LRB invasion of *S. rostrata* (Santos et al., 2001; D'Haeze et al., 2003).Once an infection thread reaches the base of a root haircell, it has to traverse cell walls and reinitiate growth in cortical cells (Kijne, 1992). Cortical cells that prepare for infection thread passage develop a pre-infection thread, which is a cytoplasmic bridge. Pre-infection threads are only observed in cortical cells, not in epidermal cells. Thus, infection thread growth through epidermal cells requires different cellular processes. In summary, the fundamental difference between the LRB and RHC invasions resides in the primary colonization and entry: for RHC invasion the response is epidermal, where as, for LRB invasion it is cortical (Figure 1).By colonizing the cortical cells, the epidermis has been circumvented during LRB invasion. Both processes come together at the level of intracellular infection thread growth in cortical cells (Figure 1).

Why must epidermal invasion be circumvented under submergence?

Submergence of vermiculite-grown *S. rostrata* roots at the time of inoculation blocks the RHC process. Root hair deformations are still observed but shepherd's crooks with bacterial colonies are lacking, which indicates that the aquatic conditions inhibit this epidermal response (Goormachtig et al., 2004). A key regulator of aquatic growth and water-adapted responses of plants is ethylene, a gaseous hormone that diffuses 1000 times more slowly in water than in air. Ethylene is also a key regulator of nodulation: it controls the nodule position opposite protoxylem poles (Heidstra et al., 1997) as well as RHC invasion, but how it does this and at which level varies depending on the plant species (Guinel and Geil, 2002; Ferguson and Mathesius, 2003). In legumes such as M. truncatula, L. japonicus and vetch, but not in bean and soybean, ethylene regulates the number of successful infections. In *M. truncatula*, only 3–8% of the infections that are initiated in root hairs persist; the other infection threads are arrested in the epidermis (Penmetsa and Cook, 1997). A mutant of *M. truncatula, skl*, which is insensitive to ethylene, has far more persistent root hair infections, which indicates that ethylene is involved in the inhibition of infection thread growth in the epidermis (Penmetsa and Cook, 1997).

Ethylene inhibits the Ca^{2+}-spiking response within *M. truncatula* root hairs that are exposed to Nod factors and interferes with the Nod factor signal transduction pathway in the root hair (Oldroyd et al., 2001). As well as interfering with the RHC response of accessible root hairs, ethylene also hinders the initiation of root hairs in semiaquatic legumes (Figure 2). Roots of *S. rostrata* and *Neptunia* grown hydroponically have no root hairs, whereas those grown under well-aerated conditions have plenty of root hairs in the zone I (Goormachtig et al., 2004). Root hair growth is restored partially by pharmacological blocking of ethylene synthesis under hydroponic conditions, and these root hairs are sensitive to curling. Taken together, ethylene that accumulates upon waterlogging inhibits initiation of root hair growth and some steps of the RHC process. To cope with the variable conditions of their habitat, semiaquatic legume plants had to evolve an alternative infection pathway, independent of the root

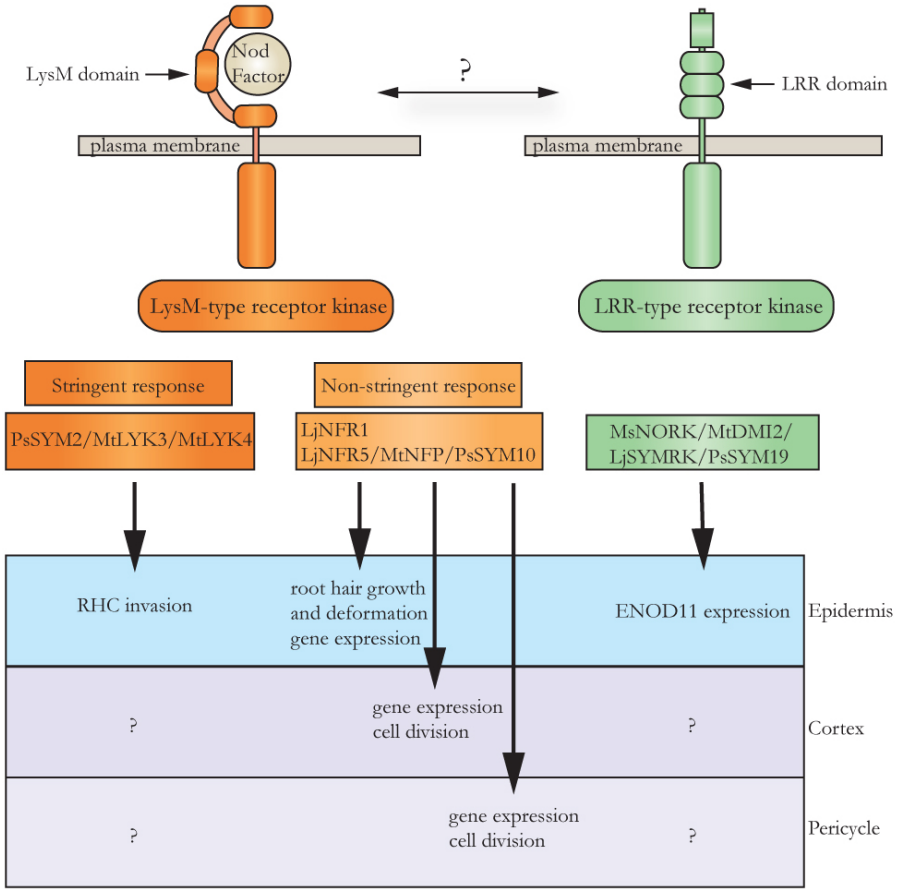

Fig. 3. Overview of receptor kinases involved in nodule initiation via root hair curl (RHC) invasion along with the processes they might control.
LysM-type receptor kinases might bind the nodulation factor (NF), could work as (hetero)dimers and might interact with leucine-rich-repeat (LRR) receptors, whose ligands are unknown. NF structure requirements for different downstream processes could be more stringent for epidermal intracellular invasion (RHC). The LRR receptor kinases are required for both vesicular arbuscular mycorrhiza and rhizobial symbiosis and could play a role in entry and establishment of the invading symbiont {Parniske, 2000 #222}. PsSYM2, MtLYK3 and MtLYK4; LjNFR5, MtNFP and PsSYM10; MsNORK, MtDMI2, LjSYMRK and PsSYM19 are orthologues. Abbreviations: Lj, Lotus japonicus; Ms, Medicago sativa; Mt, Medicago truncatula; Ps, Pisum sativum.

epidermis. To nodulate in water, an invasion track has been recruited that depends on ethylene. Indeed, ethylene is essential for infection pocket formation, an important stage of the LRB invasion and reminiscent of aerenchyma formation (D'Haeze et al., 2003).

Structural requirements of Nod factors and the consequences for signalling in RHC and LRB nodulation

Nod factors are perceived by specific receptors, and components of the signal transduction mechanism have recently been cloned (Endre et al., 2002; Stracke et al., 2002; Limpens et al., 2003; Madsen et al., 2003; Radutoiu et al., 2003; Ané et al., 2004; Lévy et al., 2004; Mitra et al., 2004) (Figure 3). A two-receptor model for Nod factor perception has been proposed: a signalling receptor (complex) that has only a low structural Nod factor requirement would be essential for nodule formation, whereas a second perception system would be involved in the bacterial uptake during the RHC process and would only recognize specific Nod factor structures (Ardourel et al., 1994; Geurts et al., 1997; Walker and Downie, 2000). The recently cloned receptor kinases *Nfr5* and *Nfr1* from L. japonicus might correspond to signalling receptors because mutations result in a NodK phenotype (Madsen et al., 2003; Radutoiu et al., 2003) (Figure 3). By contrast, the *Sym2* gene of pea and its putative *M. truncatula* orthologues *Lyk3* and *Lyk4* could correspond to uptake receptors (Limpens et al., 2003). Within their extracellular domains, all these receptor-like kinases have LysM motifs that are known to be involved in binding of bacterial peptidoglycan, thus making them good candidates to bind Nod factors directly (Spaink, 2004) (Figure 3). The presence of the Sym2A allele of *Pisum sativum cv. Afghanistan* allows uptake only of *Rhizobium leguminosarum bv. viciae* strains that produce Nod factors with an acetyl group modification at the reducing end sugar (Geurts et al., 1997). Production of Nod factors without this acetyl group by *R. leguminosarum bv. viciae* could provoke cortical cell division in the inner cortex and Enod12 expression in the epidermis but hardly any infection threads were formed and the few that were observed were arrested in the root epidermis. It is interesting that the *Sym2* gene is only active in the epidermis, as shown with a temperature sensitive allele (Geurts et al., 1997). If the uptake receptor system functioned only in the epidermis, as suggested by the experimental evidence, bacterial invasion via LRB invasion would not need structural requirements as stringent as those for RHC invasion. *Azorhizobium caulinodans*, the *S. rostrata* microsymbiont, produces mainly pentameric Nod factors with a common fatty acid, an N-methyl and a 6-O-carbamoyl group at the non-reducing-end GlcNAc residue, and with a D-arabinosyl group, an L-fucosyl group or both at the reducing-end GlcNAc (Mergaert et al., 1993). By using bacterial mutants that produce altered Nod factors, none of the substituents has been shown to be strictly required for LRB nodulation, although the nodulation frequency is determined by their synergistic presence (D'Haeze et al., 2000). By contrast, *A. caulinodans* that produces Nod factors without the glycosyl groups at the reducing end and the arabinosyl moiety at the non-reducing end cannot enter the host by the RHC mechanism. Root hair deformations, root

hair curls and cortical cell division are still observed, but no intracellular infections are seen within the root hairs (Goormachtig et al., 2004). Thus, uptake in the epidermal root hair requires more stringent Nod factor structures than does the cortical LRB entry, supporting the presence of a more specific uptake receptor in the epidermis. LysM protein kinases are now being cloned from *S. rostrata* to generate knockout lines to study their role in RHC and LRB invasion. We expect the uptake receptor not to be involved in LRB infection, whereas knockout lines of the signalling receptor homologues should give a NodK phenotype in both RHC and LRB nodulation. Another receptor-like kinase involved, this time in both rhizobial and mycorrhizal symbioses, is *NORK* of *Medicago sativa* and *SymRK* of *L. japonicus* (Endre et al., 2002; Stracke et al., 2002) (Figure 3). This receptor has an extracellular domain with leucine-rich repeats potentially recognizing a ligand of proteinaceous nature and might be part of a receptor complex with a basic function in the establishment of intracellular symbioses (Parniske, 2000). Recently, the arrested curling part of the nodulation phenotype of the NORK mutants has been suggested to be attributed to an elevated touch sensitivity (Esseling et al., 2004). Touch responses might play a role in bacterial uptake because the root hair or cortical cells should have a mechanism to sense the mechanical force needed for plasma membrane invagination. Therefore, it will be interesting to analyse the role of NORK in LRB invasion. Plenty of questions still need to be answered, making the picture more complex as more information is becoming available. It is clear that the study of LRB invasion can enrich our knowledge of rhizobial infection in general. It has been a long-standing goal of legume researchers to understand the legume–rhizobia symbiosis sufficiently to be able to transfer the process to important crops such as rice. Because rice is a water-stress-tolerant plant, lessons learnt from working with *S. rostrata* might be important to keep in mind.

Chapter 6

Transcript profiles of *S. rostrata* nodulation reveal important differences between inter- and intracellular invasion

Infection thread formation in curled root hairs is the common way of entry for rhizobia to initiate a N_2-fixing symbiosis with legumes. As this epidermal invasion is inhibited by ethylene, aquatic legumes provide a second mode of entry that involves intercellular cortical invasion at lateral root bases. Depending on the physiological conditions one of both modes of invasion is offered to *Azorhizobium caulinodans* to infect the semi-aquatic legume *S. rostrata*. The main difference between both processes is the circumvention of the epidermis during lateral root based nodulation. To distinguish both invasion ways at the molecular level, a large-scale cDNA-AFLP based comparison of the respective transcript profiles has been performed. We identified clusters that can be linked to known morphological events during nodule formation, implicating them in the regulation of these events. Several new regulatory pathways can be predicted based on the dataset and are discussed.

Introduction

Legume plants can thrive in nitrogen poor habitats because of their ability to engage in a symbiotic interaction with a group of soil borne bacteria collectively called rhizobia. Bacterial Nod factors (NF) are the key signaling molecules that prime the plants for nodule initiation. (D'Haeze and Holsters, 2002; Geurts and Bisseling, 2002; Limpens and Bisseling, 2003). Nod factors are lipochitoöligosaccharide molecules with strain-specific decorations that determine the host-specific recognition between the two symbionts. The concerted actions of several developmental programmes resulting in bacterial invasion and *de novo* cortical cell division give rise to nodules which are specialized and highly complex organs, in which the differentiated bacteria fix atmospheric nitrogen.

Two different invasion strategies have been studied in detail (reviewed in Goormachtig et al., 1998; Patriarca et al., 2004). The best-studied one involves the deformation and subsequent curling of susceptible root hair cells in the elongation zone I of the root. A bacterial microcolony becomes entrapped in the curl and the bacteria invade this root hair cell intracellularly. Local cell wall hydrolysis and invagination of the membrane precedes the formation of the infection thread (IT). This tubular IT of both plant and bacterial origin guides the bacteria through the epidermal and cortical cell layers towards an incipient nodule primordium. Once the ITs reach the nodule primordium a meristematic zone is established and the offspring of this meristem are the cells that eventually take up the differentiating bacteria resulting in the central tissue of the nodule where nitrogen fixation ensues (Gage, 2004). The meristem can either be persistent in indeterminate nodules, or not, resulting in a determinate nodule type. Indeterminate nodules are cylindrical in shape and maintain a zonated structure. A single longitudinal section shows an apical meristem, the adjacent infection zone, were bacteria are released from the ITs and the fixation zone where bacteria have differentiated and fill the complete plant cell (Mylona et al., 1995). Determinate nodules are characterized by a round shape because the meristem rapidly shuts off. Further growth is achieved through cell (Mylona et al., 1995).

Nod factor signaling is responsible for the induction of root hair curling and IT formation and for the initiation of cell division. Upon NF recognition by specific receptors, an abundance of responses, including ion fluxes, membrane depolarization, phosholipase activity, phospholipid signaling and calcium spiking is activated (D'Haeze and Holsters, 2002). Studying bacterial as well as plant mutants that show defects in the root hair curling invasion has led to the hypothesis that Nod factor perception and action can be split into two pathways. The first pathway, the signaling pathway, primes the plant for bacterial entry and cortical cell division and only requires low NF structural demands, while a second NF sensing mechanism is activated by recognition of strictly host specific Nod factors and allows IT formation and bacterial entry in the curled root hair. It has been proposed that this stringent recognition is only active within the epidermis (Geurts et al., 1997), which is also

the site for other nodulation checkpoints such as the sensitivity to ethylene.

Another invasion track involves the direct cortical colonization of lateral (LRB) and adventitious root bases, the best studied example is the interaction between the semi-aquatic legume *Sesbania rostrata* and *Azorhizobium caulinodans*. Here, no epidermal entry stages are apparent and the bacteria gain direct access to the cortex via epidermal cracks at the sites of lateral or adventitious root protrusion (Den Herder et al., 2006). A few cortical cells undergo a Nod factor dependent form of programmed cell death to form cavities that are colonized by the bacteria. These so-called infection pockets (IP) serve as a launching point for inter- and intracellular infection threads growing towards the incipient nodule primordium (D'Haeze et al., 2003; Goormachtig et al., 2004a). Subsequent nodule development is of a chimeric nature. During the early stage of nodule development, the nodule primordium surrounds the IPs in a basket shape. Distally in this 'open basket', a meristem is visible, also an infection zone and a young fixation zone are present. Later on, however, the meristem activity ceases resulting in a determinate nodule (Goormachtig et al., 1998).

Recently it was shown that both aforementioned invasion strategies occur in *S. rostrata*, depending on physiological conditions (Goormachtig et al., 2004a; Goormachtig et al., 2004b). Under well-aerated conditions, the bacteria invade the plant by means of root hair curling invasion (RHC). Under hydroponic conditions however, when ethylene that accumulates in the roots block epidermal entry, a switch is made to the intercellular invasion at the lateral root bases (LRB), enabling the roots to nodulate upon submergence (Goormachtig et al., 2004a; Goormachtig et al., 2004b).

The occurence of both invasion strategies on the same plant allows a comparison of the molecular mechanisms governing both processes. As mentioned before, hydroponic nodulation occurs without intervention of epidermal responses, in contrast to nodulation in aerated conditions where the epidermal root hairs are involved in the initial stages of the response (Goormachtig et al., 2004a). The Nod factor structural requirements are higher for root hair curling invasion compared to crack entry invasion (Goormachtig et al., 2004b), supporting the hypothesis of the presence of stringent epidermal checkpoints for entry (Ardourel et al., 1994).

The advent of high throughput expression analysis tools such as cDNA-AFLP, micro-array platforms, suppressive subtractive hybridization, SAGE (Serial Analysis of Gene Expression) analysis and EST library sequencing has greatly improved our knowledge of the molecular mechanisms governing nodule initiation and development (Fedorova et al., 2002; Poulsen and Podenphant, 2002; Colebatch et al., 2004; El Yahyaoui et al., 2004; Kuster et al., 2004; Manthey et al., 2004; Mitra and Long, 2004; Schroeyers et al., 2004; Asamizu et al., 2005; Lohar et al., 2005). So far, however, all studies were limited to one invasion system. Here we describe a large-scale analysis in which we compared transcription profiles of root hair curling and lateral root based invasion in *S.*

rostrata. We applied the PCR-based transcript profiling method cDNA-AFLP because of its high sensitivity and reproducibility (Bachem et al., 1996; Breyne et al., 2003). Approximately 7000 genes were screened, resulting in 646 differentially expressed tags. Statistical analysis of the dataset revealed a core group of genes common to both invasion ways. A large number of genes however, were specifically expressed in one of both invasion systems. We will discuss this dataset, and integrate these findings into the existing knowledge of the system and put forth several hypotheses concerning the physiology of the nodule.

Materials and methods

Plant material and bacterial strains

S. rostrata seedlings were germinated and subsequently grown in either tubes containing liquid medium or in Leonard jars as described (Goormachtig et al., 1995; Fernandez-Lopez et al., 1998). Plants were inoculated with *A. caulinodans* ORS571(pBBR5-hem-gfp5-S65T) or ORS571-V44(pBBR5-hem-gfp5-S65T) (Van den Eede et al., 1987; D'Haeze et al., 2004).

RNA extraction and cDNA synthesis

Samples from appropriate stages were excised and frozen in liquid nitrogen until RNA purification. RNA was extracted as described (Kiefer et al., 2000). Subsequently, template preparation was performed using 2 μg of total RNA (Breyne et al., 2003). Preamplification was done using an MseI primer without selective bases and a BstYI primer with a T at the 3' end, thus reducing mixture complexity by a factor of 2. Finally, selective amplification was performed with the most selective nucleotides (+2/+2), resulting in 128 possible primer combinations. This resulted in a maximal reduction in template complexity, thus simplifying later analysis and band isolation.

cDNA-AFLP experiments

Subsequent cDNA-AFLP experiments were performed as described (Breyne *et al.,* 2002, see material and methods). Gels were scored using the AFLP-QuantarTMPro (Keygene, Wageningen, The Netherlands) and were further analyzed using a Microsoft Access based software application (ArrayAN) (Vandenabeele et al., 2003). Normalization was done based on the intensity levels of constitutive bands in each primer combination. A correction factor was introduced to account for differences in lane intensity due to loading differences. This factor was calculated by dividing the sum of all individual band intensities within one lane by the average of all sums within the respective primer combination. Each band intensity value was then divided by this correction factor. A coefficient of variation (CV) was then calculated as the standard deviation on all values of the time course divided by the average expression over the time course.

Within each primer combination, 5% of the genes with the lowest CV value were marked as constitutively expressed. Per lane (time point) the intensities of these bands were summed and divided by the average of the sum. This generated a second correction factor that was used to normalize the raw expression

data generated by AFLP-QuantarTMPro. The CV was again calculated on these normalized data for each gene. This CV value was used as a selection criterion for differential expression (Vandenabeele et al., 2003). A cut off value of $\log_2(CV) = 0.1$ was used as the criterion for differential expression. Hierarchical clustering was performed using the Multiple Experiment Viewer (MeV, TIGR) software (Saeed et al., 2003).

Fragment isolation, sequencing and identification

Fragments of interest were excised by superimposing the dried gel with an autoradiography of the gel. Fragments were eluted by incubating in 100 μl distilled water for 1 hour. 5 μl of the eluate was then used as a template for subsequent reamplification. PCR reactions were performed with the corresponding +2/+2 primer combinations. The resulting amplicons were sequenced directly and low quality sequences were removed from the dataset.

The obtained sequences were analyzed as follows. All sequences were compared to the non redundant protein database at EMBL and to the *Medicago truncatula* Gene Index (MTGI) at TIGR using BLASTX and BLASTN algorithms respectively (Altschul et al., 1997). Tags showing homology (cut off: $E<10^{-3}$) to accessions in either database were withheld in the final database.

qRT-PCR analysis

qRT-PCR analysis was done a described using tissue obtained from a biological repeat (Vlieghe et al., 2005). First strand cDNA was synthesized using a Superscript RT II cDNA synthesis kit (Invitrogen, Carlsbad, USA). qRT-PCRs were performed using the SYBR Green kit (Eurogentec, Seraing, Belgium). Reactions were run on the iCycler iQ (Bio-Rad, Hercules, USA). A ubiquitin gene was used as a constitutive control (Corich et al., 1998). All reactions were performed in triplicate and averaged. Normalization of qRT-PCR data was performed using the $2^{-\Delta\Delta C_T}$ method as described (Livak and Schmittgen, 2001).

gene	Sense Primer	Anti-sense Primer
Srubiquitine1	GGGAAGCAGTTGGAGGATGG	AGACGCAGAACAAGGTGAAGG
WC002-BT11M22-259.3	TTGCCGCGCATAGACAGATG	TCTTTCAAACGCTTCACGTCAG
WC020BT23M14-343.0	CTGTGAGAGCCTGGTTAGACTG	CATCATAAGGCCACCGGATAGG
WC022BT24M13-265.0	GGGTTATGGAATATGTGCTGCTTG	GCTGCCACAACCACCTCTG
WC024BT24M42-288.2	TTCGGTTGTGTGCTCTGATCC	GGCAGCGATGAATAAGTTGTGG
WC029T31M41-395.6	GGAAGCCTAGCCACCAATTTAGC	TACAGTGATGGGACTCCTTACTTG
WC041BT42M22-281.9	ACCGCATTGTGATCCAACG	ACAAAGGCATTAGGATGAGGTC
WC043BT43M22-372.0	AATGTGGAAGAGGGCAGGATAG	CATACCCAACGCCAAGTAAGTC
WC048BT32M12-658.6	GAAGTGGCGGCGGTTATGG	AGACCAGCAAACCCTTCATCG

Results

Experimental setup and cDNA analysis

Wild type *S. rostrata* plants were grown either in Leonard jars to favor root hair curling invasion (RHC) or in tubes containing liquid medium to favor lateral root base nodulation

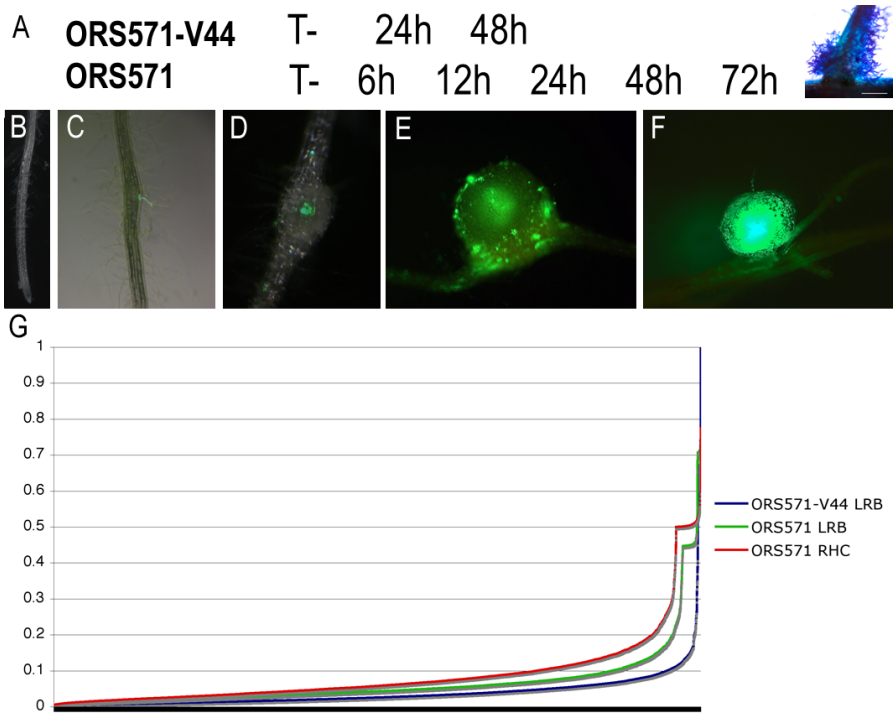

Fig. 1 Tissue sampling and analysis of differentially expressed cDNA-AFLP tags
A. For the series in hydroponic conditions plants were inoculated with either *A. caulinodans* ORS571-V44, a strain deficient in NF production, or *A. caulinodans* ORS571, both of which contain a gfp expressing plasmid for visualization with fluorescence microscopy (see material and methods). Timepoints at which lateral root bases (inset) were harvested are indicated. As a negative control LRBs of uninoculated plants were harvested (T-). B-F To avoid signal dilution, a morphology based approach was used for plants grown in vermiculite. As a negative control, 1.5 cm long root root segments without the apical meristem were harvested (B). From inoculated plants, small root fragments with infection threads were excised (C, rhc1, ± 24-36 hpi), root fragments with infection threads and bumps indicative of cortical cell divisions were harvested next (D, rhc2, ±48-60 hpi). Primordia before the onset of nitrogen fixation (E, rhc3, ±72-100 hpi) and young fixing nodules (F, rhc4, ±140 hpi) were also harvested. G. Plot of sorted log CV values. RHC samples contain more differentially expressed tags compared to hydroponic samples and LRB samples have more differentially expressed than ORS571-V44 inoculated samples.

(Goormachtig et al., 2004b). Approximately 900 plants in Leonard jars were inoculated with *A. caulinodans* ORS571 (pBBR5-*hem*-gfp5-S65T) containing a gfp reporter plasmid driven by the constitutive *Sinorhizobium meliloti* ∂-aminolevulinic acid synthase promoter (D'Haeze et al., 2004). The hydroponically grown plants were inoculated with either the same gfp expressing wild type strain or with a mutant strain ORS571-V44 (pBBR-*hem*-gfp-S65T) that contains a Tn5 insertion in the *nodA* gene impairing Nod factor production (D'Haeze et al., 1998). Use of this mutant strain enabled us to distinguish between differentially expressed genes as a result of growth conditions and differential expression linked to nodule development.

Fluorescent stereomicroscopy was used to specifically harvest tissues in the process of invasion, thus allowing a significant enrichment of reactive tissue. For the hydroponically grown material a time based harvesting strategy was chosen based on the high synchronicity of the system. Uninoculated LRBs and LRBs 6, 12, 24, 48 and 72 hours post inoculation (hpi) were collected. For the time course with *A. caulinodans* ORS-571-V44 (pBBR-*hem*-gfp-S65T), uninoculated LRBs and LRBs 24 and 48 hpi were taken. Because

nodulation in Leonard jars for root hair curling invasion is not synchronized a morphology based harvesting procedure was used (Figure 1A). As a negative control, uninoculated lateral root fragments corresponding to the zone directly behind the root apical meristem were harvested, and the root apical meristem (RAM) was removed (designated rhc0) (Fig. 1B). From inoculated plants, small root fragments with infection thread containing root hairs (rhc1, ± 24-36 hpi) (Fig. 1C), root fragments with infection threads and small bumps indicating cortical cell activation (rhc2, ±48-60 hpi)(Fig. 1D), young primordia before the onset of nitrogen fixation (rhc3, ±72-100 hpi)(Fig. 1E) and young fixing nodules (rhc4, ±140 hpi)(Fig. 1F) were excised.

Using these samples, a cDNA-AFLP transcript profiling experiment was performed to identify genes that were differentially regulated during nodule initiation in *S. rostrata* in hydroponic or aeroponic conditions (see material and methods). In total 128 primer combinations were analyzed, which allowed visualization of some 7000 transcript derived tags (Fig. 1G). In order to determine what could be considered differential, a graph was made plotting about 3000 tags, arranged by ascending $\log_2$(CV) (see material and methods). A distinct change in the curve was visible around $\log_2$(CV) = 0.1 (Fig. x). As a consequence, a tag was considered differential if its $\log_2$(CV) was 0.1 or higher in any of the three time series. This resulted in 646 genes that were withheld for further study. These showed a significantly differential expression pattern in either the RHC or LRB nodulation systems or in both and gave a significant blast hit (E-value < 10^{-3}) to sequences in public databases (Altschul et al., 1997).

Cluster analysis

In order to get a first insight into similarities between the transcript pools of each sample, hierarchical clustering of all experiments was performed with the Pearson correlation as a statistical tool (see material and methods). As seen in Figure 2A, the base of the tree consists of the V44 series corresponding to unresponsive tissue and the inoculated tissues are separated in three different clusters. The early LRB stages, crack 6h, 12h and 24 h form a subcluster, the RHC 24h forms a separate cluster and the late time points of both the RHC and LRB samples, i.e. from 48 hours after inoculation onward, cluster together. This suggests that the onset of each invasion way is characterized by specific gene expression and that there are a high number of commonalities between the two invasion ways at later stages, corresponding to primordium formation and nodule differentiation.

Next, cluster analysis of all gene tags revealed several distinct expression profiles. For convenience, tags were separated into ‘common’ and ‘non-common’ groups. ‘Common’ refers to genes similarly regulated in both LRB and RHC nodulation (fig. 2B), whereas ‘non-common’ refers to genes that are specifically expressed in one experiment, being either LRB nodulation, root hair curling

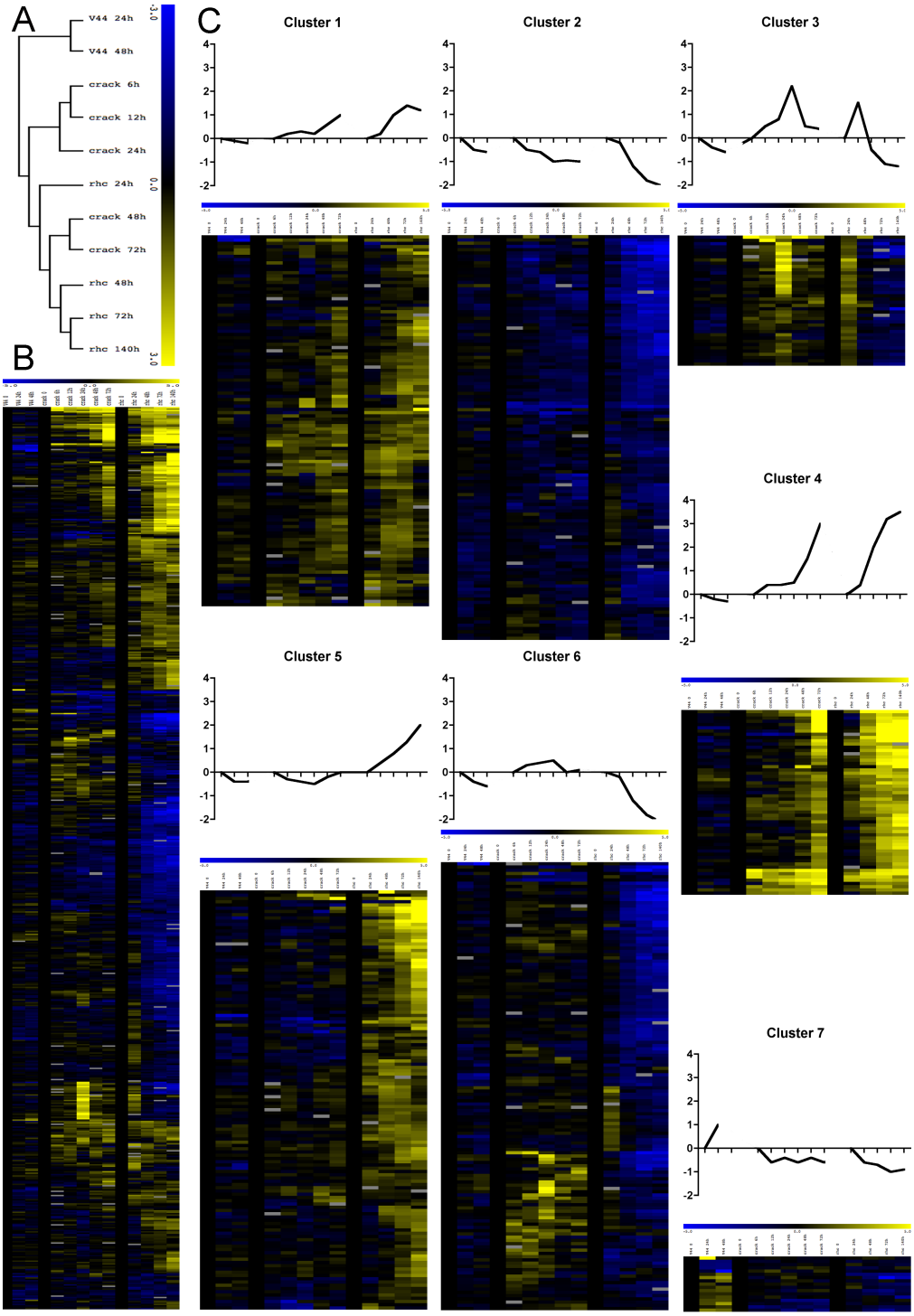

Fig. 2 Cluster analysis
A. Hierarchical clustering of sample expression profiles visualizes the similarities in expression patterns of late time points. Before 48 hours after inoculation, differences between samples are more pronounced than after 48 hours, roughly corresponding with nodule development. B. Hierarchical clustering of all 646 differentially expressed tags. Gene tags with a log CV of at least 0.1 (corresponding to a 2 fold change in expression) were sequenced and expression profiles of the corresponding genes were clustered. The blue color indicates downregulation, yellow indicates upregulation. C. K Means Clustering of differentially expressed gene tags. Clusters 1 to 4 are considered common clusters, Cluster 5 harbours the root hair curling specific genes, whereas cluster 6 contains crack entry specific tags. Finally, clusters 7 contains tags specifically upregulated upon ORS571-V44 inoculation. Time points are given in Fig. 1, inoculation series from left to right are V44, hydroponically grown roots inoculated with *A.caulinodans* ORS571-V44; crack, hydroponically grown roots inoculated with wild type *A.caulinodans* ORS571; rhc, aerated roots inoculated with wild type *A.caulinodans* ORS571.

nodulation, LRBs treated with ORS571-V44 or expressed in LRBs treated with both ORS571 and ORS571-V44 indicating specific gene expression for hydroponic conditions.

K means clustering of common and specific genes resulted in 7 discernable clusters (Fig. 2C) (Full scale images of the clusters with the annotation of the tags, along with the dataset and the MultiExperiment Viewer software, can be found on the accompanying CD). Although distinctions between clusters are not always clear-cut, i.e. some clusters are more heterogeneous than others, this method does enable a comprehensive overview of the data (In what follows, cluster number will be given between brackets for clarity). Clusters 1 to 4 consist of the 337 common gene tags. On average, Cluster 1 contained tags that are upregulated in either invasion way. Cluster 2 consists of tags that show a down-regulation during both RHC and LRB nodulation. As seen in Figure 2, those tags are also down regulated in LRBs after ORS571-V44 infection, however the level of down regulation was much lower compared to both nodulation ways. Cluster 3 contains tags corresponding to genes that are transiently and commonly upregulated and finally, cluster 4 represents tags that are common but whose transcript level does not reach a plateau level at later time points. In the non-common, series specific tags, cluster 5 displays a predominantly root hair curling specific pattern, whereas cluster 6 contains tags from genes that are specifically expressed during the LRB nodulation, accompanied by some very early transient up-regulated or down regulated root hair curling genes. Cluster 7 contains genes upregulated only in the serie inoculated with ORS571-V44.

qRT-PCR analysis of differential tags confirms their differential expression during nodule initiation

In order to confirm the robustness of the data, a biological repeat was performed and qRT-PCR on a subset of tags was performed (see material and methods, Figure 3). Overall, expression profiles of tested genes was consistent with the expected expression based on the cDNA-AFLP data (Fig. 3). It often proved difficult to design suitable primers due to the short nature of many AFLP tags. Of the 14 gene tags tested in this way, 10 corresponded the pattern found previously (Fig. 3), for 2 tags the expression pattern differed in one time series but not the other (data not shown).

The presence of different functional classes in the dataset

About 32% of all tags identified in this screening consisted of genes with similarity to genes of unknown function, expressed proteins or putative genes. They were equally distributed over the different clusters. An exhaustive list of all functional classes identified in the different clusters can be found in the supplementary materials added as addendum. Although the often short length of cDNA-AFLP tags and the use of *S. rostrata* as a model, this comparison can easily obscure one to one identification of orthologous

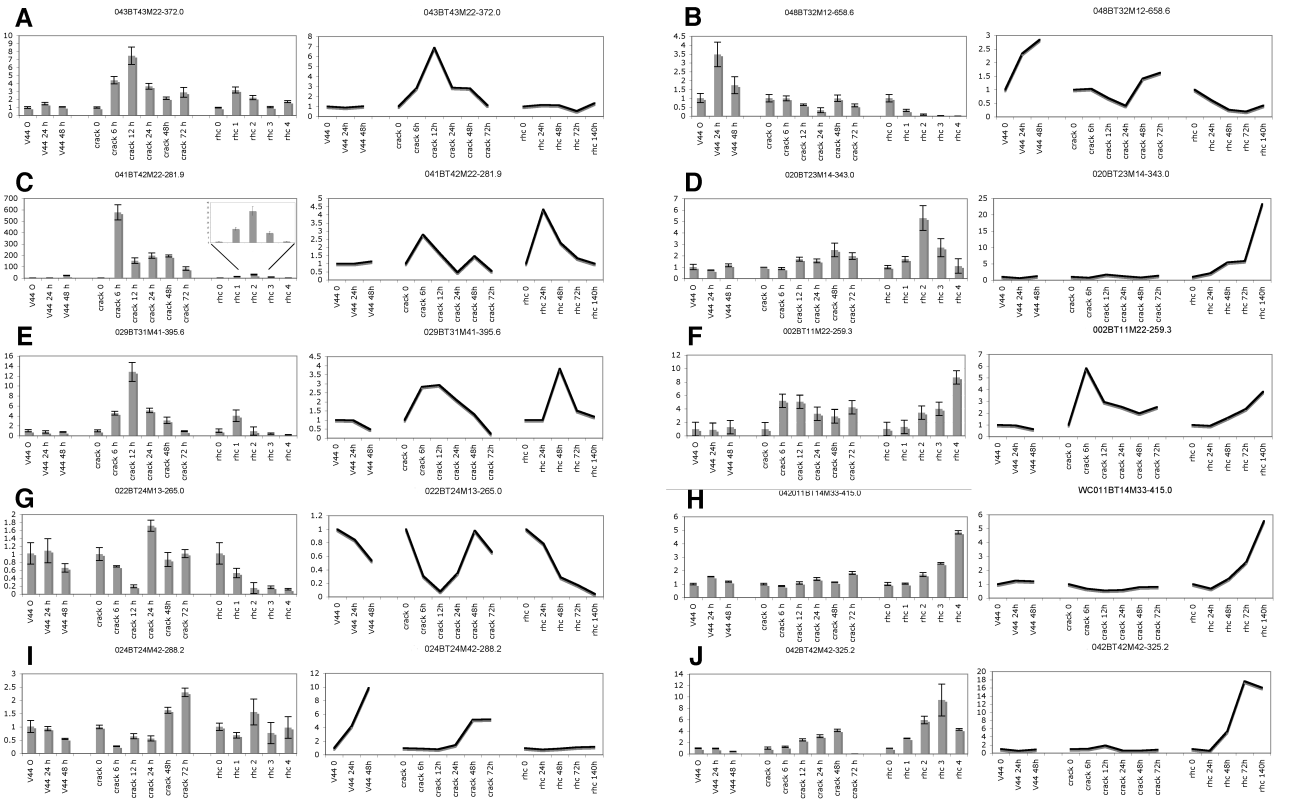

Fig. 3 qRT-PCR verification of a subset of differential tags.
A biological repeat was performed and qRT-PCR reactions were done as described (Material and Method). For every tag, qRT-PCR results are shown left (bars) and the cDNA-AFLP profile on the right (right). Expression levels are given as fold change, relative to the noninoculated controls for each series. Abbreviations: V44, hydroponically grown roots inoculated with *A.caulinodans* ORS571-V44; crack, hydroponically grown roots inoculated with wild type *A.caulinodans* ORS571; rhc, aerated roots inoculated with wild type *A.caulinodans* ORS571. Tag identity is as follows: A. 043BT43M22-372.0, Chitinase; 048BT32M12-658.6, B. L-asparaginase, C. 041BT42M22-281.9, Gibberellin 20-oxidase; D. 020BT23M14-343.0, MAP kinase NTF6; E. 029BT31M41-395.6, Subtilisin-like protease; F. 002BT11M22-259.3, response regulator protein; G. 022BT24M13-265.0, Putative low-affinity nitrate transporter; H. 011BT14M33-415.0, Yippee-like protein; I. 024BT24M42-288.2, GDSL motif lipase/hydrolase-like protein; J. 042BT42M42-325.2, MtN21 nodulin.

sequences identified in other transcript profiles (predominantly *M. truncatula*), some similarities are obvious in these datasets. 41 common or root hair curling specific tags had similar expression patterns in other, previously published transcript profiles (Table 1) (Gyorgyey et al., 2000; Colebatch et al., 2004; El Yahyaoui et al., 2004; Lohar et al., 2005). These were identified based on annotation, however, proteins with limited functional information (e.g. kinase, phosphatases, … with no known role) were not added to the set. This means that at least 7 % of the dataset has been shown to be upregulated in other transcriptome experiments, but the actual percentage is no doubt higher.

Discussion

Root hair curling invasion and lateral root base invasion in the tropical legume *Sesbania rostrata* are clearly different. LRB nodulation, as the word says, happens at lateral root bases during hydroponic growth while RHC

This work	pattern	annotation	Colebatch *et al.*, 2004	Gyorgyey *et al.*, 2000	Lohar *et al.*, 2005	El Yahyaoui *et al.*, 2004
WC003BT11M44-404.8	common up	nodulin 26 (aquaporin)				
WC004BT12M21-217.7	common up	copper amine oxidase				
WC005BT12M24-260.3	rhc up	PEP carboxylase				
WC008BT13M41-222.1	rhc up	cytochrome b				
WC009BT14M13-239.2	common up	endo-β-glucanase				
WC010BT14M21-346.2	common up	nucleoid binding protein				
WC010BT14M31-285.1	common up	7 transmembrane protein				
WC010BT14M32-538.2	common up	ribosomal protein L10A				
WC011BT14M34-368.1	common up	cellulase				
WC011BT14M44-357.8	rhc up	glutamine synthetase				
WC014BT21M12-288.3	common up	CCAAT-binding TF				
WC015BT21M24-214.5	rhc up	invertase				
WC018BT22M41-268.1	common up	peroxidase				
WC020BT23M33-210.5	common down	peroxidase				
WC023BT24M24-192.7	rhc up	SPF1 protein				
WC025BT21M33-141.8	common up	metallothionein				
WC025BT22M24-261.5	rhc up	MtN21				
WC025BT22M24-345.4	common up	ferritin				
WC026BT22M43-250.2	common up	Ca-dependent protein kinase				
WC029BT31M44-432.4	common down*	Hs1Pro				
WC030BT32M23-163.8	rhc up	ankyrin				
WC034BT33M43-354.7	common up	purple acid phosphatase				
WC035BT34M12-163.6	common up	histone H2A				
WC035BT34M13-238.4	rhc down	phosphate transporter				
WC035BT34M14-177.7	common up	carbonic anhydrase				
WC035BT34M22-143.0	rhc up	amino acid transporter				
WC035BT34M22-332.6	rhc up	cellulose synthase				
WC037BT34M42-158.5	rhc up	dynamin				
WC037BT34M44-595.7	common up	AP2/EREBP domain TF				
WC037BT44M11-660.0	common up	elongation factor 1-alpha				
WC038BT41M14-183.1	rhc up	alpha-dioxygenase				
WC040BT42M12-553	common up	peptide transporter				
WC041BT42M21-195.6	comomn up	histone H4				
WC041BT42M22-146.2	common u	thioredoxin				
WC041BT42M31-268.2	rhc up	inorganic pyrophosphatase				
WC041BT42M32-170.0	rhc up	ADP ribosylation factor				
WC044BT43M23-448.9	V44 up, common down	trypsin inhibitor				
WC044BT43M34-229.8	common up	ATPase				
WC046BT44M13-377.5	rhc up	asparagine synthase (glutamine hydrolising)				
WC047BT44M31-127.4	rhc up	MtN6				
WC047BT44M42-554.0	common up	chalcone reductase				

Table 2 Comparison with other published transcripts profiles
Analysis of existing transcriptome datasets for *M. truncatula* and *L. japonicus* revealed 41 common or root hair curling specific tags had similar expression patterns with these datasets {Colebatch, 2004 #349; El Yahyaoui, 2004 #351; Gyorgyey, 2000 #339; Lohar, 2005 #381}. These commonalities were identified based on annotation, proteins with no published function (proteins with general annotations such as protein kinase, protein phosphatase, transcription factor ...) were not withheld due to uncertain one on one relationships.

invasion occurs at root hairs in the elongation zone I of the root during aerated growth. RHC involves the complex process of root hair curling within the epidermis, and presumably requires a specific stringent NF recognition is needed which is lacking during LRB invasion as the epidermis is skipped (Goormachtig et al., 2004b), while during LRB nodulation, infection pockets are formed as the result of Nod factor induced death of some cortical cells (D'Haeze et al., 2003). Common to both invasion ways is the NF dependent signaling that primes the plant for organ formation. ITs and primordia are formed, be it at different locations and in different physiological contexts, indicating that the mechanisms that underlie these processes are common to both.

A transcript profiling has been performed to identify genes that function in these different processes. Three series of samples have been compared. In one experiment, hydroponic LRBs were infected with ORS571-V44, a Nod factor deficient strain. In a second experiment, hydroponic roots were inoculated with ORS571 and in a third experiment, aeroponic roots were used. Clustering of these experiments revealed a strong correlation between early and late time points of the two nodulation series, and this provided a good control on sample quality. The clustering also elegantly showed differences between early crack entry and root hair curling time points and commonalities between late time points in both nodulation series.

A group of ‘core nodulins’ is similarly expressed in both LRB and RHC nodule formation

Of the 646 tags that were withheld for analysis, 337 tags were categorized as commonly regulated in both root hair curling and crack entry nodulation. Hierarchical clustering revealed a more refined pattern with 4 different groups. Compared to uninoculated roots, 124 tags showed a significant downregulation and some 212 tags showed upregulation. The latter belonged to 3 groups depending on intensity and timing of expression. Cluster 4 with highly upregulated tags contains several genes that have been previously reported to be nodulation-induced, among these are an aquaporin (Catalano et al., 2004), a chalcon reductase (Goormachtig et al., 1999), and ENOD18 (Hohnjec et al., 2000). Cluster 3 consists of transiently upregulated tags, the expression of which peaks between 6 and 48 hours post inoculation and then gradually returns to the basal level. Cluster 1 contains tags that are expressed at a lower level than tags in cluster 4 but also are continuously upregulated during the time-course of the experiment.

nodule functioning and maintenance

Common clusters 1 and 4 mostly consist of pathways involved in nodule functioning and maintenance. A large number of genes involved in transport of metabolites can be found. A total of 33 tags (representing 5% of the entire dataset) encode for a range of transport proteins such as nitrate transporters (1,4), an aquaporin (4), several putative amino acid transporters (2,4,), H^+-ATPases (2,), sugar transporters (1,4), several ABC type transporters (2,4,5,6) and a peptide transporter (4). Also tags that are involved in primary metabolism and respiration belong to this common cluster. indicative of the high energy demands for nodule (Prell, 2006).

Cell wall modification

IT formation and IT progression involves intensive cell wall modification (Brewin, 2004). Proline-rich proteins are essential components of cell walls and the IT matrix, (Brewin, 2004). Tags putatively coding for several (hydroxy) prolin-rich proteins (4), a lignin biosynthesis gene caffeic acid O-methyltransferase (1,4) and a cellulase (4) show a continuous upregulation throughout nodulation. Moreover ROS components have been localized in ITs and it has been put forward that H_2O_2 driven cross-linking of extensins within the IT matrix is the driving force of IT progression (Brewin, 2004). Seventeen tags displayed homology to genes known to be involved in ROS-production and metabolismm among those are tags homologous to peroxidases (2,3,4), amine oxidases (1,2), respiratory burst oxidases (NADPH oxidases, 2,6), a copper amino-oxidases (1) belong to the common class and thus might be involved in IT progression.

ROS and defense

ROS production and metabolism is also highly involved in defenses against pathogens. A significant number of tags were derived from pathogenesis related genes. Some defense-related genes were upregulated during nodulation, whereas others were downregulated. Among the downregulated genes were a TIR domain containing protein TSDC, an Hs1pro1 homolog, which is involved in nematode resistance, a beta-glucan elicitor receptor protein, a polygalacturonase-inhibitor

(2). To the upregulated clusters belonged tags homologous to genes coding for a putative avr9 elicitor response protein (3), a protein with homology to an XA21-like receptor kinase (4) and several cytochrome P450s. About 90 % of all infection events abort prematurely in *M. truncatula* probably through defense responses mounted by the plant (Pauly et al., 2006). Rhizobia need to repress defense responses and trick the plant into allowing infection, which probably requires active repression of certain defense pathways (Mithofer, 2002). On the other hand, a nodule is rich in nutrients and consequently an attractive target for pathogens, this no doubt requires the plant to become more vigilant, leading to upregulation of certain pathways. It seems likely that the plant needs to perform a molecular 'balancing act' to accomplish these endeavors. Previous transcript profiling experiments in *M. truncatula* revealed a similar behavior of known defense related genes (El Yahyaoui et al., 2004; Manthey et al., 2004).

Signal transduction and transcriptional regulation

Signaling is ubiquitously important in all aspects of development and representatives of these classes are found throughout all stages of this analysis. A lot of tags could be identified as kinases, receptor-like kinases and protein phosphatases for which functional data are lacking. Some however have been previously characterized and provide clues to their function in nodulation. Most notably, a tag homologous to an unknown LysM domain containing RLK was identified as commonly upregulated (3). The LysM domains showed 35% similarity to LjNFR5 (Madsen et al., 2003; Radutoiu et al., 2003). The gene belongs to a new, third subfamily of LysM domain containing RLKs in legumes, and RNAi-analysis revealed a possible novel role in nodulation in both *S. rostrata* and *M. truncatula* (Capoen *et al.,* in preparation).

Also a wide range of TFs was present in the dataset, some of them upregulated, others repressed. Among these are the GRAS protein GAI (a negative regulator of gibberellin action), confirming the predicted need for tight regulation of GA during nodule initiation (Lievens et al., 2005). Two Myb1-like transcripts (2,3), 2 AP2 domain containing TFs (1,2) and two WRKY transcription factors (most similar to 28 (1) and 69 (4)) were found, the *Arabidopsis* orthologues of which are differentially upregulated during biotic stress responses (www.genevestigator.ethz.ch).

Calcium signal transduction

Several tags bearing homology to calmodulin or calmodulin-like proteins (3) and a Ca^{2+}-dependent protein kinase (3) were identified. Calcium has long been proposed to play a role in signaling events during nodulation. One of the earliest cellular responses to NF within the root hairs is a rhythmic Ca^{2+}-oscillation (Ca^{2+}-spiking) that ensues within 20 minutes of NF addition, it is proposed to be one of the major signaling events preceding nodule inception (Oldroyd and Downie, 2006). No role for calcium signaling has been attributed yet to crack entry invasion but as inhibitors of Ca^{2+}-spiking inhibit nodule formation, it will surely also play an important role (Capoen *et al.,* unpublished data). The observation that those tags are present in the transiently upregulated

cluster shows that calcium signaling is important in both nodulation systems.

Phospholipid signaling

Several tags involved in phospolipid signaling were repressed during nodulation, e.g. tags showing homology to a phosphatidylinositol 3-kinase (2), an inositol 4-methyltransferase (6) and 3 tags for putative inositol polyphosphate 5-phosphatases (2,6) were found. This is striking since a role for phospholipids during early NF signaling has been proposed based on pharmacological evidence (den Hartog et al., 2003; Charron et al., 2004). Expression profiles suggest that transcripts for genes involved in these processes are present in roots but disappear rapidly, which may indicate that, although phospolipid signaling is required during early stages, it may no longer play an essential role later on during nodule development.

Meristem functions

Nodulation involves primordium formation and the differentiation of an apical nodule meristem that is transient or continuous in hydroponic or aerated conditions respectively. Interestingly, several tags showed similarity to genes involved in apical and floral meristem maintenance and differentiation and inflorescences, among these are genes coding for PETAL LOSS (2), the MADS box gene FRUITFULL (2), Nam-like protein 10 (2) and 14 (4), CONSTANS (4), the KNAT3 homeobox gene (6), GIGANTEA (6), CYCLOIDEA (5), LEUNIG (6), an interactor of IRK (for inflorescence and root apices receptor-like kinase), named IRKI (1) (Hattan et al., 2004) and a tag similar to the dem protein (defective embryo and meristem, 3 (Fig. 4) (Irish, 1999; Ferrandiz et al., 2000; Kieffer and Davies, 2001; Komeda, 2004; Veit, 2004). It has been proposed that functions from shoot and floral apical meristems have been recruited for nodule mersitem activity. For instance expression of a gibberellin-20-oxidase was observed in the direct progeny of the nodule meristem *in S. rostrata* (Lievens et al., 2005) whereas knotted homologues were localized in the nodule mersitem of *M. truncatula* (Koltai et al., 2001). Current scientific consensus states 4 pathways that control flowering time, gibberellin, the autonomous pathway, vernalization and a light-dependent pathway. It seems that elements of at least 2 of these pathways might have been recruited for nodule meristem diffentiation, i.e. gibberellin and the light dependent pathway (via the CONSTANS-like protein) (Komeda, 2004). Although literature about the presence of these gene products in roots is scarce at best, most of the genes involved in floral and apical meristem determination have ESTs in root-derived tissues (see table 2). It will be interesting to see whether or not these genes indeed play important roles during nodule initiation and development.

RHC specific gene expression

190 tags were found that are specific for root hair curling. This is about 3 times more than for the crack entry specific tags. This demonstrates that the epidermis adds an additional layer of complexity to nodule formation. Among the 190 tags that were found to be root hair curling specific, 88 were strongly downregulated, whereas 102 were

Expression Report for TC101055

Total ESTs found in TC101055: 14

Cat#	Library	# of ESTs	% of library total
#9D5	Developing flower	3	0.05
5413	Drought	2	0.02
#9D6	Germinating Seed	2	0.03
5414	Insect herbivory	2	0.02
T1617	GVN	1	0.02
T10173	HOGA	1	0.02
T10493	GPOD	1	0.03
#A8V	Phoma-infected	1	0.03
#GFK	Virus-Infected Leaves	1	0.01

Expression Report for TC102252

Total ESTs found in TC102252: 10

Cat#	Library	# of ESTs	% of library total
#9D6	Germinating Seed	3	0.04
T11031	BNIR	2	0.06
#9D5	Developing flower	2	0.03
T10494	GESD	1	0.02
T11127	GLSD	1	0.02
4047	Nodulated root	1	0.03

Expression Report for TC104631

Total ESTs found in TC104631: 3

Cat#	Library	# of ESTs	% of library total
T10493	GPOD	2	0.06
#GFM	Methyl Jasmonate-Elicited Root Cell Suspension Culture	1	0.01

Expression Report for TC109137

Total ESTs found in TC109137: 7

Cat#	Library	# of ESTs	% of library total
5520	MtBC	2	0.02
T1682	MHAM	1	0.01
T10173	HOGA	1	0.02
T11958	MTUS	1	0.02
4048	Developing root	1	0.03
#GFK	Virus-Infected Leaves	1	0.01

Expression Report for TC106609

Total ESTs found in TC106609: 52

Cat#	Library	# of ESTs	% of library total
4049	Developing stem	9	0.09
T1815	KV0	4	0.15
T1707	KV3	3	0.05
T1682	MHAM	3	0.04
T12494	Leguminosins	3	0.17
5414	Insect herbivory	3	0.03
#GFL	Aphid-Infected Shoots	3	0.06
5519	MtBB	2	0.03
5520	MtBC	2	0.02
T1510	KV2	2	0.06
T1581	DSIR	2	0.08
T1748	DSIL	2	0.03
T10494	GESD	2	0.04
#A8V	Phoma-infected	2	0.06
#GFK	Virus-Infected Leaves	2	0.03
T1617	GVN	1	0.02
T1841	KV1	1	0.04
#G8F	MtSNF	1	0.14
T10014	MGHG	1	0.04
T10493	GPOD	1	0.03
5413	Drought	1	0.01
4047	Nodulated root	1	0.03
4046	Developing leaf	1	0.01

Expression Report for TC100528

Total ESTs found in TC100528: 17

Cat#	Library	# of ESTs	% of library total
7263	Elicited cell culture	6	0.07
T1748	DSIL	4	0.07
#G8J	MtSTW	1	0.24
T11958	MTUS	1	0.02
T12308	6KUG	1	0.01
T10174	kiloclone	1	0.07
#A8V	Phoma-infected	1	0.03
4046	Developing leaf	1	0.01
4049	Developing stem	1	0.01

MtGI EST Search: BF646615

EST ID	GB #	Clone	Clone End	Cat #	TC#	Linked EST
NF066C08EC1F1065	BF646615	NF066C08EC	5'	7263	singleton	n/a

Fig. 4 TIGR expression reports for genes known to be involved in shoot apical and floral meristems.
Several tags were identified with previously published roles in floral and shoot apical meristem signaling. To further corroborate their root expression, expression data of the best hit in the *Medicago* EST database at www.TIGR.org was analysed for root and or nodule expression. TC101055, Constans-like protein 1; TC102252, Cycloidea PlCYC4 protein; TC104631, EuFUL FRUITFULL-like mads-box; TC109137, LEUNIG; TC106609, GIGANTEA protein; TC100528, NAC-domain protein 3; BF646615, Trihelix transcription factor (PETAL LOSS).
Library abbreviations; GVN, one month old nitrogen-fixing root nodules one month old nitrogen-fixing root nodules; HOGA, oligogalacturan treated roots; GPOD, pods; BNIR, nematode infected roots; GESD, early seed development, GLSD, late seed development; KV0, immediately prior to *Sinorhizobium* infection, KV3, 3 days post *Sinorhizobium* infection; MHAM, roots colonized with *Glomus versiforme*; MtBB, 4 days post *Sinorhizobium* infection; MtBC, 3 weeks post inoculation with *Glomus intraradices*; KV2, 2 days post *Sinorhizobium* infection, DSIR, roots infected with Phytophthora medicaginis; DSIL, leaves infected with Colletotrichum trifolii; KV1, 24 hours post *Sinorhizobium* infection; MtSNF, nitrogen starved roots; MGHG, *Phytophtora* elicitor treated roots; MTUS, *Medicago truncatula* unigene set; inoculated supernodulating roots.

upregulated. Two known nodulin genes *MtN6* (5) and *MtN21* (5) were strongly and specifically upregulated upon nodulation in aerated conditions. In *M. truncatula MtN6* expression was shown to precede infection and was thus proposed to play a role in the preparation of cells for infection thread passage (Mathis et al., 1999). As LRB nodulation also involves IT formation, differences in physiological conditions might account for the specific involvement of this tag in RHC invasion.

Although metabolic genes were mostly common in their expression patterns, several genes involved in amino acid biosynthesis were root hair curling specific. This is surprising as these tags are involved in processes that are thought to belong to the basic nodule physiology. It is possible that differences in tissue physiology between aerated and hydroponic growth are partly responsible. Indeterminate nodules predominantly use glutamine and asparagine as vectors for ammonium incorporation, whereas determinate nodules use ureides to this end (Prell and Poole, 2006). *S. rostrata* nodule development is in essence indeterminate, although meristem activity ceases prematurely in hydroponic conditions, explaining the presence of genes that are involved in glutamine and asparagine metabolism.

A tag homologous to the auxin efflux carrier PIN2 was identified to be root hair curling specific. It has been shown in *M. truncatula* that this tag is specifically upregulated during nodulation (Schnabel and Frugoli, 2004). Also a tag encoding an ADP-ribosylation factor (ARF) shows a highly similar expression pattern to PIN2. ARFs have been implicated in the correct targeting of both PIN2 and a ROP GTPase in growing root hair cells (Xu and Scheres, 2005a). This implicates these 3 proteins in polarization of top growing structures. Their expression pattern, exclusive to RHC invasion corroborates this and identifies these genes for further functional analysis.

Crack entry specific gene expression

Cluster 6 contains several crack entry specific tags that might be of interest in unraveling the molecular mechanisms of infection pocket formation. IP formation occurs about 24-36 hours after inoculation, hence preparation for this event would occur in this time period. A number the crack entry specific tags had a transient expression pattern during the first 24 hours. Among these, a tag similar to a hexose transporter. Recently, expression of a hexose transporter has been shown in *Arabidopsis thaliana* to correlate with the induction of programmed cell death (Norholm et al., 2006). Cluster 6 (Fig. 2C) also contains a papain-like cysteine proteinase. Papain-like proteinases have been involved in a large number of cell death related processes (Beers et al., 2000). Additionally, a GPI-anchor transamidase, a type 2A protein phosphatase, a 7 transmembrane protein and the cytokinin receptor CRE1 were present. We also found a tag similar to an Arabidopsis hydrolase (At2g14110) that was slightly differentially expressed upon osmotic stress and senescence induced PCD, and a basic helix

loop helix transcription factor (At4g37850), the Arabidopsis homolog of which was strongly upregulated upon *Pseudomonas* infection, salt stress and jasmonate treatment (www.genevestigator.ethz.ch). It would be interesting to investigate whether any of these genes are indeed involved in signaling mechanisms leading to programmed cell death and IP formation. To date, markers that are highly specific for IP formation are scarce and none so far are believed to be direct effectors of cell death in plants (Den Herder et al., 2006). The identification of effector proteins would significantly improve our understanding of the regulation of this process essential for hydroponic nodulation of *S. rostrata.*

Different regulation of members of gene families during different invasions

When considering broader functional classes as opposed to single tags, clear differences emerge between the two invasion systems. Taking reactive oxygen metabolism as an example, tags for similar genes show differences in regulation between LRB and RHC nodulation. Although representatives of some ROS production and metabolic genes are found in both systems, it appears that different isoforms may be involved. Several tags encoding peroxidase genes were found, some of these are common, one however was crack entry specific, implying different roles and substrates. Similarly, three NADPH oxidase encoding tags were found, 1 was common, the two others were specific to either root hair curling or crack entry. Conversely, 2 distinct amine oxidase were found to be common, so was a copper amino-oxidase. Amine oxidases are interesting since they might be involved in cross-linking of glycoproteins in the IT matrix (Brewin, 2004). Their expression profile has been confirmed by RT-PCR and analysis of their function in nodulation is ongoing (J. Den Herder *et al.,* unpublished results).

Several tags involved in vesicle transport and targeting were identified in our screen. A number of GTP binding proteins were differentially regulated. Small GTPases are involved in almost all aspects of eukaryotic life, so it is not surprising to find them in this study and activation of G protein activity by Nod factor has been reported previously (Yang et al., 1994; Kelly and Irving, 2003). Interesting however, is the very early, common expression of a tag similar to ROP9 (cluster 1). ROPs have been implicated in tip growth mechanisms and H_2O_2 production and might thus be involved in infection thread progression during nodulation (Yang et al., 1994; Maunoury et al., 2006). Also the root hair curling specificity of an ADP ribosylation factor (ARF) deserves mentioning here. It is thought that ARF mediated targeting of certain ROP proteins is involved in establishing cell polarity in tip growing structures such as root hair cells, suggesting ARF function during root hair curling (Xu and Scheres, 2005b). Additionally, a syntaxin was strongly upregulated during root hair curling invasion (5), whereas a SNAP protein (7) was upregulated in the series inoculated with ORS571-V44. Syntaxins and SNAP proteins are SNARE proteins involved in regulated exocytosis (Hepp et al., 2005). Tip growing structures rely heavily on targeted exocytosis.

The specific downregulation of a SNAP protein upon inoculation with NF producing rhizobia may reflect a change in the nature of vesicles targeted to the site of infection, thus allowing IT formation.

Other patterns revealed by cluster analysis

16 tags showed differential expression upon inoculation with *A. caulinodans* ORS571-V44 (cluster 7) that did not show similar changes in the two nodulation series. Of these tags, 5 had homology to proteins with no known function, others were a putative transcriptional regulator, a protein similar to a high affinity nitrate transporter, a pathogenesis related protein, a SNAP protein (described above), a periaxin like protein, a pyruvate kinase and a trypsin inhibitor. No clear explanation is available for these data although some annotations point towards pathogenesis related functions, indicating a possible role for NF in the repression of defense responses (Mithofer, 2002). Because this cluster consists of tags that are expressed upon recognition of bacterial compounds, it is likely that some defense response genes belong to this cluster. The lack of functional data for most of these genes, however, does not allow for founded hypothesizing.

Conclusion

The presence of phenotypic plasticity during *S. rostrata* enables for a high throughput comparison of transcriptional profiles during nodulation. Besides genes involved in both infection systems, the core nodulins, we also identified large subsets of genes that were either crack entry or root hair curling specific, reflecting the differences in infection strategy and the lack of epidermal invasion during lateral root base nodulation. It has been shown that NF structure requirements differ between lateral root base nodulation and root hair curling nodulation in *S. rostrata* and it was proposed that the stringent entry receptor complex that governs infection of root hairs plays no role during LRB nodulation (Ardourel et al., 1994; Goormachtig et al., 2004b). This is supported by the observation that manipulating Ca^{2+} spiking frequencies restores root hair invasion of *S. rostrata* in hydroponic conditions, showing that hydroponic conditions inhibit the stringent response (Capoen *et al.,* in preparation). Further investigation of the root hair curling specific genes dependent on the stringent response that are present in our data may reveal interesting novel functions involved in nodulation. Similarly, genes specific to LRB nodulation expressed the first 2 days after inoculation are potential markers for infection pocket formation, the hallmark event of LRB nodulation. A rich source of information is available now and mining these data is no doubt an important step in our understanding of both inter- and intracellular invasion of rhizobia.

Supplementary data: K Means Clustering

Cluster 1

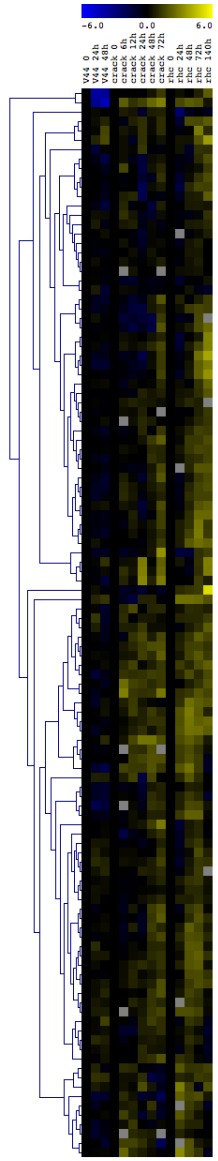

WC020BT23M21-595.5=
"WC014BT21M14-190.8=similar to GP 2398523 emb CAA74049.1 Transcription factor {Arabidopsis thaliana}, partial (24%) "
"WC041BT42M21-497.1=Pyruvate dehydrogenase E1 component alpha subunit, mitochondrial precursor (EC 1.2.4.1) (PDHE1-A). "
"WC036BT34M34-354.0=similar to PIR B86227 B86227 hypothetical protein [imported] - Arabidopsis thaliana, partial (84%) "
WC005BT12M23-246.9=NADH:ubiquinone oxidoreductase-like protein (At5g18800).
"WC002BT11M31-204.8=similar to GP 6688808 emb CAB65279.1 O-diphenol-O-methyl transferase {Medicago sativa subsp. x varia}, complete "
"WC005BT12M33-348.9=similar to GP 21592566 gb putative malonyl-CoA:Acyl carrier protein transacylase {Arabidopsis thaliana}, partial (7%) "
WC040BT42M13-330.0=
"WC038BT41M23-122.6=similar to GP 20259195 gb AAM14313.1 unknown protein {Arabidopsis thaliana}, partial (83%) "
WC041BT42M22-613.1=IRK-interacting protein.
WC022BT24M12-415.9=Putative carrier protein (AT4G01100/F2N1_16).
WC041BT42M32-392.1=Hypothetical protein.
"WC028BT31M23-167.9=similar to GP 22655368 gb AAM98276.1 At2g17760/At2g17760 {Arabidopsis thaliana}, partial (48%) "
WC038BT41M22-523.8=Isovaleryl-CoA dehydrogenase (EC 1.3.99.10).
WC047BT44M33-156.2=Hypothetical protein.
WC029BT31M41-658.1=P0431G06.23 protein (B1139B11.1 protein).
WC001BT11M14-445.7=Ubiquitin extension protein.
WC002BT11M32-350.2=60S acidic ribosomal protein P0.
WC001BT11M13-195.6=Translocon Tic40-like protein (AT5g16620/MTG13_6) (At5g16620).
WC036BT34M24-227.7=Hypothetical protein (At1g67530).
WC005BT12M32-323.3=Probable NADH-ubiquinone oxidoreductase subunit B17.2 (Complex I-B17.2) (CI-B17.2).
"WC037BT34M43-215.4=similar to PIR G96811 G96811 unknown protein T11I11.17 [imported] - Arabidopsis thaliana, partial (31%) "
WC038BT41M23-381.7=Caffeic acid O-methyltransferase.
WC025BT21M33-328.0=Putative sugar transporter.
WC024BT24M44-188.8=Phosphate/phosphoenolpyruvate translocator.
WC039BT41M33-292.7=Expressed protein (Hypothetical protein).
WC041BT42M22-324.8=Putative phytosulfokine peptide precursor.
WC004BT12M12-319.0=Transporter-like protein.
WC026BT11M41-177.5=O-diphenol-O-methyl transferase (EC 2.1.1.6).
"WC020BT23M21-411.9=similar to GP 13430446 gb AAK25845.1 putative multispanning membrane protein {Arabidopsis thaliana}, partial (93%) "
"WC031BT32M34-201.0=similar to PIR E84781 E847 hypothetical protein At2g36500 [imported] - Arabidopsis thaliana, partial (3%) "
WC035BT34M21-107.8=
"WC041BT42M22-146.2=similar to SP Q9SEU7 THM3_ARATH Thioredoxin M-type 3 chloroplast precursor (TRX-M3). [Mouse-ear cress] {Arabidopsis thaliana}, partial (63%) "
"WC024BT24M44-127.6=similar to PIR F96570 F96570 unknown protein MQ33-82175 [imported] - Arabidopsis thaliana, partial (89%) "
"WC018BT22M34-100.2=homologue to GP 4835752 gb AADJ0219.1 Is a member of the PF 00069 Eukaryotic protein kinase family. ESTs gb T46484 gb AF066875 and gb , partial (13%) "
WC026BT22M43-180.5=Ubiquinol-cytochrome C reductase complex ubiquinone-binding protein QP-C (EC 1.10.2.2) (Ubiquinol-cytochrome C reductase complex 8.2 kDa protein).
WC002BT11M32-521.7=60S acidic ribosomal protein P0 (Fragment).
WC041BT42M32-372.6=P0682B08.13 protein.
WC029BT31M43-149.7=Putative mitochondrial NAD-dependent malate dehydrogenase.
WC045BT43M44-544.7=Chloroplast 1-deoxy-D-xylulose-5-phosphate synthase.
WC029BT31M41-152.4=ADP-glucose pyrophosphorylase large subunit CagpL2 (EC 2.7.7.27) (Glucose-1-phosphate adenylyltransferase) (ADP-glucose synthase).
WC047BT44M31-341.2=ATP-dependent Clp protease proteolytic subunit (EC 3.4.21.92) (Endopeptidase Clp).
"WC042BT42M42-551.3=similar to PIR T51575 T51575 2-hydroxyphytanoyl-CoA lyase-like protein - Arabidopsis thaliana, partial (75%) "
WC044BT43M33-149.6=F3F20.4 protein.
"WC047BT44M31-313.3=weakly similar to GP 14596113 gb AAK68784.1 Unknown protein {Arabidopsis thaliana}, partial (73%) "
WC033BT33M22-222.8=Hypothetical protein.
"WC022BT24M12-230.7=weakly similar to GP 17978926 gb AAL47430.1 AT3g47210/F13I12_260 {Arabidopsis thaliana}, partial (6%) "
WC037BT34M43-210.9=Ribosomal protein L28-like.
WC015BT21M24-403.9=Putative extensin.
"WC036BT34M34-208.3=similar to PIR A84830 A848 hypothetical protein At2g40480 [imported] - Arabidopsis thaliana, partial (6%) "
WC029BT31M43-355.2=Purple acid phosphatase precursor (EC 3.1.3.2).
WC034BT33M43-354.7=Purple acid phosphatase precursor (EC 3.1.3.2).
WC003BT11M33-223.4=21 kDa extracellular calmodulin-binding protein.
WC015BT21M31-188.7=Nicotianamine synthase 2 (EC 2.5.1.43) (S-adenosyl-L-methionine:S- adenosyl-L-methionine:S-adenosyl-methionine 3-amino-3- carboxypropyltransferase 2) (AtNAS2).
WC008BT13M41-265.5=40S ribosomal protein S17.
WC046BT43M33-369.4=DEAD-box RNA helicase-like protein.
WC001BT11M14-269.5=Beta-xylosidase.
WC005BT12M33-303.8=Probable WRKY transcription factor 28 (WRKY DNA-binding protein 28).
WC044BT43M34-233.3=HMG-CoA synthase 2.
WC040BT42M12-434.6=Hypothetical protein.
WC045BT43M43-374.0=Hypothetical protein.
WC041BT42M32-508.0=Similarity to unknown protein.
WC047BT44M42-342.0=Kinesin-like protein.
WC002BT11M22-259.3=Response regulator protein.
WC046BT43M32-277.6=Auxin-responsive GH3-like protein.
WC037BT34M42-160.8=Ribosomal protein S3a.
WC003BT11M44-149.9=small G-protein ROP9 [Medicago truncatula]
WC013BT13M21-307.7=UVB-resistance protein UVR8 (AT5g63860/MGI19_6).
WC003BT11M44-M75.9=Cytosolic aldehyde dehydrogenase RF2C.
"WC002BT11M32-195.6=Genomic DNA, chromosome 5, TAC clone:K19P17 (Hypothetical protein)."
WC036BT34M24-243.9=Diamine oxidase (Copper amino oxidase) (EC 1.4.3.6).
"WC004BT12M12-131.1=similar to PIR G96836 G9 unknown protein T21F11.18 [imported] - Arabidopsis thaliana, partial (19%) "
WC037BT34M44-595.7=AP2/EREBP transcription factor.
WC037BT44M11-660.0=Elongation factor 1-alpha (EF-1-alpha).
WC037BT34M42-208.2=Putative C2H2-type zinc finger protein (At2g02080).
WC001BT11M14-300.0=Hypothetical protein.
WC024BT22M41-630.0=Isopentenyl-diphosphate delta-isomerase II (EC 5.3.3.2) (IPP isomerase II) (Isopentenyl pyrophosphate isomerase II).
WC035BT34M12-170.7=B-like cyclin.
"WC004BT12M21-217.7=similar to GP 12597838 gb AAG60148.1 copper amine oxidase putative {Arabidopsis thaliana}, partial (66%) "
WC045BT43M42-441.5=ATP citrate lyase b-subunit (EC 4.1.3.8).
WC044BT43M32-445.5=ATP citrate lyase b-subunit (EC 4.1.3.8).
"WC044BT43M34-439.8=homologue to GP 15919089 emb CAC86996. ATP citrate lyase b-subunit {Lupinus albus}, complete "
WC005BT12M23-912.0=Similarity to protein kinase (Hypothetical protein) (At5g63940).
"WC011BT14M41-316.3=similar to GP 23617012 dbj BAC20708. putative translational inhibitor protein {Oryza sativa (japonica cultivar-group)}, partial (68%) "
WC035BT34M21-283.1=Geranylgeranyl reductase.
WC002BT11M22-220.0=40S ribosomal protein S7.
WC041BT42M24-364.0=At2g27240 protein.
WC043BT43M12-429.4=ATP citrate lyase b-subunit (EC 4.1.3.8).
"WC046BT44M14-272.8=similar to GP 10177467 dbj BAB10858. permease 1 {Arabidopsis thaliana}, complete "
WC047BT44M33-259.7=Hypothetical protein.
WC035BT34M21-390.7=Putative cytochrome P450.
WC044BT43M34-314.4=MSS5-like protein (Fragment).
WC041BT42M21-195.6=Histone H4.
WC039BT41M32-170.7=Microtubule-associated protein MAP65-1c.
"WC036BT34M34-501.0=similar to GP 19179315 emb transcription factor E2Fe {Arabidopsis thaliana}, partial (25%) "
"WC048BT44M44-411.4=similar to GP 6091722 gb AAF03434.1 putative ribosomal protein L13 {Arabidopsis thaliana}, partial (87%) "
WC045BT44M11-182.1=Histone H4.
WC029BT31M41-450.6=Kinesin 1 (Kinesin-like protein A).
"WC024BT23M41-278.2=Putative endo-1,4-beta-glucanase."
WC025BT22M24-587.0=Cyclophilin (EC 5.2.1.8) (Peptidyl-prolyl cis-trans isomerase) (PPIase) (Rotamase).
"WC021BT23M42-374.2=Homologue to PIR T00795 T00795 26S proteasome regulatory subunit [imported] - Arabidopsis thaliana, partial (59%) "
WC046BT44M24-254.0=
WC035BT34M12-163.6=Histone H2A.
WC024BT23M42-448.6=Putative nucleotide-binding protein.
"WC035BT34M12-130.3=similar to GP 13161397 dbj BAB33033. CPRD2 {Vigna unguiculata}, partial (75%) "
"WC024BT23M42-208.7=similar to GP 17381218 gb AAL36421.1 unknown protein {Arabidopsis thaliana}, partial (81%) "
"WC047BT44M33-467.3=Inner membrane ALB1NO3-like protein 1, chloroplast precursor (Ath4)."
WC037BT34M41-162.2=Defective gibberellin 3B-hydroxylase.
WC046BT44M22-222.2=Kinesin-like protein.
WC041BT42M22-281.9=Gibberellin 20-oxidase.
WC047BT44M41-272.9=Hypothetical 214.8 kDa protein ycf1.
WC036BT34M24-486.0=Gb|AAC63835.1.
WC029BT31M41-395.6=Subtilisin-like protease C1.
"WC019BT23M11-251.5=Putative endo-1,4-beta-glucanase."

Cluster 2

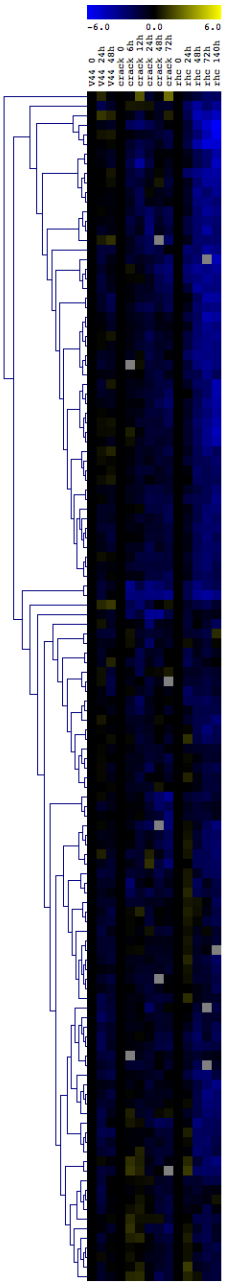

WC020BT23M14-143.3=bZIP transcription factor ATB2.
WC022BT24M12-153.8= unknown
WC012BT12M43-528.5=Amine oxidase.
WC011BT14M42-215.4=Low affinity sulphate transporter 3.
"WC012BT12M43-326.3=Lysine and histidine specific transporter, putative."
WC008BT13M42-389.6=Emb|CAB86085.1.
WC011BT14M42-229.0=Low affinity sulphate transporter 3.
WC022BT24M13-269.0=Putative low-affinity nitrate transporter.
WC008BT13M42-308.2=Putative aspartate-tRNA ligase.
WC035BT34M13-326.2=PDR15 ABC transporter.
"WC043BT43M22-263.9=homologue to SP P49107 PSAN_ARATH Photosystem I reaction centre subunit N chloroplast precursor (PSI- N). [Mouse-ear cress], partial (62%) "
WC042BT42M34-268.8=P0452F10.18 protein.
WC014BT21M21-218.3=Glycine-rich protein (Hypothetical protein).
"WC005BT12M24-267.7=similar to GP 6714564 dbj BAA89498.1 cyc07 {Daucus carota}, complete"
WC022BT24M12-532.5=F8K7.10 protein (Hypothetical protein).
"WC031BT32M42-268.4=weakly similar to GP 4530585 gb AAD22104.1 B12D protein {Ipomoea batatas}, partial (96%) "
"WC037BT34M42-302.9=similar to PIR D86157 D86157 hypothetical protein AAF02892.1 [imported] - Arabidopsis thaliana, partial (17%) "
"WC021BT23M41-234.9=SP P29388 NU5 NADH-ubiquinone oxidoreductase chain 5 (EC 1.6.5.3). [Mouse-ear cress] {Arabidopsis thaliana}, partial (18%) "
WC022BT24M13-359.1=1-aminocyclopropane-1-carboxylate oxidase homolog (ACC oxidase).
WC022BT24M14-187.2=Cinnamate 4-hydroxylase (EC 1.14.13.11).
WC029BT31M43-186.5=EST AU029428(E30359) corresponds to a region of the predicted gene.
WC045BT43M44-282.9=Cation diffusion facilitator 2.
"WC044BT43M32-338.3=Membrane protein, putative."
WC013BT13M21-335.4=Transcription factor Myb1.
WC043BT43M22-226.1=ATP synthase alpha subunit (Fragment).
WC025BT21M31-632.9=Carboxypeptidase II (Fragment).
WC022BT24M13-461.7=Hypothetical protein (Apospory-associated protein C).
WC025BT21M31-415.0=Putative AP2 domain containing protein.
"WC026BT22M43-347.6=Ser/Thr protein kinase isolog, 46094-44217."
WC040BT41M43-285.2=
"WC042BT42M33-150.7=similar to GP 5262203 emb CAB45800.1 nodulin-like protein {Arabidopsis thaliana}, partial (77%) "
WC023BT24M32-161.8=Syringolide-induced protein B13-1-9.
WC043BT43M12-564.4=NADP-malic enzyme.
WC044BT43M32-363.8=TIR-similar-domain-containing protein TSDC.
WC035BT34M14-149.9=Homoglutathione synthetase.
WC037BT34M42-468.2=Polygalacturonase inhibitor-like protein (Hypothetical protein).
WC042BT42M33-310.7=Hypothetical protein.
"WC042BT42M41-186.7=similar to GP 1644427 gb AAB17995.1 glyoxalase II {Arabidopsis thaliana}, partial (96%) "
WC014BT21M12-625.6=F14M2.8 protein (At1g33800/F14M2_23) (Hypothetical protein).
"WC040BT42M12-485.4=homologue to SP P27520 CB23_PEA Chlorophyll A-B binding protein 21S chloroplast precursor (LHCII type II CAB-21S) (LHCP)., complete "
"WC001BT11M14-205.0=similar to GP 16930473 gb AAL31922.1 At1g09660/F21M12_5 {Arabidopsis thaliana}, partial (65%) "
WC022BT24M21-157.7=Plasma membrane H+-ATPase.
WC025BT21M33-486.0=OJ1200_C08.22 protein.
"WC025BT21M31-213.1=similar to GP P21745 EA30_VICFA Embryonic abundant protein VF30.1 precursor. [Broad bean] {Vicia faba}, complete "
WC035BT34M14-410.0=Putative inositol polyphosphate 5-phosphatase At5P2.
WC038BT41M21-304.5=P-glycoprotein (Fragment).
WC015BT21M24-347.9=Hypothetical protein.
"WC043BT43M14-389.5=similar to GP 9758042 dbj BAB08505.1 gb AAD56319.1-gene_id:MYC6.4-similar to unknown protein {Arabidopsis thaliana}, partial (68%) "
WC023BT24M34-349.0=Putative PREG1-like negative regulator.
WC023BT24M32-391.5=SuFUL FRUITFULL-like MADS-box (Fragment).
WC048BT32M41-357.3=Hypothetical protein.
WC015BT21M31-415.9=Putative AP2 domain containing protein.
WC022BT24M12-610.7=Respiratory burst oxidase protein.
"WC004BT12M13-158.0=similar to GP 15010698 gb AT3g22600/F16J14_17 {Arabidopsis thaliana}, partial (26%) "
WC037BT34M42-403.0=Polygalacturonase inhibitor-like protein (Hypothetical protein).
WC037BT34M43-403.3=Similar to prokaryotic DNA polymerase III gamma subunit (ST1CHEL).
WC014BT21M21-390.0=At1g48370/F11A17_27.
"WC009BT14M13-308.9=Genomic DNA, chromosome 5, TAC clone:K9I9 (AT5g67480/K9I9_4)."
"WC020BT23M21-449.3=weakly similar to GP 16604342 gb AAL24177.1 At2g46080/T3F17.27 {Arabidopsis thaliana}, partial (38%) "
WC007BT13M24-340.8=Hypothetical protein.
WC005BT12M24-250.8=F26F24.22.
"WC018BT22M34-317.1=similar to PIR T05188 T05188 protein kinase F4I10.10 (EC 2.7.1.-) - Arabidopsis thaliana, partial (68%) "
WC005BT12M32-410.6=F2Z14.9 protein (Hypothetical protein).
WC035BT34M11-443.1=Emb|CAA19725.1 (Hypothetical protein) (At3g21150).
WC045BT43M44-649.1=Plastidic aldolase NPALDP1.
"WC005BT12M31-217.1=similar to PIR A95535 A95535 unknown protein 11341-13243 [imported] - Arabidopsis thaliana, partial (97%) "
WC040BT42M13-160.5=Hypothetical protein (Putative harpin-induced protein).
WC041BT42M22-203.3=DNA-directed RNA polymerase beta'' chain (EC 2.7.7.6) (PEP) (Plastid- encoded RNA polymerase beta'' subunit) (RNA polymerase beta'' subunit).
WC005BT12M24-203.8=OJ1058_A12.25 protein.
WC001BT11M11-264.9=OJ1007_H09.1 protein (P0474G09.1 protein).
WC035BT34M13-462.7=Putative bHLH transcription factor.
WC020BT23M33-210.5=Peroxidase precursor.
WC045BT43M44-167.4=OSJNBa0014K14.5 protein.
"WC039BT41M34-315.6=6-phosphogluconate dehydrogenase, decarboxylating (EC 1.1.1.44)."
WC039BT41M33-270.6=Beta-glucan-elicitor receptor.
WC038BT41M21-603.2=SAR1/GTP-binding secretory factor.
WC027BT31M21-317.3=Pectin methylesterase 5 (Fragment).
WC029BT31M44-432.4=Putative Hslpro-1 homolog.
WC043BT43M22-153.3=Beta-glucan binding protein.
WC021BT23M44-212.2=Putative polyprotein (Fragment).
WC039BT41M34-139.3=Peroxidase (Fragment).
WC018BT22M41-177.4=Wound-inducible P450 hydroxylase.
WC021BT23M43-221.5=phosphatidylinositol 3-kinase [Medicago truncatula]
"WC015BT21M31-199.4=similar to GP 9279576 dbj gene_id:MLN21.7-unknown protein {Arabidopsis thaliana}, partial (19%) "
WC005BT12M32-384.3=Putative centromere protein.
WC028BT31M34-375.6=Zinc finger protein 3.
"WC014BT21M14-576.6=ATP-dependent Clp protease, ATP-binding subunit (AT5g50920/K3K7_7)."
WC048BT32M12-414.4=Putative photosystem I antenna protein.
WC042BT42M42-200.0=AML5.
WC027BT31M22-250.7=Helicase-like protein.
WC048BT44M44-395.4=Nam-like protein 10.
WC028BT31M23-227.4=Phenylalanine ammonia-lyase (EC 4.3.1.5).
"WC027BT31M21-264.8=similar to PIR G84825 G84825 probable CCCH-type zinc finger protein [imported] - Arabidopsis thaliana, partial (56%) "
"WC039BT41M31-143.6=similar to PIR T05181 T05181 S-receptor kinase (EC 2.7.1.-) T6K22.120 precursor - Arabidopsis thaliana, partial (28%) "
WC042BT42M34-207.0=Hypothetical protein.
WC021BT23M41-291.2=F20P5.13 protein.
WC011BT14M42-700.0=Alpha tubulin (Fragment).
WC020BT23M22-219.3=Ribosomal protein L5.
"WC028BT31M32-287.9=PIR A26014 A26 histone H3 - wheat, partial (98%)"
WC020BT23M22-326.1=Hypothetical protein (AT4G29790/F27B13_30).
WC026BT22M43-324.1=Putative ARGONAUTE9 protein.
WC021BT23M41-271.2=F6F9.4 protein.
WC001BT11M11-381.0=MTGI TC84033
"WC029BT31M43-259.0=homologue to GP 6539600 gb amino acid transporter a {Vicia faba}, partial (60%) "
WC010BT14M31-304.4=putative receptor kinase
"WC020BT23M22-103.9=similar to GP 22022560 gb AAM83237.1 At1g03250/F15K9_13 {Arabidopsis thaliana}, partial (82%) "
WC023BT24M33-284.8=Hypothetical protein.
WC025BT21M33-398.6=Putative nitrate transporter (NTL1).
"WC025BT22M24-142.4=similar to GP 16930433 gb AAL31902.1 AT4g17230/d14650c {Arabidopsis thaliana}, partial (62%) "
WC046BT44M13-465.0=Putative disease resistance protein (Fragment).
WC043BT43M22-317.8=At3g14067.
WC038BT41M22-379.4=Putative polyprotein (Fragment).
WC018BT22M34-149.6=Hypothetical protein K1AA1542 (Fragment).
"WC040BT42M13-277.6=Plastocyanin A, chloroplast precursor."
WC003BT11M44-241.6=Mini-chromosome maintenance protein MCM6.
"WC001BT11M14-127.3=similar to PIR T49190 T49190 ribosomal protein L1-like protein - Arabidopsis thaliana, partial (70%) "
"WC023BT24M24-392.9=similar to GP 12597759 gb AAG60072.1 pheromone receptor putative (AR401) {Arabidopsis thaliana}, partial (79%) "
WC025BT21M33-333.6=Highly similar to YUP8H12R.39.
WC020BT23M31-168.2=Trihelix transcription factor PETAL LOSS.
WC025BT21M33-141.8=Metallothionein.
"WC023BT24M24-347.1=similar to PIR T05688 T05688 hypothetical protein F20M13.160 - Arabidopsis thaliana, partial (40%) "
WC046BT44M21-385.0=
"WC009BT13M43-415.9=similar to GP 20160656 dbj BAB89601. contains EST AU058101(S2419)-similar to Arabidopsis thaliana chromosome5 At5g58640-unknown protein, partial (60%) "
WC021BT23M43-346.1=OSJNBa0067K08.20 protein.

Cluster 3

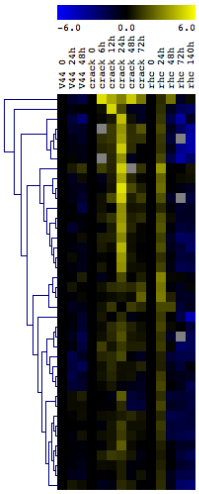

WC010BT14M32-538.2=Putative 60S ribosomal protein L10A (RPL10aC).
WC024BT24M42-267.0=Putative calmodulin-related protein.
WC001BT11M14-159.7=NADH dehydrogenase subunit 4.
WC024BT23M41-437.3=SAR DNA-binding protein-1.
"WC021BT23M41-435.7=similar to GP 15292729 gb AAK92733.1 putative polygalacturonase PG1 {Arabidopsis thaliana}, partial (51%) "
"WC023BT24M33-147.4=similar to GP 17978960 gb AT5g10020/T31P16_9 {Arabidopsis thaliana}, partial (8%) "
WC026BT22M43-250.2=Putative calcium-dependent protein kinase.
WC031BT32M42-386.3=GAI-like protein.
"WC008BT13M32-224.0=similar to PIR A96749 A96749 unknown protein T10D10.5 [imported] - Arabidopsis thaliana, partial (27%) "
WC044BT43M34-229.8=ATPase alpha subunit.
"WC021BT23M41-199.0=similar to GP 17381034 gb AAL36329.1 putative protein phosphatase type 2C {Arabidopsis thaliana}, partial (71%) "
WC039BT41M41-315.4=ATP synthase F0 subunit 1.
"WC040BT41M43-233.7=Phosphoribosylformylglycinamidine cyclo-ligase, chloroplast precursor (EC 6.3.3.1) (AIRS) (Phosphoribosyl-aminoimidazole synthetase) (AIR synthase). "
"WC044BT43M31-106.0=homologue to PIR T48580 T48580 hypothetical protein T31B5.150 - Arabidopsis thaliana, partial (33%) "
WC001BT11M14-253.2=Proteasome subunit alpha type 5 (EC 3.4.25.1) (20S proteasome alpha subunit E) (20S proteasome subunit alpha-5).
"WC032DT33M13-141.0=similar to SP P49231 PRO1_PHAVU Profilin 1. [Kidney bean French bean] {Phaseolus vulgaris}, complete "
"WC024BT23M42-116.2=similar to GP 9759344 dbj BAB09999.1 cleft lip and palate associated transmembrane protein-like {Arabidopsis thaliana}, partial (32%) "
WC009BT14M13-293.4=26S proteasome subunit RPN9b.
"WC004BT12M12-355.5=similar to GP 15809986 gb AAL06920.1 AT3g19540/T31J18_4 {Arabidopsis thaliana}, partial (20%) "
"WC014BT21M11-398.0=weakly similar to PIR T02414 T02414 probable protein kinase [imported] - Arabidopsis thaliana, partial (12%) "
WC026BT11M43-359.2=Hypothetical protein (Fragment).
WC041BT42M23-203.8=Dem protein (defective embry and meristem)
"WC009BT13M44-126.9=similar to PIR T08460 T08 hypothetical protein F22O6.230 - Arabidopsis thaliana, partial (51%) "
WC018BT22M41-268.1=Peroxidase precursor.
WC021BT23M41-192.5=At2g32080/F22D22.17.
"WC021BT23M43-247.7=similar to GP 11876272 emb CAC18917. unnamed protein product {Glycine max}, partial (49%) "
"WC010BT14M31-285.1=similar to GP 4587571 gb AAD25802.1 Belongs to the PF 01027 Uncharacterized protein family UPF0005 with 7 transmembrane domains., partial (92%) "
WC021BT23M43-493.0=ABC1 protein.
"WC045BT43M42-156.3=similar to GP 459533 emb CAA54968.1 orf224; homology to ribosomal protein S1 of E. coli {Oenothera berteriana}, partial (83%) "
"WC035BT34M13-139.6=weakly similar to GP 3928543 dbj BAA34687.1 UDP-glucose glucosyltransferase {Arabidopsis thaliana}, partial (59%) "
WC025BT21M33-211.5=Putative avr9 elicitor response protein.
WC044BT43M32-507.0=ATP citrate lyase b-subunit (EC 4.1.3.8).
WC037BT34M42-224.8=Myb-related transcription factor (Fragment).
WC025BT21M31-297.1=Hydroxycinnamoyl transferase.
WC025BT21M33-322.0=Putative receptor-like protein kinase.
WC041BT42M31-208.3=Coatomer alpha subunit-like protein.
"WC040BT42M13-125.9=similar to GP 4587575 gb AAD25806.1 Belongs to PF 01121 Uncharacterized protein family UPF0038 containing ATP/GTP binding domain. ESTs, partial (77%) "
"WC036BT34M34-622.0=Auxin-induced basic helix-loop-helix transcription factor, putative (At1g58100). "
WC003BT11M44-296.0=Putative ribosomal protein L2 (Fragment).
WC022BT24M23-184.7=At3g44220.

Cluster 4

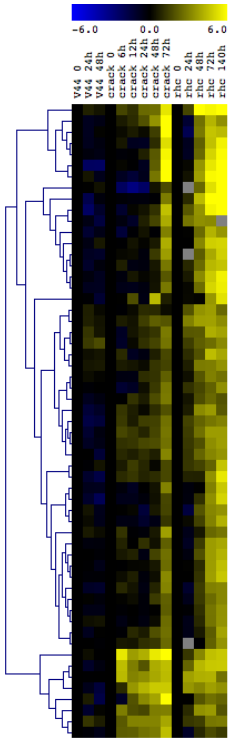

WC047BT44M42-554.0=Chalcone reductase.
"WC025BT21M33-188.9=weakly similar to GP 5020217 gb AAD38040.1 acyl CoA reductase {synthetic construct}, partial (36%) "
"WC009BT14M13-239.2=Endo-1,4-beta glucanase precursor."
WC004BT12M12-503.3=RING/C3HC4/PHD zinc finger-like protein.
WC002BT11M21-177.6=O-diphenol-O-methyl transferase (EC 2.1.1.6).
WC003BT11M44-404.8=multifunctional aquaporin [Medicago truncatula]
"WC040BT42M12-196.6=similar to PIR S51171 S51171 amino acid transport protein AAT1 - Arabidopsis thaliana, partial (55%) "
WC027BT31M12-151.4=
WC042BT42M33-206.1=L-ascorbate oxidase precursor (EC 1.10.3.3) (Ascorbase) (ASO).
"WC008BT13M32-167.1=similar to GP 21732311 emb hypothetical protein {Homo sapiens}, partial (4%) "
WC024BT24M44-340.8=Hypothetical protein B1307A11.10.
WC048BT44M44-290.8=NAC-domain protein 14.
WC042BT42M42-422.5=Putative glucosyltransferase.
WC027BT31M12-251.7=Early nodulin ENOD18.
"WC010BT14M23-346.3=Chloroplast nucleoid DNA binding protein, putative."
WC042BT42M34-412.5=ZR1 protein.
"WC037BT34M44-215.8=similar to GP 19347791 gb AAL86346.1 unknown protein {Arabidopsis thaliana}, partial (97%) "
WC037BT44M11-274.9=Hypothetical protein.
WC035BT34M22-176.9=Plasma membrane MIP protein.
WC011BT14M34-368.1=Putative cellulase CEL2 (Fragment).
WC024BT24M42-337.8=Putative glucosyltransferase.
WC035BT34M14-177.7=Carbonic anhydrase (EC 4.2.1.1).
WC040BT42M12-553.9=Peptide transporter.
WC004BT12M21-462.5=Emb|CAB72181.1 (hypothetical protein).
"WC025BT22M24-345.4=similar to PIR T08124 T08124 ferritin 2 precursor - cowpea, partial (84%) "
"WC019BT23M12-556.0=similar to GP 15991736 gb AAL13045.1 WRKY transcription factor 69 {Arabidopsis thaliana}, partial (40%) "
WC005BT12M33-131.2=Protein phosphatase-2C.
WC022BT24M21-459.2=Adenosylhomocysteinase.
"WC004BT12M12-180.8=similar to GP 9366656 emb C probable similar to ring-h2 finger protein rhala. {Trypanosoma brucei}, partial (18%) "
WC004BT12M12-241.2=OSJNBa0088H09.3 protein.
WC010BT14M24-509.1=F19K23.20 protein.
WC042BT42M34-391.3=Hypothetical protein.
WC044BT43M24-178.1=Putative prolyl endopeptidase (Fragment).
WC002BT11M21-167.4=O-diphenol-O-methyl transferase (EC 2.1.1.6).
WC031BT32M34-175.5=
"WC009BT14M12-112.8=similar to GP 22597162 gb AAN03468.1 bZIP transcription factor ATB2 {Glycine max}, partial (65%) "
WC011BT14M43-562.0=Hypothetical protein B1003C08.2.
WC019BT23M11-362.9=CONSTANS-like protein 1.
WC043BT43M13-311.9=Putative invertase inhibitor precursor (Pollen allergen Pla a 1).
WC028BT31M32-273.9=Early nodulin ENOD18.
"WC041BT42M32-146.3=similar to PIR G84590 G84590 probable heat shock protein [imported] - Arabidopsis thaliana, partial (88%) "
"WC037BT34M42-300.3=similar to GP 6523547 emb CAB62280.1 hydroxyproline-rich glycoprotein DZ-HRGP {Volvox carteri f. nagariensis}, partial (11%) "
WC041BT42M31-216.8=Sugar transporter like protein.
WC004BT12M12-211.5=Transporter-like protein.
WC010BT14M23-555.0=Hypothetical protein B1003C08.2.
WC040BT41M43-378.9=Caffeic acid O-methyltransferase.
WC035BT34M14-389.4=Expressed protein (Hypothetical protein).
WC005BT12M23-872.0=Putative serine/proline-rich protein (At3g45230).
WC046BT44M22-200.2=Cytochrome P450-dependent fatty acid hydroxylase.
"WC010BT14M21-346.2=Chloroplast nucleoid DNA binding protein, putative."
WC004BT12M13-265.8=Peroxidase precursor.
WC023BT24M34-265.7=HcrVf1 protein.
WC032BT32M44-700.7=Gb|AAC63835.1.
WC039BT41M31-196.7=Putative sulfate transporter-like.
"WC014BT21M12-288.3=similar to GP 2398523 emb CAA74049.1 Transcription factor {Arabidopsis thaliana}, partial (24%) "
"WC046BT44M13-211.6=similar to GP 19347818 gb AAL86322.1 unknown protein {Arabidopsis thaliana}, partial (17%) "
WC003BT11M33-336.3=Citrate binding protein.

Cluster 5

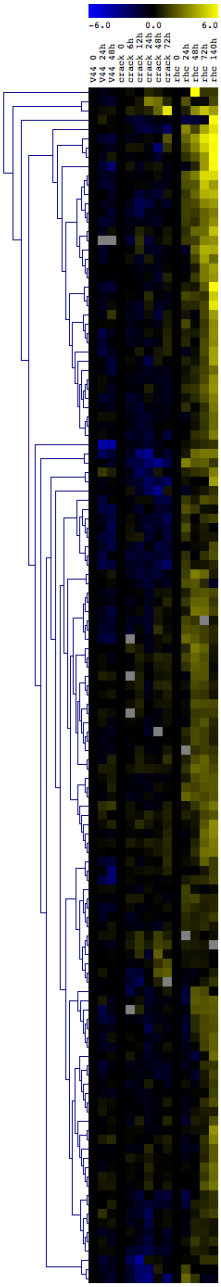

WC045B744M11-262.0=T9L6.1 protein.
WC034B733M33-308.6=similar to PIR T04124 T04124 receptor-like protein kinase (EC 2.7.1.-) - rice. partial (29%)
WC035B734M12-329.6=Ethylene-induced esterase.
WC046B744M24-238.5=similar to GP 13508844 emb CAC35167. arbutin synthase {Rauvolfia serpentina}. partial (34%)
WC041B742M22-197.5=similar to PIR S51171 S51171 amino acid transport protein AAT1 - Arabidopsis thaliana. partial (55%)
WC047B744M34-633.2=Hypothetical protein.
WC011B714M43-269.0=Tyrosine aminotransferase (EC 2.6.1.5).
WC046B744M13-M91.6=auxin efflux carrier protein [Medicago truncatula]
WC038B741M13-679.3=Putative nitrate transporter NRT1-3.
WC026B722M44-133.6=Microtubule-associated protein EB1-like protein.
WC030B732M23-163.8=Putative C3HC4-type RING zinc finger/ankyrin protein (Putative RING zinc finger ankyrin protein).
WC041B742M32-170.0=ADP-ribosylation factor.
WC041B742M21-217.9=
WC037B734M42-158.5=similar to GP 2576411 gb AAC61784.1 similar to dynamin-like protein encoded by GenBank Accession Number X99669 {Arabidopsis thaliana}. partial (65%)
WC035B734M22-143.0=Putative amino acid transporter.
WC020B723M14-343.0=Mitogen-activated protein kinase homolog NTF6 (EC 2.7.1.37) (P43).
WC025B721M33-234.0=Multidrug resistance associated protein 1.
WC042B742M42-325.2=MtN21 nodulin protein-like.
WC026B722M44-384.7=similar to GP 17065224 gb AAL32766.1 Unknown protein {Arabidopsis thaliana}. partial (17%)
WC032B733M13-195.0=RAC-like GTP binding protein RAC2.
WC026B711M43-210.4=Putative PAP-specific phosphatase.
WC046B744M21-290.3=Benzoyl coenzyme A: benzyl alcohol benzoyl transferase.
WC046B744M24-207.0=Peptide/glutathione transporter OPT1 (Fragment).
WC005B712M34-159.3=similar to PIR T11852 T11852 lipoxygenase (EC 1.13.11.12) - kidney bean. partial (93%)
WC002B711M31-286.5=similar to GP 6688808 emb CAB65279.1 O-diphenol-O-methyl transferase {Medicago sativa subsp. x varia}. complete
WC037B734M44-161.4=Enolase (EC 2.3.1.16).
WC048B732M41-269.6=similar to GP 7940285 gb AAF70844.1 F24O1.19 {Arabidopsis thaliana}. partial (12%)
WC025B721M33-128.3=similar to PIR T49904 T499 hypothetical protein T24H18.70 - Arabidopsis thaliana. partial (2%)
WC026B711M41-348.5=Polyprotein. putative.
WC038B741M13-255.1=Syntaxin 132 (AtSYP132).
WC013B713M21-197.2=Mitochondrial energy transfer protein precursor.
WC014B721M14-184.9=Selenium-binding protein-like protein.
WC021B723M44-531.4=similar to GP 21594011 gb AAM65929.1 unknown {Arabidopsis thaliana}. partial (71%)
WC038B741M14-269.1=T19F06.6 protein (AT4g24140/T19F6_130).
WC035B734M13-176.5=Phosphoenolpyruvate carboxylase (EC 4.1.1.31) (PEPCase).
WC011B714M33-415.0=Yippee-like protein (Hypothetical protein) (At2g40110 protein).
WC046B744M13-557.0=RNA-directed RNA polymerase (Fragment).
WC011B714M44-357.8=Glutamine synthetase, cytosolic isozyme (EC 6.3.1.2) (Glutamate-- ammonia ligase).
WC006B712M41-170.0=F16P17.19 protein (RNA polymerase IIA largest subunit. putative. 12353-6556).
WC047B744M31-127.4=MtN6; nodulin 6
WC012B711M12-377.7=homologue to PIR F86214 F86214 protein T6D22.2 [imported] - Arabidopsis thaliana. partial (47%)
WC047B744M32-298.4=At5g63160.
WC025B721M31-187.9=Nicotianamine synthase 2 (EC 2.5.1.43) (S-adenosyl-L-methionine:S- adenosyl-L-methionine:S-adenosyl-methionine 3-amino-3- carboxypropyltransferase 2) (AtNAS2).
WC004B712M13-423.8=NADH:ubiquinone oxidoreductase-like protein (At5g18800).
WC048B732M12-146.8=similar to GP 18491139 gb AAL69538.1 At2g25910/F17H15.6 {Arabidopsis thaliana}. partial (87%)
WC018B722M41-148.0=homologue to GP 13878137 gb AAK44146.1 unknown protein {Arabidopsis thaliana}. partial (43%)
WC045B744M11-434.3=weakly similar to GP 4335795 gb AAD17432.1 unknown protein {Arabidopsis thaliana}. partial (29%)
WC046B744M13-334.8=Type 5 protein serine/threonine phosphatase 62 kDa isoform.
WC046B744M13-377.5=Asparagine synthetase [glutamine-hydrolyzing] 1 (EC 6.3.5.4) (Glutamine-dependent asparagine synthetase 1).
WC003B711M34-496.7=similar to GP 15146224 gb AAK83595.1 AT5g25280/F18G18_20 {Arabidopsis thaliana}. partial (47%)
WC046B744M14-M89.4=SP Q02735 CAPP_MEDSA Phosphoenolpyruvate carboxylase (EC 4.1.1.31) (PEPCASE). [Alfalfa] (Medicago sativa}. partial (70%)
WC005B712M24-260.3=Phosphoenolpyruvate carboxylase (EC 4.1.1.31) (PEPCase).
WC022B724M13-582.0=similar to PIR Y17005 Y17005 major allergen Mal d 1 - apple tree. partial (18%)
WC009B713M44-159.2=similar to GP 13397927 emb CAC34625. putative calmodulin-related protein (Medicago sativa}. partial (69%)
WC047B744M32-592.0=Nucleoid DNA-binding-like protein.
WC022B724M21-663.8=T9L6.1 protein.
WC031B732M34-363.0=similar to GP 22136892 gb AAM91790.1 unknown protein {Arabidopsis thaliana}. partial (3%)
WC021B723M41-M82.1=Microtubule associated protein.
WC005B712M31-538.3=similar to PIR A44803 A4480 pG1 protein - human (fragment). partial (61%)
WC024B723M41-139.1=similar to PIR T40546 T40546 60s ribosomal protein l38 - fission yeast (Schizosaccharomyces pombe). partial (94%)
WC042B742M43-267.0=Endo-1,4-beta-glucanase.
WC035B734M22-332.6=F22D16.26 protein.
WC035B734M22-255.8=Emb|CAB82688.1.
WC026B722M43-385.0=OSJNBa0017B10.12 protein.
WC037B734M43-351.0=Exoribonuclease-like.
WC005B712M31-257.0=40S ribosomal protein S2.
WC042B742M33-293.2=PIR A25642 HSEM4 histone H4 - maize. complete
WC024B723M41-348.8=Photosystem I assembly protein ycf3.
WC037B734M43-307.0=26S proteasome subunit RPN9b.
WC031B732M42-529.0=similar to GP 21740815 emb CAD41005. OSJNBa0042L16.3 {Oryza sativa}. partial (92%)
WC022B724M21-484.7=Adenosylhomocysteinase.
WC027B731M12-567.2=(1-4)-beta-mannan endohydrolase.
WC043B743M13-642.0=Hypothetical protein.
WC024B724M42-299.0=40S ribosomal protein S30-like.
WC048B732M41-138.0=homologue to SP P34922 G3PC_ Glyceraldehyde 3-phosphate dehydrogenase cytosolic (EC 1.2.1.12). [Garden pea] {Pisum sativum}. partial (15%)
WC037B734M44-236.7=EAR7 protein (Hypothetical protein) (Allergen-like protein BNSn20).
WC036B734M23-219.6=similar to GP 21536603 gb unknown {Arabidopsis thaliana}. partial (27%)
WC032B733M14-292.8=Peroxidase precursor (Fragment).
WC024B724M42-235.8=
WC022B724M23-392.7=weakly similar to GP 17529172 gb unknown protein {Arabidopsis thaliana}. partial (14%)
WC030B732M21-184.7=similar to GP 3335335 gb AAC27137.1 ESTs gb F14113 and gb T42122 come from this region. {Arabidopsis thaliana}. partial (78%)
WC022B724M22-356.8=Purple acid phosphatase (EC 3.1.3.2).
WC015B721M24-201.4=Putative glucan 1,3-beta-glucosidase.
WC023B724M24-192.7=SPF1 protein.
WC044B743M33-247.2=Gamma-glutamyl hydrolase precursor (EC 3.4.19.9) (Gamma-Glu-X carboxypeptidase) (Conjugase) (GH).
WC001B711M11-400.0=Ribosomal protein L33.
WC005B712M34-275.3=similar to GP 21624281 dbj BAC01127. P1CYC4 {Pueraria montana var. lobata}. partial (30%)
WC029B731M24-291.1=Hypothetical protein.
WC046B744M24-202.5=At3g10650.
WC046B744M13-216.5=S-adenosyl-methionine-sterol-C-methyltransferase.
WC006B712M41-181.1=Heat shock protein (Fragment).
WC046B744M22-398.6=Similar to Mus musculus (Mouse). sex-determining region Y protein (Testis-determining factor).
WC024B724M44-328.9=similar to PIR T02607 T02607 probable cytochrome P450 T19L18.2 [similarity] - Arabidopsis thaliana. partial (76%)
WC037B744M11-255.9=Seed tetraubiquitin.
WC027B731M11-253.8=2'-hydroxydihydrodaidzein reductase.
WC019B723M12-521.0=Methionine synthase.
WC018B722M34-434.7=SAR DNA-binding protein-1.
WC041B742M31-237.8=Histone H4.
WC018B722M41-318.5=TAF5.
WC026B722M43-166.5=Putative ubiquitin carboxyl-terminal hydrolase.
WC025B721M31-328.3=Hypothetical protein.
WC011B714M43-487.0=Serine/threonine protein phosphatase BSL2 (EC 3.1.3.16) (BSU1-like protein 2) Brassinosteroid signaling.
WC037B734M43-151.6=similar to GP 21553767 gb AAM62860.1 unknown {Arabidopsis thaliana}. partial (74%)
WC020B723M21-243.2=bZIP transcription factor ATB2.
WC038B741M21-110.5=Calmodulin-like protein.
WC015B721M24-214.5=similar to GP 21594008 gb AAM65926.1 putative invertase {Arabidopsis thaliana}. partial (94%)
WC002B711M22-320.3=Cystathionine-gamma-synthase precursor (EC 4.2.99.9).
WC003B711M34-423.8=similar to GP 15146224 gb AAK83595.1 AT5g25280/F18G18_20 {Arabidopsis thaliana}. partial (47%)
WC040B741M43-263.2=Respiratory burst oxidase homolog.
WC043B743M11-413.1=homologue to GP 13016806 emb CAC29435. P-type H+-ATPase {Vicia faba}. partial (19%)
WC007B713M24-264.1=Aldehyde dehydrogenase (NAD+) (EC 1.2.1.3).
WC007B713M13-351.1=similar to PIR T05512 T05512 hypothetical protein F13M23.50 - Arabidopsis thaliana. partial (17%)
WC036B734M23-272.4=Hypothetical protein Atu4185.
WC047B744M33-233.9=Dbj|BAA78736.1 (Hypothetical protein).
WC014B721M11-216.0=POLYUBIQUITIN-like protein.
WC045B744M11-159.0=Metal transport protein.
WC036B734M23-153.6=homologue to GP 15215820 gb AAK91455.1 At4g28240/F26K10_120 {Arabidopsis thaliana}. partial (19%)
WC048B732M41-228.6=similar to GP 7940285 gb AAF70844.1 F24O1.19 {Arabidopsis thaliana}. partial (12%)
WC022B724M22-230.2=similar to GP 16209656 gb AAL14388.1 At4g15940/dl4011w {Arabidopsis thaliana}. partial (91%)
WC039B741M32-447.5=Disease resistance response/ dirigent-like protein.
WC045B744M11-320.4=Putative purple acid phosphatase.
WC020B723M31-600.8=Glutamate 1-semialdehyde aminotransferase (EC 5.4.3.8).
WC004B712M21-318.3=similar to PIR T05308 T05308 hypothetical protein F26P21.120 - Arabidopsis thaliana (fragment). partial (45%)
WC033B733M32-186.4=similar to GP 11177137 dbj nuclear coiled-coil protein AT4g30200 {Arabidopsis thaliana}. partial (9%)
WC046B744M13-292.1=Hypothetical protein.
WC029B731M43-172.5=Ribosomal protein L9, putative.
WC047B744M34-275.0=Granule-bound starch synthase Ib precursor (EC 2.4.1.21).
WC043B743M21-311.8=Putative RNA binding protein precursor.
WC038B741M13-133.7=similar to PIR T07623 T07623 extensin homolog HRGP2 - soybean (fragment). partial (61%)

Cluster 6

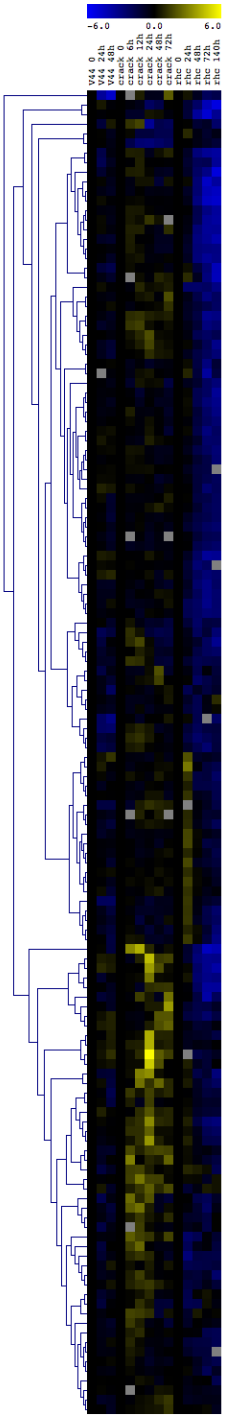

WC024BT23M41-500.6=similar to PIR T05188 T05188 protein kinase F4I10.10 (EC 2.7.1.-) - Arabidopsis thaliana. partial (68%)
WC020BT23M31-166.2=Peroxidase precursor.
WC044BT43M23-275.1=homologue to SP P49107 PSAN_ARATH Photosystem I reaction centre subunit N chloroplast precursor (PSI- N). [Mouse-ear cress]. partial (62%)
WC008BT13M33-192.2=Inositol 4-methyltransferase (EC 2.1.1.129).
WC043BT43M21-319.3=Chlorophyll a/b-binding protein (Fragment).
WC037BT34M42-205.2=Chalcone synthase (EC 2.3.1.74).
WC025BT21M33-204.0=Nucleoid DNA-binding protein cnd41-like protein.
WC004BT12M12-112.0=similar to GP 20127022 gb AAM10937.1 putative bHLH transcription factor {Arabidopsis thaliana}. partial (27%)
WC036BT34M33-207.6=Hypothetical protein.
WC043BT43M21-641.8=Amino acid transporter-like protein.
WC038BT41M14-183.1=Putative alpha-dioxygenase (Fragment).
WC009BT14M11-344.4=Putative gag-pol polyprotein.
WC031BT32M32-409.5=Respiratory burst oxidase homolog.
WC018BT22M34-206.0=Isopentenyl-diphosphate delta-isomerase II (EC 5.3.3.2) (IPP isomerase II) (Isopentenyl pyrophosphate isomerase II).
WC020BT23M22-627.5=BSD protein (Fragment).
WC002BT11M21-386.5=S-receptor kinase-like protein 2.
WC048BT32M12-399.6=At1g10600.
WC027BT31M14-552.4=Putative inositol polyphosphate-5-phosphatase.
WC021BT23M43-270.8=CTV.2.
WC024BT23M41-383.2=Wound-inducible P450 hydroxylase.
WC005BT12M31-271.9=similar to PIR P84920 P84920 probable glutaredoxin [imported] - Arabidopsis thaliana. partial (97%)
WC040BT41M44-M94.7=weakly similar to GP 21039116 gb AAM33509.1 60 kDa glycoprotein (Cryptosporidium parvum). partial (11%)
WC024BT23M42-430.0=similar to GP 15290113 dbj BAB63805. contains ESTs AU031749(R1464) D24170(R1464)-unknown protein {Oryza sativa (japonica cultivar-group)}. partial (10%)
WC037BT34M42-484.3=Putative LRR receptor protein kinase.
WC013BT14M14-273.4=Protein phosphatase-2c (Fragment).
WC040BT41M44-360.0=Hypothetical protein (Fragment).
WC028BT31M33-164.4=Beta-adaptin-like protein C (Fragment).
WC047BT44M34-293.0=similar to PIR P86427 P86427 auxin response factor 6 (ARF6) [imported] - Arabidopsis thaliana. partial (17%)
WC032BT32M43-342.9=ABC transporter. putative.
WC004BT12M22-220.4=weakly similar to GP 10039641 gb AAG12204.1 Orf122 {Chlorobium tepidum}. partial (66%)
WC009BT13M43-356.3=Putative mitochondrial glyoxalase II (Fragment).
WC033BT33M24-328.8=weakly similar to GP 6729048 gb AAF27044.1 unknown protein 3' partial {Arabidopsis thaliana}. partial (11%)
WC005BT12M32-319.3=Syringolide-induced protein B13-1-9.
WC035BT34M13-238.4=Putative phosphate transporter (At1g76430).
WC009BT14M12-282.2=Sucrose synthase.
WC038BT41M21-153.7=
WC025BT22M24-261.5=weakly similar to GP 21593499 gb AAM65466.1 putative nodulin protein N21 {Arabidopsis thaliana}. partial (16%)
WC043BT43M11-199.6=weakly similar to GP 4105798 gb AAD02556.1 PGPD14 {Petunia x hybrida}. partial (53%)
WC041BT42M21-366.8=KCBP interacting Ca2+-binding protein.
WC011BT14M41-229.2=similar to GP 22597162 gb AAN03468.1 bZIP transcription factor ATB2 {Glycine max}. partial (65%)
WC038BT41M14-522.0=Centromere protein.
WC010BT14M21-283.6=Hypothetical protein.
WC048BT32M12-468.3=similar to GP 17381208 gb AAL36416.1 unknown protein {Arabidopsis thaliana}. complete
WC003BT11M33-404.8=Citrate binding protein.
WC046BT44M23-181.6=weakly similar to PIR D85437 D85437 hypothetical protein AT4g37030 [imported] - Arabidopsis thaliana. partial (41%)
WC045BT43M44-680.7=OSJNBa0065B15.8 protein.
WC036BT34M24-232.8=Putative polygalacturonase.
WC014BT21M21-285.0=Genomic DNA. chromosome 3. BAC clone:T5M7 (Hypothetical protein) (At3g25590).
WC009BT14M11-374.8=Basic chitinase (AT3g16920/K14A17_4).
WC011BT14M41-221.4=similar to GP 22136716 gb AAM91677.1 unknown protein {Arabidopsis thaliana}. partial (37%)
WC014BT21M12-276.4=Ras-related protein Rab11A.
WC029BT31M43-390.7=similar to PIR B96836 B96836 unknown protein T21F11.23 [imported] - Arabidopsis thaliana. partial (13%)
WC003BT11M44-289.1=Cytosolic aldehyde dehydrogenase RF2C.
WC045BT44M11-462.0=Hypothetical protein.
WC022BT24M13-378.9=similar to PIR T51937 T51937 probable inositol-1 4 5-trisphosphate 5-phosphatase (EC 3.1.3.56) At5P2 [imported] - Arabidopsis. partial (53%)
WC013BT14M14-366.5=Putative receptor protein kinase.
WC038BT41M22-576.9=ATMRP4 (MRP-like ABC transporter).
WC044BT43M32-171.7=Translation elongation factor-1 alpha (Fragment).
WC042BT42M33-368.6=GIGANTEA protein.
WC014BT21M13-241.8=60S ribosomal protein L7-1.
WC003BT11M33-258.0=ATP synthase B chain (EC 3.6.3.14) (Subunit I).
WC037BT44M11-217.3=GP 21322711 e pherophorin-dz1 protein {Volvox carteri f. nagariensis}. partial (4%)
WC004BT12M12-230.0=weakly similar to GP 10039641 gb AAG12204.1 Orf122 {Chlorobium tepidum}. partial (66%)
WC006BT12M41-266.3=SP O22552 VATL_PHAAU Vacuolar ATP synthase 16 kDa proteolipid subunit (EC 3.6.3.14). [Mung bean Vigna radiata]. complete
WC027BT31M14-273.0=homologue to GP 4240227 dbj BAA74892.1 KIAA0869 protein {Homo sapiens}. partial (2%)
WC021BT23M41-495.0=similar to SP P29677 MPPA_SOLTU Mitochondrial processing peptidase alpha subunit mitochondrial precursor (EC 3.4.24.64) (Alpha-MPP). partial (93%)
WC020BT23M21-618.0=Hexose transporter.
WC042BT42M43-346.7=Type 2A protein phosphatase-3 (EC 3.1.3.16) (Serine/threonine protein phosphatase).
WC009BT13M44-330.0=Histidine kinase. (CRE1 cytokinin receptor)
WC008BT13M41-222.1=Cytochrome b.
WC036BT34M23-238.4=weakly similar to GP 11141605 gb AAG32022.1 LEUNIG {Arabidopsis thaliana}. partial (8%)
WC043BT43M12-159.2=weakly similar to GP 9758223 dbj FRO2 homolog {Arabidopsis thaliana}. partial (13%)
WC005BT12M33-381.1=F20P5.3 protein.
WC038BT41M22-154.8=
WC027BT31M12-196.4=Acid phosphatase.
WC036BT34M24-240.0=At1g12170.
WC008BT13M31-303.1=Nematode resistance-like protein.
WC036BT34M34-140.3=similar to PIR A84830 A848 hypothetical protein At2g40480 [imported] - Arabidopsis thaliana. partial (6%)
WC004BT12M11-528.3=similar to GP 1985024 gb cytosolic aldehyde dehydrogenase RF2C {Zea mays}. partial (27%)
WC047BT44M41-153.3=similar to GP 9967495 emb CAC03535.2 putative protein {Arabidopsis thaliana}. partial (74%)
WC045BT43M43-356.2=similar to GP 15425641 dbj BAB64308. TOM3 {Arabidopsis thaliana}. partial (90%)
WC041BT42M31-268.2=Vacuolar proton-inorganic pyrophosphatase.
WC047BT44M41-143.1=similar to GP 15292697 gb AAK97717.1 putative RNA-binding protein {Arabidopsis thaliana}. partial (4%)
WC048BT32M12-512.6=Octapeptide-repeat protein T2.
WC033BT33M32-160.5=
WC002BT11M31-168.5=weakly similar to PIR D96693 D96 protein Putative ABC transporter [imported] - Arabidopsis thaliana. partial (5%)
WC038BT41M24-141.8=similar to PIR C84473 C84473 probable protein kinase [imported] - Arabidopsis thaliana. partial (69%)
WC013BT13M21-214.0=weakly similar to GP 19310745 gb AAL85103.1 unknown protein {Arabidopsis thaliana}. partial (17%)
WC044BT43M32-290.3=cycloartenol synthase
WC014BT21M12-314.6=Hypothetical protein OJ1012B02.18 (Hypothetical protein OJ1364E02.2).
WC028BT31M23-237.1=Protein kinase-like protein.
WC021BT23M44-377.2=similar to GP 21594011 gb AAM65929.1 unknown {Arabidopsis thaliana}. partial (71%)
WC036BT34M23-423.3=similar to PIR T00593 T02480 sec13-related protein At2g30050 - Arabidopsis thaliana. complete
WC003BT11M33-517.0=weakly similar to PIR T01996 T01996 nucleoid DNA-binding protein cnd41 chloroplast - common tobacco. partial (63%)
WC032BT32M44-M97.9=similar to GP 21025977 gb AAM14389.1 putative nodulin protein {Arabidopsis thaliana}. partial (81%)
WC004BT12M21-210.5=similar to PIR T02456 T02456 protein kinase homolog F4I18.11 - Arabidopsis thaliana. partial (19%)
WC011BT14M42-334.6=Putative peroxidase.
WC036BT34M23-157.3=weakly similar to GP 21592507 gb unknown {Arabidopsis thaliana}. partial (44%)
WC044BT43M34-318.5=homologue to PIR T06570 T06570 superoxide dismutase (EC 1.15.1.1) (Cu-Zn) - garden pea. complete
WC007BT13M13-296.6=similar to PIR E85097 E8509 hypothetical protein At4g09550 [imported] - Arabidopsis thaliana. partial (33%)
WC046BT44M22-188.8=Plasma membrane MIP protein.
WC021BT23M44-332.6=similar to SP O23714 PS21_ARATH Proteasome subunit beta type 2-1 (EC 3.4.25.1) (20S proteasome alpha subunit D1). [Mouse-ear cress]. partial (97%)
WC021BT23M43-408.5=At2g14110.
WC037BT44M11-376.8=NAD(P)H-quinone oxidoreductase chain J. chloroplast (EC 1.6.5.-) (NAD(P)H dehydrogenase. chain J) (NADH-plastoquinone oxidoreductase subunit J).
WC001BT11M11-169.4=GP 21322711 e pherophorin-dz1 protein {Volvox carteri f. nagariensis}. partial (4%)
WC005BT12M24-645.0=NAD(P)H-quinone oxidoreductase chain H. chloroplast (EC 1.6.5.-) (NAD(P)H dehydrogenase. chain H) (NADH-plastoquinone oxidoreductase 49 kDa subunit).
WC023BT24M41-124.5=similar to SP Q41001 BCP_PEA Blue copper protein precursor. [Garden pea] {Pisum sativum}. partial (87%)
WC005BT12M32-247.2=homologue to PIR S40240 S40240 ubiquitin/ribosomal protein S27a fusion protein - white lupine. complete
WC005BT12M32-276.1=homologue to SP O82043 ILV5_PEA Ketol-acid reductoisomerase chloroplast precursor (EC 1.1.1.86). complete
WC002BT11M32-197.4=Genomic DNA. chromosome 5. TAC clone:K19P17 (Hypothetical protein).
WC003BT11M33-508.0=Citrate binding protein.
WC042BT42M33-487.5=Cytochrome P450.
WC035BT34M12-210.6=similar to GP 20453070 gb AAM19780.1 AT5g66920/MUD21_18 {Arabidopsis thaliana}. partial (86%)
WC043BT43M22-372.0=Chitinase.
WC046BT44M23-525.0=weakly similar to PIR D85437 D85437 hypothetical protein AT4g37030 [imported] - Arabidopsis thaliana. partial (41%)
WC005BT12M33-364.5=Catechol O-methyltransferase (EC 2.1.1.6).
WC005BT12M31-140.0=Gigantea homologue (Fragment).
WC042BT42M43-613.9=Hypothetical protein.
WC024BT23M41-365.7=F10A5.18.
WC012BT11M12-215.2=F26G16.2 protein.
WC040BT42M13-227.2=60S ribosomal protein L7-3.
WC023BT24M33-163.9=Papain-like cysteine proteinase isoform II.
WC005BT12M33-309.3=similar to GP 14719339 gb AAK73157.1 putative protein kinase {Oryza sativa}. partial (82%)
WC037BT44M11-209.2=KNAT3 homeodomain protein.
WC046BT44M13-231.1=HMG-CoA synthase 2.
WC044BT43M23-367.6=Hypothetical protein.
WC026BT22M43-649.0=weakly similar to GP 10176848 dbj BAB10054. amino acid transporter {Arabidopsis thaliana}. partial (43%)
WC033BT33M22-129.8=similar to GP 16226251 gb AAL16115.1 AT4g14500/d13290w {Arabidopsis thaliana}. partial (30%)
WC045BT43M41-218.0=Poly(A)-binding protein.

Cluster 7

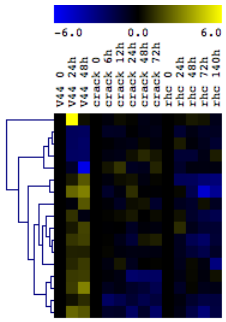

"WC046BT44M24-136.5=similar to GP 18377783 gb AAL67041.1 unknown protein {Arabidopsis thaliana}, partial (24%) "
WC036BT34M34-578.0=F8K7.13 protein (Putative transcriptional regulatory protein).
"WC047BT44M42-146.0=GP 4521190 db Pib {Oryza sativa}, partial (0%)"
WC014BT21M14-294.8=Hypothetical protein.
WC036BT34M32-400.0=Alkaline alpha galactosidase I (Fragment).
"WC040BT41M43-169.2=similar to GP 15451136 gb periaxin-like protein {Arabidopsis thaliana}, partial (26%) "
"WC010BT14M31-324.0=similar to GP 15081628 gb At1g79260/YUP8H12R_40 {Arabidopsis thaliana}, partial (89%) "
"WC012BT11M24-153.3=similar to PIR H96816 H96 hypothetical protein F9K20.18 [imported] - Arabidopsis thaliana, partial (47%) "
WC022BT24M23-353.5=Hypothetical protein.
WC045BT43M44-417.1=Hypothetical protein.
WC048BT32M12-658.6=L-asparaginase (EC 3.5.1.1).
WC007BT13M24-259.6=Aldehyde dehydrogenase 1 precursor (EC 1.2.1.3).
WC043BT43M12-672.2=AT5g52920/MXC20_15 (EC 2.7.1.40) (Pyruvate kinase) (PK).
WC044BT43M23-448.9=Trypsin inhibitor.
"WC043BT43M14-131.9=similar to GP 15021754 gb root nodule extensin {Pisum sativum}, partial (54%) "
"WC003BT11M34-231.6=similar to SP Q9SPE6 SNAA_ARATH Alpha-soluble NSF attachment protein (Alpha-SNAP), complete "
WC047BT44M32-286.4=F13K23.20 protein.

Chapter 7

SrSymRK, a plant receptor essential for symbiosome formation

Published as: Capoen, W., Goormachtig, S., De Rycke, R., Schroeyers, K., and Holsters, M. (2005). SrSymRK, a plant receptor essential for symbiosome formation. Proc Natl Acad Sci U S A 102, 10369-10374.

The symbiosis between legumes and rhizobia is essential for the nitrogen input into the life cycle on our planet. New root organs, the nodules, are established, which house N_2-fixing bacteria internalized into the host cell cytoplasm as horizontally acquired organelles, the symbiosomes. The interaction is initiated by bacterial invasion via epidermal root hair curling and cell division in the cortex, both triggered by bacterial nodulation factors. Of the several genes involved in nodule initiation that have been identified, one encodes the leucine-rich repeat-type receptor kinase SymRK. In SymRK mutants of *Lotus japonicus* or its orthologs in *Medicago* sp. and *Pisum sativum,* nodule initiation is arrested at the level of the root hair interaction. Because of the epidermal block, the role of SymRK at later stages of nodule development remained enigmatic. To analyze the role of SymRK downstream of the epidermis, the water-tolerant legume *Sesbania rostrata* was used that has developed a nodulation strategy to circumvent root hair responses for bacterial invasion. Evidence is provided that SymRK plays an essential role during endosymbiotic uptake in plant cells.

Introduction

Leguminous plants can engage into a symbiotic interaction with rhizobia and form new root organs, the nodules, in which the bacteria reside and fix atmospheric dinitrogen. Rhizobia belong to diverse phylogenetic taxa but have in common the capacity to induce nodules on the appropriate legume host. The nodulation process is initiated by a complex signal exchange between both partners. The principal signal molecules, the bacterial nodulation factors (NFs), are lipochitooligosaccharides decorated with specific chemical groups at both the reducing and nonreducing end (D'Haeze and Holsters, 2002).

Recognition of compatible NFs triggers developmental and cellular host responses, such as rapid ion fluxes, membrane depolarization, calcium oscillations, cytoskeletal reorganization, root hair deformations and curling, gene expression, and cell division (Geurts and Bisseling, 2002); Oldroyd, 2004 #235}. Rhizobial invasion usually takes place via root hairs. Upon NF perception, developing root hairs deform and eventually curl (Gage, 2004). The bacteria are entrapped in this curl and a microcolony is formed. Local cell wall hydrolysis and invagination of the plasma membrane lead to the formation of a tubular structure: the infection thread (IT) that proceeds through the root hair and underlying cell layers to guide the bacteria toward a nodule primordium, which develops in the cortex (Gage, 2004). An elaborate IT network spreads into the nodule primordium to provide bacteria to plant cells for endosymbiotic release. Uptake is initiated by local IT wall hydrolysis; unwalled infection droplets are formed from which bacteria are pinched off, thus creating symbiosomes (Brewin, 2004). Symbiosomes contain one or a few bacteria, now called bacteroids, surrounded by a plant-derived membrane, the peribacteroid or symbiosome membrane (Vasse et al., 1990). Considerable progress has been made in analyzing the plant mechanisms that regulate initiation and development of nodules and control of bacterial invasion.

Several candidate NF receptors have been identified, which are all receptor-like kinases with extracellular lysin motif (LysM) domains (Limpens et al., 2003; Madsen et al., 2003; Radutoiu et al., 2003)). Bacterial LysM domains bind peptidoglycan or chitin (Amon et al., 1998; Bateman and Bycroft, 2000); hence, plant LysM-receptor-like kinases are good candidates for NF binding and perception. In addition, other NF signal transduction elements act downstream from the LysM-receptor-like kinases, because the corresponding mutants still respond to NFs by root hair swelling, but no longer show a root hair curling (RHC) response. In *Medicago truncatula,* the Dmi1, Dmi2, and Dmi3 (Catoira et al., 2000) genes encode a putative ligand-gated cation channel, a leucine-rich repeat (LRR)-type receptor kinase, and a putative calcium and calmodulin-dependent protein kinase, respectively (Endre et al., 2002; Stracke et al., 2002; Ané et al., 2004; Lévy et al., 2004). Orthologs of Dmi2 have been described in *M. sativa* (MsNork), *Lotus japonicus* (LjSymRK), and *Pisum sativum* (Pssym19) (Endre et al., 2002; Stracke et al., 2002). Remarkably, mutations in these genes also impair arbuscular mycorrhization, which is

an ancient and widespread that facilitates phosphate acquisition and involves 80% of the land plants and fungi belonging to the Glomeromycota (Parniske, 2004). Hence, the pathways of nodulation and mycorrhization share common genetic elements for the establishment of endosymbiotic structures (Parniske, 2004). Recently, a nonsymbiotic, NF independent phenotype of enhanced touch sensitivity has been observed for the MsNork, the MtDmi2, and the LjSymRK mutant lines. When care is taken not to disturb root hairs during experimental manipulations, they curl upon application of rhizobia, but the curling is arrested when the root hair tip touches its own shank. Hence SymRK and its relatives are not needed for the curling process itself, although they do remain necessary for downstream, NF-dependent gene expression (Esseling et al., 2004).

We have investigated the role of SrSymRK, the unique *Sesbania rostrata* ortholog of *MsNork-LjSymRK* in the establishment of lateral root base (LRB) nodules. The tropical legume S. rostrata is adapted to nodulate in temporarily flooded habitats and has versatile nodulation features. Under well-aerated conditions, nodules form in the zone of developing root hairs via RHC invasion of the microsymbiont *Azorhizobium caulinodans* (Goormachtig et al., 2004a). However, on hydroponic roots, N_2-fixing nodules develop at LRBs (Goormachtig et al., 2004a), azorhizobia invade the cortex intercellularly via cracks, resulting from lateral root protrusion, thereby circumventing the epidermis (Goormachtig et al., 1998). Cortical infection pockets (IPs) are formed by NF-dependent local cell death induction and subsequent colonization of bacteria. Presumably, IPs function as signaling centers, similar to rhizobial colonies within 3D root hair curls (Goormachtig et al., 2004a). From IPs, ITs guide bacteria toward the target cells for symbiotic uptake. A very comparable process takes place at the bases of adventitious rootlets that are located on the stem of S. rostrata and that can develop into ‘‘stem’’ nodules upon inoculation. Because LRB nodulation with intercellular invasion strictly depends on NFs (D'Haeze et al., 1998), it is an excellent tool to analyze the requirement for and consequences of NF-linked perception transduction systems in cell layers, which are deeper than the epidermis. Here, we demonstrate that RNA interference (RNAi)-mediated knockdown of *SrSymRK* inhibits release of bacteria from infection droplets into the plant cytoplasm.

Materials and Methods

Plant and Bacterial Material.

S. rostrata Brem and A. caulinodans ORS571 (pRG960SD-32) were grown as described (Goormachtig et al., 2004b).

Southern Analysis.

DNA gel blot analysis was performed as described (Sambrook et al., 1989). Labeled probes were generated from the extracellular domain with SrNORKRTF1 (5’-CCAAACAGACGTGGAAGTGA- 3’) and SrNORKRTR2 (5’-CTTCGCTCATGTGTTGGTTGC- 3’).

Identification of the Full-Length SrSymRKSequence.

Plaques (10^5) of a λ-fix II S. rostrata genomic library were screened with a probe

corresponding to the extracellular and kinase domains of *M. truncatula* DMI2 (Sambrook et al., 1989). The full-length cDNA sequence was obtained by 5' and 3' RACE (Smart RACE cDNA amplification kit, Clontech). The fragments were cloned in a pGEMTeasy vector (Promega).

Expression Analysis.

In situ hybridization was as described (Goormachtig et al., 1997; Gage, 2004). The LRR region was used as template to produce ^{35}S-labeled antisense probe. RT-PCR was performed (Corich et al., 1998; Kiefer et al., 2000) with specific probes generated by SrNORKrtF1 (5'-CCAAACAGACGTGGAAGTGA- 3') and SrNORKrtR2 (5'-CTTCGCTCATGTGTTGGTTGC- 3') primers.

Transgenic Roots.

To produce the knockout constructs (pK7GWIWG27F2-SymRKKO1 and pK7GWIWG27F2-Sym- RKKO2), two non overlapping regions of the LRR domain were recombined in the pK7GWIWG27F2 binary GATEWAY vectors (Invitrogen) (Karimi et al., 2002). For the pK7GWIWG27F2-SymRKKO1 and pK7GWIWG27F2-SymRKKO2 constructs, the primers SrSymRKRTF1attB1 (5'-GGGGACAAGTTTGTACAAAAAAGCAGGCTCCAACCAAACAGACGTGGAAGTGA- 3') and SrSymRKR13attB2 (5'-GGGACCACTTTGTACAAGAAAGCTGGGTCACTGGAAGGAATTGGTCCT- 3'); and SrSymRKF16attB1 (5'-GGGGACAAGTTTGTACAAAAAAGCAGGCTTGAGCCACAACAGT- 3') and SrSymRKRTR2attB2 (5'-GGGGACCACTTTGTACAAGAAAGCTGGGTCTTCGCTCATGTGTTGGTTGC- 3') were used, respectively. S. rostrata embryonic axes were transformed as described (Van de Velde et al., 2003).

Light Microscopy and Transmission EM.

Staining with β-glucuronidase was as described (D'Haeze et al., 1998). For semithin sections, the tissues were embedded in Technovit 7100 (Heraeus), cut, and stained with toluidine blue (Goormachtig et al., 1998; Van de Velde et al., 2003). GFP analysis (Van de Velde et al., 2003) and transmission EM (D'Haeze et al., 1998) were performed as described.

Fig. 1. *SrSymRK*, the *SymRK* ortholog of *S. rostrata*. (*A*) Sequence of the SrSymRK protein and orthologs. SrSymRK shows a90%and86%similarity to *L. japonicus LjSymRK* and *M. truncatula MtDMI2*, respectively. Conserved amino acids are highlighted. (*B*) Southern analysis with the extracellular domain of *SrSymRK* as a probe.

Results

SrSymRK Transcripts Accumulate in the Infection Zone of LRB Nodules.

The full-length cDNA of *SrSymRK* was obtained by genomic library hybridization and RT-PCR (see Materials and Methods) SrSymRK is 86% and 90% similar at the amino acid level to MtDmi2 and LjSymRK, respectively (Fig. 1A). Southern hybridization with the extracellular domain (Fig. 1B) of *MtDmi2* as probe revealed one band in each digest, demonstrating that *SrSymRK* is a unigene. RT-PCR was performed to analyze the expression levels of *SrSymRK* during LRB nodulation. cDNA was prepared from stem-located adventitious root primordia before and at 2, 4, 6, and 15 days post inoculation (dpi) with *A. caulinodans* (Fig. 2A). As seen in Fig. 2A, a basal expression was observed in adventitious root primordia, the expression was rapidly induced between 2 and 4 dpi, and the transcript levels dropped again in mature nodules at 15 dpi. Similarly, but less pronounced, *SrSymRK* transcripts accumulated during LRB nodulation of hydroponic roots.Uninfected roots and infected LRBs were harvested 12, 24, 36, 72, and 84 h after inoculation. RT-PCR analysis showed that the transcript levels were already slightly elevated 12 h after inoculation. *SrSymRK*

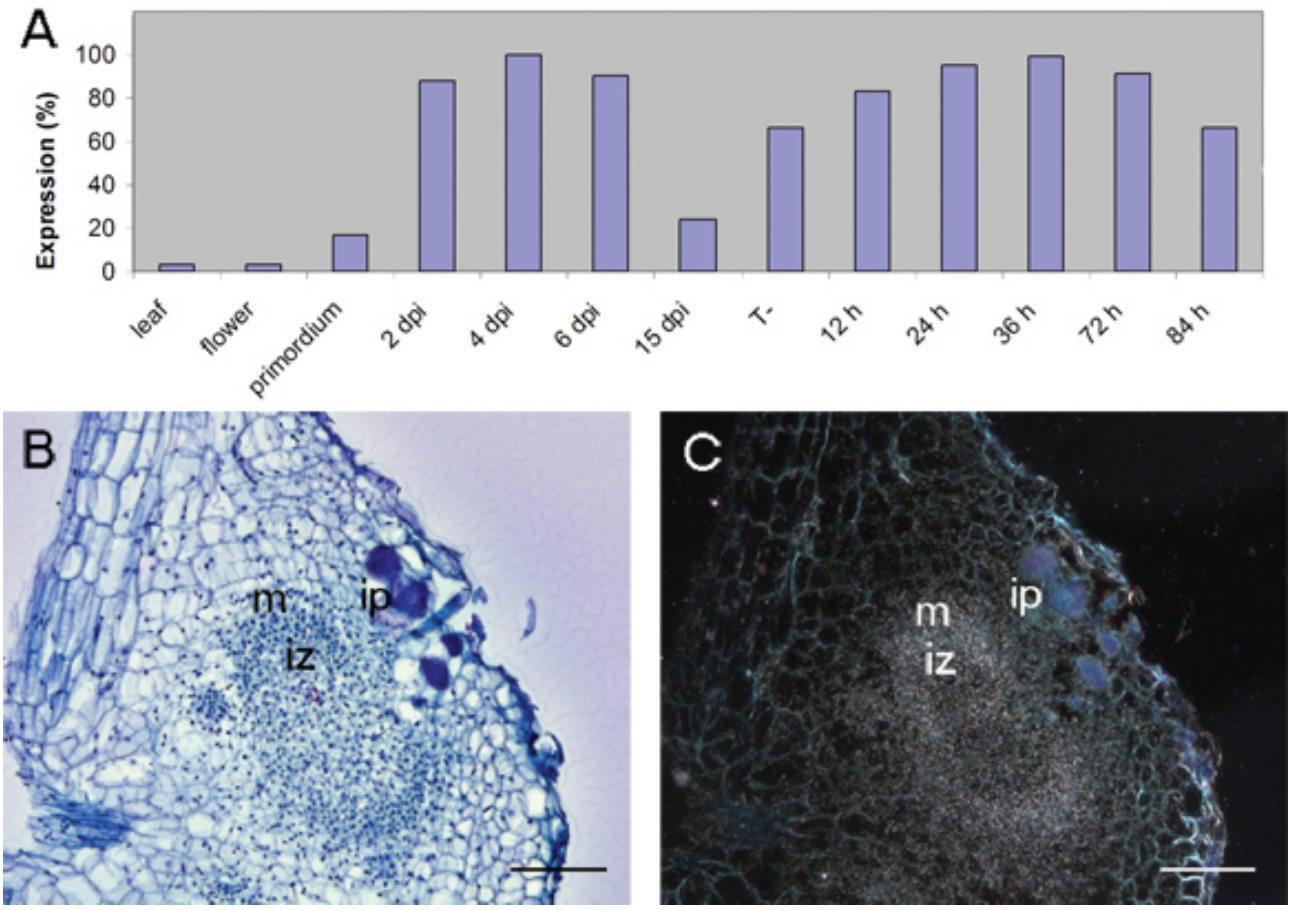

Fig. 2. Expresssion analysis of *SrSymRK*. (*A*) RT-PCR analysis. *SrSymRK* expression levels are shown for leaves, flowers, uninfected adventitious root primordia (primordium), in adventitious root primordia infected with ORS571 after 2, 4, and 6 dpi, in hydroponic roots (T-), and in hydroponic roots 12, 24, 36, 72, and 84 h after inoculation. (*B*) Bright-field image of an *in situ* mRNA localization in a semithin section through a nodule primordium 72 h after inoculation. (*C*) Dark-field image of *B*; signal is visible as silver grains in the infection zone. ip, infection pocket; iz, infection zone; m, meristem. (Scale bars, 100 μm.)

levels were low in flowers and leaves (Fig. 2A). To analyze the transcript localization during nodule development, developing adventitious root nodules were hybridized *in situ* at 3 dpi. At this stage, ITs have reached the nodule primordium, which has the shape of an open basket with a meristem and an infection zone where bacteria are released into plant cells. *SrSymRK* transcripts were detected in the infection zone of the developing nodule (Fig. 2 B and C).

Knock down of *SrSymRK* Affects Bacterial Release from ITs.

To investigate the role for *SrSymRK* in LRB nodulation, two independent RNAi constructs were made, each with a 200-bp fragment of the *SrSymRK* LRR-coding sequence. These constructs were introduced into *S. rostrata* via *Agrobacterium rhizogenes*-mediated transformation (see Materials and Methods) with a ^{35}S-enhanced GFP as cotransformation marker (Van de Velde et al., 2003). In total, 91 cotransformed roots were selected for analysis. Chimeric plants with transgenic roots were inoculated with *A. caulinodans*, and

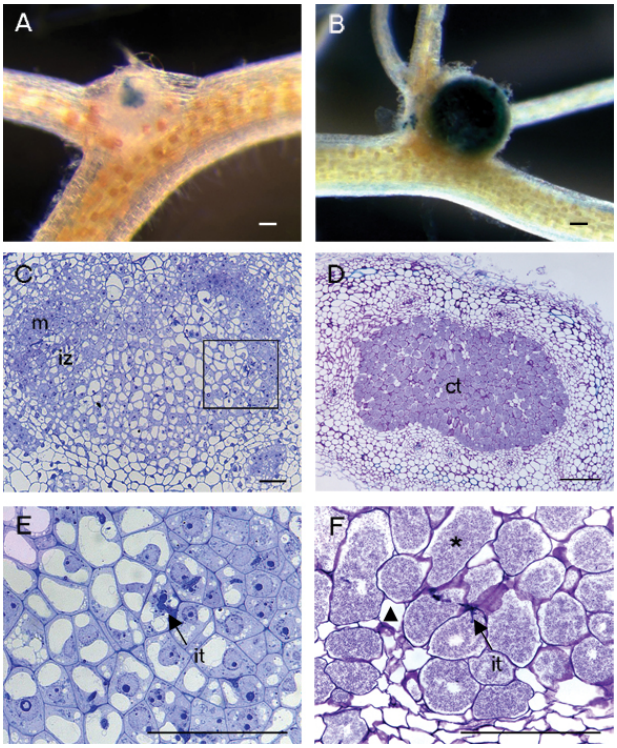

Fig. 3. Knockdown phenotype of *SrSymRK*. (*A*) Low magnification view of a *SrSymRK* knockdown line, 10 dpi. Bacteria are labeled with _-glucuronidase. (*B*) Low magnification view of a functional WT nodule, 10 dpi. Bacteria are labeled with β-glucuronidase. (*C*) Semithin section through *A*. IPs, ITs, and a primordium are formed, but no cells are infected. (*D*) Semithin section through *B*, 10 dpi. (*E* and *F*) Details of *C* and *D*. Uninfected and infected cells are marked by triangles and asterisks, respectively. ct, central tissue; ip, infection pocket; it, infection thread; iz, infection zone; m, meristem. (Scale bars, 100 μm.)

nodulation was scored between 8 and 14 dpi. At this stage, control lines transformed with the empty vector, all contained round, N_2-fixing nodules (Fig. 3B). Nine lines containing RNAi constructs developed small, white, nodule-like structures at the base of the lateral roots of hydroponically grown roots (Fig. 3A). Infection with ORS571(pRG960–32), which can be visualized by β-glucuronidase staining, revealed that the primary invasion into the infection center was not hampered, but spreading into the cells of the nodule primordium was inhibited. In contrast, the central tissue of the stained control nodules was completely invaded (compare Fig. 3 A with B). RT-PCR analysis of clonally propagated offspring of the nine lines showed a down-regulation of 65–92% in *SrSymRK* transcript levels when compared to control lines (data not shown). Microscopic analysis of semithin, toluidine blue-stained sections through a nodule-like structure derived from a *SrSymRK* RNAi line at 10 dpi revealed a nodule primordium in the typical open-basket conformation as is normally seen for WT nodules at 3–6 dpi. IPs were visible, with ITs progressing toward an infection zone adjacent to the meristem (Fig. 3 C and E). Nevertheless, no fixation zone with infected cells was observed but, instead, a zone of differentiated cells that were vacuolated and not filled with bacteria (Fig. 3E). In contrast, the control nodules had a fully differentiated central tissue containing cells with N_2-fixing symbiosomes (Fig. 3 D and F).

Ultrastructural Analysis of SrSymRK RNAi Lines Reveals Multiple Nodulation Defects.

To better investigate eventual morphological abnormalities, in vitro-propagated transgenic roots of a 70% *SrSymRK* knockdown line were grafted on WT shoots of *S. rostrata*. This particular line showed nodule primordium and IT formation, but no bacterial uptake, in accordance with the phenotype for *SrSymRK*

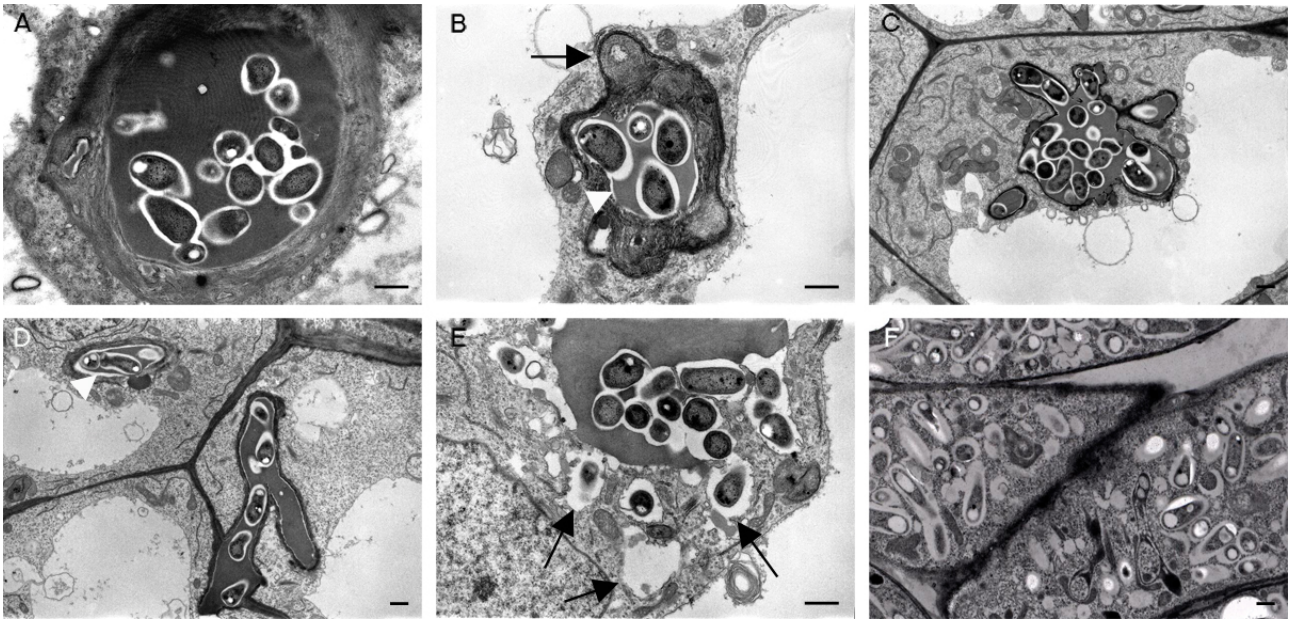

Fig. 4. Ultrastructural analysis of the *SrSymRK* knockdown phenotype. (*A*) Transverse section through a WT intracellular IT. (*B*) Transverse section through an intracellular IT in an *SrSymRK* knockdown background, 10 dpi. Arrowhead and arrow indicate low electron-dense rim and abnormal cell wall depositions in *SrSymRK* knockdown lines, respectively. (*C*) Section through a bag-like intracellular IT consisting of numerous branches, 10 dpi. (*D*) Section through an intracellular IT in an *SrSymRK* knockdown background. Low electron-dense rim is indicated by an arrowhead. (*E*) Rare release of bacteria, resulting in abnormal symbiosomes, which are indicated by arrows. (*F*) WT bacteroids at 6 dpi. (Scale bars, 1 μm.)

knockdown lines described above. The grafts responded to bacterial inoculations in exactly the same manner as the primary transformed roots (data not shown). Ten days after inoculation with *A. caulinodans,* small, nodule-like structures were harvested for EM analysis (Materials and Methods). High magnifications of ITs in the infection zone showed that, in contrast to WT, a low electron-dense rim was present between the IT matrix and the IT wall (Fig. 4 A, B, and D). The rim was continuous with the low electron-dense bacterial surface polysaccharides. ITs seemed to lose rigidity and became bag-like in appearance, with unusually protruding bulges (Fig. 4 C and D). Extensive cell wall depositions (Fig. 4B) were also obvious that had never been seen in WT ITs (Fig. 4A). Infection droplets were observed, but only a few symbiosome-like structures could be detected in the plant cell cytoplasm. They were different from WT symbiosomes (Fig. 4F) and had an irregular shape (Fig. 4E). The bacteroids were surrounded by a large and irregular peribacteroid space (Fig. 4E).

Discussion

The search for functions involved in NF perception and signal transduction has revealed a set of genes that are required for nodulation as well as for mycorrhization, the ancient plant-fungi endosymbiosis from which nodulation has been derived (Kistner and Parniske, 2002). We provide more insight into the function of SymRK, a component of the common signal transduction cascade. *LjSymRK* and its orthologs *MtDmi2*, *MsNork*, and *Pssym19* code for LRR-type receptor kinases, and mutations in these genes cause a

very early arrest and almost completely block epidermal responses to rhizobia resulting in impaired RHC (Endre et al., 2002; Stracke et al., 2002). During mycorrhization, *LjSymRK* mutants are arrested at the level of intracellular fungal entry in the exodermis-outer cortical cells, indicating that SymRK also functions downstream of the epidermis, in other plant tissues (Demchenko et al., 2004).

The question of whether during nodulation SymRK plays also a role in tissues other than the epidermis is difficult to answer in legumes that use RHC invasion. However, it can be easily addressed in host plants that offer crack entry invasion, which avoids the epidermis and the root hairs and provides direct intercellular entry in the outer cortex at positions of LRBs. The water-tolerant tropical legume *S. rostrata* has recruited such a cortical invasion track to nodulate on submergence when accumulating ethylene blocks RHC invasion and root hair development (Goormachtig et al., 2004b) as well as during nodulation at the bases of stem-located adventitious rootlets where root hairs are absent. During LRB nodulation on S. rostrata, the bacteria enter directly in the cortical plant tissues and infection proceeds intercellularly in the outer cortex, without root hair involvement, yet the process depends strictly on NFs (D'Haeze et al., 1998).

To analyze the role of SymRK downstream of the epidermis, the *S. rostrata* ortholog was isolated. SrSymRK is ~85–90% similar to its relatives from other legumes. Southern hybridizations indicated that it is a unigene and expression analysis revealed that it could indeed function downstream of the epidermis. RT-PCR showed that the *SrSymRK* transcripts were up-regulated during adventitious and lateral root-based nodulation to disappear again in mature nodules. The induction level during adventious root nodulation was more pronounced, reflecting the ease of specific and synchronous sampling of the stem-located adventitious root tissues. In situ hybridization indicated that *SrSymRK* transcripts were present in cells underlying the nodular meristem, i.e., in the infection zone where bacteria will be released into the plant cell cytoplasm to differentiate into N_2-fixing bacteroids. To obtain an insight into an eventual function of *SrSymRK* in the infection zone, RNAi knockdown roots were constructed with *A. rhizogenes*-mediated root transformation. Lines with 4- to -10-fold reduced transcript levels exhibited the same impaired LRB nodulation phenotype. After 2 weeks, only small, non fixing nodule-like structures were detected that were barely infected with *A. caulinodans*. Light microscopy and EM revealed two main defects in these nodule-like structures. First, ITs were formed, indicating that the underlying mechanism was not hampered, but they had an irregular appearance with protruding bulges containing mainly IT matrix. Also the walls of the ITs were irregular with large cell wall deposits. At the ultrastructural level, the matrix of the ITs was separated from the IT wall by a layer of low electron-dense material that seemed continuous with the low electron-dense surface polysaccharide layer of the bacteria. A flooding of the surface polysaccharides along the edges of the ITs could imply a change in the physico-chemical nature of the IT matrix. Cross-linking of the matrix concomitant with bacterial cell division has been proposed to be

the driving force for IT progression (Brewin, 2004); hence, changes in the matrix composition might give rise to irregular IT structures. A second defect is observed at the level of bacterial uptake when rhizobia are released into the plant cell cytoplasm to form symbiosomes. This process is initiated by local hydrolysis of the IT cell wall and formation of an infection droplet, a small bulge surrounded by a plant cell membrane containing a few bacteria and IT matrix (Brewin, 2004). From the infection droplets, individual bacteria are released in the cytoplasm (Parniske, 2000). As shown by transmission EM analysis, in the *SrSymRK* RNAi line, infection droplets were formed, but hardly any individual symbiosome was present. The few symbiosomes that were detected in the cytoplasm had an irregular structure, indicating a defect in bacterial uptake into the plant cells, possibly as a consequence of disabled vesicle trafficking. Similar features were observed in M. truncatula (Limpens et al., 2005). Hence, SymRK is involved in control of IT structure and in bacterial uptake for symbiosome formation. Taking into consideration these observations, the known role of SymRK in rhizobial root hair entry and mycorrhizal invasion, as well as recent findings on the mechanisms of invasion of biotrophic pathogens, we propose that SymRK might be part of a molecular complex for intracellular residence of endosymbionts that incorporates cell wall integrity control and targeted exocytosis (Schulze-Lefert, 2004). Intracellular penetrations of biotrophic pathogens and symbiotic mycorrhiza have much in common and might depend on related programs (Parniske, 2000). During arbuscular myccorhizal initiation in *LjSymRK* mutants, the fungus invades epidermal cells, but is arrested after appressoria have been formed, at the intracellular passage through the exodermis-outer cortex (Demchenko et al., 2004), an arrest that might be explained by a defect in a common pathogen-symbiont entry system. Moreover, part of the phenotype observed in SymRK mutants during the initial steps of the RHC nodulation process is related to elevated touch sensitivity (Esseling et al., 2004). A possible role for SymRK in connection to the recruitment of exocytosis-mediated resistance or mechanical stress-sensing mechanisms for symbiont entry could be suppression of touch related plant responses. NFs, the main bacterial signals for nodule development, trigger nodulation-related effects in the epidermis, as well as changes in cortex and pericycle cells. The latter effects are provoked from a distance because it is very unlikely that NFs migrate through symplast or apoplast since they are immobilized in the plant cell walls (Goedhart et al., 2000). Hence, NFs probably activate secondary signals that, together with signals coming from the stele, determine the landscape for nodule development and preparation for invasion (Geurts and Bisseling, 2002). During LRB nodulation in *S. rostrata*, the distant NF-dependent response of nodule primordium formation is not disturbed in roots with ~10-fold SrSymRK silencing, suggesting that it may not be linked to SymRK function. In contrast, the well established coupling of SymRK to NF signal transduction in RHC nodulation (Catoira et al., 2000; Wais et al., 2000; Madsen et al., 2003; Radutoiu et al., 2003; Esseling et al.,

2004; Oldroyd and Downie, 2004) would provide an early epidermal checkpoint, which is circumvented in LRB nodulation that uses direct cortical responses. Besides signaling from a distance, NFs may affect adjacent cells in the epidermis and during the passage of the ITs in the cortex. In the epidermal root hairs, bacterial entry requires both NF perception (presumably via LysM-type receptors) and active SymRK (Endre et al., 2002; Stracke et al., 2002; Limpens et al., 2003; Madsen et al., 2003; Radutoiu et al., 2003; Oldroyd and Downie, 2004)). In the infection zone, where SymRK transcripts are up-regulated, a cell-autonomous role in uptake is plausible and presumably uncoupled from local bacterial NFs. Although genes responsible for NF production are transcribed in ITs and NFs have been localized in the infection zone (Timmers et al., 1998), a few cases have been described of NF-deficient strains that could reach the interior of a nodule and were internalized to fix nitrogen as long as NFs were added to the root medium (Relic et al., 1994; D'Haeze et al., 1998) (J. Den Herder and M. Holsters, unpublished results). The NF-deficient strains NGR234 of *Rhizobium* sp. and USDA110 of *Bradyrhizobium japonicum* were able to invade and nodulate *Vigna unguiculata* and *Glycine ma*x when NFs of NGR234 were added at a concentration of 10^{-7} to 10^{-6} M (Relic et al., 1994). An analogous observation has been made for the LRB nodulation on hydroponic roots of S. rostrata by coinoculating a bacterial mutant with defective surface polysaccharides (ORS571-X15), but normal NFs, and a mutant without NF production (ORS571-V44; (D'Haeze et al., 1998)). The ORS571-V44 strain cannot enter the host because of the absence of NFs and does not provoke any nodulation-related effect (Goethals et al., 1989), whereas ORS571- X15 induces nodule primordia at LRBs, but is arrested in superficially located IPs. However, ORS571-X15 can complement ORS571-V44 for nodule invasion and functional nodules are formed, which are exclusively occupied by ORS571-V44 bacteria (D'Haeze et al., 1998). Presumably, NFs trigger developmental gradients from a distance, without being required in situ at the moment of SymRK-dependent internalization. In summary, SymRK is required at the heart of endosymbiosis in leguminous plants to release bacteria into nodule cells during a process that might testify of common origins of bacterial and fungal endophytic lifestyles and biotrophic pathogen invasion strategies.

Chapter 8

Nod factor induced Ca^{2+}-spiking frequency in Sesbania rostrata is linked to infection strategy.

Upon waterlogging, *Sesbania rostrata* is able to nodulate via an intercellular invasion way in which bacteria gain entry through cracks at lateral root bases. Ethylene accumulating under hydroponic conditions inhibits root hair invasion, while promoting lateral root base nodulation.

We investigated Ca^{2+}-spiking events in axillary root hairs of hydroponically grown roots. These root hairs respond to Nod factors but do not allow bacterial entry. Microinjection of Ca^{2+}-sensitive dyes revealed Ca^{2+}-spiking, the frequency and shape of which is significantly different from those observed for zone I root hairs in other legumes and responds differently to ethylene, but not jasmonate. Manipulation of Ca^{2+}-spiking frequency in hydroponic culture leads to the induction of root hair invasion but not nodule formation. Hence, successful root hair invasion is strictly correlated with a specific Ca^{2+}-spiking signature.

Introduction

Nod factors (NF) are the major rhizobial signal molecules that enable the establishment of a nitrogen fixing symbiosis with legume plants. NFs are lipochito-oligosaccharide molecules that are recognized by the host plant, presumably via specific NF receptors, thus initiating signal cascades that lead to nodule formation (Cullimore and Denarie, 2003; Limpens and Bisseling, 2003; Geurts et al., 2005). NF structure varies among rhizobia, but always consists of an N-acetyl glucosamine backbone (GlucNAc, usually 4 to 6 residues), from which the GlucNAc residue at the non-reducing end is acylated. Variety in NF structure is achieved by acyl chains with different length and saturation and different decorations at the reducing or non-reducing end of the NF backbone, e.g. acetyl-, carbamoyl-, sulphate-, fucosyl- and arabinosyl-moieties, depending on the species (D'Haeze and Holsters, 2002).

In legumes such as *M. truncatula* and *L. japonicus,* bacterial infection occurs in root hair cells right behind the root hair tip, called zone I root hairs, called root hair curling invasion or RHC. Upon NF recognition, cytoskeletal changes result in bulging, deformation and ultimately in curling of the root hair cell, thus entrapping bacteria within the curl (Timmers et al., 1999; Esseling and Emons, 2004). Within the curl, local wall hydrolysis precedes the invagination of the plasma membrane, thus initiating the formation of an infection thread. In concert, inner cortical cells dedifferentiate to form the nodule primordium (Ferguson and Mathesius, 2003). Ultimately, the ITs reach the nodule primordium, the bacteria are released into the plant cell cytoplasm to form a functional nodule.

The NF dependent signalling networks involved in the initiation of these processes are starting to become apparent. NFs are putatively perceived by a family of LysM domain containing receptor-like kinases (Limpens et al., 2003; Madsen et al., 2003; Radutoiu et al., 2003). Almost immediately upon NF application, a rapid influx of Ca^{2+} occurs, followed by a Cl^- efflux, leading to membrane depolarization, and ultimately the membrane is repolarized by a K^+ efflux and H^+ pump activity (reviewed in (Esseling and Emons, 2004)). Within minutes of these events, oscillations in cytosolic Ca^{2+}-concentrations occur in and around the nucleus (Oldroyd and Downie, 2006). These oscillations, called Ca^{2+}-spiking, are NF structure specific, as wild type NFs were shown to induce Ca^{2+}-spiking at picomolar concentrations in *M. truncatula*, whereas removal of decorations resulted in a rapid drop in Ca^{2+}-spiking inducing activity (Oldroyd et al., 2001b). The importance of NF induced Ca^{2+}-spiking for nodule initiation is emphasized by the isolation of numerous plant mutants that are impaired in both nodulation and Ca^{2+}-spiking initiation. Among these are mutants in several LysM domain containing receptor-like kinases (RLK) presumed to recognize NF (LjNFR1 and 5, MtNFP), a LRR

domain containing RLK (MsNORK, MtDMI2, LjSymRK, PsSym19, SrSymRK), a nucleoporin (LjNup133) and a putative plastidial ion channel (MtDMI1, CASTOR, POLLUX) (Oldroyd and Downie, 2004; Kanamori et al., 2006). Other nod$^-$ mutants still initiate Ca^{2+}-spiking One such mutant was identified as a calcium and calmodulin dependent protein kinase (CCaMK) similar to CaM kinase II in animals, suggesting its role in the interpretation of the calcium signal (MtDMI3, PsSYM9) (Lévy et al., 2004; Mitra et al., 2004).

Epidermal root hair invasion in zone I of the roots is inhibited by ethylene in *M. truncatula* (Penmetsa and Cook, 1997)as well as in *S. rostrata*, which accummulates upon waterlogging. To cope with this, water-tolerant legumes evolved an alternative invasion strategy to allow nodulation. In *S. rostrata* and *Neptunia* spp., the microsymbiont enters at lateral root bases, directly colonizing the outer cortex via cracks at sites of lateral root protrusion, called lateral root base nodulation or LRB (Den Herder et al., 2006). This invasion is also dependent on NF, although the structural requirements are less stringent than for root hair curling (RHC) invasion, and it is not inhibited by ethylene (Goormachtig et al., 2004).

A major target of the ethylene-mediated inhibition of RHC invasion is Ca^{2+}-spiking (Oldroyd et al., 2001a). The ethylene insensitive *M. truncatula* mutant *skl* shows a decreased Ca^{2+}-spiking frequency as compared to wild type plants, suggesting a role for ethylene in the regulation of spiking frequency (Oldroyd et al., 2001a). An additional factor influencing NF induced Ca^{2+}-spiking in *M. truncatula* has recently been identified. Jasmonic acid (JA) has been reported to have a slowing influence on Ca^{2+}-spiking in zone I root hairs (Sun et al., 2006).

While Ethylene inhibits RHC in *S. rostrata*, it is an absolute requirement for LRB nodulation in hydroponic culture (D'Haeze et al., 2003). Not only are the effects of ethylene in the epidermis circumvented, an ethylene-dependent pathway has been recruited for the formation of infection pockets (IPs) in the outer cortex via local, induced cell death (D'Haeze et al., 2003). No epidermal invasion occurs during LRB nodulation, nevertheless a number of axillary root hair initials maintain the ability to respond to NF. These axillary root hair initials lie adjacent to the lateral root bases and grow out and deform upon NF addition (Mergaert et al., 1993). These root hairs have been used in pharmacological approaches to unravel down stream signaling pathways involved in NF perception at LRBs (D'Haeze et al., 2003). Ethylene and ROS antagonists inhibit NF dependent root hair outgrowth in the same manner as they inhibit hydroponic nodulation itself (D'Haeze et al., 2000).

Here we show that axillary root hairs at the LRB of *S. rostrata* respond to NF with Ca^{2+}-spiking. Compared to zone I root hair responses of other legumes, Ca^{2+}-spiking was significantly

faster and the shape of the spikes was different. Similar to observations in *M. truncatula* (Sun et al., 2006), JA treatment slowed down spiking. However, Ca^{2+}-spiking responded differently to ethylene, since an ethylene antagonist inhibit Ca^{2+}-spiking rather than promoting it as in *M. truncatula*. Modulation of Ca^{2+}-spiking frequency by exogenous application of AVG and JA partially restored infection of these root hairs by rhizobia, while LRB nodulation was blocked. These finding suggest that a strict Ca^{2+}-spiking frequency is a determining factor in the potential for invasion of a given root hair.

Materials and Method

Plant material and bacterial strains

S. rostrata seedlings were germinated and subsequently grown in either tubes containing liquid medium or on plates with BNM medium as described (Ehrhardt et al., 1992; Goormachtig et al., 1995). Plants were inoculated with *A. caulinodans* ORS571 (pBBR5-hem-gfp5-S65T) as described (D'Haeze et al., 2004).

Calcium spiking analysis

Spiking analysis was performed as described (Ehrhardt et al., 1996; Wais et al., 2000). Micropipettes were pulled from borosilicate capillaries using an electrode puller (model 773, Campden Instruments). Needles were preloaded with dextran linked Oregon green (10,000 MW, Molecular Probes Inc.). Ionthophoretic injections were performed using a cell amplifier (model Intra 767, World Precision Instruments) and a stimulus generator (World Precision Instruments). Plants were mounted on slides containing BNM medium for microinjection of suitable root hairs and subsequent imaging. For visualisation, an inverted epifluorescence microscope (TE2000, Nikon) equipped with a monochrometer (optoscan, Cairns Research) was used. Imaging was performed with a ccd camera (ORCA-ER, Hamamatsu). Subsequent data analysis was done using the MetaFluor software (Universal Imaging).

Pharmacology

Concentrations of inhibitors were 1, 3 or 7 μM L-α-(2-aminoethoxyvinyl)-glycine (AVG), 25, 50 or 100 μM jasmonic acid, 0.1 % n-butanol and 10 μM Cyclopiazonic acid (CPA). Inhibitors were purchased from Sigma-Aldrich. For the Ca^{2+} spiking experiments, spiking cells were visualized for at least 30 minutes before addition of compounds. For the pharmacological treatments in infection assays, all experiments were done at least twice per time point. At the concentrations used, the inhibitors had no influence on plant or bacterial growth. 1000 x stock solutions were made according to the manufacturers instructions. Equal amounts of the solvent were tested as controls to dismiss negative effects of the solvents on plant or bacterial growth.

Microscopical analysis

Light microscopical analysis was performed as described (D'Haeze et al., 1998). Plant

material was harvested and fixed using 2.5% glutaraldehyde, embedded in Technovit 7100 (Kulzer Histo-Technik, Wehrheim, Germany). 4 μm sections were made, stained with 0.5% toluidine blue and mounted with Depex (Sigma). The sections were then analysed using a Diaplan bright field microscope (Leitz).

Results

Nod factor induced Ca^{2+}-spiking in axillary root hairs under hydroponic conditions.

Microinjections of the calcium responsive dye Oregon green into the axillary root hair initials that are present on hydroponically grown *S. rostrata* roots were performed. Subsequent application of *A. caulinodans* Nod factors resulted in rapid calcium oscillations within 5 to 20 minutes (see also the video file on the accompanying CD, Fig. 1A). Of 28 plants analysed, 65 cells that showed continuous cytoplasmic streaming after injection were visualized. Of these 65 cells, 57 cells showed spiking.

Subsequently, spike shape was determined. To this end, from a number of representative spikes from several traces, both the time to reach a maximum, and the time to return to background levels were measured. An average spike took 24.26 s ± 6.10 to complete (n = 43).

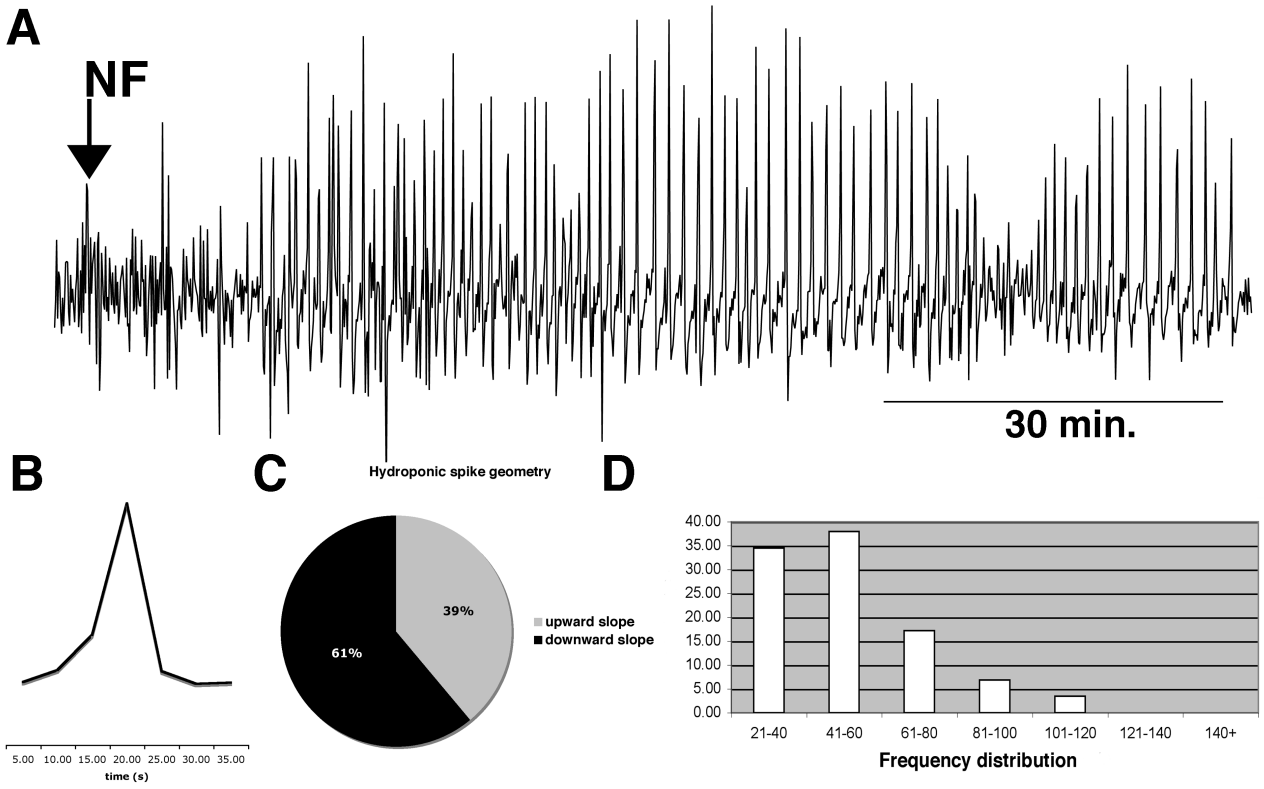

Fig. 1 Hydroponic spiking characteristics.
A. Ca^{2+} spiking pattern of an axillary root hair initial. Spiking commences some 5 to 10 minutes after NF application. B. Spike shape of a typical spike. C. Comparison o upward and downward slopes of Ca^{2+} spikes. Typically, the upward slope represents about 39 % of the total spike, whereas the downward slope is remarkably steep and consists of about 61 % of the total spike. D. Frequency distribution of spike periods. The majority of cells analysed showed a spiking period of less than 80 seconds.

The average time to reach a maximum was 9.35 s ± 2.58 and the average downward slope was 14.91 s ± 4.71 (Fig. 1A). Overall, this means that for hydroponic NF induced Ca^{2+}-spiking, the upward part accounts for about 39% of the total spike surface (Fig. 1C). Ca^{2+}-spiking frequency ranged from 35 s to 118 s between maxima. The average period was 55.50 s ± 20.83 (n = 57) (Fig 1D).

Involvement of type IIA calcium ATPases and Phospholipase D in Ca^{2+}-spiking.

In order to establish a link to Ca^{2+}-spiking in other legumes, we tested some antagonists of Ca^{2+}-spiking (den Hartog et al., 2001; Engstrom et al., 2002). Application of 1 μM CPA, an inhibitor of Type IIA calcium ATPases, rapidly inhibited NF-induced Ca^{2+}-spiking (n = 2/3 (plants/cells), data not shown). Similar results were obtained using 0.5% n-butanol, an antagonist of phospholipase D activity (n = 2/3 (plants/cells), data not shown). These data suggest a signaling cascade that is similar to what is known for Ca^{2+}-spiking in zone I root hairs of other legumes.

Effect of ethylene and ethylene inhibitors on NF dependent Ca^{2+}-spiking in axillary root hairs.

NF responses in zone I root hairs are blocked by ethylene (Oldroyd et al., 2001a). To test the influence of ethylene on axillary root hair spiking, 40 μM ACC, an ethylene biosynthesis precursor, was applied to the medium. We found no effect of ACC on Ca^{2+}-spiking frequency (n = 2/5 (plants/cells), data not shown).

NF dependent axillary root hair deformation is inhibited by AVG, an inhibitor of ethylene biosynthesis, so the effect of AVG on spiking frequency was analysed. Addition of 7 μM AVG resulted in rapid changes in Ca^{2+}-spiking frequency (n = 8/14 (plants/cells), Fig. 2A, C). The average period was established at 74.20 s ± 31.20 and did not significantly differ from wild type spiking. However, the spike shape changed significantly under these conditions. The upward slope accounted for only 16 % of the total spike duration, whereas the downward slope was significantly slower at 84 % of the total spike (n=54, Fig. 2C). The average total spike time was 53.37 s ± 18.12, which is different from the spike time in control conditions (24.26 s ± 6.10, Fig. 2C).

Effect of JA on NF induced axillary root hair Ca^{2+}-spiking.

It has recently been shown that, apart from ethylene, JA also affects Ca^{2+}-spiking in zone I root hairs of *M. truncatula* (Sun et al., 2006). We therefore investigated the influence of JA on Ca^{2+}-spiking in *S. rostrata* axillary root hairs in hydroponic conditions. Two concentrations were tested: 20 μM and 50 μM JA. Both concentrations did influence NF induced Ca^{2+}-spiking in a similar manner, but since more

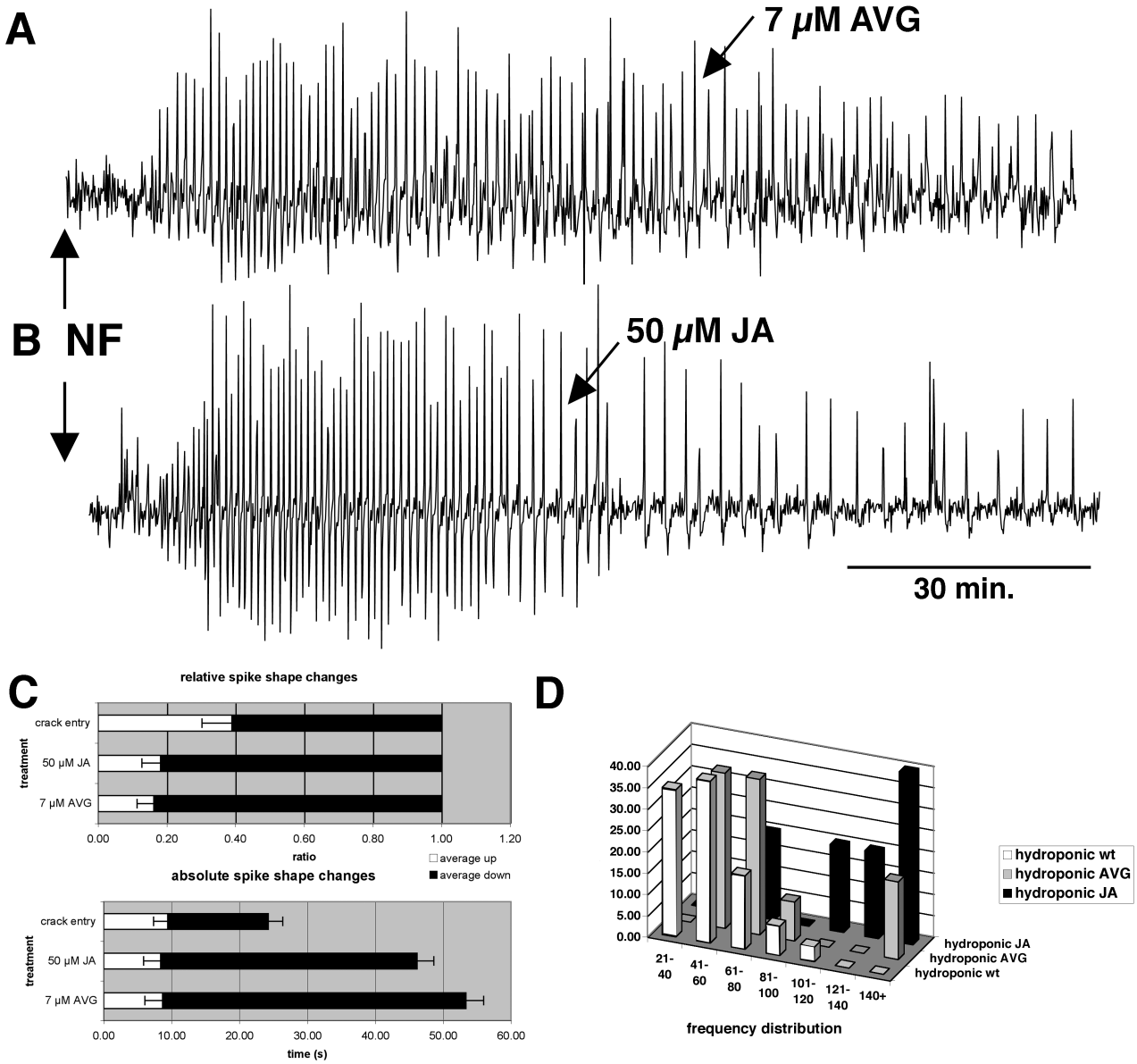

Fig. 2 Pharmacological manipulation of Ca^{2+} spiking.
A. Application of 7 μM AVG significantly alters spike shape. B. Application of 50 μM JA significantly alters Ca^{2+} spike shape and frequency. C. Both AVG and JA treatments significantly alter the upward/downward slope ratio (upper graph). Also the spike period changes significantly, but only the downward slope is affected (lower graph). D. A shift in Ca^{2+} spiking frequency is induced by JA treatment, but not by AVG treatment, as shown by a histogram plotting the frequency distribution for wild type hydroponic spiking and spiking upon AVG or JA application.

cells responded to 50 μM JA (95 % of all cells opposed to 50 % of all cells for 20 μM JA) we proceeded with 50 μM JA as a challenge in our system.

The average spiking frequency changed rapidly upon JA addition, the average time between maxima was 117.17 s ± 37.73 (as opposed to 53.37 s ± 18.12 for wild type hydroponic spiking, Fig. 2B). An average spike took 46.15 s ± 10.16 (n = 65) to complete, the upward slope accounted for some 18 % of the total spike, whereas the downward slope accounted for 82 % of the total spike (Fig. 2C).

wild type				[]	AVG				[]	JA			
2dpi		6dpi			2 dpi		6 dpi			2 dpi		6 dpi	
epidermis	cortex	epidermis	cortex		epidermis	cortex	epidermis	cortex		epidermis	cortex	epidermis	cortex
n=57 deformation 1 plant with 1 IT	n=57 ccd and IP formation	n=45 N/A	n=45 start of fixing nodule	**1 µM 2 days before**	n=4 2 with ITs	n=4 3 with ccd	x	n=8 8 with wild type nodules	**25 µM 2 days before**	n=4 deformations	n=4 IP formation and ccd	n=14 5 with ITs	n=14 13 with nodules
				3 µM 2 days before	n=1 ITs	n=1 no ccd	n=9 all 9 with ITs	n=9 small, delayed nodules	**50 µM 2 days before**	n=6 x	n=6 no IPs or ccd	n=12 3 with Its	n=12 9 delayed nodules 3 without nodules
				7 µM 2 days before	x	x	n=10 no Its	n=10 no nodules	**100 µM 2 days before**	n=5 x	n=5 no IPs or ccd	n=13 x	n=13 3 dead 7 without nodules 3 with delayed nodules
				7 µM 2 hours before	n=20 9 with ITs 11 with nothing	no ccd	x	x	**25 µM 2 hours before**	n=2 both with ITs	n=2 both with ccd	n=10 x	n=10 nodules
									50 µM 2 hours before	n=18 12 with ITs	n=18 none with ccd	n=6 x	n=6 small delayed nodules

Table 1 Pharmacological manipulation of hydroponic invasion and root hair invasion.
The table gives an overview of the different treatments that were performed using either AVG or JA. Plants were analyzed at 2 or 6 days post infection. Especially presence of axillary root hair deformation, intracellular infection threads (IT) or infection pockets (IP) and cortical cell division (ccd, 2dpi) or primordium formation (6dpi) were scored. Plants were treated either 2 days or 2 hours before inoculation with *A. caulinodans*. Concentrations used are indicated.

The influence of the addition of AVG and JA on infection and nodule formation.

We next compared the effect of AVG and JA on the infection and nodule formation at LRBs in hydroponic conditions. Three different AVG concentrations were applied 2 days prior to inoculation with a gfp labeled *A. caulinodans* ORS571 strain. At 5 days post inoculation, no effect on nodulation on plants treated with 1 µM AVG was seen. A reduction in the number of nodules was seen when plants were treated with 3 µM AVG and a nearly complete block of nodulation was observed using 7 µM AVG (1 plant out of 10 still had small, delayed primordia, table 1).

The bacterial infection was analyzed by fluorescent microscopy. As the concentration of AVG was increasing, axillary root hairs were observed that contained infection threads with GFP-labeled bacteria. When using 7 µM AVG (as in the Ca^{2+}-spiking experiments), at least 50 % of all plants assessed contained ITs in axillary root hairs.

Semithin sections through lateral root bases treated with 7 µM AVG were analysed and compared to untreated plants. In the LRBs treated with AVG, a large number of ITs was

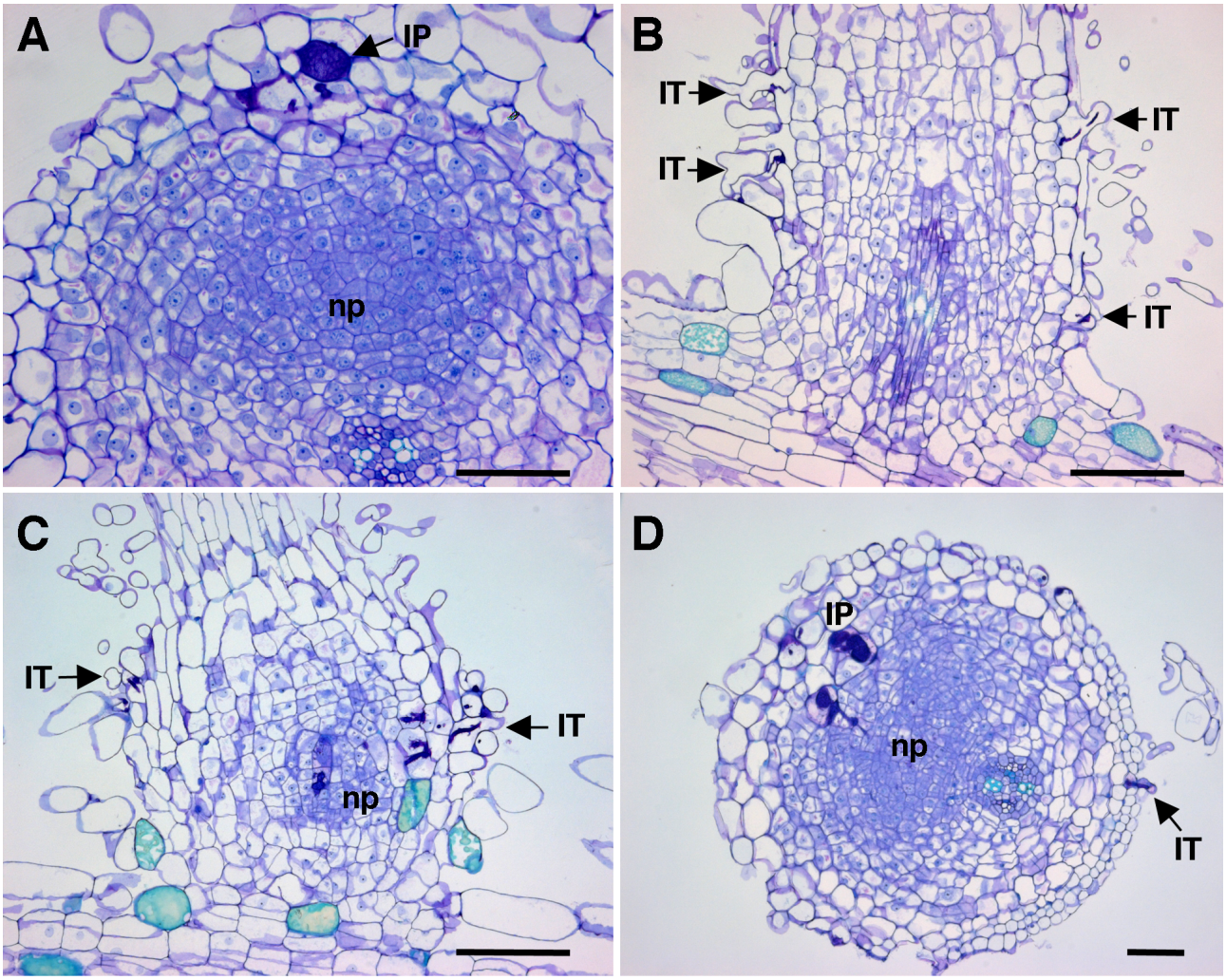

Fig. 3 Changes in infection strategy can be induced by altering Ca^{2+} spiking frequency.
Plant were grown hydroponically and pretreated with either AVG or JA (see text). Inoculated plants were screened 3 and 5 days after inoculation for the presence of intracellular infection threads. A. Wild type nodule primordium 3 days after inoculation. B. Cross section through a lateral root base after treatment with 7 μM AVG, intracellular infection threads are indicated with arrows. C. Cross section through a lateral root base after application of 50 μM JA, a small, delayed nodule primordium is visible and several intracellular infection threads are indicated. D. Cross section through a nodule primordium after treatment with 50 μM JA. The primordium originates from a crack entry infection event, an infection pocket is clearly visible. Also an intracellular infection thread is visible but no nodule primordium is present. Abbreviations: IP, infection pocket; np, nodule primordium; IT, intracellular infection thread. Bars are 100 μm.

indeed visible in axillary root hair cells. This was only infrequently observed in control roots. ITs that proceeded into deeper tissue were never observed (Fig. 3B).

JA was applied at 3 concentrations, 25, 50 and 100 μM JA, and 2 different stages, 2 days or 2 hours before inoculation. When 25 μM JA was added at either stage, 23 out of 24 plants had nodules 6 days after inoculation. When 50 μM JA was applied 2 days before, only 50% of the plants had nodules, whereas most plants had delayed nodules when 50 μM JA was applied 2 hours before inoculation. Application of 100 μM JA, 2 days before inoculation, blocked nodulation in 70 % of plants and the remaining plants showed significant delays in nodule formation (table 1).

Analysis by fluorescent microscopy showed an increasing number of ITs in axillary root hairs with increasing JA concentrations, except for

100 μM JA, which totally blocked IT formation. 20 % of the plants developed ITs in axillary root hairs when 20 μM JA was applied 2 days or 2 hours before inoculation. The same percentages were seen when 50 μM JA was applied two days before inoculation. However, when applied 2 hours before inoculation, 75% of the plants had axillary root hairs with intracellular ITs.

Semithin sections through lateral root bases treated with 25 and 50 μM JA were analysed. As for AVG, infrequent infection threads were sometimes visible in axillary root hair cells, and JA treatment strongly enhances the number of intracellular infection threads in these axillary root hairs. A few primordia from roots treated with 50 μM JA were found not to originate from IPs but from infection events in axillary root hairs (Fig. 3C). For both concentrations of JA used, some functional nodules were still formed and microscopic analysis showed these nodules originated from IPs (Fig. 3D).

Discussion

Water-tolerant legumes like *Sesbania rostrata*, adopted the crack entry nodulation program to enable nitrogen-fixing symbiosis upon submergence. On hydroponic roots, the microsymbionts do not enter via curled root hairs in zone I of the root, instead they directly enter the cortex via infection pocket formation at lateral root bases (Den Herder et al., 2006). Although not used for invasion, submerged lateral root bases carry incipient axillary root hairs that respond by deformation to Nod factors with identical NF structural and secondary signal requirements as for LRB nodulation.

Ca^{2+}-spiking in zone I root hairs plays a central role in the NF induced signal transduction leading to zone I nodule formation and several environmental factors have been shown to influence nodulation via changing Ca^{2+}-spike traits. Also the axillary root hairs of *S. rostrata* respond to Nod factors with Ca^{2+}-spiking. Known antagonists of Ca^{2+}-spiking in other legumes, such as CPA and n-butanol, inhibited hydroponic Ca^{2+}-spiking, suggesting a similar mechanism. However, upon analysis of the frequency and spike shape, we found striking differences with what has been published for *M. truncatula, L. japonicus* and *P. sativum* (Ehrhardt et al., 1996; Walker et al., 2000; Oldroyd et al., 2001a).

S. rostrata nodulates via zone I root hair curling when grown in aeroponic conditions. Preliminary results have shown that also in *S. rostrata* root zone I root hairs respond to Nod factors by spiking with traits similar to Ca^{2+}-spiking that has been seen in other legumes (data not shown). However, the number of cells that showed Ca^{2+}-spiking was significantly less than what was observed for other legumes (1 out of 90 cells tested, data not shown), indicating a shift in the zone of responsive root hairs to other slightly older root hairs that can not be sampled with microinjection.

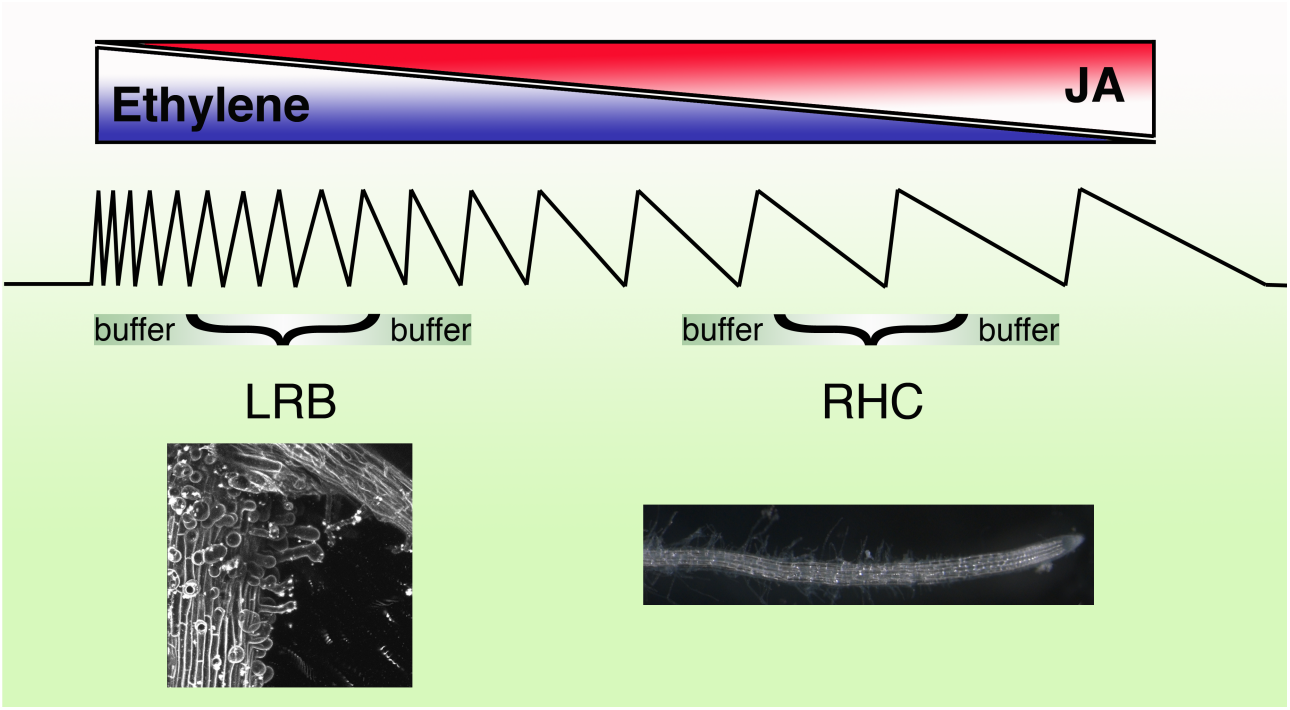

Fig. 4 Model of the establishment of a Ca^{2+}-spiking frequency range
Ca^{2+}-spiking can occur at distinct frequencies, depending on signal, position of the cell on the root and hormone status. NF induced Ca^{2+}-spiking frequency will depend on these factors and can influence NF signaling to the extent that nodulation is inhibited. Although Ca^{2+}-spiking frequency is modulated by ethylene and jasmonate in similar ways in hydroponic and aeroponic conditions, the sensitivity of Ca^{2+}-spiking to these molecules is different. Adding ACC to spiking cells in *M. truncatula* immediately inhibits spiking, whereas no effect can be seen in hydroponic conditions. Conversely adding AVG has no effect on Ca^{2+}-spiking in *M. truncatula* but inhibits spiking in *S. rostrata*. It thus seems that the molecular mechanisms involved in the initiation of Ca^{2+}-spiking are differently conditioned and buffered to changes in hormone levels in both root hair types. This can be explained using a model that encompasses the influence of JA and ethylene on the range of spiking frequencies. Adding ACC to root hair curling cells rapidly inhibits spiking by shifting the frequency, beyond the capabilities of the buffering system, to 'unphysiological' levels. However, cells in hydroponic culture are adapted to high ethylene levels and adding more ethylene has no discernable effect. Similarly, adding AVG to hydroponic, spiking cells, beyond it's buffering system, has a dramatic effect but not on root hair curling cells.

These observations suggested that the spike patterns observed in the axillary root hairs are specific for LRBs in hydroponic conditions.

While ethylene had no effect on the spiking traits of axillary, hydroponically grown root hairs whereas AVG, an inhibitor of ethylene, influenced Ca^{2+}-spiking and reduced the downward slopes of the spikes. This response is opposite for what has been shown for zone I root hair spiking, but correlates with the demand for ethylene during lateral root base nodulation as AVG blocks LRB nodulation as well as NF dependent axillary root hair deformation (D'Haeze et al., 2003). The particular spiking pattern of axillary root hairs at lateral root bases is not correlated with root hair infection but could play a role in signaling for nodule primordium and infection pocket formation. It is quite possible that also cortical cells show a similar spiking pattern. This question can not be addressed since microinjections in cortical cells is impossible due to technical problems. *S. rostrata* also nodulates at adventitious root primordia on its stem. At these locations, a similar invasion

mechanism is used as for lateral root base nodulation. No axillary root hairs are present at those locations (Goormachtig et al., 1998), nevertheless the question remains open whether epidermal or cortical cell responses are the primary origin of the signaling cascade leading to LRB nodulation (D'Haeze et al., 2003; Lievens et al., 2005). In *M. truncatula,* epidermis-specific complementation of the *dmi3* mutant could shed light on the need for cortical spiking and its detection during nodulation.

Addition of JA resulted in rapid changes in Ca^{2+}-spiking properties, leading to Ca^{2+}-spiking characteristics reminiscent of what has been seen in *M. truncatula* zone I root hairs. Moreover, as for zone I nodulation, also LRB nodulation was blocked by the addition of JA (Sun et al., 2006), showing that JA has a general effect on nodulation, independent of the physiological conditions in which the plants are growing and in which nodulation occurs.

A vast array of signals needs to be integrated into the nodulation signalling pathway. Among these signals are ethylene and JA, that seem to act, at least partially, upstream of Ca^{2+}-spiking. The number of signals found to interplay at this level will probably expand in the future, other plant hormones will no doubt influence JA and ethylene concentrations, and NF structure specific signals are also known to act at this stage (Oldroyd et al., 2001b). JA has a slowing effect on spiking frequency (this work, (Sun et al., 2006)). For ethylene the effect is opposite to JA. In *M. truncatula* direct effects of ethylene on spiking frequency are impossible to detect since addition of even minute amounts of ACC immediately and completely block Ca^{2+}-spiking (Oldroyd et al., 2001a). However, indirectly, it can be extrapolated that ethylene works as a throttle on spiking frequency. Sun and coworkers (2006) observed an additive effect on the reduction of spiking upon addition of suboptimal concentrations of both AVG and JA, suggesting opposite functions on frequency for ethylene and JA, since AVG is an ethylene biosynthesis inhibitor. Moreover, the authors show that the *M. truncatula* ethylene insensitive mutant *skl* is hypersensitive to JA-inhibition of Ca^{2+}-spiking, confirming this model (Sun et al., 2006). The main difference between *S. rostrata* and *M. truncatula* seems to be an altered sensitivity to ethylene. While *M. truncatula* is sensitive to even the mildest increase in ethylene levels, *S. rostrata*, adapted to submergence, had to alter its sensitivity to ethylene and has an attenuated response to ethylene.

Pharmacological manipulation of Ca^{2+}-spiking with both AVG and JA resulted in frequencies and/or spike shapes changes leading to patterns more similar to those described in *M. truncatula,* pea. and *M. sativa*. By adding those compounds, intracellular infection threads were observed in the axillary root hairs. Hence, creating conditions that slow down Ca^{2+}- spiking are sufficient to allow intracellular infection of these root hairs and

root hairs that spike within a certain predetermined range will be capable of accommodating infection threads (Box 1). Similar conclusions have been arrived at by Miwa and coworkers by analyzing the Ca^{2+}-spiking frequencies of zone I root hairs in several developmental stages (Miwa et al., 2006). Similarly, preconditioning of hydroponically grown *S. rostrata* seedlings with AVG also leads to a restoration of intracellular invasion (Goormachtig et al., 2004). This however, was different from the experiments described here, since long term conditioning leads to the presence of root hairs in the zone I of the root, where normally no root hairs are present in hydroponic conditions. These zone I root hairs could be infected by bacteria and lead to nodule formation (Goormachtig et al., 2004).

The particular range of Ca^{2+}- spiking that allows intracellular infection thread formation is not compatible with the physiological conditions of lateral root base nodulation as cortical cell divison and nodulation was hampered by adding AVG and JA. When spiking antagonist concentrations in the medium were increased, an increase in the number of plants with infection threads was seen but inversely the number of plants with delayed nodule formation or no nodules increased. Moreover, the presence of intracellular infection threads in the axillary root hairs was not usually connected with the formation of a nodule primordium and that the infection threads were almost never able to grow in deeper tissues and colonize the plant.

Recent years have seen great improvements in our understanding of early Nod factor signal transduction. Combining forward and reverse genetics with pharmacological approaches has proven to be a powerful way of dissecting these pathways. Here we show that hydroponic Ca^{2+}-spiking is significantly different from what has been reported for other legumes and that modulation of Ca^{2+}-spike geometry and period is important to allow for intracellular invasion of root hairs, whilst being incompatible with local (at LRB sites) nodule development. These findings further substantiate the long held belief that NF induced Ca^{2+}-spiking is one of the central signalling mechanisms during nodule initiation and show that modulation of this signal by endogenous signals is a key feature of the symbiosis.

Chapter 9

Functional analysis of a novel type of LysM receptor-like kinase involved in legume nodulation

Legumes engage in a symbiotic interaction with soil-borne rhizobia to form nitrogen-fixing root organs, called nodules. Via a molecular cross-talk between both partners the plant prepares for infection and organ formation. Nod factors are the major bacterial signaling molecule and they are assumed to be recognized by LysM domain containing receptor-like kinases. Two major classes of LysM-RLKs have been identified thus far, both are involved in the very early stages of the symbiosis. Here we report on the identification of a third subfamily of LysM-RLKs with distinct features. Phylogenetic analysis suggests these belong to a third lineage of LysM-RLKs that is conserved in the non-legume *Arabidopsis thaliana.* Knock down of at least one member of this subfamily results in a nodulation phenotype in both *Sesbania rostata* and *Medicago truncatula*, which suggests other roles for LysM-RLKs than previously assumed. This preliminary analysis allows us to hypothesize about the evolutionary origin of NF perception and could point out new directions for research into LysM-RLKs.

Introduction

In the legume-rhizobium symbiosis, complex signaling between both partners lead to the formation of a novel organ, the nodule, which is invaded by bacteria that will fix nitrogen and feed the plant with ammonia. This process requires recognition of compatible strains and is as complex as any other organ development.

The primary signal molecule produced and secreted by the bacteria is the Nod factor (NF). NFs are lipochitooligosaccharides usually consisting of a tetra- or pentameric N-acetyl-D-glucosamine (GlucNAc) backbone with an acyl chain at the non-reducing end sugar and several modifying moieties at the terminal sugar residues (for a review see D'Haeze and Holsters, 2002). NFs are active at picomolar concentrations and therefore the existence of specific plant receptors had been hypothesized. Recently, the mapping of nodulation defective mutants that show almost no responses to NF has led to the identification of two LysM domain containing receptor-like kinases (RLK) *LjNFR1* and *5* in *Lotus japonicus* (Madsen et al., 2003; Radutoiu et al., 2003). In *M. truncatula*, synteny based mapping was used to identify a *M. truncatula* locus that imposes NF structure specific limitations on bacterial invasion, thus suggesting a role in NF perception (Geurts et al., 1997; Limpens et al., 2003). This locus contains a cluster of seven LysM type RLKs (*MtLYK1-7*) (Limpens et al., 2003). LYK3 and LYK4 are involved in infection thread initiation and progression and are structurally similar to NFR1. It thus appears that NFs are perceived by the LysM domains and downstream signaling likely involves a phosphorylation cascade originating from the activity of the intracellular kinase domains of these proteins.

Based on their structure, the identified LysM-RLKs separate into two groups. The NFR1 type that contains 2 LysM domains and consists of multiple exons while the NFR5 type has 3 LysM domains and consists of a single exon. Interestingly, the NFR5 type does not contain an activation loop, nor an ATP binding pocket in its kinase domain, suggesting that heterodimerization with a functional partner protein is needed for downstream signaling (Madsen et al., 2003; Riely et al., 2006).

The presence of different NF receptor complexes or receptors with different stringencies has been proposed more than a decade ago by Ardourel and coworkers (1994), who, by using a set of bacterial mutants with altered NF structure, found different NF structure requirements for the induction of cortical cell division and root hair deformations compared to bacterial entry into root hairs. This model served as a suitable basis to explain the majority of observations and experimental data concerning NF signaling.

One of the main questions is how the cloned NF receptors relate to these two types of NF receptor complexes. LjNFR1 and 5 were

proposed to be signaling receptors, whereas MtLYK3 and 4 would be potential entry receptors. Overall, this shows that a more intricate model is required to address these obvious differences between species as sequence analysis shows a high level of homology between LjNFR1 and MtLYK3 (Oldroyd and Downie, 2004). Although the former do not respond to NF by any known physiological response except for a diminished membrane depolarization in certain *nfr1* alleles, LYK3 knock down still allows for root hair deformation and sometimes curling, showing species specific differences in LysM-RLK function (Limpens et al., 2003; Madsen et al., 2003; Radutoiu et al., 2003). It seems that although some pieces of the puzzle have fallen into place, several pieces are missing and an important next step in our knowledge of NF signaling will come from investigations concerning the existence and composition of these receptor complexes and NF binding properties of the LysM domains involved, combinatorial heterodimerization could result in a much broader spectrum of specificities and activities than initially thought.

LysM domains are dispersed throughout the eukaryotic lineage and are thought to have been acquired by horizontal transfer from prokaryotic lineages (Bateman and Bycroft, 2000). They occur in proteins with peptidoglycan binding properties and certain certain chitinases (Amon et al., 1998; Bateman and Bycroft, 2000). Chitin, peptidoglycan and the Nod factor backbone all contain GlucNAc residues and this similarity suggests that the aforementioned LysM-RLKs are involved in NF binding. Although so far no biochemical data is available, modeling experiments with the *M. truncatula* NFP domains suggest that the LysM domains can each bind one NF molecule and binding sites for each of the *Rhizobium meliloti* NF decorations could be predicted (Mulder et al., 2006).

During a wide scale transcript profiling experiment in *S. rostrata,* a differentially expressed tag was identified that showed similarity to a LysM-RLK from *Arabidopsis thaliana* and to a lower extent to *Lotus japonicus* NFR5 (Capoen *et al.*, in preparation). Because of the nodulation specific expression pattern and the similarity to a putative NF receptor, an initial functional analysis was performed. Here we show that indeed, knock-down lines in *S. rostrata* and the corresponding gene in *M. truncatula* show a similar, novel nodulation phenotype. Plants carrying the knock-down construct show an early cessation of nodule meristem activity, leading to small, globular but nitrogen fixing nodules. We also present data on several other LysM-RLKs in *M. truncatula* that belong to this novel subfamily that is structurally distinct from the known NFR1 and NFR5 type LysM-RLKs.

Materials and Method

in silico analysis

Using the *S. rostrata LysM* tag (Capoen *et al., in preparation*) as a query, both the genomic sequence database at www.ncbi.nlm.nih.gov and the *Medicago* EST database at www.tigr.org were searched using blastx and tblastn (Altschul et al., 1997). Of the sequences retrieved, redundant ones were removed by one on one aligments using ClustalW. The resultant non-redundant set was then subjected to phylogenetic analysis. Alignments were performed using ClustalW and alignments were curated with the BioEdit software (Thompson et al., 1994; Hall, 1999). Neighbour-joining trees were constructed using the TreeCon software (Van de Peer and De Wachter, 1997). 1000 iterations were performed to test node significance for bootstrap analysis.

Isolation of full-length sequences

In order to obtain the full-length cDNA sequence of *SrLysM,* 5' and 3' RACE was performed (Smart RACE cDNA amplification kit, Clontech). The fragments were cloned in a pGEMTeasy vector (Promega). The full length cDNA of *MtLysM* could be amplified immediately from *M. truncatula* root cDNA based on the *in silico* obtained full length sequence using MtLysMORFF3 5'-TTACACCCCATTCTCTGCAA-3' and MtLysMORFR3 5'-AGGCCCTGCTTAACCCTTAG-3'.

Plant material and bacterial strains

S. rostrata seedlings were germinated and subsequently grown in either tubes containing liquid medium or in Leonard jars as described (Goormachtig et al., 1995; Fernandez-Lopez et al., 1998). *S. rostrata* plants were grown in hydroponic or aeroponic conditions and were inoculated with *A. caulinodans* ORS571 (pBBR5-hem-gfp5-S65T) or ORS571-V44 (pBBR5-hem-gfp5-S65T) allowing the use of gfp as a visual marker (Van den Eede et al., 1987; D'Haeze et al., 2004). For LRB nodulation, timepoints at which lateral root bases were harvested 24 and 48 hours after inculation for ORS571-V44 and 6, 12, 24, 48 and 72 hours post inoculation wit h ORS571. LRBs of uninoculated plants were harvested as control (T-). A morphology based approach was used for plants grown in conditions that favor root hair curling. 1.5 cm long root root segments without the apical meristem were harvested (B). Small root fragments with infection threads were excised (rhc1), root fragments with infection threads and bumps indicating nodule initiation (rhc2), primordia before the onset of nitrogen fixation (rhc3) and young fixing nodules (rhc4) were also specifically excised.

Medicago truncatula Jemalong J5 and *Sinorhizobium meliloti* 1021 were grown and inoculated as described (Mergaert et al., 2003). Plants were grown *in vitro* on petri dishes (12 × 12 cm) containing 0.8% Kalys agar (HP 696-7470 Kalys, France) and SOLi medium (as described at www.isv.cnrs-gif.fr/embo2/manuels/index.html). Tissue was

sampled similar to rhc samples for *S. rostrata,* timepoints used were 6, 9, 16, 28 and 48 days after inoculation.

qRT-PCR analysis

qRT-PCR analysis was done a described (Vlieghe et al., 2005). *M. truncatula* root fragments corresponding to the region 2 cm above the root tips were excised at given timepoints (see text). For *S. rostrata* samples, lateral root bases were specifically excised at given time points. For the root hair curling samples, a morphology based harvesting strategy is preferred. As negative control, 1.5 cm root tip fragments without the root apical meristem were excised (rhc0). Similar fragments containing curling cells with infection threads were excised and collected (rhc1). Fragments with bumps, indicating cortical cell divisions were considered another stage (rhc2). Young non-fixing nodules with gfp signal in the nodule, indicating ITs in the central tissue (rhc3) and young fixing nodules were the last stages harvested (rhc4). *S. rostrata* RNA was extracted as described (Kiefer et al., 2000), *M. truncatula* RNA was extracted using the RNeasy Plant Mini Kit (Qiagen, the Netherlands) following manufacturers specifications. First strand cDNA was synthesized using a Superscript RT II cDNA synthesis kit (Invitrogen, Carlsbad, USA). qRT-PCRs were performed using the SYBR Green kit (Eurogentec, Seraing, Belgium). Reactions were run on the iCycler iQ (Bio-Rad, Hercules, USA). For *M. truncatula* and *S. rostrata* RNA samples, an Elongation factor 1α and a ubiquitin gene were used as a constitutive control respectively (for primer sequences, see table)(Corich et al., 1998; Van de Velde et al., 2006). All reactions were performed in triplicate and averaged. Normalization of qRT-PCR data was performed using the $2^{-\Delta\Delta C_T}$ method as described (Livak and Schmittgen, 2001). As an internal control for sample quality, MtENOD40 expression was tested in all *M. truncatula* samples.

Gene	Sense Primer	Anti-sense Primer
AC148994_1	ACAACAACACAGATGGCGAAAG	TCATCAACACCATAAGCCTCTCC
AC148994_2	TTTCGGCTTCTATTCCAATCTTCC	TACCTTGGCACTAAAGTTACTGTC
AC184241_1	TTTTCTGCCACCCATATCCTAC	AGTTTGGAGAGTTAGCAAAGTATG
CR936328_1	ACTCCTCCGCATCTCTCATCTC	GTTGGTAGTAGGTGTTGTTGTTGG
MtLysM	AAGCATACCTCACCTTCAGAAC	CGGCGAGTTGAGATGGATTTG
AC126779_1	ACTTATGTGTGGCAGGATAATGAC	CGGTTGGTTGAAGCAGTGAAG
AC148141_1	no primers found	no primers found
MtLYK3	CAAGCATCGTCCGAATTTCTCTGG	CAATATCCAATCAACCGCACCAG
SrLysM	TTCCAGAACACAGACACCTACC	TGGGACAAGCACATCTAAGAGG
ELF1-α	ACTGTGCAGTAGTACTTGGTG	AAGCTAGGAGGTATTGACAAG
MtENOD40	CCCTCCATTTTCCTAAACAGTTTGC	ACTTGCCGGTTTGCCATGC

Generation of transgenic roots

To produce a *MtLysM* promoter::GUS fusion, the region 2 kb upstream of the *MtLysM* ORF was identified and isolated via PCR, using MtLysMpromF3 5'-TGAGCATGACACATTGACACA-3' and MTLysMpromR3 5'-TTGCAGAGAATGGGGTGTAA-3' as primers. The fragment was cloned into the pBWG43-Dnew binary GATEWAY vector (Invitrogen) (Karimi et al., 2002), recombining the promoter sequence with the β-glucuronidase open

reading frame and a 35S terminator sequence as described. *M. truncatula* seedlings were transformed as described (Boisson-Dernier et al., 2001). Plant roots were inoculated and at given time points harvested and staining with β-glucuronidase was done for 24 hours as described (D'Haeze et al., 1998).

To produce the knockout constructs (pK7GWIWG27F2-SrLysMKO and pK7GWIWG27F2-MtLysMKO), similar regions over the LysM domains were recombined in the pK7GWIWG27F2 binary GATEWAY vectors (Invitrogen) (Karimi et al., 2002). For the pK7GWIWG27F2-SrLysMKO and pK7GWIWG27F2-MtLysMKO constructs, the primers SrLysMtagF2 (5'-TCCCTGAATGACACCTTTGA-3') and SrLysMtagR2 (5'-TGAGAGGCCCTCAAAAGTG-3'); and MtLysMRTF1 (5'-CGAAACATTCGAAACAAACA-3') and MtLysMRTR2 (5'-CACCCCAATCAACCAAATAAA-3') were used, respectively. *S. rostrata* embryonic axes and *M. truncatula* seedlings were transformed as described (Boisson-Dernier et al., 2001; Van de Velde et al., 2003). As a control, roots were transformed with the pB7WG2D construct, overexpressing gfp as a visual marker. *S. rostrata* roots were inoculated with *A. caulinodans* ORS571 (pRG960SD-32), which can be visualized by staining β-glucuronidase activity (Goormachtig et al., 2004b). Hairy roots were propagated *in vitro* as described (Van de Velde et al., 2003). Seeds of the ENOD11 promoter::gus lines were kindly provide by Dr. David Barker.

Microscopical analysis

Light microscopical analysis was performed as described (D'Haeze et al., 1998). Plant material was harvest and fixed using 2.5% glutaraldehyde, embedded in Technovit 7100 (Kulzer Histo-Technik, Wehrheim, Germany). 4 μm sections were made, stained with 0.5% ruthenium red or 0.5% toluidine blue and mounted with Depex (Sigma). The sections were then analysed using a Diaplan bright field microscope (Leitz).

Results

Identification of a novel LysM type receptor-like kinase in *Sesbania rostrata* and *Medicago truncatula.*

In a transcript profiling experiment in *S. rostrata,* a tag has been identified that shows a low level of homology to genes encoding LysM type receptor-like kinases. This tag belonged to a cluster of genes that were upregulated during nodule formation in *S. rostrata* (Capoen *et al.,* in preparation). The tag spanned two LysM domains and because of these characteristics, was withheld for further analysis. Blastx analysis using the region containing the two LysM domains showed that the tag, designated *SrLysM,* was most homologous to two LysM-RLKs in Arabidopsis, At2g23770 and At2g33580 (43 and 42% amino

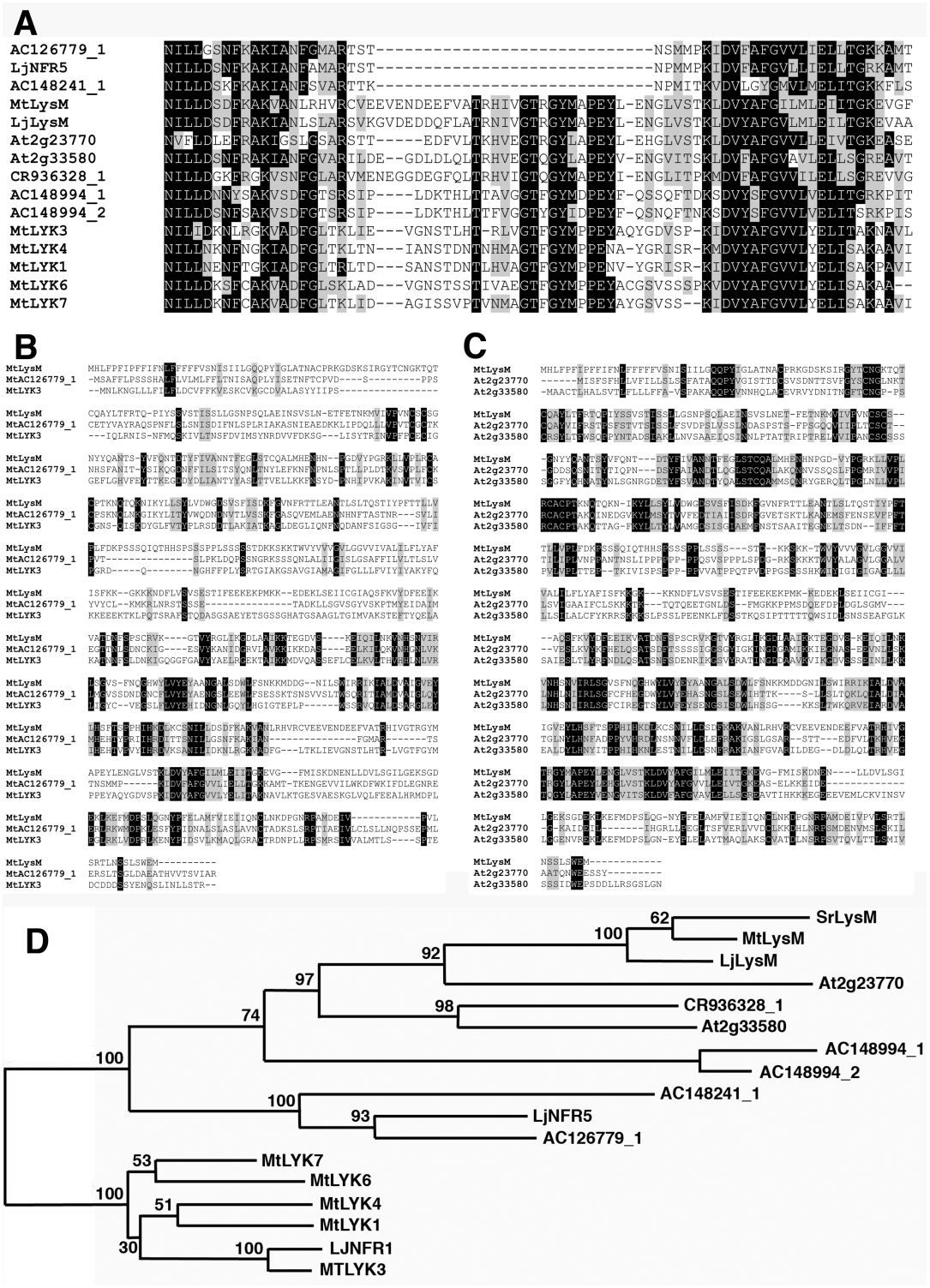

Fig.1 Sequence analysis of LysM-RLK proteins

A. . Alignment of a part of the kinase domain of all LysM-RLKs discussed in the text. The region directly surrounds the activation loop of the serine/threonine kinase domain, not the lack of the activation loop in NFR5 like proteins, but not in MtLysM-like or LYK3-like proteins. Shading threshold is set at 50%, black shading indicates identical residues, grey shading indicates similar residues. B. Alignment of MtLysM with MtLYK3 and MtAC126779_1 showing significant differences between members of the three different subfamilies of LysM-RLKs in *M. truncatula*. Shading threshold is set at 100%, black shading indicates identical residues, grey shading indicates similar residues. C. Alignment of MtLysM with 2 putative paralogs in *A. thaliana*. Shading threshold is set at 100%, black shading indicates identical residues, grey shading indicates similar residues. D. Phylogenetic tree depicting the presence of three different lineages of LysM-RLKs in legumes. Bootstrap values are indicated at the nodes and are based on 1000 iterations. For more explanation, see text.

acid similarity respectively). Also, homology was seen with LjNFR5 (35% similarity) and PsSYM10, the pea orthologue of LjNFR5 (30% simmilarity).

Next, the *Medicago* and *Lotus* genome sequences (NCBI) and EST databases (TIGR) were queried via blastx and tblastn using *SrLysM* and this analysis revealed several sequences with varying degrees of similarity (see material & methods). In *M. truncatula*, 6 full-length open reading frames were found that encode previously unknown LysM-RLKs. Closer analysis revealed two ORFs that were highly similar to *LjNFR5*. These open reading frames, designated *AC148241_1* and *AC126779_1* both encode LysM-RLKs containing 3 LysM domains and lacking an activation loop in the kinase domain (Fig1A). Moreover, the corresponding genes consisted of one exon. *AC148241_1* and *AC126779_1* are 72 and 82% similar to *LjNFR5* at the amino acid level, suggesting close homology. AC126779_1 might be identical to *MtNFP,* as a mutation was discovered in this gene in the *nfp* mutant in *M. truncatula* (unpublished, cited in Zhu et al., 2006).

The remaining 4 ORFs were different from both the NFR5 and NFR1/LYK3 type LysM-RLKs as shown by their overall similarity. They contain 2 LysM domains and an activation loop in the kinase domain (Fig. 1A). On the gene level, *MtLysM* (*AC126779_2*), the closest homologue to *SrLysM,* and CR936328_1 consists of only one exon, whereas *AC148994_1* and *AC148994_2* consists of 3 and 2 exons respectively. Overall similarity clearly separates these four sequences from the other 2 subfamilies. Whereas individual similarity among these 4 sequences is at least 60% at the amino acid level, similarity with either NFR1 or LYK3 type genes is no more than 45%.

Also, close homologues were found in the *Arabidopsis* genome. Two genes with relatively high similarity, At2g23770 and At2g33580 show around 60% overall similarity with *MtLysM* (43 and 42% in the LysM domains, respectively), hence they are closer homologues to *MtLysM* than the *Medicago* proteins from both the NFR5 and LYK3 type subfamilies (overall similarity within *Medicago* is around 40% for all genes) (Fig. 1A-C). Also, At2g23770 and At2g33580 were recently identified independently as close homologues of *Medicago* LysM-RLKs in *Arabidopsis* (Zhu et al., 2006). Furthermore, one *L. japonicus* homologue of *MtLysM* was also identified and named *LjLysM* (BAC clone LjT13I23). LjLysM shows 80% similarity to MtLysM at the protein level. We could not identify more members of this subfamily, likely due to the unfinished state of the *L. japonicus* genome sequence.

Phylogenetic analysis using sequences from *S. rostrata, M. truncatula, L. japonicus* and *A. thaliana* reveals 3 clear subfamilies (Fig. 1C). Subfamily one contains the LYK3/NFR1 type receptors, subfamily two consists of the NFR5 type receptors and subfamily 3 contains the

newly identified receptor-like kinases. Overall, proteins in subfamily 3 are 60 to 85% similar at the protein level, regardless of species, whereas similarity between subfamilies is lower, typically around 40 to 50% similarity (data not shown).

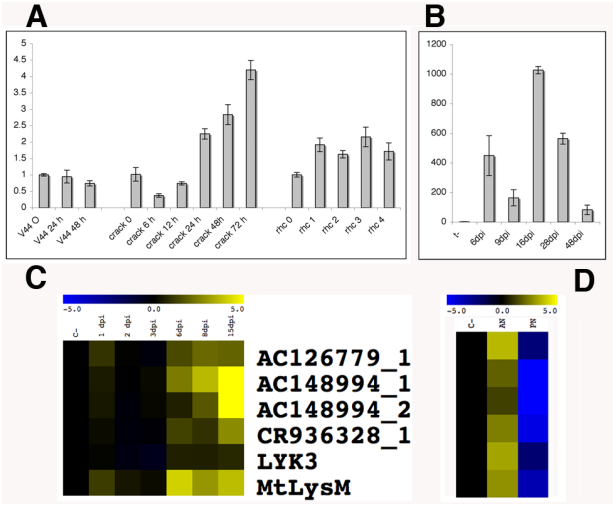

Fig. 2 Expression analysis
A. qRT-PCR analysis of *SrLysM* in hydroponic conditions after inoculation with ORS571-V44 as a negative control, in hydroponic conditions inoculated with wild type azorhizobia (crack) and in aeroponic conditions (rhc). B. qRT-PCR analysis of *MtLysM* in *M. truncatula roots* inoculated with *S. meliloti*. C. Expression of LysM-RLK representatives of all 3 subfamilies, yellow color indicates induction, blue indicates repression. D. $\log_{10}$ fold expression of LysM-RLK representatives of all 3 subfamilies. AN: apical part of root nodule, PN: proximal part of nodule.

Cloning of *the SrLysM* and *MtLysM* open reading frames

Subsequently, 5' and 3' RACE was performed to isolate the full length *SrLysM* open reading frame, however, to date, this yielded only the 5' sequence containing the first 900 base pairs of the open reading frame. Cloning of the full-length open reading frame (ORF) of *SrLysM* is ongoing. Also, via PCR the open reading frame of *MtLysM*, the closest homologue to *SrLysM* (see next paragraph) was amplified and cloned (see material and methods).

Expression analysis

S. rostrata is characterized by two invasion ways, in aerated conditions, the default root hair curling invasion (RHC) occurs. However, upon waterlogging, this invasion strategy is inhibited and nodules arise at sites of lateral root protrusion (LRB invasion), where bacteria use the resulting cracks to colonize the cortex directly (Goormachtig et al., 2004a). To determine the expression of *SrLysM* in both conditions, uninoculated and inoculated tissue was excised and RNA was prepared as described (see Material & Methods). Subsequent qRT-PCR quantifcation showed that *SrLysM* is differentially expressed upon inoculation with wild type rhizobia in both conditions, but not after inoculation with ORS571-V44, a NF deficient strain (Fig. 2A). However, during LRB invasion, the expression level was still rising at 72 hpi, a stage at which the experiment was stopped. Conversely, in tissues harvested for root hair invasion, *SrLysM* expression already reached a plateau in the rhc1 stage, corresponding to roots with infection threads but no cell division (Fig. 2A).

Also, *MtLysM* is induced upon inoculation of *M. truncatula* with compatible rhizobia, here, expression of *MtLysM* is very strongly induced, reaching a maximum of 1000 fold expression at 16 days post inoculation, corresponding to young fixing nodules, and a gradual decrease can be seen in later time points (Fig. 2B). We then proceeded by analyzing the expression

pattern of other members of the LysM-RLK family in *M. truncatula*. To this end, primer pairs were designed for *AC126779_1, AC148994_1* and *AC148994_2, CR936328_1* and *MtLYK3.* It was not possible to design high quality primers for *AC148241_1,* consequently, no data are available for this sequence. All genes were differentially expressed during nodulation, although a slight variation in induction level can be discerned, *AC148994_1* and *AC148994_2* are most strongly upregulated, a milder upregulation can be seen for *CR936328_1* and *MtLysM* (Fig. 2C), even lower was expression of *AC126779_1* (putative MtNFP) and expression of *MtLYK3* was the least induced, consistent with previously published observations (Limpens et al., 2005). In order to get a better understanding of the spatial expression pattern, mature nodules were cut in half and the proximal and distal parts of the nodules were collected separately. Expression of all genes tested was detected in the distal zone containing the meristem and infection zones, but not in the proximal fixation zone (Fig. 2D).

To get an overview of the expression patterns of the 2 *Arabidopsis* homologues, an *in silico* analysis was performed using the online micro-array compendium at www.genevestigator.ethz.ch (see addendum).

For At2g23770, upregulation was more than twofold in several treatments, all connected in one way or another with biotic and abiotic stress responses. These include challenges with *M. persicae* aphid nymphs and *Erisyphe cichoracearum*, treatment with hydrogen peroxide, cycloheximide, chitin, ozone and syringolin. Also, At2g23770 was upregulated upon programmed cell death in cell culture and nitrogen starvation. Similarly, or At2g33580, expression was reported upon treatments with cycloheximide, chitin, ozone, hydrogen peroxide, mannitol and salicylic acid, and upon challenge with *E. cichoracearum* and *Pseudomonas syringae* (for a full account of all expression patterns, see addendum). Except for the cycloheximide treatments, induction levels for At2g33580 were lower than for At2g23770 in corresponding treatments.

MtLysM promoter analysis.

A 2kb genomic region upstream of the *MtLysM* open reading frame was amplified from *M. truncatula* genomic DNA via PCR and recombined into a GATEWAY compatible expression system (see material and methods). Transgenic roots containing the *MtLysM*-promoter::GUS fusion were inoculated with *S. meliloti* and stained for GUS activity. Expression in non-inoculated roots was compared with roots 7, 14, 21 and 30 days after inoculation with *S. meliloti.* Within uninoculated roots, expression was sometimes visible in the root tips (Fig. 3A) and in parts of the vascular tissue, which, due its unpredictable occurrence was viewed as background (data not shown). Uninoculated roots showed GUS staining in the zone of the root directly behind the root tip (Fig. 3A).

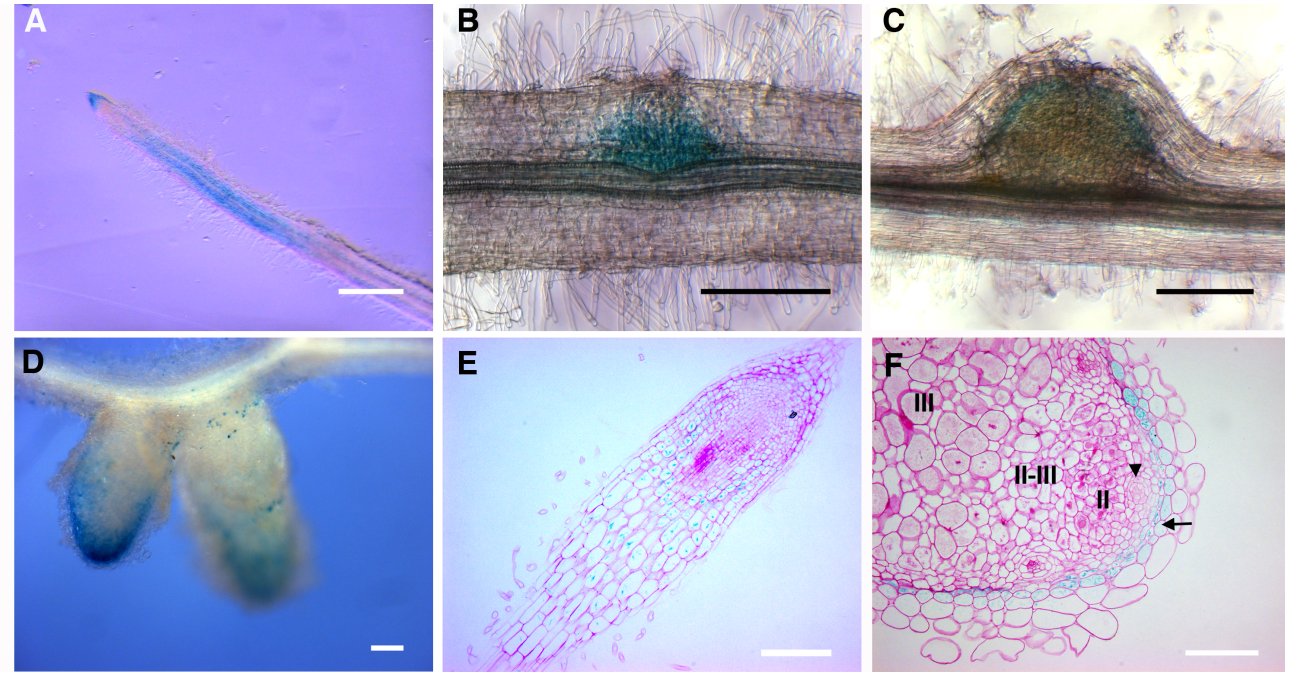

Fig. 3 Analysis of the *MtLysM* promoter activity
A-F. pMtLysM::gus transformed roots were stained for GUS activity 24 hours before analysis. A. uninoculated roots with background GUS activity in root tips and in the zone directly behind the root tips. B. GUS activity in lateral root primordia. C. GUS activity in developing nodule becomes restricted to the outer layers of the central tissue. D. in mature nodules, GUS activity is visible in the apical parts of the nodule. E-F: Rhutenium Red stained sections. E. Semithin section through root tips shows GUS precipitates in cortical cells in the zone behind the root tip. F. Semithin section through mature nodule. Expression is restricted to the inner cortical cell layer of the nodule tissue. Abbreviations: I Meristem, II infection zone, II-III transition zone, III infection zone. Arrowhead: nodule vascular bundle, arrow: inner cortical cell layer showing GUS staining indicative of *MtLysM* promoter activity. Bars are 200 μM.

Expression was visible in the cortical cells of this region but not in the vascular tissue. Semithin sections showed GUS staining in cortical cells in the zone directly behind the root tips (Fig. 3B). Lateral root primordia also showed GUS staining (Fig. 3B), however the very tip of the primordium was often devoid of staining, and the expression was often restricted to a ring around the primordium (data not shown).

Upon inoculation, the expression visible in the zone behind the root tip seems to disappear in the majority of roots. Next, expression was restricted to the outermost cell layers of the growing nodule primordium, with a faint blue staining barely visible in the center of the primordium (Fig 3C). In mature nodules, expression become more and more restricted to the apical part of the nodule where GUS staining can be seen in the zone containing the meristem and infection zone (Fig. 3D). Semithin sectioning showed that expression in mature root nodules was restricted to a few cell layers on the outside of the nodules (Fig. 3F). The inner cortical cell layer showed the strongest expression, although often the outer cell layer of the nodule parenchyma also stained blue with GUS.

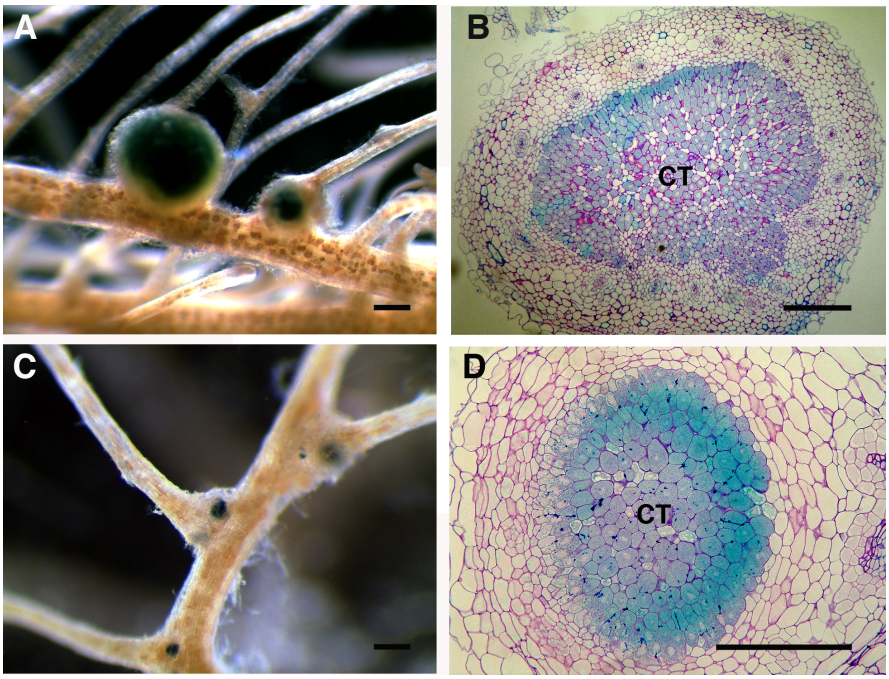

Fig. 4 RNAi phenotype of *SrLysM*
A. Low magnification view of control roots 8 days after inoculation with *A. caulinodans.* Blue staining indicates bacteria in the central tissue. B. Semithin section through a nitrogen fixing control nodule, 8 days after inoculation. C. Low magnification view of *SrLysM* knock down line with small nodule like structures containing bacteria at 8 dpi. D. Semithin section through small knock down nodules at 8 dpi. Central tissue is smaller in surface than for control roots, however, the central cells have differentiated normally en cells look like nitrogen fixing control cells. Abbreviations: CT, central tissue. Bars are 200 μm.

RNAi knock down reveals a novel symbiotic function for *SrLysM* and *MtLysM.*

Knock down of *SrLysM.*

To investigate the potential role of *SrLysM* during nodule development, an RNAi construct spanning the two LysM domains was introduced into *S. rostrata* transgenic roots, in parallel, a construct with 35S driven gfp was used as a positive control (see material & methods). Transformants were inoculated with an *A. caulinodans* that can be visualized by staining for GUS activity, and assessed 8 days after inoculation, at which stage the control plants contained functional, round nodules (Fig. 4A). Of the 40 lines containing the knock down constructs that were obtained, 6 lines showed small nodule like structures containing *A. caulinodans* (Fig. 4C). Semithin sections through these small nodules revealed nitrogen fixing cells in the central tissue. These cells appeared normal and infection threads had no discernable defects. However, the number of fixing cells in cross sections was markedly lower compared to nodules of control lines (compare Fig. 4B with 4D).

Knock down of *MtLysM.*

An RNAi construct spanning the two LysM domains was also made for *MtLysM* and introduced into *M. truncatula* roots using *A. rhizogenes* mediated hairy root transformation. Three independent transformations were performed in parallel with a gfp expressing

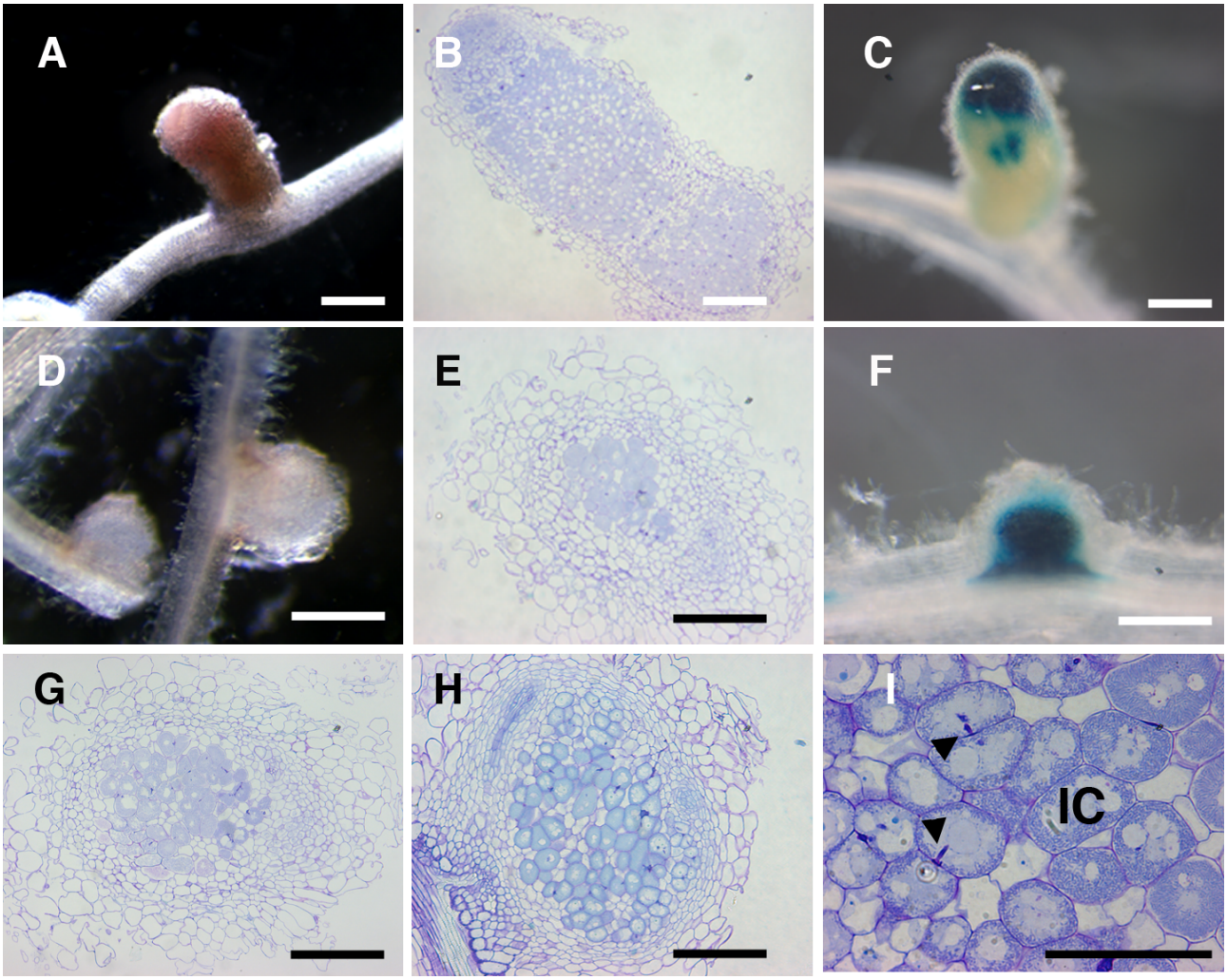

Fig. 5 RNAi phenotype of *MtLysM*
A-C: control lines. A. Low magnification view of 35S-gfp expression control roots 30 dpi. Nitrogen fixing nodules are present and semithin sections confirm zonated habit of the control nodules as seen in panel B. C. 35S-gfp expressing lines in pENOD11::gus background shows wild type ENOD11 expression pattern at 30 dpi. D-F. *MtLysM* knock down lines. D. Low magnification view of small white nodules found on knock down lines 30 dpi. E. Semithin sections through small white nodules in D. F. Small nodules 30 dpi on *MtLysM* knock down lines in pENOD11::gus background. G-H. The amount of nitrogen fixing cells in knock down lines differs significantly between lines (compare G to H), depending on timing of meristematic arrest. I. Nitrogen fixing cells develop normally in knock down lines. Abbreviations: IC, infected cells. Arrowheads indicate infection threads. Bars 250 μm.

control construct. In total, the nodulation phenotype of 84 individual transformants was analysed 30 days after inoculation with rhizobia. 24 roots contained pink nodules of the indeterminate type, 35 contained small white nodules (Fig. 5D) and 25 had no nodules, although often deformed root hairs were visible (data not shown). Of 29 transformants with the gfp expressing empty vector, 26 contained pink indeterminate nodules 30 days after inoculation (Fig. 5A), whereas 3 bore no nodules.

Nodules were harvested for microscopical analysis and semithin sections through the small white nodules showed a limited number of infected, seemingly healthy differentiated and bacteria containing central cells (Fig. 6E, G-I). The number of fixing cells varied between lines but was markedly lower than for control nodules (compare Fig. 6B with 6G-H).

Cross sections revealed no meristem and generally no infection zone could be discerned in these small, white nodules. Occasionally, a small infection zone was still present. Infection threads were present in these nodules and were comparable in size and shape to infection threads in control nodules.

To investigate whether or not nodulin gene expression was affected upon *MtLysM* knock down, we repeated the RNAi experiments in pMtENOD11::GUS (line L416 Journet et al., 2001) background. These plants contain a promoter::GUS construct with the upstream region of the early nodulin gene ENOD11 (Journet et al., 2001). Nodules stained for gus activity 30 days after inoculation in control lines showed a typical expression pattern in the apical region of the nodule, conforming to the published expression pattern (Fig. 5C) (Journet et al., 2001). When knock down lines were stained, strong GUS expression off the ENOD11 promoter sequence was visible throughout the small round nodule (Fig. 5F).

Quantification of expression levels in *S. rostrata* and *M. truncatula* knock down lines.

From all lines described for both *S. rostrata* and *M. truncatula* root cultures were grown and RNA was extracted. Using qRT-PCR, expression levels of the respective *LysM* genes was determined for knock-down and control lines. Unfortunately, expression levels in hairy roots were very inconsistent, even so in control lines (Data not shown). This impeded straightforward identification of lines with markedly lower expression levels and subsequent correlation to the phenotype obtained for those lines.

Discussion

During a cDNA-AFLP transcript profiling experiment in *S. rostrata* evidence was found for a novel LysM domain containing RLK that was upregulated during both lateral root base and root hair curling nodulation. Two genes were similar to *LjNFR5*, *AC126779_1* and *AC148241_1*, the former likely being the orthologue of NFR5 and the latter a closely related gene. Indeed, both genes consist of one exon, have 3 extracellular LysM domains and no activation loop in the kinase domain, as was reported for *LjNFR5* (Madsen et al., 2003). The closest homologue to *SrLysM* was designated *MtLysM,* It contains the activation loop and only two discernable LysM domains, although it also is a single exon gene like NFR5. Three tags were highly similar to *MtLysM*, *MtCR936328_1* and *MtAC148994_1* and *MtAC148994_2* and cluster together in the new subfamily, as well as two *Arabidopsis* genes, At2g23770 and At2g33580. The *Arabidopsis* genes might represent the ancestral forms from which, through duplications and neofunctionalization, the NF perception system has evolved. The majority of these results are in agreement with a recent wide scale phylogenetic analysis of genes involved in nodulation (Zhu et al., 2006). However, Zhu and coworkers do not mention

the lack of the activation loop, nor the number of LysM domains and group all *NFR5* like sequences in what is designated the LysMb clade, as opposed to the *NFR1* and *LYK3* like genes in the LysMa clade (Zhu et al., 2006). The sequences called *MtNFR5a* and *c* in the Zhu *et al.* paper correlate to the genes *MtAC126779_1* and *MtAC148241_1* respectively, and *MtNFR5b* correlates to *MtLysM.* We thus propose to split the so called LysMb clade in two, one cluster containing the true *NFR5* genes in one branch and the *MtLysM* like genes in the other branch.

Subsequent analysis focused on this third subfamily with *MtLysM*, *MtCR936328_1, MtAC148994_1* and *MtAC148994_2* as the prime representative, based on its presumed orthology to *SrLysM,* as representatives of the other subfamilies, *MtLYK3, MtAC126779_1* and *MtAC148241_1* were used. *MtAC126779_1* is induced upon inoculation, which fits with the observation that in *Pisum sativum, PsSYM10* is present in indeterminate nodules, whereas *LjNFR5* was not present in determinate nodules (Madsen et al., 2003). Determinate nodules differ from indeterminate type nodules since indeterminate nodules maintain a zonated structure with an apical meristem constantly adding new cells to the nodule that need to be infected, requiring the continued expression of genes involved in infection of central tissue cells. Compared to the representatives of the other subfamilies, the *MtLysM* homologues were strongly induced during nodule development. *MtAC148994_1* and *MtAC148994_2* were most strongly upregulated, a milder upregulation was found for *MtCR936328_1* and *MtLysM.* The presence of the majority of known LysM-type RLKs in the apical part of older nodules points towards a role for these proteins in the processes that govern late stages of the symbiosis. *MtLYK3* was only very mildly induced during nodulation, nevertheless *MtLYK3* was mainly expressed in the apical part of the nodule, as was described in literature (Limpens et al., 2005). This suggests roles for all *Medicago* LysM-RLKs identified to date in later stages of nodule development, in the zone where the progeny of the nodule meristem differentiates and is infected by bacteria.

Analysis of the *MtLysM* promoter using a GUS reporter construct revealed a basal expression pattern in the zone behind the root tip of non-inoculated roots and around lateral root primordia. Expression narrows down in nodule primordia to the outer cell layers of the primordium and in mature nodules expression is restricted to the distal part of the nodule. Microscopical analysis confirmed cortical expression in root tips. In mature nodules expression is limited to the inner cortical layer of the nodule and perhaps the outer parenchymal layer. *In situ* hybridizations are being performed for all members of the subfamily to deepen our understanding of the accummulation patterns of these genes. Also a more in depth analysis of the early *MtLysM* promoter activity is in progress.

Knock down of *SrLysM* in *S. rostrata* and *MtLysM* in *M. truncatula* resulted in smaller nodules and the absence of a meristem or infection zone. *S. rostrata* nodules initially have a meristem which switches of eventually. Premature arrest of the meristem activity is likely to lead to smaller nodules with fewer cells in the central tissue. Also the *M. truncatula* phenotype is most likely due to a premature arrest of the nodule meristem, and differences in nodule size might be due to differences in residual expression levels, resulting in a different timing of meristem cessation in different lines. This novel phenotype hints at a role for LysM-RLKs in signaling for meristem maintenance in nodules. How this is achieved mechanistically is uncertain but functional analysis of downstream targets will no doubt shed light on this issue. Additionally, it is possible that a complete knock down has an even more severe phenotype since a significant proportion of the lines tested in *M. truncatula* had no nodules, whereas in control lines this was only rarely seen. However, for the time being, the lack of expression quantifications precludes us from making strong statements in this regard. The identification of TILLING lines might address this problem and several promising mutants in the GLIP TILLING population were identified (http://www.eugrainlegumes.org).

Given the expression of *MtLysM* in primordia and in the nodule parenchyma and cortex, where the protein would most likely not come into contact with bacteria or NF, it seems plausible that endogenous signals rather than NFs are ligands for some of these newly found LysM-RLKs. Although the association with rhizobia is essentially a legume specific trait, several reports of NF responses in non-legumes add a shroud of mystery to this bacterial signal molecule. NF can induce alkalinization and an oxidative burst in tobacco cell cultures, similar to elicitor treated cultures, whereas alfalfa cell cultures respond by slight acidification and no oxidative burst (Baier et al., 1999), indicating that non-legumes have perception systems that can recognize NF. Legumes may have evolved a new type of elicitor receptor that accommodates for this new kind of biotic interaction. Most likely, the chitin perception pathway in plants is at the evolutionary origin of the NF perception pathway. The identification of two highly homologous *Arabidopsis* genes which are differentially expressed during biotic stress conditions strongly supports this hypothesis.

Also, somatic embryogenesis of several plant species has been shown to be correlated with or require NF like compounds. Cell cultures of a carrot somatic embryogenesis mutant can be rescued by *S. meliloti* Nod factor (De Jong et al., 1993). This rescue can also be achieved by addition of an endochitinase, suggesting that molecules derived from this endochitinase activity and structurally similar to rhizobial NF are involved in signaling for somatic embryogenesis. Moreover, in the conditioned

medium of embryogenic spruce cell cultures, the presence of a lipophilic fraction containing GlucNAc cross-reacting molecules was correlated with embryogenesis (Dyachok et al., 2002). These data suggest similar perception systems for NFs on the one hand and for elicitors and a putative embryogenic signal with structural similarities to NF on the other hand. Such pathways are good candidates to have been usurped and adapted to accommodate for symbiosis by gene duplications and neofunctionalization events.

Conclusions and future perspectives

We have conducted a preliminary analysis of a novel subfamily of LysM domain containing RLKs that are related to the two known classes of putative NF receptors in legumes (for a review, see Geurts et al., 2005). This novel subfamily is likely to have certain members that also play key roles in nodule development, since knock down of *MtLysM* resulted in a previously unreported phenotype in which the meristem activity ceases prematurely. Whether or not bacterial NF, other bacterial signals or endogenous plant signals are involved in this process is unknown and will be investigated. Nodulation is an extremely finetuned process and that most of the intricacies of the interaction remain unexplored to date.

A At2g23770

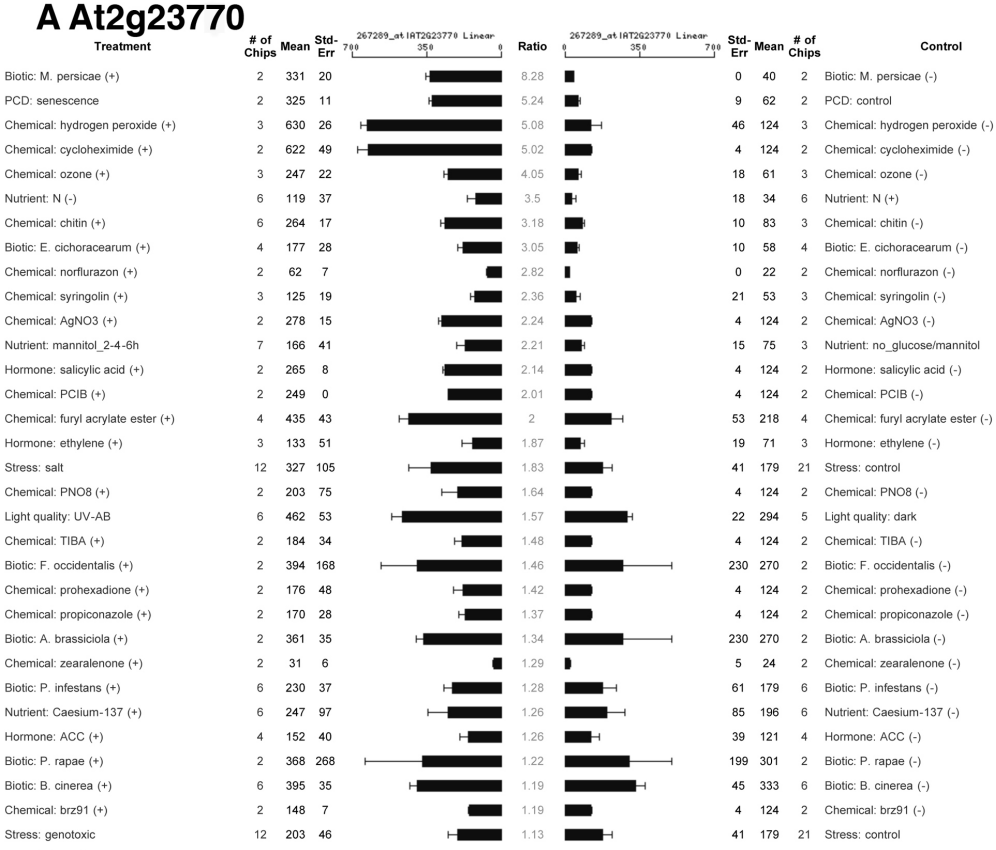

Treatment	# of Chips	Mean	Std-Err	Ratio	Std-Err	Mean	# of Chips	Control
Biotic: M. persicae (+)	2	331	20	8.28	0	40	2	Biotic: M. persicae (-)
PCD: senescence	2	325	11	5.24	9	62	2	PCD: control
Chemical: hydrogen peroxide (+)	3	630	26	5.08	46	124	3	Chemical: hydrogen peroxide (-)
Chemical: cycloheximide (+)	2	622	49	5.02	4	124	2	Chemical: cycloheximide (-)
Chemical: ozone (+)	3	247	22	4.05	18	61	3	Chemical: ozone (-)
Nutrient: N (-)	6	119	37	3.5	18	34	6	Nutrient: N (+)
Chemical: chitin (+)	6	264	17	3.18	10	83	3	Chemical: chitin (-)
Biotic: E. cichoracearum (+)	4	177	28	3.05	10	58	4	Biotic: E. cichoracearum (-)
Chemical: norflurazon (+)	2	62	7	2.82	0	22	2	Chemical: norflurazon (-)
Chemical: syringolin (+)	3	125	19	2.36	21	53	3	Chemical: syringolin (-)
Chemical: AgNO3 (+)	2	278	15	2.24	4	124	2	Chemical: AgNO3 (-)
Nutrient: mannitol_2-4-6h	7	166	41	2.21	15	75	3	Nutrient: no_glucose/mannitol
Hormone: salicylic acid (+)	2	265	8	2.14	4	124	2	Hormone: salicylic acid (-)
Chemical: PCIB (+)	2	249	0	2.01	4	124	2	Chemical: PCIB (-)
Chemical: furyl acrylate ester (+)	4	435	43	2	53	218	4	Chemical: furyl acrylate ester (-)
Hormone: ethylene (+)	3	133	51	1.87	19	71	3	Hormone: ethylene (-)
Stress: salt	12	327	105	1.83	41	179	21	Stress: control
Chemical: PNO8 (+)	2	203	75	1.64	4	124	2	Chemical: PNO8 (-)
Light quality: UV-AB	6	462	53	1.57	22	294	5	Light quality: dark
Chemical: TIBA (+)	2	184	34	1.48	4	124	2	Chemical: TIBA (-)
Biotic: F. occidentalis (+)	2	394	168	1.46	230	270	2	Biotic: F. occidentalis (-)
Chemical: prohexadione (+)	2	176	48	1.42	4	124	2	Chemical: prohexadione (-)
Chemical: propiconazole (+)	2	170	28	1.37	4	124	2	Chemical: propiconazole (-)
Biotic: A. brassiciola (+)	2	361	35	1.34	230	270	2	Biotic: A. brassiciola (-)
Chemical: zearalenone (+)	2	31	6	1.29	5	24	2	Chemical: zearalenone (-)
Biotic: P. infestans (+)	6	230	37	1.28	61	179	6	Biotic: P. infestans (-)
Nutrient: Caesium-137 (+)	6	247	97	1.26	85	196	6	Nutrient: Caesium-137 (-)
Hormone: ACC (+)	4	152	40	1.26	39	121	4	Hormone: ACC (-)
Biotic: P. rapae (+)	2	368	268	1.22	199	301	2	Biotic: P. rapae (-)
Biotic: B. cinerea (+)	6	395	35	1.19	45	333	6	Biotic: B. cinerea (-)
Chemical: brz91 (+)	2	148	7	1.19	4	124	2	Chemical: brz91 (-)
Stress: genotoxic	12	203	46	1.13	41	179	21	Stress: control

B At2g33580

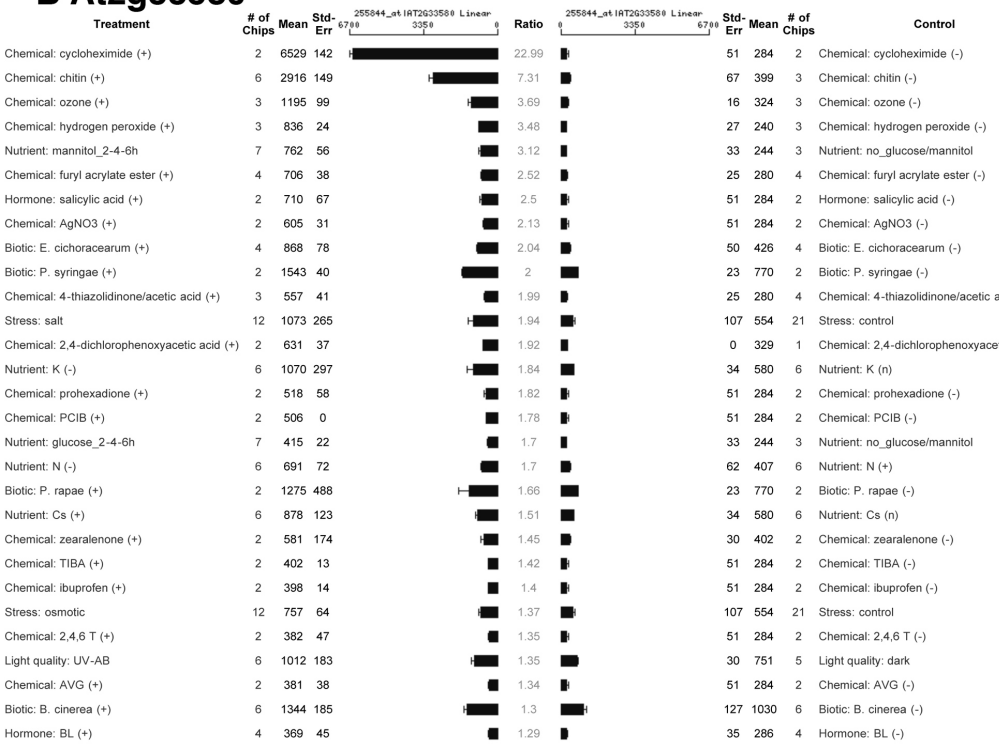

Treatment	# of Chips	Mean	Std-Err	Ratio	Std-Err	Mean	# of Chips	Control
Chemical: cycloheximide (+)	2	6529	142	22.99	51	284	2	Chemical: cycloheximide (-)
Chemical: chitin (+)	6	2916	149	7.31	67	399	3	Chemical: chitin (-)
Chemical: ozone (+)	3	1195	99	3.69	16	324	3	Chemical: ozone (-)
Chemical: hydrogen peroxide (+)	3	836	24	3.48	27	240	3	Chemical: hydrogen peroxide (-)
Nutrient: mannitol_2-4-6h	7	762	56	3.12	33	244	3	Nutrient: no_glucose/mannitol
Chemical: furyl acrylate ester (+)	4	706	38	2.52	25	280	4	Chemical: furyl acrylate ester (-)
Hormone: salicylic acid (+)	2	710	67	2.5	51	284	2	Hormone: salicylic acid (-)
Chemical: AgNO3 (+)	2	605	31	2.13	51	284	2	Chemical: AgNO3 (-)
Biotic: E. cichoracearum (+)	4	868	78	2.04	50	426	4	Biotic: E. cichoracearum (-)
Biotic: P. syringae (+)	2	1543	40	2	23	770	2	Biotic: P. syringae (-)
Chemical: 4-thiazolidinone/acetic acid (+)	3	557	41	1.99	25	280	4	Chemical: 4-thiazolidinone/acetic acid (-)
Stress: salt	12	1073	265	1.94	107	554	21	Stress: control
Chemical: 2,4-dichlorophenoxyacetic acid (+)	2	631	37	1.92	0	329	1	Chemical: 2,4-dichlorophenoxyacetic acid
Nutrient: K (-)	6	1070	297	1.84	34	580	6	Nutrient: K (n)
Chemical: prohexadione (+)	2	518	58	1.82	51	284	2	Chemical: prohexadione (-)
Chemical: PCIB (+)	2	506	0	1.78	51	284	2	Chemical: PCIB (-)
Nutrient: glucose_2-4-6h	7	415	22	1.7	33	244	3	Nutrient: no_glucose/mannitol
Nutrient: N (-)	6	691	72	1.7	62	407	6	Nutrient: N (+)
Biotic: P. rapae (+)	2	1275	488	1.66	23	770	2	Biotic: P. rapae (-)
Nutrient: Cs (+)	6	878	123	1.51	34	580	6	Nutrient: Cs (n)
Chemical: zearalenone (+)	2	581	174	1.45	30	402	2	Chemical: zearalenone (-)
Chemical: TIBA (+)	2	402	13	1.42	51	284	2	Chemical: TIBA (-)
Chemical: ibuprofen (+)	2	398	14	1.4	51	284	2	Chemical: ibuprofen (-)
Stress: osmotic	12	757	64	1.37	107	554	21	Stress: control
Chemical: 2,4,6 T (+)	2	382	47	1.35	51	284	2	Chemical: 2,4,6 T (-)
Light quality: UV-AB	6	1012	183	1.35	30	751	5	Light quality: dark
Chemical: AVG (+)	2	381	38	1.34	51	284	2	Chemical: AVG (-)
Biotic: B. cinerea (+)	6	1344	185	1.3	127	1030	6	Biotic: B. cinerea (-)
Hormone: BL (+)	4	369	45	1.29	35	286	4	Hormone: BL (-)

Addendum

Response viewer outputs for At2g23770 and At2g33580 as documented in the genevestigator micro-array compendium (www.genevestigator.ethz.ch). A. partial output for At2g23770 showing the treatments with strongest upregulation for this gene. B. partial output for At2g33580. Treatments or controls upon which the respective genes are induced are indicated left, whereas controls or treatments with lower expression are indicated right. Centrally located are the ratio values for treatment over control, showing relative induction of the gene in each experiment.

Summary & Perspectives

Although often invisible to the naked eye, life on earth is inseparably linked on all levels. From the ecosystem level to the molecular level, organisms interact with each other and without this link, no life would be possible. This is nicely illustrated by the symbiotic interaction between nearly all land plants with fungi of the *glomeromycota*, during which the fungi penetrate the plant roots and form intracellular structures called arbuscules, a process called Arbuscular Mycorrhization (Kistner and Parniske, 2002). These arbuscules can be thought of as heavily branched synapses that allow both interactors to exchange nutrients, resulting in an improved phosphorous and mineral uptake by the plant. This interaction was likely a pivotal step in the conquest of land by early land plants, illustrating the importance of cooperation in evolution.

Several 100 million years later, another symbiosis emerged in a small lineage in the Eurosids I clade. Several groups of nitrogen fixing microorganisms started cooperating with plants to form nodule like structures on the roots of host plants wherein the bacteria fix highly inert atmospheric nitrogen and provide the plant with ammonia as the reduced nitrogen source. In return the plant provides its guests with carbon sources and a specialized niche. The best-known example of this symbiotic nitrogen fixation is a group of gram-negative soil bacteria collectively called rhizobia, which interact with leguminous host plant species to form the typical nodule. Evidence suggests that certain hurdles that exist for a microorganism to penetrate a plant were overcome by recruiting pathways (called the 'common sym' pathway) from the more ancient mycorrhizal symbiosis (Parniske, 2000). Invasion, although instigated by a bacterial lipochitooligosaccharide signal called the NF, is tightly regulated by the plant. The most widely studied infection procedure is called root hair curling invasion. Here, bacterial recognition by the appropriate host leads to curling of root hair cells and in the entrapment of a bacterial microcolony in that curl. From there, bacteria penetrate the root hair cell, in a tubular structure called an infection thread that leads the dividing bacteria towards the root cortex. In the inner cortex, cells have started to redifferrentiate to form the root nodule, where bacteria are released into the central nodule tissue and differentiate to form a novel, nitrogen-fixing organelle called the symbiosome (reviewed in Patriarca et al., 2004) (Chapter 1). Legumes have adopted several other infection strategies, presumably in a response to environmental obstacles that affect the plants ability to form nodules via the default pathway (Guinel and Geil, 2002; Goormachtig et al., 2004a). As a model for this plasticity, *Sesbania rostrata* has enjoyed some attention, as it can be infected via fissures resulting from lateral or adventitious root protrusion, called lateral root base or LRB nodulation (Chapter 3). *S. rostrata* is a tropical, semi-aquatic legume that is adapted to seasonal flooding, which leads to high levels of accumulating ethylene that inhibits root hair curling (Den Herder et al., 2006). Contrary to root hair curling, LRB

nodulation is not inhibited but promoted by ethylene (D'Haeze et al., 2003). Ethylene is required for the formation of the infection pocket (IP), a small group of outer cortical cells that die in a process reminiscent of programmed cell death. The IP serves as a signaling center from which ITs proceed towards the incipient nodule primordium, analogous to the function of the root hair curl (Goormachtig et al., 2004a). Work in *S. rostrata* with bacterial mutants with altered NF structure suggests that NF structure specificity is more stringent for root hair curling than for LRB nodulation (Goormachtig et al., 2004b). A long lasting paradigm in nodulation research states the existence of two receptor complexes with different stringencies towards NF structure, a stringent entry receptor and a less stringent signaling receptor (Ardourel et al., 1994). This suggests that LRB nodulation, which basically skips the epidermal entry step via direct colonization of the outer cortex, has circumvented the entry receptor complex in the epidermis. It also suggests that the entry receptor complex or its downstream targets are partially regulated by ethylene (Chapter 4-5).

These unique features of *S. rostrata* nodulation allow several questions concerning rhizobial infection to be addressed from a fresh angle. Infection strategies can be compared within the same species, greatly facilitating analysis. Since infection is presumed to circumvent entry receptor mediated events in the epidermis, questions pertaining to putative roles for NF signal transduction pathways in the cortex can readily be studied. And it is these questions that dominated the second part of this work.

Using cDNA-AFLP based transcript profiling, a wide scale comparison of root hair curling and LRB nodulation was conducted (Chapter 6). This resulted in the identification of more than 600 genes that are differentially expressed in either root hair curling or LRB nodulation, or in both, and the identification of promising marker genes possibly involved in IP formation on the one hand and epidermal NF responses on the other. Broad similarities were found between both processes. Although bacterial invasion strategies differ significantly, the development of the nodule itself relies on the same processes in both nodulation types. As a consequence, a wealth of data is now available and elements of the dataset can be cherry-picked for future functional analysis.

A multitude of data is present in literature concerning pathways, processes and genes essential for the earliest plant responses to NF (Riely et al., 2006). However, these data are strongly biased towards their roles in epidermal events, since mutation of these genes in plants that nodulate via root hair curling are all blocked at the epidermal stage. To address this, the role of *SrSymRK* was investigated. *SymRK/NORK* encodes a LRR type receptor like kinase that is necessary for both nodulation and mycorrhization and was presumed to act exclusively in the epidermis. However, knock down of the gene in *S. rostrata* resulted in the formation of nodules that, on closer inspection,

did not contain nitrogen-fixing bacteria in the central tissue. *SrSymRK* knock down did not significantly affect nodule formation or IT formation, but had an effect on IT morphology and on bacterial release from the ITs into the host cell cytoplasm (Chapter 7). Other recent work suggests that mutations in *SymRK*, and by analogy several other genes in the common sym pathway, are also affected in the touch sensitivity of root hairs, leading to the arrest of cytoplasmic streaming and vesicle targeting to the point of bacterial attachment (Esseling et al., 2004; Geurts et al., 2005). Mechanical sensing might thus also be involved during appressorium formation and fungal entry during mycorrhization and the possibility that this pathway was recruited downstream of NF signaling is enticing. While progression of ITs through the cortex most likely (ab)uses the basic cell cycle machinery to gain access to the successive cortical cell layers (Yang et al., 1994), the final release of bacteria requires targeting of specialized vesicles to the infection thread tip, likely making the process functionally analogous to the initial root hair cell entry. More reports of the possible role of these early nodulation genes at later stages are now cropping up and expression analysis places most of the known NF receptors and common sym genes in the zone of bacterial release in mature nodules (Limpens et al., 2005).

The common sym genes have been implicated in the mediation of an enigmatic NF response known as Ca^{2+}-spiking. Within minutes of NF perception, (peri)nuclear oscillations in calcium concentrations can be detected in root hairs (Oldroyd and Downie, 2006). By analogy with animal systems, these oscillations are thought to have signaling capacity and to be essential for the propagation of the signaling cascade originating from NF perception event. Furthermore it has been shown that Ca^{2+}-spiking is inhibited by ethylene, making Ca^{2+}-spiking a likely target for the ethylene mediated inhibition of root hair curling (Oldroyd et al., 2001). Paradoxically, ethylene is a prerequisite for LRB nodulation. These conflicting observations needed to be addressed. The inhibition of Ca^{2+}-spiking by ethylene is likely to be the reason why the circumvention of epidermal responses have to be circumvented in LRB nodulation. While during LRB nodulation no root hair cells are involved, axillary root hair initials present at the lateral root base do respond to NF by deforming (Mergaert et al., 1993). Microinjection of calcium sensitive dyes into these cells showed that they have retained the ability to initiate NF induced Ca^{2+}-spiking but at frequencies that are much higher than those reported in other legumes (Chapter 8). Contrary to what is known for Ca^{2+}-spiking in *M. truncatula*, hydroponic Ca^{2+}-spiking is insensitive to ethylene and is inhibited by ethylene antagonists. Application of jasmonate also leads to a decrease in frequency, as was observed in *M. truncatula* (Sun et al., 2006). Pharmacological modulation of Ca^{2+}-spiking frequency resulted in the initiation of infection of these axillary root hair cells, but not in nodule formation. Several conclusions and

hypotheses follow from these observations. This does not mean, however, that the signaling events in these root hairs is necessary for nodulation in hydroponic culture since the adventitious root sites on the stem of *S. rostrata* do not carry root hairs but can form nodules. It does suggest that a range of Ca^{2+}-spiking frequencies is present *in vivo*. Hydroponic spiking frequencies are at the extreme of this range and do not accommodate for intracellular invasion anymore. Furthermore, the data presented here suggest that ethylene is partly responsible for this shift in frequency, since the addition of ethylene biosynthesis inhibitors slows down Ca^{2+}-spiking. First and foremost, a causal link between Ca^{2+}-spiking and intracellular invasion can now be established, which is an observation of great importance to the future direction of research into calcium signaling during nodule development.

At the very forefront of NF perception are a family of LysM domain containing receptor-like kinases that are presumed to recognize the NFs and initiate the symbiosis. Thus far, two types of LysM-RLKs have been identified, candidate entry receptors are the NFR1 type receptors whereas the NFR5 type receptors are the presumed signaling receptors (Cullimore and Denarie, 2003). Although this model is most likely a crude oversimplification of the actual situation, it currently serves as the most suitable model of action. Alternatively, the different hetero- and homodimers that can be formed using members of these subfamilies could account for a combinatorial treasure trove of NF specific responses. The identification of a novel type of LysM-RLK that was upregulated in the previously mentioned cDNA-AFLP experiment may add to this emerging complexity (Chapter 9). This third subfamily of LysM-RLKs contains several genes with characteristics that can best be described as chimaeric since they show several characteristics that are essentially a mix of both previously described classes. The existence of several highly homologous sequences in *Arabidopsis* and rice (This work, Zhu et al., 2006) suggests that neofunctionalization of duplicated sequences has resulted in the evolution of NF perception. At least for one member of this new subfamily, *MtLysM,* a novel nodulation phenotype has been established. Nodule meristem maintenance is impaired in knock down lines of both *SrLysM* and *MtLysM* without affecting the differentiation of the central, nitrogen-fixing tissue. We are currently investigating NF specificity of these receptors by heterologous expression of *SrLysM* in *Medicago* roots. This might provide clues as to where our focus should be directed for future analysis.

In conclusion, we have taken full advantage of the unique features of *S. rostrata*'s unique nodulation features to investigate both the unique aspects of LRB nodulation and to add to the growing body of knowledge of root hair curling nodulation. We have identified gene clusters in both invasion types that merit future analysis. We have also shown the use of *S. rostrata* as a model for the functional analysis

of cortical functions for genes that also act in the epidermis without the need for laborious and often difficult techniques like the use of inducible constructs. Finally, the identification of Ca^{2+}-spiking as a potential target of the adaptation to hydroponic conditions has deepened our understanding of LRB nodulation.

Samenvatting & Toekomstperspectieven

De transitie van water naar land is tijdens de evolutie van de huidige landplanten naar alle waarschijnlijkheid mede mogelijk gemaakt door het aangaan van een nauwe samenwerking met bepaalde fungi van de de *glomeromycota*, Arbusculaire Mycorrizatie of AM genaamd (Kistner and Parniske, 2002). Hierbij invaderen fungale hyphen de wortels en in de diepste corticale cellagen dringen deze hyphen binnen in een aantal cellen en vertakken zich tot boomvormige structuurtjes, de arbuscules, waarmee het contactoppervlak met de plantenmembraan aanzienlijk toeneemt. Hierdoor kan de plant eficiënter fosfaten en mineralen opnemen. Het zijn deze boomvormige structuren waar deze interactie haar naam dankt. De AM symbiose is een fundamenteel kenmerk van alle landplanten en slechts een kleine minderheid is niet in staat om deze symbiotische interactie aan te gaan.

Hoewel AM de meest universele symbiotische interactie is, zijn er tal van andere symbioses gekend. Agronomisch is de symbiotische stikstoffixatie veruit de belangrijkste. Een klein aantal ordes binnen de cladistische lijn van de Eurosids I is in staat om een interactie aan te gaan met bepaalde groepen van bodembacteriën, de rhizobia, met als resultaat een nieuw plantenorgaan, de nodule, waarin de gedifferentieerde bacteriën atmospherische stikstof fixeren en in de vorm van ammonium aan de plant geven. Deze symbiose is zo'n 65 miljoen jaar geleden ontstaan, enkele honderden miljoen jaar na het ontstaan van de AM associatie (Kistner and Parniske, 2002). Er wordt aangenomen dat een aantal hindernissen die genomen dienden te worden bij het binnendringen van de plant evolutief zijn opgelost door de recrutering van verschillende signaaltransductiepathways uit de AM symbiose (Kistner and Parniske, 2002). Verschillende plantenmutanten met vroege defecten in nodulatie zijn ook niet meer in staat om te associëren met AM fungi. Intussen zijn, afhankelijk van de soort, minstens 5 loci geïdentificeerd met defecten in beide symbioses, deze worden de 'common sym' genen genoemd (Kistner and Parniske, 2002). Het lijkt aannemelijk dat deze genen betrokken zijn in de intracellulaire accomodatie van de symbiotische partners, een proces dat voorlopig enkel is waargenomen bij deze symbioses (Parniske, 2000).

De invasie van bacteriën tijdens nodulatie wordt strikt gereguleerd door de plant zelf, hoewel de interactie wordt geïnitieerd door bacteriële lipochitooligosaccharides, de Nod factoren of NF. De standaard invasieweg die wordt gevolgd begint wanneer wortelhaarcellen in de zone naast het worteltopje deze NF waarnemen en beginnen te krullen. Deze krullende wortelharen zullen een bacteriële microkolonie insluiten. Vanuit deze microkolonie invaderen de bacteriën de wortelhaarcel, waarbij een buisvormige structuur, de infectiedraad (IT), de bacteriën zal begeleiden naar de diepere cellagen. In de diepere cortex zijn intussen een aantal cellen gededifferentieerd en hebben een nodule primordium gevormd. Dit uitgroeiende nodule

primordium zal worden geïnfecteerd door bacteriën wanneer de ITs deze cellen bereiken. De bacteriën differentiëren vervolgens tot nieuwgevormde organellen, de stikstoffixerende symbiosomen (voor een overzicht van nodule organogenese, zie Patriarca et al., 2004) (Hoofdstuk 1-2).

Niet alle planten worden geïnfecteerd volgens dit stramien en het vermoeden bestaat dat alternatieve invasiewegen zijn ontstaan omdat bepaalde plantensoorten zich moesten aanpassen aan omstandigheden waarin de wortelhaarinvasie onmogelijk is (Goormachtig et al., 2004). Een voorbeeld hiervan is de tropische legumineus *Sesbania rostrata*. Deze semi-aquatische plant is aangepast aan verhoogde ethyleen niveaus in de wortels, waar dit gasvormig plantenhormoon accummuleert tijdens overstromingen. Ethyleen kan wortelhaarkrulling blokkeren in planten zoals *Medicago truncatula* en er wordt aangenomen dat dit probleem overwonnen werd door het omzeilen van de wortelhaarinvasie in waterverzadigde omstandigheden. In *S. rostrata* wordt, onder waterverzadigde omstandigheden, de cortex direct gekoloniseerd via scheuren ter hoogte van uitgroeiende zij- of adventiefwortels (ook LRB nodulatie genoemd, naar lateral root base nodulation). Daar induceren de bacteriën een vorm van geprogrammeerde celdood, waardoor een infectiepocket (IP) ontstaat. Deze IP dient dan als uitgangspunt voor de inter- en later intracellulaire infectiedraden die naar het nodule primordium groeien. Voor dit proces is ethyleen een absolute vereiste, in tegenstelling tot infectie via wortelharen. *S. rostrata* heeft dus niet alleen de epidermale inhibitie van ethyleen omzeild maar ook de hoge ethyleenconcentraties aangewend om een alternatieve infectiestrategie te ontwikkelen (Hoodstuk 3).

Wanneer *S. rostrata* echter in goed geaereerde condities wordt gegroeid schakelt de plant opnieuw over naar de standaard wortelhaarinvasie (Hoofdstuk 4). Deze invasieweg is nagenoeg identiek aan deze beschreven in andere legumineuzen en wordt door ethyleen geïnhibeerd. Er kon voorts worden aangetoond dat de NF structuurvereisten strenger zijn voor wortelhaarinvasie dan voor LRB invasie. Dit strookt met de gangbare hypothese dat twee NF receptorcomplexen bestaan, een stringente ‘entry receptor’ en een minder stringente ‘signaling receptor’ (Ardourel et al., 1994). Het is waarschijnlijk dat de entry receptor een belangrijke rol speelt in de epidermis. De waarneming dat de stringente respons niet nodig is tijdens LRB nodulatie kan erop wijzen dat ethyleen een invloed uitoefent op deze stringente respons.

Deze waarnemingen aangaande de phenotypische plasticiteit tijdens de invasie van *S. rostrata* hebben tot een aantal belangrijke vragen en hypotheses geleid die in het tweede deel van dit werk werden aangekaart. De aanwezigheid van twee invasiewegen binnen dezelfde plant laat een

diepgaande vergelijking van beide toe, wat het voorkomen van species-afhankelijke variatie vermijdt. Voorts kan de rol van de vroege 'common sym' genen worden nagegaan in de corticale cellagen, hetgeen niet voor de hand liggend is in soorten waar alle corticale responsen reeds bij voorbaat worden geblokkeerd in mutanten voor deze sym genen door het epidermale fenotype.

Er werd een cDNA-AFLP transcriptoomanalyse uitgevoerd waarbij de LRB nodulatie met de wortelhaarinvasie werd vergeleken (Hoofdstuk 6). Hierbij werden meer dan 600 genen ontdekt die differentieel tot expressie kwamen in beide invasiewegen of specifiek in een van beide. Hierbij werd onder andere een belangrijke cluster geïdentificeerd met een aantal potentiële merkergenen voor infectiepocketvorming. Voorts werden ook een groot aantal genen gevonden die specifiek tot expressie kwamen tijdens de wortelhaarinvasie. Deze cluster bevat waarschijnlijk een groot aantal genen die betrokken zijn bij de epidermale responsen en hier bevinden zich dan ook waarschijnlijk doelwitgenen van het entry receptorcomplex. Daarnaast werden ook een groot aantal genen geïdentificeerd die gemeenschappelijk werden opgereguleerd tijdens beide nodulatieprocessen. Dit wijst op de hoge graad van gemeenschappelijkheid tijdens het vormen van de nodule zelf, want alhoewel de initiële invasiestrategiën sterk van elkaar verschillen, zijn de eindproducten uiteindelijk nagenoeg identiek. Deze dataset zal vrij toegankelijk zijn en is een rijke bron aan kandidaat genen voor verdere functionele analyse.

Een belangrijke vraag met betrekking tot de 'common sym' genen is of ze ook een rol spelen in andere celtypes. Dit is moeilijk uit te maken in modellegumineuzen zoals *M. truncatula* aangezien alle tot nu toe gekarakteriseerde NF receptoren en common sym genen een defect vertonen nog voor de bacteriën de wortelhaarcel kunnen binnendringen. Aangezien *S. rostrata* de epidermis onder bepaalde omstandigheden omzeilt, is deze analyse hier eenvoudiger. Hiervoor werd *SrSymRK* gekozen, een LRR type receptor-achtig kinase betrokken bij de allervroegste responsen op NF. Uitschakelen van *SrSymRK* met behulp van RNAi resulteerde in de vorming van nodules. Wanneer deze nodules microscopisch werden geanalyseerd was een normaal ontwikkelend centraal weefsel zichtbaar, de infectiedraden vertoonden echter zakvormige uitstulpingen en er werden geen bacteriën aangetroffen in de cellen van het centraal noduleweefsel. In dezelfde periode werd ook een niet-symbiotisch fenotype van mutanten in *M. truncatula* waargenomen, hierbij werd een verhoogde gevoeligheid van de wortelharen voor mechanische stimuli vastgesteld (Esseling et al., 2004). De cytoplasmatische stromingen die tijdelijk stoppen na aanraken konden niet opnieuw worden opgewekt in de mutant, hetgeen er op wijst dat SymRK betrokken zou kunnen zijn in de recrutering

van vesikels naar de plaats van NF geinduceerde tip groei. Samen met de gebrekkige IT groei en de defecten in symbiosoom formatie wijst dit op een mogelijk defect tijdens de gerichte excretie die verantwoordelijk wordt geacht voor de aanvoer van materiaal nodig voor de correcte groei van infectiedraden en symbiosomen. Hoe SymRK dit proces precies medieert is nog onbekend maar identificatie van doeleiwitten zal zeker bijdragen tot ons begrip van dit proces.

Een centraal signaaltransductie element in de 'common sym' pathway is Ca^{2+}-spiking. Enkele minuten na herkenning van compatibele bacteriën zijn in en rond de wortelhaarkern ritmische oscillaties in calcium concentraties zichtbaar. Deze oscillaties zijn NF structuurspecifiek en worden geïnhibeerd door ethyleen (Oldroyd et al., 2001; Oldroyd and Downie, 2006). Naar analogie met dierlijke systemen wordt verwacht dat de eigenschappen van deze Ca^{2+}-spiking belangrijke informatie overbrengen die vertaald zal worden in veranderde genexpressie. Ca^{2+}-spiking wordt als een centrale zuil van de NF signaaltransductie in wortelharen beschouwd, maar aangezien Ca^{2+}-spiking door ethyleen kan geïnhibeerd worden rees de vraag naar de relevantie van Ca^{2+}-spiking tijdens LRB nodulatie. Rond laterale wortelbasissen van hydropoon gegroeide *S. rostrata* bevinden zich kleine primordiale axillaire wortelharen die, hoewel ze niet geïnfecteerd worden door bacteriën, wel uitgroeien en deformeren na herkenning van NF (Mergaert et al., 1993). Nader onderzoek wees uit dat deze wortelharen inderdaad Ca^{2+}-spiking initiëren. De frequentie van deze Ca^{2+}-spiking was echter opmerkelijk veel hoger dan in andere legumineuzen en ze werd niet geïnhibeerd door ethyleen (Hoofdstuk 8). Toevoegen van ethyleen inhibitoren en jasmonaat had wel een sterke invloed op de frequentie. Ook bleek de farmacologische manipulatie van de Ca^{2+}-spiking frequentie met deze producten te leiden tot het herstellen van de wortelhaarinvasie in hydropone cultuur. Dit wijst op het belang van Ca^{2+}-spiking frequentie voor intracellulaire invasie. Deze observatie heeft verstrekkende gevolgen en wijst voor het eerst onomstotelijk op een link tussen beide fenomenen. De zoektocht naar het moleculair mechanisme dat Ca^{2+}-spiking frequentie reguleert en de manier waarop Ca^{2+}-spiking frequentie de 'entry pathway' beïnvloedt zal van groot belang zijn om dit proces beter te begrijpen.

Stroomopwaarts van de common sym genen bevindt zich een pathway die niet gemeenschappelijk is met AM symbiose en van belang is bij de perceptie van NF. Een aantal genen betrokken in dit deel van de pathway zijn de NF receptoren zelf, waarvan recent een aantal kandidaten werden geïdentificeerd. Deze genen coderen voor LysM domein bevattende receptor-achtige kinases, waarvan tot nog toe 2 klasses werden geïdentificeerd. In de eerder vernoemde cDNA-AFLP analyse kwam een transcript naar voor dat een lage homologie vertoonde met

LjNFR5, een recent gekloneerde kandidaat NF receptor. Nader onderzoek wees uit dat het inderdaad om een LysM-RLK ging, maar dat deze niet tot een van de voornoemde klasses van NF receptoren behoorde. Phylogenetische analyse wees uit dat dit gen, *SrLysM,* inderdaad tot een derde subfamilie van LysM-RLKs behoorde. Deze subfamilie omvat enkele genen in *M. truncatula* en bovendien werden twee nauwe verwanten teruggevonden in *Arabidopsis thaliana*. RNAi van zowel *SrLysM* als diens ortholoog in *M. truncatula MtLysM*, wees op een nieuw symbiotisch fenotype waarbij de meristematische activiteit van het nodulemeristeem vroegtijdig stopt, wat leidt tot een fixerende nodule met slechts een klein aantal fixerende cellen. Geen gebreken werden waargenomen in IT vorming en groei of in differentiatie van de cellen van het centrale weefsel. Momenteel wordt onderzocht of deze eiwitten inderdaad bona fide NF receptoren zijn door heterologe expressie van *SrLysM* in *M. truncatula* wortels, hierbij zal gekeken worden naar mogelijke responsen op *A. caulinodans* NF, hetgeen enkel kan wijzen op perceptie door *SrLysM.*

Samenvattend kan worden gesteld dat de unieke karakteristieken van *S. rostrata* nodulatie het mogelijk hebben gemaakt om onderzoek naar symbiotische stikstoffixatie vanuit een nieuw perspectief te benaderen. Vergelijking van beide invasiewegen heeft geleid tot de identificatie van interessante genclusters voor zowel LRB nodulatie en wortelhaarinvasie en toekomstige functionele analyse zal hier zonder twijfel uit kunnen putten. Voorts konden ook late stappen van de symbiose op een elegante manier benaderd worden. De onafhankelijkheid van epidermale responsen tijdens LRB nodulatie laat toe om genen met een duale functie in vroege en late stappen te analyseren zonder omslachtige omwegen zoals induceerbare constructen. Een verdere verfijning van het LRB nodulatie model, waarbij de rol van ethyleen in de fenotypische adaptatie aan watertolerante nodulatie werd ontdekt en de identificatie van de betrokkenheid van Ca^{2+}-spiking frequentie heeft niet alleen geleid naar nieuwe inzichten in de nodulatie van *S. rostrata* maar van nodulatie in legumineuzen in het algemeen. *S. rostrata* heeft de capaciteit om ook de toekomst een rol te spelen als alternatieve modelplant voor de studie van bacteriële invasie van rhizobia.

References

Aharon, G.S., Gelli, A., Snedden, W.A., and Blumwald, E. (1998). Activation of a plant plasma membrane Ca2+ channel by TGalpha1, a heterotrimeric G protein alpha-subunit homologue. FEBS Lett **424,** 17-21.

Alazard, D., and Duhoux, E. (1990). Development of Stem Nodules in a Tropical Forage Legume, Aeschynomene-Afraspera. Journal of Experimental Botany **41,** 1199-1206.

Altschul, S.F., Madden, T.L., Schaffer, A.A., Zhang, J., Zhang, Z., Miller, W., and Lipman, D.J. (1997). Gapped BLAST and PSI-BLAST: a new generation of protein database search programs. Nucleic Acids Res **25,** 3389-3402.

Amon, P., Haas, E., and Sumper, M. (1998). The sex-inducing pheromone and wounding trigger the same set of genes in the multicellular green alga Volvox. Plant Cell **10,** 781-789.

Amor, B.B., Shaw, S.L., Oldroyd, G.E., Maillet, F., Penmetsa, R.V., Cook, D., Long, S.R., Denarie, J., and Gough, C. (2003). The NFP locus of Medicago truncatula controls an early step of Nod factor signal transduction upstream of a rapid calcium flux and root hair deformation. Plant J **34,** 495-506.

Ané, J.M., Kiss, G.B., Riely, B.K., Penmetsa, R.V., Oldroyd, G.E., Ayax, C., Levy, J., Debelle, F., Baek, J.M., Kalo, P., Rosenberg, C., Roe, B.A., Long, S.R., Denarie, J., and Cook, D.R. (2004). Medicago truncatula DMI1 required for bacterial and fungal symbioses in legumes. Science **303,** 1364-1367.

Ardourel, M., Demont, N., Debelle, F., Maillet, F., de Billy, F., Prome, J.C., Denarie, J., and Truchet, G. (1994). Rhizobium meliloti lipooligosaccharide nodulation factors: different structural requirements for bacterial entry into target root hair cells and induction of plant symbiotic developmental responses. Plant Cell **6,** 1357-1374.

Asamizu, E., Nakamura, Y., Sato, S., and Tabata, S. (2005). Comparison of the transcript profiles from the root and the nodulating root of the model legume Lotus japonicus by serial analysis of gene expression. Mol Plant Microbe Interact **18,** 487-498.

Assmann, S.M. (2002). Heterotrimeric and unconventional GTP binding proteins in plant cell signaling. Plant Cell **14 Suppl,** S355-373.

Bachem, C.W., van der Hoeven, R.S., de Bruijn, S.M., Vreugdenhil, D., Zabeau, M., and Visser, R.G. (1996). Visualization of differential gene expression using a novel method of RNA fingerprinting based on AFLP: analysis of gene expression during potato tuber development. Plant J **9,** 745-753.

Baier, R., Schiene, K., Kohring, B., Flaschel, E., and Niehaus, K. (1999). Alfalfa and tobacco cells react differently to chitin oligosaccharides and sinorhizobium meliloti nodulation factors. Planta **210,** 157-164.

Bateman, A., and Bycroft, M. (2000). The structure of a LysM domain from E-coli membrane-bound lytic murein transglycosylase D (MltD). Journal of Molecular Biology **299,** 1113-1119.

Beers, E.P., Woffenden, B.J., and Zhao, C. (2000). Plant proteolytic enzymes: possible roles during programmed cell death. Plant Mol Biol **44,** 399-415.

Bersoult, A., Camut, S., Perhald, A., Kereszt, A., Kiss, G.B., and Cullimore, J.V. (2005). Expression of the Medicago truncatula DMI2 gene suggests roles of the symbiotic nodulation receptor kinase in nodules and during early nodule development. Mol Plant Microbe Interact **18,** 869-876.

Bethke, P.C., and Jones, R.L. (2001). Cell death of barley aleurone protoplasts is mediated by reactive oxygen species. Plant J **25,** 19-29.

Boisson-Dernier, A., Chabaud, M., Garcia, F., Becard, G., Rosenberg, C., and Barker, D.G. (2001). Agrobacterium rhizogenes-transformed roots of Medicago truncatula for the study of nitrogen-fixing and endomycorrhizal symbiotic associations. Molecular Plant-Microbe Interactions **14,** 695-700.

Bono, J.J., Riond, J., Nicolaou, K.C., Bockovich, N.J., Estevez, V.A., Cullimore, J.V., and Ranjeva, R. (1995). Characterization of a binding site for chemically synthesized lipooligosaccharidic NodRm factors in particulate fractions prepared from roots. Plant J **7,** 253-260.

Boogerd, F.C., and vanRossum, D. (1997). Nodulation of groundnut by Bradyrhizobium: a simple infection process by crack entry. Fems Microbiology Reviews **21,** 5-27.

Borisov, A.Y., Madsen, L.H., Tsyganov, V.E., Umehara, Y., Voroshilova, V.A., Batagov, A.O., Sandal, N., Mortensen, A., Schauser, L., Ellis, N., Tikhonovich, I.A., and Stougaard, J. (2003). The Sym35 gene required for root nodule development in pea is an ortholog of Nin from Lotus japonicus. Plant Physiol **131,** 1009-1017.

Brewin, N.J. (1991). Development of the legume root nodule. Annu Rev Cell Biol **7,** 191-226.

Brewin, N.J. (2004). Plant Cell Wall Remodelling in the Rhizobium-Legume Symbiosis. Crit. Rev. Plant Sci. **23,** 293-316.

Breyne, P., Dreesen, R., Cannoot, B., Rombaut, D., Vandepoele, K., Rombauts, S., Vanderhaeghen, R., Inze, D., and Zabeau, M. (2003). Quantitative cDNA-AFLP analysis for genome-wide expression studies. Mol Genet Genomics **269,** 173-179.

Capoen, W., Goormachtig, S., De Rycke, R., Schroeyers, K., and Holsters, M. (2005). SrSymRK, a plant receptor essential for symbiosome formation. Proc Natl Acad Sci U S A **102,** 10369-10374.

Cardenas, L., Vidali, L., Domnguez, J., Prez, H., Snchez, F., Hepler, P.K., and Quinto, C. (1998). Rearrangement of actin microfilaments in plant root hairs responding to rhizobium etli nodulation signals. Plant Physiol **116,** 871-877.

Catalano, C.M., Lane, W.S., and Sherrier, D.J. (2004). Biochemical characterization of symbiosome membrane proteins from Medicago truncatula root nodules. Electrophoresis **25,** 519-531.

Catoira, R., Timmers, A.C., Maillet, F., Galera, C., Penmetsa, R.V., Cook, D., Denarie, J., and Gough, C. (2001). The HCL gene of Medicago truncatula controls Rhizobium-induced root hair curling. Development **128,** 1507-1518.

Catoira, R., Galera, C., de Billy, F., Penmetsa, R.V., Journet, E.P., Maillet, F., Rosenberg, C., Cook, D., Gough, C., and Denarie, J. (2000). Four genes of Medicago truncatula controlling components of a nod factor transduction pathway. Plant Cell **12,** 1647-1666.

Chandler, M.R., Date, R.A., and Roughley, R.J. (1982). Infection and Root-Nodule Development in Stylosanthes Species by Rhizobium. Journal of Experimental Botany **33,** 47-57.

Charron, D., Pingret, J.L., Chabaud, M., Journet, E.P., and Barker, D.G. (2004). Pharmacological evidence that multiple phospholipid signaling pathways link Rhizobium nodulation factor perception in Medicago truncatula root hairs to intracellular responses, including Ca2+ spiking and specific ENOD gene expression. Plant Physiol **136,** 3582-3593.

Colebatch, G., Desbrosses, G., Ott, T., Krusell, L., Montanari, O., Kloska, S., Kopka, J., and Udvardi, M.K. (2004). Global changes in transcription orchestrate metabolic differentiation during symbiotic nitrogen fixation in Lotus japonicus. Plant J **39,** 487-512.

Complainville, A., Brocard, L., Roberts, I., Dax, E., Sever, N., Sauer, N., Kondorosi, A., Wolf, S., Oparka, K., and Crespi, M. (2003). Nodule initiation involves the creation of a new symplasmic field in specific root cells of medicago species. Plant Cell **15,** 2778-2791.

Corich, V., Goormachtig, S., Lievens, S., Van Montagu, M., and Holsters, M. (1998). Patterns of ENOD40 gene expression in stem-borne nodules of Sesbania rostrata. Plant Mol Biol **37,** 67-76.

Cullimore, J., and Denarie, J. (2003). Plant sciences. How legumes select their sweet talking symbionts. Science **302,** 575-578.

Cullimore, J.V., Ranjeva, R., and Bono, J.J. (2001). Perception of lipo-chitooligosaccharidic Nod factors in legumes. Trends Plant Sci **6,** 24-30.

D'Haeze, W., and Holsters, M. (2002). Nod factor structures, responses, and perception during initiation of nodule development. Glycobiology **12,** 79R-105R.

D'Haeze, W., Gao, M., and Holsters, M. (2004). A gfp reporter plasmid to visualize Azorhizobium caulinodans during nodulation of Sesbania rostrata. Plasmid **51,** 185-191.

D'Haeze, W., Mergaert, P., Prome, J.C., and Holsters, M. (2000). Nod factor requirements for efficient stem and root nodulation of the tropical legume Sesbania rostrata. J Biol Chem **275,** 15676-15684.

D'Haeze, W., Gao, M.S., De Rycke, R., Van Montagu, M., Engler, G., and Holsters, M. (1998). Roles for azorhizobial nod factors and surface polysaccharides in intercellular invasion and nodule penetration, respectively. Mol Plant Microbe Interact **11,** 999-1008.

D'Haeze, W., De Rycke, R., Mathis, R., Goormachtig, S., Pagnotta, S., Verplancke, C., Capoen, W., and Holsters, M. (2003). Reactive oxygen species and ethylene play a positive role in lateral root base nodulation of a semiaquatic legume. Proc Natl Acad Sci U S A **100,** 11789-11794.

Dazzo, F.B., Truchet, G.L., Hollingsworth, R.I., Hrabak, E.M., Pankratz, H.S., Philip-Hollingsworth, S., Salzwedel, J.L., Chapman, K., Appenzeller, L., Squartini, A., and et al. (1991). Rhizobium lipopolysaccharide modulates infection thread development in white clover root hairs. J Bacteriol **173,** 5371-5384.

de Faria, S.M., Hay, G.T., and SPRENT, J.I. (1988). Entry of rhizobia into roots of *Mimosa scabrella* Bentham occurs between epidermal cells. J. Gen. Microbiol. **134,** 2291-2296.

De Jong, A.J., Heidstra, R., Spaink, H.P., Hartog, M.V., Meijer, E.A., Hendriks, T., Schiavo, F.L., Terzi, M., Bisseling, T., Van Kammen, A., and De Vries, S.C. (1993). Rhizobium Lipooligosaccharides Rescue a Carrot Somatic Embryo Mutant. Plant Cell **5,** 615-620.

De Koninck, P., and Schulman, H. (1998). Sensitivity of CaM Kinase II to the frequency of Ca2+ oscillations. Science **279,** 227-230.

Demchenko, K., Winzer, T., Stougaard, J., Parniske, M., and Pawlowski, K. (2004). Distinct roles of Lotus japonicus SYMRK and SYM15 in root colonization and arbuscule formation. New Phytologist **163,** 381-392.

den Hartog, M., Musgrave, A., and Munnik, T. (2001). Nod factor-induced phosphatidic acid and diacylglycerol pyrophosphate formation: a role for phospholipase C and D in root hair deformation. Plant J **25,** 55-65.

den Hartog, M., Verhoef, N., and Munnik, T. (2003). Nod factor and elicitors activate different phospholipid signaling pathways in suspension-cultured alfalfa cells. Plant Physiol **132,** 311-317.

Den Herder, G., Schroeyers, K., Holsters, M., and Goormachtig, S. (2006). Signaling and Gene Expression for Water-Tolerant Legume Nodulation. Critical Reviews in Plant Sciences **Submitted**.

Diaz, C.L., Logman, T., Stam, H.C., and Kijne, J.W. (1995). Sugar-Binding Activity of Pea Lectin Expressed in White Clover Hairy Roots. Plant Physiol **109,** 1167-1177.

Dolmetsch, R.E., Lewis, R.S., Goodnow, C.C., and Healy, J.I. (1997). Differential activation of transcription factors induced by Ca2+ response amplitude and duration. Nature **386,** 855-858.

Doyle, J.J. (1998). Phylogenetic perspectives on nodulation: evolving views of plants and symbiotic bacteria. Trends Plant Sci **3,** 473-478.

Doyle, J.J., and Luckow, M.A. (2003). The rest of the iceberg. Legume diversity and evolution in a phylogenetic context. Plant Physiol **131,** 900-910.

Drinkwater, L.E., Wagoner, P., and Sarrantionio, M. (1998). Legume-based cropping systems have reduced carbon and nitrogen losses. Nature **396,** 262-265.

Duhoux, E. (1984). The Ontogenesis of Stem Nodules in Sesbania-Rostrata (Legume). Canadian Journal of Botany-Revue Canadienne De Botanique **62,** 982-994.

Dyachok, J.V., Wiweger, M., Kenne, L., and von Arnold, S. (2002). Endogenous Nod-factor-like signal molecules promote early somatic embryo development in Norway spruce. Plant Physiol **128,** 523-533.

Ehrhardt, D.W., Atkinson, E.M., and Long, S.R. (1992). Depolarization of alfalfa root hair membrane potential by Rhizobium meliloti Nod factors. Science **256,** 998-1000.

Ehrhardt, D.W., Wais, R., and Long, S.R. (1996). Calcium spiking in plant root hairs responding to Rhizobium nodulation signals. Cell **85,** 673-681.

El Yahyaoui, F., Kuster, H., Ben Amor, B., Hohnjec, N., Puhler, A., Becker, A., Gouzy, J., Vernie, T., Gough, C., Niebel, A., Godiard, L., and Gamas, P. (2004). Expression profiling in Medicago truncatula identifies more than 750 genes differentially expressed during nodula-

tion, including many potential regulators of the symbiotic program. Plant Physiol **136,** 3159-3176.

Endre, G., Kereszt, A., Kevei, Z., Mihacea, S., Kalo, P., and Kiss, G.B. (2002). A receptor kinase gene regulating symbiotic nodule development. Nature **417,** 962-966.

Engstrom, E.M., Ehrhardt, D.W., Mitra, R.M., and Long, S.R. (2002). Pharmacological analysis of nod factor-induced calcium spiking in Medicago truncatula. Evidence for the requirement of type IIA calcium pumps and phosphoinositide signaling. Plant Physiol **128,** 1390-1401.

Erhardt, D.W., Atkinson, E.M., and Long, S.R. (1992). Depolarization of alfalfa root hair membrane potential by *Rhizobium meliloti* Nod factors. Science **256,** 998-1000.

Eshete, F., and Fields, R.D. (2001). Spike frequency decoding and autonomous activation of Ca2+-calmodulin-dependent protein kinase II in dorsal root ganglion neurons. J Neurosci **21,** 6694-6705.

Esseling, J.J., and Emons, A.M. (2004). Dissection of Nod factor signalling in legumes: cell biology, mutants and pharmacological approaches. J Microsc **214,** 104-113.

Esseling, J.J., Lhuissier, F.G., and Emons, A.M. (2003). Nod factor-induced root hair curling: continuous polar growth towards the point of nod factor application. Plant Physiol **132,** 1982-1988.

Esseling, J.J., Lhuissier, F.G., and Emons, A.M. (2004). A nonsymbiotic root hair tip growth phenotype in NORK-mutated legumes: implications for nodulation factor-induced signaling and formation of a multifaceted root hair pocket for bacteria. Plant Cell **16,** 933-944.

Etzler, M.E., Kalsi, G., Ewing, N.N., Roberts, N.J., Day, R.B., and Murphy, J.B. (1999). A nod factor binding lectin with apyrase activity from legume roots. Proc Natl Acad Sci U S A **96,** 5856-5861.

Fedorova, M., van de Mortel, J., Matsumoto, P.A., Cho, J., Town, C.D., VandenBosch, K.A., Gantt, J.S., and Vance, C.P. (2002). Genome-wide identification of nodule-specific transcripts in the model legume Medicago truncatula. Plant Physiol **130,** 519-537.

Felle, H., Kondorosi, E., Kondorosi, A., and Schultze, M. (1995). Nod signal-induced plasma membrane potential changes in alfalfa root hairs are differentially sensitive to structural modifications of the lipochitooligosaccaride. Plant J. **7,** 939-947.

Felle, H., Kondorosi, E., Kondorosi, A., and Schultze, M. (1996). Rapid alkalinization in alfalfa root hairs in response to rhizobial lipochitooligosaccharide signals. Plant J. **10,** 295-301.

Felle, H.H., Kondorosi, E., Kondorosi, A., and Schultze, M. (1998). The role of ion fluxes in Nod factor signalling in *Medicago sativa*. Plant J **13,** 455-463.

Felle, H.H., Kondorosi, E., Kondorosi, A., and Schultze, M. (2000). How alfalfa root hairs discriminate between Nod factors and oligochitin elicitors. Plant Physiol **124,** 1373-1380.

Ferguson, B., and Mathesius, U. (2003). Signaling interactions during nodule development. JOURNAL OF PLANT GROWTH REGULATION **22,** 47-72.

Fernandez-Lopez, M., Goormachtig, S., Gao, M., D'Haeze, W., Van Montagu, M., and Holsters, M. (1998). Ethylene-mediated phenotypic plasticity in root nodule development on sesbania rostrata. Proc Natl Acad Sci U S A **95,** 12724-12728.

Ferrandiz, C., Gu, Q., Martienssen, R., and Yanofsky, M.F. (2000). Redundant regulation of meristem identity and plant architecture by FRUITFULL, APETALA1 and CAULIFLOWER. Development **127,** 725-734.

Fields, R.D., Lee, P.R., and Cohen, J.E. (2005). Temporal integration of intracellular Ca2+ signaling networks in regulating gene expression by action potentials. Cell Calcium **37,** 433-442.

Gage, D.J. (2004). Infection and invasion of roots by symbiotic, nitrogen-fixing rhizobia during nodulation of temperate legumes. Microbiology and Molecular Biology Reviews **68,** 280-+.

Gage, D.J., and Margolin, W. (2000). Hanging by a thread: invasion of legume plants by rhizobia. Curr Opin Microbiol **3,** 613-617.

Geurts, R., and Bisseling, T. (2002). Rhizobium nod factor perception and signalling. Plant Cell **14,** S239-249.

Geurts, R., Fedorova, E., and Bisseling, T. (2005). Nod factor signaling genes and their function in the early stages of Rhizobium infection. Curr Opin Plant Biol **8,** 346-352.

Geurts, R., Heidstra, R., Hadri, A.E., Downie, J.A., Franssen, H., vanKammen, A., and Bisseling, T. (1997). Sym2 of pea is involved in a nodulation factor-perception mechanism that controls the infection process in the epidermis. Plant Physiol **115,** 351-359.

Gleason, C., Chaudhuri, S., Yang, T., Munoz, A., Poovaiah, B.W., and Oldroyd, G.E. (2006). Nodulation independent of rhizobia induced by a calcium-activated kinase lacking autoinhibition. Nature **441,** 1149-1152.

Godfroy, O., Debelle, F., Timmers, T., and Rosenberg, C. (2006). A Rice Calcium- and Calmodulin-Dependent Protein Kinase Restores Nodulation to a Legume Mutant. Mol Plant Microbe Interact **19,** 495-501.

Goedhart, J., Hink, M.A., Visser, A.J., Bisseling, T., and Gadella, T.W., Jr. (2000). In vivo fluorescence correlation microscopy (FCM) reveals accumulation and immobilization of Nod factors in root hair cell walls. Plant J **21,** 109-119.

Goethals, K., Gao, M., Tomekpe, K., Vanmontagu, M., and Holsters, M. (1989). Common Nodabc Genes in Nod Locus-1 of Azorhizobium-Caulinodans - Nucleotide-Sequence and Plant-Inducible Expression. Molecular & General Genetics **219,** 289-298.

Goormachtig, S., Van Montagu, M., and Holsters, M. (1998a). The early nodulin gene ENOD2 shows different expression patterns during Sesbania rostrata stem nodule development. Mol Plant Microbe Interact **11,** 237-241.

Goormachtig, S., Capoen, W., and Holsters, M. (2004a). Rhizobium infection: lessons from the versatile nodulation behaviour of water-tolerant legumes. Trends Plant Sci **9,** 518-522.

Goormachtig, S., Mergaert, P., Van Montagu, M., and Holsters, M. (1998b). The symbiotic interaction between Azorhizobium caulinodans and Sesbania rostrata molecular cross-talk in a beneficial plant-bacterium interaction. Subcell Biochem **29,** 117-164.

Goormachtig, S., Capoen, W., James, E.K., and Holsters, M. (2004b). Switch from intracellular to intercellular invasion during water stress-tolerant legume nodulation. Proc Natl Acad Sci U S A **101,** 6303-6308.

Goormachtig, S., Alves-Ferreira, M., Van Montagu, M., Engler, G., and Holsters, M. (1997). Expression of cell cycle genes during Sesbania rostrata stem nodule development. Mol Plant Microbe Interact **10,** 316-325.

Goormachtig, S., Lievens, S., Herman, S., Van Montagu, M., and Holsters, M. (1999). Chalcone reductase-homologous transcripts accumulate during development of stem-borne nodules on the tropical legume Sesbania rostrata. Planta **209,** 45-52.

Goormachtig, S., Valerio-Lepiniec, M., Szczyglowski, K., Van Montagu, M., Holsters, M., and de Bruijn, F.J. (1995). Use of differential display to identify novel Sesbania rostrata genes enhanced by Azorhizobium caulinodans infection. Mol Plant Microbe Interact **8,** 816-824.

Graham, P.H., and Vance, C.P. (2003). Legumes: importance and constraints to greater use. Plant Physiol **131,** 872-877.

Gressent, F., Drouillard, S., Mantegazza, N., Samain, E., Geremia, R.A., Canut, H., Niebel, A., Driguez, H., Ranjeva, R., Cullimore, J., and Bono, J.J. (1999). Ligand specificity of a high-affinity binding site for lipo-chitooligosaccharidic nod factors in medicago cell suspension cultures. Proc Natl Acad Sci U S A **96,** 4704-4709.

Gualtieri, G., and Bisseling, T. (2000). The evolution of nodulation. Plant Molecular Biology **42,** 181-194.

Guinel, F.C., and Geil, R.D. (2002). A model for the development of the rhizobial and arbuscular mycorrhizal symbioses in legumes and its use to understand the roles of ethylene in the establishment of these two symbioses. Can. J. Bot. **80,** 695-720.

Gyorgyey, J., Vaubert, D., Jimenez-Zurdo, J.I., Charon, C., Troussard, L., Kondorosi, A., and Kondorosi, E. (2000). Analysis of Medicago truncatula nodule expressed sequence tags. Mol Plant Microbe Interact **13,** 62-71.

Hall, T. (1999). BioEdit program. In Nucleic Acids Symposium Series

Harris, J.M., Wais, R., and Long, S.R. (2003). Rhizobium-Induced calcium spiking in Lotus japonicus. Mol Plant Microbe Interact **16,** 335-341.

Harrison, M.J. (1999). Molecular and cellular aspects of the arbuscular mycorrhizal symbiosis. Annu. Rev. Plant Physiol. Plant MOl. Biol. **50,** 361-389.

Hattan, J., Kanamoto, H., Takemura, M., Yokota, A., and Kohchi, T. (2004). Molecular characterization of the cytoplasmic interacting protein of the receptor kinase IRK expressed in the inflorescence and root apices of Arabidopsis. Biosci Biotechnol Biochem **68,** 2598-2606.

Heidstra, R., Yang, W.C., Yalcin, Y., Peck, S., Emons, A.M., van Kammen, A., and Bisseling, T. (1997). Ethylene provides positional information on cortical cell division but is not involved in Nod factor-induced root hair tip growth in Rhizobium- legume interaction. Development **124,** 1781-1787.

Hepp, R., Puri, N., Hohenstein, A.C., Crawford, G.L., Whiteheart, S.W., and Roche, P.A. (2005). Phosphorylation of SNAP-23 regulates exocytosis from mast cells. J Biol Chem **280,** 6610-6620.

Hogg, B.V., Cullimore, J.V., Ranjeva, R., and Bono, J.J. (2006). The DMI1 and DMI2 early symbiotic genes of medicago truncatula are required for a high-affinity nodulation factor-binding site associated to a particulate fraction of roots. Plant Physiol **140,** 365-373.

Hohnjec, N., Kuster, H., Albus, U., Frosch, S.C., Becker, J.D., Puhler, A., Perlick, A.M., and Fruhling, M. (2000). The broad bean nodulin VfENOD18 is a member of a novel family of plant proteins with homologies to the bacterial MJ0577 superfamily. Mol Gen Genet **264,** 241-250.

Imaizumi-Anraku, H., Takeda, N., Charpentier, M., Perry, J., Miwa, H., Umehara, Y., Kouchi, H., Murakami, Y., Mulder, L., Vickers, K., Pike, J., Downie, J.A., Wang, T., Sato, S., Asamizu, E., Tabata, S., Yoshikawa, M., Murooka, Y., Wu, G.J., Kawaguchi, M., Kawasaki, S., Parniske, M., and Hayashi, M. (2005). Plastid proteins crucial for symbiotic fungal and bacterial entry into plant roots. Nature **433,** 527-531.

Irish, V.F. (1999). Patterning the flower. Dev Biol **209,** 211-220.

Jackson, M.B. (1985). Ethylene and Responses of Plants to Soil Waterlogging and Submergence. Annual Review of Plant Physiology **36**.

James, E.K., and Sprent, J.I. (1999). Development of N-2-fixing nodules on the wetland legume Lotus uliginosus exposed to conditions of flooding. New Phytologist **142,** 219-231.

James, E.K., Minchin, F.R., and Sprent, J.I. (1992). The physiology and nitrogen-fixing capability of aquatically and terrestrially grown *Neptunia plena* - the importance of nodule oxygen-supply. ANN BOT-LONDON **69,** 181-187.

James, E.K., Gyaneshwar, P., Mathan, N., Barraquio, Q.L., Reddy, P.M., Iannetta, P.P.M., Olivares, F.L., and Ladha, J.K. (2002). Infection and colonization of rice seedlings by the plant growth-promoting bacterium Herbaspirillum seropedicae Z67. Molecular Plant-Microbe Interactions **15,** 894-906.

Journet, E.P., El-Gachtouli, N., Vernoud, V., de Billy, F., Pichon, M., Dedieu, A., Arnould, C., Morandi, D., Barker, D.G., and Gianinazzi-Pearson, V. (2001). Medicago truncatula ENOD11: a novel RPRP-encoding early nodulin gene expressed during mycorrhization in arbuscule-containing cells. Mol Plant Microbe Interact **14,** 737-748.

Kalo, P., Gleason, C., Edwards, A., Marsh, J., Mitra, R.M., Hirsch, S., Jakab, J., Sims, S., Long, S.R., Rogers, J., Kiss, G.B., Downie, J.A., and Oldroyd, G.E. (2005). Nodulation signaling in legumes requires NSP2, a member of the GRAS family of transcriptional regulators. Science **308,** 1786-1789.

Kanamori, N., Madsen, L.H., Radutoiu, S., Frantescu, M., Quistgaard, E.M., Miwa, H., Downie, J.A., James, E.K., Felle, H.H., Haaning, L.L., Jensen, T.H., Sato, S., Nakamura, Y., Tabata, S., Sandal, N., and Stougaard, J. (2006). A nucleoporin is required for induction of Ca2+ spiking in legume nodule development and essential for rhizobial and fungal symbiosis. Proc Natl Acad Sci U S A **103,** 359-364.

Karas, B., Murray, J., Gorzelak, M., Smith, A., Sato, S., Tabata, S., and Szczyglowski, K. (2005). Invasion of Lotus japonicus root hairless 1 by Mesorhizobium loti involves the nodulation factor-dependent induction of root hairs. Plant Physiol **137,** 1331-1344.

Karimi, M., Inze, D., and Depicker, A. (2002). GATEWAY vectors for Agrobacterium-mediated plant transformation. Trends Plant Sci **7,** 193-195.

Kelly, M.N., and Irving, H.R. (2003). Nod factors activate both heterotrimeric and monomeric G-proteins in Vigna unguiculata (L.) Walp. Planta **216,** 674-685.

Kiefer, E., Heller, W., and Ernst, D. (2000). A simple and efficient protocol for isolation of functional RNA from plant tissues rich in secondary metabolites. Plant Molecular Biology Reporter **18,** 33-39.

Kieffer, M., and Davies, B. (2001). Developmental programmes in floral organ formation. Semin Cell Dev Biol **12,** 373-380.

Kistner, C., and Parniske, M. (2002). Evolution of signal transduction in intracellular symbiosis. Trends Plant Sci **7,** 511-518.

Koltai, H., Dhandaydham, M., Opperman, C., Thomas, J., and Bird, D. (2001). Overlapping plant signal transduction pathways induced by a parasitic nematode and a rhizobial endosymbiont. Mol Plant Microbe Interact **14,** 1168-1177.

Komeda, Y. (2004). Genetic regulation of time to flower in Arabidopsis thaliana. Annu Rev Plant Biol **55,** 521-535.

Krusell, L., Madsen, L.H., Sato, S., Aubert, G., Genua, A., Szczyglowski, K., Duc, G., Kaneko, T., Tabata, S., de Bruijn, F., Pajuelo, E., Sandal, N., and Stougaard, J. (2002). Shoot control of root development and nodulation is mediated by a receptor-like kinase. Nature **420,** 422-426.

Kuster, H., Hohnjec, N., Krajinski, F., El Yahyaoui, F., Manthey, K., Gouzy, J., Dondrup, M., Meyer, F., Kalinowski, J., Brechenmacher, L., van Tuinen, D., Gianinazzi-Pearson, V., Puhler, A., Gamas, P., and Becker, A. (2004). Construction and validation of cDNA-based Mt6k-RIT macro- and microarrays to explore root endosymbioses in the model legume Medicago truncatula. Journal of Biotechnology **108,** 95-113.

Lévy, J., Bres, C., Geurts, R., Chalhoub, B., Kulikova, O., Duc, G., Journet, E.P., Ane, J.M., Lauber, E., Bisseling, T., Denarie, J., Rosenberg, C., and Debelle, F. (2004). A putative Ca2+ and calmodulin-dependent protein kinase required for bacterial and fungal symbioses. Science **303,** 1361-1364.

Lhuissier, F.G.P., De Ruijter, N.C.A., Sieberer, B.J., Esseling, J.J., and Emons, A.M.C. (2001). Time course of cell biological events evoked in legume root hairs by Rhizobium Nod factors: State of the art. Annals of Botany **87,** 289-302.

Lievens, S. (2002). early gene expression during *Sesbania rostrata* nodule development (Universiteit Gent, België).

Lievens, S., Goormachtig, S., and Holsters, M. (2001). A critical evaluation of differential display as a tool to identify genes involved in legume nodulation: looking back and looking forward. Nucleic Acids Res **29,** 3459-3468.

Lievens, S., Goormachtig, S., Den Herder, J., Capoen, W., Mathis, R., Hedden, P., and Holsters, M. (2005). Gibberellins are involved in nodulation of Sesbania rostrata. Plant Physiol **139,** 1366-1379.

Limpens, E., and Bisseling, T. (2003). Signaling in symbiosis. Curr Opin Plant Biol **6,** 343-350.

Limpens, E., Franken, C., Smit, P., Willemse, J., Bisseling, T., and Geurts, R. (2003). LysM domain receptor kinases regulating rhizobial Nod factor-induced infection. Science **302,** 630-633.

Limpens, E., Mirabella, R., Fedorova, E., Franken, C., Franssen, H., Bisseling, T., and Geurts, R. (2005). Formation of organelle-like N2-fixing symbiosomes in legume root nodules is controlled by DMI2. Proc Natl Acad Sci U S A **102,** 10375-10380.

Livak, K.J., and Schmittgen, T.D. (2001). Analysis of relative gene expression data using real-time quantitative PCR and the 2(-Delta Delta C(T)) Method. Methods **25,** 402-408.

Lohar, D.P., Sharopova, N., Endre, G., Penuela, S., Samac, D., Town, C., Silverstein, K.A., and Vandenbosch, K.A. (2005). Transcript Analysis of Early Nodulation Events in Medicago truncatula. Plant Physiol.

Lorbiecke, R., and Sauter, M. (1999). Adventitious root growth and cell-cycle induction in deepwater rice. Plant Physiology **119,** 21-29.

Loureiro, M.F., James, E.K., Sprent, J.I., and Franco, A.A. (1995). Stem and Root-Nodules on the Tropical Wetland Legume Aeschynomene Fluminensis. New Phytologist **130,** 531-544.

Madsen, E.B., Madsen, L.H., Radutoiu, S., Olbryt, M., Rakwalska, M., Szczyglowski, K., Sato, S., Kaneko, T., Tabata, S., Sandal, N., and Stougaard, J. (2003). A receptor kinase gene of the LysM type is involved in legume perception of rhizobial signals. Nature **425,** 637-640.

Manthey, K., Krajinski, F., Hohnjec, N., Firnhaber, C., Pühler, A., Perlick, A., and Küster, H. (2004). Transcriptome Profiling in Root Nodules and Arbuscular Mycorrhiza Identifies a Collection of Novel Genes Induced During *Medicago truncatula* Root Endosymbiosis. Molecular Plant-Microbe Interactions **17,** 1063-1077.

Mathesius, U., Weinman, J.J., Rolfe, B.G., and Djordjevic, M.A. (2000). Rhizobia can induce nodules in white clover by "hijacking" mature cortical cells activated during lateral root development. Mol Plant Microbe Interact **13,** 170-182.

Mathis, R., Grosjean, C., de Billy, F., Huguet, T., and Gamas, P. (1999). The early nodulin gene MtN6 is a novel marker for events preceding infection of Medicago truncatula roots by Sinorhizobium meliloti. Mol Plant Microbe Interact **12,** 544-555.

Maunoury, M., Kondorosi, A., Kondorosi, E., and Mergaert, P. (2006). Cell biology of nodule infection and development. In Nitrogen Fixation: Origins, applications, and research progress. Leguminous Nitrogen-Fixing Symbioses, J. Sprent and W.E. Newton, eds (The Netherlands: Springer.

McAlvin, C.B., and Stacey, G. (2005). Transgenic expression of the soybean apyrase in Lotus japonicus enhances nodulation. Plant Physiol **137,** 1456-1462.

Meijer, H.J., and Munnik, T. (2003). Phospholipid-based signaling in plants. Annu Rev Plant Biol **54,** 265-306.

Mergaert, P., Van Montagu, M., Prome, J.C., and Holsters, M. (1993). Three unusual modifications, a D-arabinosyl, an N-methyl, and a carbamoyl group, are present on the Nod factors of Azorhizobium caulinodans strain ORS571. Proc Natl Acad Sci U S A **90,** 1551-1555.

Mergaert, P., Nikovics, K., Kelemen, Z., Maunoury, N., Vaubert, D., Kondorosi, A., and Kondorosi, E. (2003). A novel family in Medicago truncatula consisting of more than 300 nodule-specific genes coding for small, secreted polypeptides with conserved cysteine motifs. Plant Physiol **132,** 161-173.

Mergaert, P., D'Haeze, W., Fernandez-Lopez, M., Geelen, D., Goethals, K., Prome, J.C., Van Montagu, M., and Holsters, M. (1996). Fucosylation and arabinosylation of Nod factors in Azorhizobium caulinodans: involvement of nolK, nodZ as well as noeC and/or downstream genes. Mol Microbiol **21,** 409-419.

Messens, E., Geelen, D., Vanmontagu, M., and Holsters, M. (1991). 7,4'-Dihydroxyflavanone Is the Major Azorhizobium-Nod Gene-Inducing Factor Present in Sesbania-Rostrata Seedling Exudate. . Mol Plant Microbe Interact **4,** 262-267.

Miles, G.P., Samuel, M.A., Jones, A.M., and Ellis, B.E. (2004). Mastoparan rapidly activates plant MAP kinase signaling independent of heterotrimeric G proteins. Plant Physiol **134,** 1332-1336.

Mithofer, A. (2002). Suppression of plant defence in rhizobia-legume symbiosis. Trends Plant Sci **7,** 440-444.

Mitra, R.M., and Long, S.R. (2004). Plant and bacterial symbiotic mutants define three transcriptionally distinct stages in the development of the Medicago truncatula/Sinorhizobium meliloti symbiosis. Plant Physiol **134,** 595-604.

Mitra, R.M., Shaw, S.L., and Long, S.R. (2004a). Six nonnodulating plant mutants defective for Nod factor-induced transcriptional changes associated with the legume-rhizobia symbiosis. Proc Natl Acad Sci U S A **101,** 10217-10222.

Mitra, R.M., Gleason, C.A., Edwards, A., Hadfield, J., Downie, J.A., Oldroyd, G.E., and Long, S.R. (2004b). A Ca2+/calmodulin-dependent protein kinase required for symbiotic nodule development: Gene identification by transcript-based cloning. Proc Natl Acad Sci U S A.

Miwa, H., Sun, J., Oldroyd, G., and Downie, J.A. (2006). Analysis of Ca2+ spiking using a cameleon Ca2+ sensor in Medicago truncatula indicates roles for optimal spiking frequency and spiking number for nodulation gene induction. . in preparation.

Mulder, L., Lefebvre, B., Cullimore, J., and Imberty, A. (2006). LysM domains of Medicago truncatula NFP protein involved in Nod factor perception. Glycosylation state, molecular modeling and docking of chitooligosaccharides and Nod factors. Glycobiology.

Munnik, T. (2001). Phosphatidic acid: an emerging plant lipid second messenger. Trends Plant Sci **6,** 227-233.

Munnik, T., Irvine, R.F., and Musgrave, A. (1998). Phospholipid signalling in plants. Biochim Biophys Acta **1389,** 222-272.

Mylona, P., Pawlowski, K., and Bisseling, T. (1995). Symbiotic Nitrogen Fixation. Plant Cell **7,** 869-885.

Ndoye, I., de Billy, F., Vasse, J., Dreyfus, B., and Truchet, G. (1994). Root nodulation of Sesbania rostrata. J Bacteriol **176,** 1060-1068.

Niebel, A., Bono, J.J., Ranjeva, R., and Cullimore, J. (1997). Identification of a High Affinity Binding Site for Lipooligosaccharidic NodRm Factors in the Microsomal Fraction of *Medicago* Cell Suspension Cultures. Mol Plant Microbe Interact **10,** 132-134.

Nishimura, R., Hayashi, M., Wu, G.J., Kouchi, H., Imaizumi-Anraku, H., Murakami, Y., Kawasaki, S., Akao, S., Ohmori, M., Nagasawa, M., Harada, K., and Kawaguchi, M. (2002). HAR1 mediates systemic regulation of symbiotic organ development. Nature **420,** 426-429.

Norholm, M.H., Nour-Eldin, H.H., Brodersen, P., Mundy, J., and Halkier, B.A. (2006). Expression of the Arabidopsis high-affinity hexose transporter STP13 correlates with programmed cell death. FEBS Lett **580,** 2381-2387.

Oldroyd, G.E., and Geurts, R. (2001). Medicago truncatula, going where no plant has gone before. Trends Plant Sci **6,** 552-554.

Oldroyd, G.E., and Long, S.R. (2003). Identification and characterization of nodulation-signaling pathway 2, a gene of Medicago truncatula involved in Nod actor signaling. Plant Physiol **131,** 1027-1032.

Oldroyd, G.E., and Downie, J.A. (2004). Calcium, kinases and nodulation signalling in legumes. Nat Rev Mol Cell Biol **5,** 566-576.

Oldroyd, G.E., and Downie, J.A. (2006). Nuclear calcium changes at the core of symbiosis signalling. Curr Opin Plant Biol.

Oldroyd, G.E., Engstrom, E.M., and Long, S.R. (2001a). Ethylene inhibits the Nod factor signal transduction pathway of Medicago truncatula. Plant Cell **13,** 1835-1849.

Oldroyd, G.E., Mitra, R.M., Wais, R.J., and Long, S.R. (2001b). Evidence for structurally specific negative feedback in the Nod factor signal transduction pathway. Plant J **28,** 191-199.

Oldroyd, G.E.D. (2001). Dissecting symbiosis: Developments in Nod factor signal transduction. Annals of Botany **87,** 709-718.

Olsson, J.E., and Rolfe, B.G. (1985). Stem and Root Nodulation of the Tropical Legume Sesbania-Rostrata by Rhizobium Strains Ors-571 and We7. Journal of Plant Physiology **121,** 199-210.

Parniske, M. (2000). Intracellular accommodation of microbes by plants: a common developmental program for symbiosis and disease? Curr Opin Plant Biol **3,** 320-328.

Parniske, M. (2004). Molecular genetics of the arbuscular mycorrhizal symbiosis. Curr Opin Plant Biol **7,** 414-421.

Patriarca, E.J., Tate, R., Ferraioli, S., and Iaccarino, M. (2004). Organogenesis of legume root nodules. International Review of Cytology - a Survey of Cell Biology, Vol. 234 **234,** 201-+.

Pauly, N., Pucciariello, C., Mandon, K., Innocenti, G., Jamet, A., Baudouin, E., Herouart, D., Frendo, P., and Puppo, A. (2006). Reactive oxygen and nitrogen species and glutathione: key players in the legume-Rhizobium symbiosis. J Exp Bot.

Penmetsa, R.V., and Cook, D.R. (1997). A Legume Ethylene-Insensitive Mutant Hyperinfected by Its Rhizobial Symbiont. Science **275,** 527-530.

Penmetsa, R.V., Frugoli, J.A., Smith, L.S., Long, S.R., and Cook, D.R. (2003). Dual genetic pathways controlling nodule number in Medicago truncatula. Plant Physiol **131,** 998-1008.

Perret, X., Staehelin, C., and Broughton, W.J. (2000). Molecular basis of symbiotic promiscuity. Microbiol Mol Biol Rev **64,** 180-201.

Peters, N.K., and Cristestes, D.K. (1989). Nodule Formation Is Stimulated by the Ethylene Inhibitor Aminoethoxyvinylglycine. Plant Physiology **91,** 690-693.

Pingret, J.L., Journet, E.P., and Barker, D.G. (1998). Rhizobium nod factor signaling. Evidence for a g protein-mediated transduction mechanism. Plant Cell **10,** 659-672.

Poulsen, C., and Podenphant, L. (2002). Expressed sequence tags from roots and nodule primordia of Lotus japonicus infected with Mesorhizobium loti. Molecular Plant-Microbe Interactions **15,** 376-379.

Prell, J., and Poole, P. (2006). Metabolic changes of rhizobia in legume nodules. Trends Microbiol **14,** 161-168.

Radutoiu, S., Madsen, L.H., Madsen, E.B., Felle, H.H., Umehara, Y., Gronlund, M., Sato, S., Nakamura, Y., Tabata, S., Sandal, N., and Stougaard, J. (2003). Plant recognition of symbiotic bacteria requires two LysM receptor-like kinases. Nature **425,** 585-592.

Relic, B., Perret, X., Estrada-Garcia, M.T., Kopcinska, J., Golinowski, W., Krishnan, H.B., Pueppke, S.G., and Broughton, W.J. (1994). Nod factors of Rhizobium are a key to the legume door. Mol Microbiol **13,** 171-178.

Riely, B.K., Mun, J.H., and Ane, J.M. (2006). Unravelling the molecular basis for symbiotic signal transduction in legumes. Molecular Plant Pathology **7,** 197-207.

Riely, B.K., Ane, J.M., Penmetsa, R.V., and Cook, D.R. (2004). Genetic and genomic analysis in model legumes bring Nod-factor signaling to center stage. Curr Opin Plant Biol **7,** 408-413.

Saeed, A.I., Sharov, V., White, J., Li, J., Liang, W., Bhagabati, N., Braisted, J., Klapa, M., Currier, T., Thiagarajan, M., Sturn, A., Snuffin, M., Rezantsev, A., Popov, D., Ryltsov, A., Kostukovich, E., Borisovsky, I., Liu, Z., Vinsavich, A., Trush, V., and Quackenbush, J. (2003). TM4: a free, open-source system for microarray data management and analysis. Biotechniques **34,** 374-378.

Sambrook, J., Fritsch, E.F., and Maniatis, T. (1989). Molecular Cloning: A Laboratory Manual. (Plainview, NY.: Cold Spring Harbor Lab. Press).

Schauser, L., Wieloch, W., and Stougaard, J. (2005). Evolution of NIN-like proteins in Arabidopsis, rice, and Lotus japonicus. J Mol Evol **60,** 229-237.

Schauser, L., Roussis, A., Stiller, J., and Stougaard, J. (1999). A plant regulator controlling development of symbiotic root nodules. Nature **402,** 191-195.

Schiefelbein, J.W. (2000). Constructing a plant cell. The genetic control of root hair development. Plant Physiol **124,** 1525-1531.

Schnabel, E.L., and Frugoli, J. (2004). The PIN and LAX families of auxin transport genes in Medicago truncatula. Mol Genet Genomics **272,** 420-432.

Schroeyers, K., Chaparro, C., Goormachtig, S., and Holsters, M. (2004). Nodulation-enhanced sequences from the water stress-tolerant tropical legume *Sesbania rostrata*. Plant Science **167,** 207-216.

Schultze, M., Kondorosi, E., Ratet, P., Buire, M., and Kondorosi, A. (1994). Cell and Molecular Biology of Rhizobium-Plant Interactions. In International Review of Cytology, G. Bourne, ed (Academic Press), pp. 1-75.

Schulze-Lefert, P. (2004). Knocking on the heaven's wall: pathogenesis of and resistance to biotrophic fungi at the cell wall. Curr Opin Plant Biol **7,** 377-383.

Searle, I.R., Men, A.E., Laniya, T.S., Buzas, D.M., Iturbe-Ormaetxe, I., Carroll, B.J., and Gresshoff, P.M. (2003). Long-distance signaling in nodulation directed by a CLAVATA1-like receptor kinase. Science **299,** 109-112.

Sharma, S.B., and Signer, E.R. (1990). Temporal and spatial regulation of the symbiotic genes of Rhizobium meliloti in planta revealed by transposon Tn5-gusA. Genes Dev **4,** 344-356.

Smit, P., Raedts, J., Portyanko, V., Debelle, F., Gough, C., Bisseling, T., and Geurts, R. (2005). NSP1 of the GRAS protein family is essential for rhizobial Nod factor-induced transcription. Science **308,** 1789-1791.

Soltis, D.E., Soltis, P.S., Morgan, D.R., Swensen, S.M., Mullin, B.C., Dowd, J.M., and Martin, P.G. (1995). Chloroplast gene sequence data suggest a single origin of the predisposition for symbiotic nitrogen fixation in angiosperms. Proc Natl Acad Sci U S A **92,** 2647-2651.

Sprent, J.I. (2002). Nodulation in Legumes. (Kew, U.K.: Royal Botanical Gardens).

Stougaard, J. (2001). Genetics and genomics of root symbiosis. Curr Opin Plant Biol **4,** 328-335.

Stracke, S., Kistner, C., Yoshida, S., Mulder, L., Sato, S., Kaneko, T., Tabata, S., Sandal, N., Stougaard, J., Szczyglowski, K., and Parniske, M. (2002). A plant receptor-like kinase required for both bacterial and fungal symbiosis. Nature **417,** 959-962.

Subbarao, N.S., Mateos, P.F., Baker, D., Pankratz, H.S., Palma, J., Dazzo, F.B., and Sprent, J.I. (1995). The Unique Root-Nodule Symbiosis between Rhizobium and the Aquatic Legume, Neptunia-Natans (L-F) Druce. Planta **196,** 311-320.

Suharsono, U., Fujisawa, Y., Kawasaki, T., Iwasaki, Y., Satoh, H., and Shimamoto, K. (2002). The heterotrimeric G protein alpha subunit acts upstream of the small GTPase Rac in disease resistance of rice. Proc Natl Acad Sci U S A **99,** 13307-13312.

Sun, J., Cardoza, V., Mitchell, D.M., Bright, L., Oldroyd, G., and Harris, J. (2006). Crosstalk between Jasmonic acid, ethylene and Nod factor signaling allows integration of diverse inputs for regulation of nodulation. Plant J **46,** 961-971.

Sutton, J.M., Lea, E.J., and Downie, J.A. (1994). The nodulation-signaling protein NodO from Rhizobium leguminosarum biovar viciae forms ion channels in membranes. Proc Natl Acad Sci U S A **91,** 9990-9994.

Thompson, J.D., Higgins, D.G., and Gibson, T.J. (1994). CLUSTAL W: improving the sensitivity of progressive multiple sequence alignment through sequence weighting, position-specific gap penalties and weight matrix choice. Nucleic Acids Res **22,** 4673-4680.

Timmers, A.C., Auriac, M.C., and Truchet, G. (1999). Refined analysis of early symbiotic steps of the Rhizobium-Medicago interaction in relationship with microtubular cytoskeleton rearrangements. Development **126,** 3617-3628.

Timmers, A.C., Auriac, M.C., de Billy, F., and Truchet, G. (1998). Nod factor internalization and microtubular cytoskeleton changes occur concomitantly during nodule differentiation in alfalfa. Development **125,** 339-349.

Tirichine, L., James, E.K., Sandal, N., and Stougaard, J. (2006). Spontaneous root-nodule formation in the model legume Lotus japonicus: a novel class of mutants nodulates in the absence of rhizobia. Mol Plant Microbe Interact **19,** 373-382.

Tirichine, L., Imaizumi-Anraku, H., Yoshida, S., Murakami, Y., Madsen, L.H., Miwa, H., Nakagawa, T., Sandal, N., Albrektsen, A.S., Kawaguchi, M., Downie, A., Sato, S., Tabata, S., Kouchi, H., Parniske, M., Kawasaki, S., and Stougaard, J. (2006). Deregulation of a Ca2+/calmodulin-dependent kinase leads to spontaneous nodule development. Nature **441,** 1153-1156.

Trusov, Y., Rookes, J.E., Chakravorty, D., Armour, D., Schenk, P.M., and Botella, J.R. (2006). Heterotrimeric G proteins facilitate Arabidopsis resistance to necrotrophic pathogens and are involved in jasmonate signaling. Plant Physiol **140,** 210-220.

Tsien, H.C., Dreyfus, B.L., and Schmidt, E.L. (1983). Initial stages in the morphogenesis of nitrogen-fixing stem nodules of Sesbania rostrata. J Bacteriol **156,** 888-897.

van Brussel, A.A., Bakhuizen, R., van Spronsen, P.C., Spaink, H.P., Tak, T., Lutgenberg, B.J.J., and Kijne, J.W. (1992). Induction of pre-infection thread structures in the leguminous host plant by mitogenic lipo-oligosaccharides of *Rhizobium*. Science **257**.

Van de Peer, Y., and De Wachter, R. (1997). Construction of evolutionary distance trees with TREECON for Windows: accounting for variation in nucleotide substitution rate among sites. Comput Appl Biosci **13,** 227-230.

Van de Velde, W., Mergeay, J., Holsters, M., and Goormachtig, S. (2003). Agrobacterium rhizogenes-mediated transformation of Sesbania rostrata. Plant Science **165,** 1281-1288.

Van de Velde, W., Perez Guerra, J.C., De Keyser, A., De Rycke, R., Rombauts, S., Maunoury, N., Mergaert, P., Kondorosi, E., Holsters, M., and Goormachtig, S. (2006). Aging in legume symbiosis: A molecular view on nodule senescence in Medicago truncatula. Plant Physiol.

Van den Eede, G., Dreyfus, B., Goethals, K., and Van Montagu, M. (1987). Identification and cloning of nodulation genes from the stem-nodulating bacterium ORS571. Mol. Gen. Genet. **206,** 291-299.

Van den Eede, G., Deblaere, R., Goethals, K., and Van Montagu, M. (1992). Broad host range and promoter selection vectors for bacteria that interact with plants. Mol. Plant-Microbe Interact. **5,** 228-234.

van Rhijn, P., Goldberg, R.B., and Hirsch, A.M. (1998). Lotus corniculatus nodulation specificity is changed by the presence of a soybean lectin gene. Plant Cell **10,** 1233-1250.

van Spronsen, P.C., vanBrussel, A.A.N., and Kijne, J.W. (1995). Nod factors produced by Rhizobium leguminosarum biovar viciae induce ethylene-related changes in root cortical cells of Vicia sativa ssp nigra. European Journal of Cell Biology **68,** 463-469.

Vance, C.P., Johnson, L.E.B., Stade, S., and Groat, R.G. (1982). Birdsfoot-Trefoil (Lotus-Corniculatus) Root-Nodules - Morphogenesis and the Effect of Forage Harvest on Structure and Function. Canadian Journal of Botany-Revue Canadienne De Botanique **60,** 505-518.

Vandenabeele, S., Van Der Kelen, K., Dat, J., Gadjev, I., Boonefaes, T., Morsa, S., Rottiers, P., Slooten, L., Van Montagu, M., Zabeau, M., Inze, D., and Van Breusegem, F. (2003). A comprehensive analysis of hydrogen peroxide-induced gene expression in tobacco. Proc Natl Acad Sci U S A **100,** 16113-16118.

Vasse, J., Debilly, F., Camut, S., and Truchet, G. (1990). Correlation between Ultrastructural Differentiation of Bacteroids and Nitrogen-Fixation in Alfalfa Nodules. Journal of Bacteriology **172,** 4295-4306.

Vega-Hernandez, M.C., Perez-Galdona, R., Dazzo, F.B., Jarabo-Lorenzo, A., Alfayate, M.C., and Leon-Barrios, M. (2001). Novel infection process in the indeterminate root nodule symbiosis between Chamaecytisus proliferus (tagasaste) and Bradyrhizobium sp. New Phytologist **150,** 707-721.

Veit, B. (2004). Determination of cell fate in apical meristems. Curr Opin Plant Biol **7,** 57-64.

Vlieghe, K., Boudolf, V., Beemster, G.T., Maes, S., Magyar, Z., Atanassova, A., de Almeida Engler, J., De Groodt, R., Inze, D., and De Veylder, L. (2005). The DP-E2F-like gene DEL1 controls the endocycle in Arabidopsis thaliana. Curr Biol **15,** 59-63.

Voesenek, L.A.C.J., Benschop, J.J., Bou, J., Cox, M.C.H., Groeneveld, H.W., Millenaar, F.F., Vreeburg, R.A.M., and Peeters, A.J.M. (2003). Interactions between plant hormones regulate submergence-induced shoot elongation in the flooding-tolerant dicot Rumex palustris. Annals of Botany **91,** 205-211.

Wais, R.J., Galera, C., Oldroyd, G., Catoira, R., Penmetsa, R.V., Cook, D., Gough, C., Denarie, J., and Long, S.R. (2000). Genetic analysis of calcium spiking responses in nodulation mutants of Medicago truncatula. Proc Natl Acad Sci U S A **97,** 13407-13412.

Walker, S.A., and Downie, J.A. (2000). Entry of Rhizobium leguminosarum bv. viciae into root hairs requires minimal nod factor specificity, but subsequent infection thread growth requires nodO or nodE. Molecular Plant-Microbe Interactions **13,** 754-762.

Walker, S.A., Viprey, V., and Downie, J.A. (2000). Dissection of nodulation signaling using pea mutants defective for calcium spiking induced by nod factors and chitin oligomers. Proc Natl Acad Sci U S A **97,** 13413-13418.

Wood, S.M., and Newcomb, W. (1989). Nodule Morphogenesis - the Early Infection of Alfalfa (Medicago-Sativa) Root Hairs by Rhizobium-Meliloti. Canadian Journal of Botany-Revue Canadienne De Botanique **67,** 3108-3122.

Xu, J., and Scheres, B. (2005a). Cell polarity: ROPing the ends together. Curr Opin Plant Biol **8,** 613-618.

Xu, J., and Scheres, B. (2005b). Dissection of Arabidopsis ADP-RIBOSYLATION FACTOR 1 function in epidermal cell polarity. Plant Cell **17,** 525-536.

Yang, W.C., de Blank, C., Meskiene, I., Hirt, H., Bakker, J., van Kammen, A., Franssen, H., and Bisseling, T. (1994). Rhizobium nod factors reactivate the cell cycle during infection and nodule primordium formation, but the cycle is only completed in primordium formation. Plant Cell **6,** 1415-1426.

Zhu, H., Riely, B.K., Burns, N.J., and Ane, J.M. (2006). Tracing nonlegume orthologs of legume genes required for nodulation and arbuscular mycorrhizal symbioses. Genetics **172,** 2491-2499.